ISSN 0021-9673

VOL. 482 NO. 1 NOVEMBER 17, 1989

JOURNAL OF CHROMATOGRAPHY

INTERNATIONAL JOURNAL ON CHROMATOGRAPHY, ELECTROPHORESIS AND RELATED METHODS

ELSEVIER

JOURNAL OF CHROMATOGRAPHY

Scope. The *Journal of Chromatography* publishes papers on all aspects of chromatography, electrophoresis and related methods. Contributions consist mainly of research papers dealing with chromatographic theory, instrumental development and their applications. The section *Biomedical Applications*, which is under separate editorship, deals with the following aspects: developments in and applications of chromatographic and electrophoretic techniques related to clinical diagnosis or alterations during medical treatment; screening and profiling of body fluids or tissues with special reference to metabolic disorders; results from basic medical research with direct consequences in clinical practice; drug level monitoring and pharmacokinetic studies; clinical toxicology; analytical studies in occupational medicine.

Submission of Papers. Papers in English, French and German may be submitted, in three copies. Manuscripts should be submitted to: The Editor of *Journal of Chromatography*, P.O. Box 681, 1000 AR Amsterdam, The Netherlands, or to: The Editor of *Journal of Chromatography, Biomedical Applications*, P.O. Box 681, 1000 AR Amsterdam, The Netherlands. Review articles are invited or proposed by letter to the Editors. An outline of the proposed review should first be forwarded to the Editors for preliminary discussion prior to preparation. Submission of an article is understood to imply that the article is original and unpublished and is not being considered for publication elsewhere. For copyright regulations, see below.

Subscription Orders. Subscription orders should be sent to: Elsevier Science Publishers B.V., P.O. Box 211, 1000 AE Amsterdam, The Netherlands, Tel. 5803 911, Telex 18582 ESPA NL. The *Journal of Chromatography* and the *Biomedical Applications* section can be subscribed to separately.

Publication. The *Journal of Chromatography* (incl. *Biomedical Applications*) has 37 volumes in 1989. The subscription prices for 1989 are:

J. Chromatogr. + *Biomed. Appl.* (Vols. 461–497):
Dfl. 6475.00 plus Dfl. 999.00 (p.p.h.) (total *ca.* US$ 3428,50)

J. Chromatogr. only (Vols. 461–486):
Dfl. 5200.00 plus Dfl. 702.00 (p.p.h.) (total *ca.* US$ 2707.25)

Biomed. Appl. only (Vols. 487–497):
Dfl. 2200.00 plus Dfl. 297.00 (p.p.h.) (total *ca.* US$ 1145.50).

Our p.p.h. (postage, package and handling) charge includes surface delivery of all issues, except to subscribers in Argentina, Australia, Brasil, Canada, China, Hong Kong, India, Israel, Malaysia, Mexico, New Zealand, Pakistan, Singapore, South Africa, South Korea, Taiwan, Thailand and the U.S.A. who receive all issues by air delivery (S.A.L. — Surface Air Lifted) at no extra cost. For Japan, air delivery requires 50% additional charge; for all other countries airmail and S.A.L. charges are available upon request. Back volumes of the *Journal of Chromatography* (Vols. 1–460) are available at Dfl. 195.00 (plus postage). Claims for missing issues will be honoured, free of charge, within three months after publication of the issue. Customers in the U.S.A. and Canada wishing information on this and other Elsevier journals, please contact Journal Information Center, Elsevier Science Publishing Co. Inc., 655 Avenue of the Americas, New York, NY 10010. Tel. (212) 633-3750.

Abstracts/Contents Lists published in Analytical Abstracts, ASCA, Biochemical Abstracts, Biological Abstracts, Chemical Abstracts, Chemical Titles, Chromatography Abstracts, Clinical Chemistry Lookout, Current Contents/Physical, Chemical & Earth Sciences, Current Contents/Life Sciences, Deep-Sea Research/Part B: Oceanographic Literature Review, Excerpta Medica, Index Medicus, Mass Spectrometry Bulletin, PASCAL-CNRS, Pharmaceutical Abstracts, Referativnyi Zhurnal, Science Citation Index and Trends in Biotechnology.

See inside back cover for Publication Schedule, Information for Authors and information on Advertisements.

0378-9673/89/$03.50

Printed in The Netherlands

CONTENTS

(Abstracts/Contents Lists published in Analytical Abstracts, ASCA, Biochemical Abstracts, Biological Abstracts, Chemical Abstracts, Chemical Titles, Chromatography Abstracts, Current Contents/Physical, Chemical & Earth Sciences, Current Contents/Life Sciences, Deep-Sea Research/Part B: Oceanographic Literature Review, Excerpta Medica, Index Medicus, Mass Spectrometry Bulletin, PASCAL-CNRS, Referativnyi Zhurnal and Science Citation Index)

(Continued overleaf)

Contents (continued)

Notes

In articles with more than one author, the name of the author to whom correspondence should be addressed is indicated in the article heading by a 6-pointed asterisk (*)

Request for manuscripts

R. Majors, F. Regnier and K. Unger will edit a special, thematic issue of the *Journal of Chromatography* entitled "LC Column Packings" (both HPLC and LC). Both reviews and research articles will be included.

Topics such as the following will be covered:

- organic packings
- inorganic packings
- non-porous particles
- macroporous particles
- restricted access media
- functionalized membranes
- solid-phase extraction materials
- commercially available packings
- physical-chemical characterization
- relative performance of packings
- packing procedures and hardware
- column care.

Only minor coverage of topics such as affinity chromatography and chiral separations is planned since these will be the topics of other thematic issues.

Potential authors of reviews should contact Roger Giese, Editor, prior to any submission. Address: 110 Mugar Building, Northeastern University, Boston, MA 02115, U.S.A.; tel.: (617) 437-3227; fax: (617) 437-2855.

The deadline for receipt of submissions is June 1, 1990. Manuscripts submitted after this date can still be published in the Journal, but then there is no guarantee that an accepted article will appear in this special, thematic issue. Five copies of the manuscript should be submitted to R. Giese. All manuscripts will be reviewed and acceptance will be based on the usual critria for publishing in the *Journal of Chromatography*.

Automatic Methods of Analysis

by **M. VALCÁRCEL** *and* **M.D. LUQUE DE CASTRO,**
Department of Analytical Chemistry, University of Córdoba, Córdoba, Spain

(Techniques and Instrumentation in Analytical Chemistry, 9)

This new book gives a comprehensive overview of the state of the art of the automation of laboratory processes in analytical chemistry. The topics have been chosen according to such criteria as the degree of consolidation, scope of application and most promising trends.

The book begins with the basic principles behind the automation of laboratory processes, then describes automatic systems for sampling and sample treatment. In the second part the principal types of analysers are discussed: continuous, batch and robotic. The third part is devoted to the automation of analytical instrumentation: spectroscopic, electroanalytical and chromatographic techniques and titrators. The last part presents examples of the application of automation to clinical chemistry, environmental pollution monitoring and industrial process control.

The text is supplemented by 290 figures and 800 literature references. It is written primarily for those directly involved in laboratory work or responsible for industrial planning and control, research centres, etc. It will also be useful to analytical chemists wishing to update their knowledge in this area, and will be of especial interest to scientists directly related to environmental sciences or clinical chemistry.

CONTENTS:

1988 xii + 560 pages
US$ 131.50 / Dfl.250.00
ISBN 0-444-43005-9

ELSEVIER SCIENCE PUBLISHERS

P.O. Box 211, 1000 AE Amsterdam, The Netherlands
P.O. Box 882, Madison Square Station, New York, NY 10159, USA

NATURAL PRODUCTS ISOLATION

Separation Methods for Antimicrobials, Antivirals and Enzyme Inhibitors

edited by **GERALD H. WAGMAN** *and* **RAYMOND COOPER,**
Schering-Plough Research, Bloomfield, NJ, USA

(Journal of Chromatography Library, 43)

This new book encompasses, in great detail, the most recent progress made in the isolation and separation of natural products. Written by experts in their respective fields, it covers antibiotics, marine and plant-derived substances, enzyme inhibitors and interferons. The book has extensive isolation schemes, tables, figures and chemical structures. In many instances a short summary of the producing organism, brief chemical description and structure and biological activity of the compounds is presented. Detailed information of extraction, separation and purification techniques follow. Each chapter has an extensive bibliography and, where applicable, an appendix showing sources of materials and equipment. A detailed index to the subject matter is also provided.

The book thus offers the reader: up-to-date reviews (including 1988) of specific topics in the natural products field not to be found elsewhere; information on new chromatographic methods and techniques described in sufficient detail to be utilized by investigators in this area of research; and extensive references to enable the serious researcher to pursue particular information. It will appeal to pharmaceutical and natural products researchers and is a valuable acquisition for university chemistry and biochemistry departments.

Contents: Countercurrent chromatography *(J.B. McAlpine, J.E. Hochlowski)*. HPLC detection methods for microbial products from fermentation broth *(R. Mierzwa et al.)*. Affinity and purification of glycopeptide antibiotics *(R.D. Sitrin, G.F. Wasserman)*. Nikkomycins and polyoxins *(H.-P. Fiedler)*. Saframycins and isoquinolines *(T. Arai)*. New cephalosporins *(S. Harada)*. Monocyclic β-lactam antibiotics *(W.L. Parker)*. Isolation of carbapenems *(K.E. Wilson)*. Avermectins and related compounds *(T. Miller, V.P. Gullo)*. Bioactive compounds from marine organisms and cultivated blue-green algae *(J.S. Mynderse et al.)*. The interferons *(S. Pestka)*. Enzyme inhibitors produced by microorganisms *(H. Umezawa)*. Alkaloidal glycosidase inhibitors from plants *(L.E. Fellows, G.W.J. Fleet)*. Chemical communication and control of development *(C.E. Smith, J.D. Orr, D.G. Lynn)*. Subject Index.

1989 xii + 618 pages
US$ 150.00 / Dfl. 285.00
ISBN 0-444- 87147-0

ELSEVIER SCIENCE PUBLISHERS

P.O. Box 211, 1000 AE Amsterdam, The Netherlands
P.O. Box 882, Madison Square Station, New York, NY 10159, USA

JOURNAL OF CHROMATOGRAPHY

VOL. 482 (1989)

JOURNAL
of
CHROMATOGRAPHY

INTERNATIONAL JOURNAL ON CHROMATOGRAPHY,
ELECTROPHORESIS AND RELATED METHODS

ELSEVIER
AMSTERDAM — OXFORD — NEW YORK — TOKYO

0021-9673/89/$03.50

Printed in The Netherlands

Journal of Chromatography, 482 (1989) 1–12
Elsevier Science Publishers B.V., Amsterdam — Printed in The Netherlands

CHROM. 21 626

ROLE OF ASSOCIATION ON PROTEIN ADSORPTION ISOTHERMS

β-LACTOGLOBULIN A ADSORBED ON A WEAKLY HYDROPHOBIC SURFACE

R. BLANCO[a], A. ARAI, N. GRINBERG[b], D. M. YARMUSH[c] and B. L. KARGER*
Barnett Institute of Chemical Analysis and Materials Science, and Department of Chemistry, Northeastern University, 341 Mugar Building, Boston, MA 02115 (U.S.A.)
(Received May 17th, 1989)

SUMMARY

This paper explores the role of association on the adsorption isotherms of β-lactoglobulin A on a weakly hydrophobic stationary phase at 4°C and mobile phases of 0.85 *M* and 1 *M* ammonium sulfate, pH 4.5. The isotherms, obtained by frontal analysis, show an S-shape and the corresponding Scatchard plots indicate positive cooperativity. The slopes and intercepts of the Scatchard plots at low solute concentration are analyzed in terms of two species —a protomer and a higher order stronger adsorbing species. An explicit equation of the isotherm is developed based on this model, and this expression is shown to reproduce the isotherm shape using the appropriate derived parameters. It is further shown from this equation that a Langmuir-shaped adsorption isotherm can be obtained if the higher order associate or aggregate binds weaker to the support than the protomer. These results indicate that protein–protein interactions and the formation of associates can play a significant role on the shape of the isotherm and ultimately on the behavior of the species in preparative scale chromatography.

INTRODUCTION

The adsorption of proteins at the liquid–solid interface is under active study for chromatography[1] and in the design of biomaterials[2,3], among other areas. The adsorption process has been studied using both static[4–6] and dynamic methods[7,8]. It has been established that the dynamic measurement of adsorption isotherms, *e.g.*, frontal analysis, provides a good general description of the process[9] and is relevant for chromatography[10].

Recently, the importance of adsorption isotherms as a tool in the prediction of

[a] Present address: Universidad de Costa Rica, Chemistry School, San Pedro 2060, Costa Rica.
[b] Present address: Merck, Sharp and Dohme Research Labs., Rahway, NJ 07065, U.S.A.
[c] Dept. of Chemical and Biochemical Engineering, Rutgers University, Piscataway, NJ 08855, U.S.A.

0021-9673/89/$03.50

elution behavior in preparative scale chromatography of small and large molecules has been emphasized[10,11]. Several important points can be learned from these studies and that of others: (1) highly precise data is required for differentiation between various adsorption mechanisms[12]; (2) the shape of the isotherm near the origin is important for determining the chromatographic elution profile[13]; and, (3) there is a lack of an understanding of the macroscopic distribution processes involved in adsorption under chromatographic conditions.

With respect to proteins, models of adsorption generally use the Langmuir isotherm to describe the non-linear adsorption behavior[14–16]. The Langmuirian isotherm is only an experimental fit of the adsorption data, since the system may be far removed from the actual Langmuir model, *e.g.* fixed homogeneous adsorption sites, no solute lateral interaction on the surface, ideal solution behavior.

In preparative scale liquid chromatography, injection of relatively high concentrations of substances is a common practice[17]. Protein–protein interactions leading to association or aggregation can be an important consideration at high concentrations; however, if precipitation does not occur, association may be neglected as a significant factor on chromatographic behavior, especially when general recommendations for preparative scale separation of proteins are presented[18]. Multiple equilibria between oligomers opens a new dimension of complexity in such systems, and subtle and/or major effects on adsorption behavior can be expected. An understanding and control of such behavior can be important in liquid chromatography, as well as in general protein adsorption phenomena.

A classical example of a protein aggregating system is β-lactoglobulin A (β-lact A)[19]. Previously, we have studied this protein at pH 4.5, 4°C, under hydrophobic interaction chromatographic (HIC) conditions, to illustrate the formation of oligomeric species and the resultant chromatographic behavior[20]. From a pure sample, several chromatographic peaks were observed whose relative amount depended on the injected concentration. Using a mass balance mathematical model, it was possible to determine that the first eluting peak was a dodecamer, the second a tetramer and the third an octamer. This stoichiometry was in agreement with molecular weight determinations using low angle laser light scattering (LALLS)[21]. The model that emerged was rapid aggregation of β-lact A upon injection into the chromatographic column.

As a continuation of this work, we have measured adsorption isotherms under weak hydrophobic surface binding conditions in order to study further the role of association or aggregation on protein adsorption. Positive cooperativity has been found, and this behavior has been interpreted in terms of associate formation with the higher order associate binding stronger to the adsorbent than the protomer. Various aspects of the adsorption behavior of β-lact A have been deduced from Scatchard plots, and an equation of the adsorption isotherm developed. Based on this equation, conditions are explored under which a Langmuir isotherm may be obtained as a result of protein association. Other studies, to be reported separately, reveal a hysteresis loop when the desorption isotherm is measured. It is not surprizing to find complex behavior in the distribution of proteins with solid surfaces.

EXPERIMENTAL

Equipment

Frontal and elution chromatography were conducted on a Model 334M liquid chromatography system (Beckman Instruments, San Ramon, CA, U.S.A.) equipped with a UV–VIS variable-wavelength detector, Model LC90 B10 (Perkin-Elmer, Norwalk, CT, U.S.A.), and a Beckman 210C sample injection valve. The absorbance signal was output to a recorder (Linear Instruments, Reno, NV, U.S.A.) and simultaneously processed by a data acquisition system (Nelson Analytical, Cupertino, CA, U.S.A.).

The column packing consisted of Vydac silica gel (Separations Group, Hesperia, CA, U.S.A.) bonded with a methyl polyether phase (particle size 5 μm, pore diameter 300 Å, specific surface area 72 m^2/g) and prepared as described elsewhere[22]. The surface coverage was 6.3 $\mu mol/m^2$, as determined by elemental analysis (assuming a stoichiometry of 2 for the binding of the silane to silica). Columns (2.78 cm × 0.29 I.D.) were slurry packed under pressure using a methanol–carbon tetrachloride solution (10:90, v/v). The temperature of the column, injection loop and tubing before the detector was regulated at 4.0°C, by a Neslab Exacal EX-300 water bath (Portsmouth, NH, U.S.A.) with an independent U-Cool Neslab cooling system.

Chemicals

HPLC water, chromatographic grade organic solvents, acetic acid, ammonium hydroxide, and reagent grade ammonium sulfate were purchased from J. T. Baker (Phillipsburg, NJ, U.S.A.). HEPES (N-2-hydroxyethyl-piperazine-N-2-ethane-sulfonic acid) and MES [2-(morpholino)ethane sulfonic acid] were obtained from Research Organics (Cleveland, OH, U.S.A.). Bovine β-lact A, electrophoretically pure, was purchased from Sigma (St. Louis, MO, U.S.A.) and used without further purification.

Procedures

Mobile phases were prepared by adding the correct weight of salt and buffer (20 m*M* HEPES, 20 m*M* MES, 20 m*M* acetic acid) to a volumetric flask containing HPLC water. The pH was adjusted to 4.5 with either ammonium hydroxide or acetic acid. Solutions were filtered and degassed under vacuum before use. Protein solutions were freshly prepared immediately before injection.

For isotherm measurements, the column was first equilibrated with the mobile phase buffer. The protein solution was then loaded through a temperature controlled loop (400 μl). When the outlet concentration of the sample reached a plateau in frontal development, the pure mobile phase buffer was switched into the column. Before each run, the column was reequilibrated with the mobile phase for 20 min. In order to detect systematic errors due to poor surface regeneration, a random procedure was followed to define the sequence of protein sample concentrations. The result of this set of experiments did not show any difference in loading (within experimental error) with samples injected in an increasing or decreasing concentration sequence. Protein concentration was monitored at a wavelength of 303 nm or 313 nm (for high concentration samples). Calibration plots were obtained at both wavelengths.

In order to obtain precise protein adsorption loadings, the flow-rate of the

mobile phase (20 μl/min) was measured during each run at 1–2 min intervals using a 1-ml calibrated Corning disposable micropipette, connected to the outlet of the detector. The volume of the stationary phase and the hold-up volume of the column were determined by a standard weight difference procedure, using methanol and carbon tetrachloride.

The amount adsorbed, Q, was determined from the area of the shaded portion of the breakthrough curve, see Fig. 1. The precision in Q between three independent injections of the same protein solution was better than 3% in the intermediate concentration region (8–12 mg/ml of protein) and less than 7% in the low concentration region (< 5 mg/ml of protein). The poorer precision at the low concentration end is due to the intrinsic error of the calculation method, in which absolute concentration errors are constant over the range of concentration, and consequently, the relative errors are larger for smaller concentrations. Nevertheless, high overall precision has been obtained for the isotherm measurements.

RESULTS AND DISCUSSION

Isotherms

Mobile phases of 0.85 *M* and 1.0 *M* ammonium sulfate were selected for frontal analysis isotherm determinations in order to reduce the adsorption coefficients of the oligomers to measurable solution concentration levels. Fig. 1 shows a typical break-through curve for β-lact A at pH 4.5 and 4°C, illustrating a diffuse front boundary. As is well known, a diffuse front is typical of an anti-Langmuir isotherm[23].

It is interesting to note that over the whole concentration range, identical isotherms were obtained with protein solutions freshly prepared and with solutions left for up to one day at 4°C. In previous studies[20], we found that protein precipitate was observed upon standing; however, the antichaotropic salt concentration was 2–3 *M*. Evidently, the salt concentrations in the present work are sufficiently low that any aggregation in solution does not lead to precipitation.

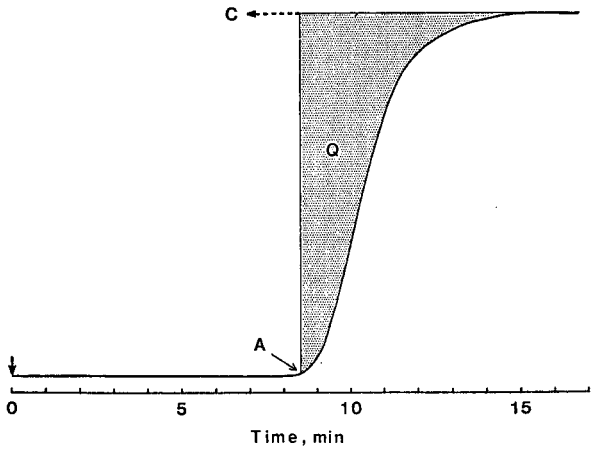

Fig. 1. Typical breakthrough curve using frontal analysis. The arrow at time 0 indicates loading of β-lact A (20 mg/ml) with a flow-rate of 20 μl/min. Point A signifies the characteristic point where the species begins to elute. Conditions: mobile phase: 0.85 *M* ammonium sulfate, 20 m*M* HEPES, 20 m*M* MES, 20 m*M* acetic acid, pH 4.5, 4°C. Column: 2.78 × 0.29 cm I.D.; packing: 5 μm C-1 ether phase.

It should also be pointed out that, from a macroscopic point of view, the information obtained from a breakthrough curve is independent of the mass transfer kinetics of the adsorption process[9]. Indeed, Q was found to be independent of flow-rate over a five-fold range for a given protein solution concentration. Therefore, the values of Q obtained from these experiments are actual measurements of the amount of protein adsorbed on the stationary phase, when the plateau-total protein concentration is C (see Fig. 1), and one can consider that the system reaches a quasi-equilibrium state that can be modeled using a mass balance approach (see below).

It is interesting to note that the desorption step (not shown) is diffuse as well. This means that the desorption isotherm is Langmuirian in shape and that there is a hysteresis loop in the adsorption–desorption isotherm. Hysteresis is a well-known phenomenon in protein adsorption where, for example, it has been shown that conformational changes on an adsorbent surface can result in altered species which bind to the surface differently (usually stronger) than the species which initially is

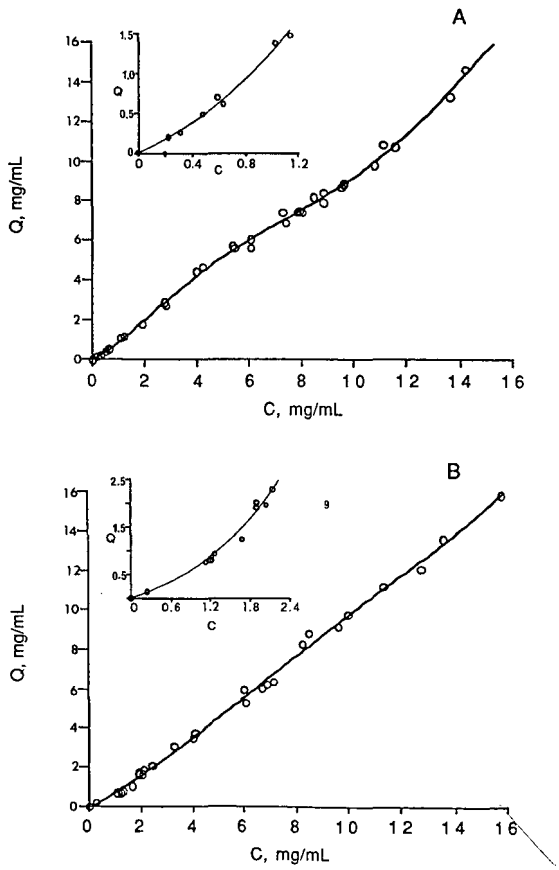

Fig. 2. (A) Adsorption isotherm of β-lact A at 0.85 M ammonium sulfate, other conditions as in Fig. 2. Inset: The low concentration region of the isotherm to emphasize the S-shape. Q = adsorbed amount of protein, C = solution concentration of protein. (B) Adsorption isotherm of β-lact A at 1.0 M ammonium sulfate, other conditions as in Fig. 1. Inset: The low concentration region of the isotherm to emphasize the S-shape.

adsorbed[24,25]. Another mechanism of hysteresis could be loss of reversible association–dissociation of aggregates on the adsorbent surface. A later paper will deal with the desorption loop and the mechanism of hysteresis for β-lact A; in this paper, we shall focus on the adsorption step. As noted, we shall model the adsorption step as a quasi-equilibrium process, as others have done when hysteresis is involved[24,25].

Fig. 2A and B present the adsorption isotherms obtained at 4.0°C, pH 4.5 at the two salt concentrations. These isotherms are S-shaped, *i.e.* proportionately greater adsorption as the sample solution concentration is increased. The S-shape is suggestive of positive cooperativity in which association occurs between molecules either by a side-by-side association on the surface[26], or by association in solution, in which one or more higher order oligomers formed at higher solution concentration adsorb more strongly than the protomer. It is to be noted that the isotherm shape in Fig. 2 is unusual in protein adsorption[27]; as already mentioned, Langmuirian shape is typically observed.

Cooperativity of biopolymers interacting with ligands has been studied using various mathematical models and plotting procedures[28–30]. The Scatchard plot is one of the most widely used approaches to obtain a macroscopic indication of the type of cooperativity in the binding reaction. This approach has also been employed in the study of adsorption of proteins on solid supports[31,32]. In order to apply this approach

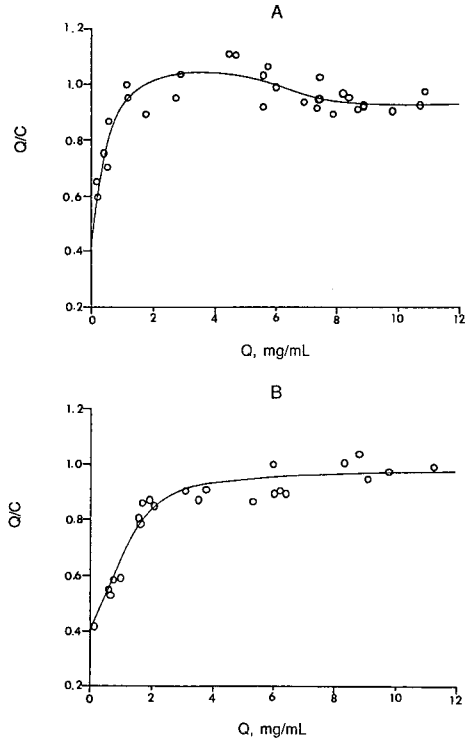

Fig. 3. (A) Scatchard plot of β-lact A derived from the data in Fig. 2A, 0.85 *M* $(NH_4)_2SO_4$. (B) Scatchard plot of β-lact A derived from data in Fig. 2B, 1.0 *M* $(NH_4)_2SO_4$.

to adsorption studies, the concentration of the ligand is maintained constant (*i.e.*, the adsorbing surface), while the concentration of protein is varied.

Fig. 3A and B present Scatchard plots derived from the isotherms in Fig. 2A and B, respectively. Q is the adsorbed amount of protein in mg/ml of adsorbent phase, and C is the plateau total protein solution concentration, in mg/ml. In agreement with the S-shaped isotherms, a positive initial slope, characteristic of positive cooperativity in the low protein concentration region[29], is observed in the two plots. Typical Scatchard plots obtained for systems of positive cooperativity generally present a well-pronounced maximum[33]. In Fig. 3A, a weakly-pronounced maximum is observed at approximately 5–6 mg/ml protein concentration, whereas no maximum can be discerned in Fig. 3B. A plateau is observed in the region beyond 6 mg/ml in both cases. One interpretation of such a plateau is the appearance at higher protein concentration of an associated species with a weaker binding affinity for the surface than the other species existing at low concentration[34]. Since a weighted average distribution coefficient is measured, changes in the relative amount of species with different affinities as a function of overall protein concentration will have an obvious effect on the measured extent of adsorption. It is interesting to note that in the previous HIC experiments[20], it was found that the highest order aggregate adsorbed the weakest.

Mass balance model

Based on the literature of β-lact A at pH 4.5 and 4°C[19] and the HIC results from our previous paper[20], it is reasonable to assume that the protein forms associates or aggregates in solution as a function of concentration. Accordingly, as previously[20], the behavior described in Fig. 3A and B has been analyzed using a mass balance model. We will focus on the low protein concentration region and assume the simplest case that two species predominate in this region of positive cooperativity of the Scatchard plot (below 5.0 mg/ml), with the higher order aggregate adsorbing more strongly than the protomer.

Consider a protomer A that can reversibly form in solution an associate, B, with n protomeric units:

$$n\mathrm{A} \rightleftharpoons \mathrm{B} \qquad [\mathrm{B}] = K_e\,[\mathrm{A}]^n \tag{1}$$

where $n > 1$ and K_e is the association constant in molar concentration units (M^{1-n}) for the reaction. The activity coefficients of the species cancel in the concentration ratio of K_e, based on the Adams-Fujita assumption[20,35].

Since a fraction of protomer A and associate B can bind to the available surface, S, each species with a variety of orientations, the adsorption process can be visualized as one of multiple steps. Each adsorption step can be defined by the number of binding sites used for each fraction of a protein species with a determined orientation. If q is identified as the mean number of binding sites of species A, and p as the mean number of adsorption sites of species B, adsorption can be represented for A as

$$\mathrm{A} + q\mathrm{S} \rightleftharpoons \mathrm{AS}_q \tag{2}$$

$$k_{q,\mathrm{A}} = [\mathrm{AS}_q]/[\mathrm{A}]\,[\mathrm{S}]^q \tag{3}$$

and for B as

$$B + pS \rightleftharpoons BS_p \tag{4}$$

$$k_{p,B} = [BS_p]/[B]\,[S]^p \tag{5}$$

where $p \leqslant nq$ and $k_{i,j}$ is the adsorption coefficient for species j, which binds the surface with a mean value of i binding sites. The value of p can be less than nq if some of the binding sites are used to form the associate.

The variables in the Scatchard plot (Q and C) can be obtained from eqns. 3 and 5. The total amount of protein on the surface, Q, in mg/ml of packing, can be defined as

$$Q = M_A([AS_q] + n[BS_p]) \tag{6}$$

or

$$Q = M_A([A][S]^q\, k_{q,A} + n[B][S]^p\, k_{p,B}) \tag{7}$$

where M_A is the molecular weight of the protomer. If we assume that the available surface, S, is much larger than the adsorbed amount of protein in the region of low protein concentration, then S can be considered to be a constant. Therefore, eqn. 7 can be simplified to

$$Q = M_A([A]\, k_A + n[B]\, k_B) \tag{8}$$

where $k_A = [S]^q\, k_{q,A}$ and $k_B = [S]^p\, k_{p,B}$. Combining eqns. 1 and 8, we obtain

$$Q = M_A(k_A\,[A] + nK_e k_B\,[A]^n) \tag{9}$$

and with the conservation of mass in the mobile phase and eqn. 1, we can write that

$$C = M_A([A] + nK_e\,[A]^n) \tag{10}$$

where C is the solution concentration of β-lact A in mg/ml. The ratio Q/C, used in the Scatchard plot, can then be written as

$$Q/C = (k_A + nK_e k_B\,[A]^{n-1})/(1 + nK_e\,[A]^{n-1}) \tag{11}$$

Eqn. 11 provides an explicit expression of an experimental quantity, Q/C, in terms of the protomer solution concentration in the mobile phase [A]. This latter parameter is not directly accessible but follows the general trend of C in the low concentration region. Since $[A] \rightarrow 0$ as $C \rightarrow 0$, from eqn. 11, the value of Q/C at zero concentration of protein reduces to k_A, the adsorption coefficient of A. The value of k_A can thus be obtained from the intercept of the Scatchard plot. The results from such an extrapolation were found to be: $k_A = 0.34 \pm 0.09$ and 0.43 ± 0.04, at 0.85 and 1.0 M ammonium sulfate, respectively. These adsorption coefficient values are reasonable given the relatively low antichaotropic salt concentration employed.

In order to obtain k_B and K_e, the initial slopes of the Scatchard plots (Q/C *vs.* Q) can be used along with the slopes of an alternative plotting procedure of Q/C *vs.* C. Defining $R = Q/C$, we have

$$dR/dQ = (dR/d[A])\,(d[A]/dQ) \tag{12}$$

and

$$dR/dC = (dR/d[A])\,(d[A]/dC) \tag{13}$$

Explicit relationships for each term in eqns. 12 and 13 can thus be derived by taking the derivatives of eqns. 9–11 with respect to [A]. These expressions evaluated in the limit when $C \rightarrow 0$ ($[A] \rightarrow 0$) yield values of the limiting slope in each plot:

$$\lim_{C\rightarrow 0}\,(dR/dQ) = 2K_e\,(k_B - k_A)/k_B \tag{14}$$

$$\lim_{C\rightarrow 0}\,(dR/dC) = 2K_e\,(k_B - k_A) \tag{15}$$

From eqns. 14 and 15, the ratio of the two limiting slopes directly yields the value of k_B. The results obtained for k_B were 1.2 ± 0.2 and 1.5 ± 0.3 at 0.85 M and 1.0 M salt concentration, respectively. These values are higher than the corresponding k_A values and reflect the increase in binding for the higher order aggregate relative to the protomer. It is noted from eqn. 14 that an initial positive slope in the Scatchard plot will always be observed if $k_B > k_A$, a condition that is fulfilled by this system. The value of K_e can be determined from k_A and k_B in eqns. 14 and 15 as: $K_e = (0.90 \pm 0.50) \cdot 10^4$ M^{1-n} and $(2.7 \pm 0.8) \cdot 10^4$ M^{1-n} at 0.85 M and 1.0 M salt concentration, respectively.

Based on these results, we next explored the numerical simulation of the data (*i.e.*, the isotherms in Fig. 3) in order to examine how well the model can predict experimental behavior. The adsorption isotherms can be reconstructed using eqns. 9 and 10, which relate experimental concentrations with the concentration of protomer [A]. Selecting the simplest case of $n = 2$ in eqn. 10, the resulting quadratic equation can be resolved for the solution concentration of (A)

$$[A] = [(1 + 8K_e^*C)^{1/2} - 1]/4K_e \tag{16}$$

where K_e^* is the apparent association constant in concentration units of mg/ml. Eqn. 16 can then be substituted into eqn. 9 to yield

$$Q = \{(k_B - k_A)\,[1 - (1 + 8K_e^*C)^{1/2}] + 4k_BK_e^*C\}/4K_e^* \tag{17}$$

Eqn. 17 provides an explicit expression for the adsorption isotherm. Fig. 4 displays the calculated isotherm at pH 4.5, 4°C and 1.0 M ammonium sulfate. There is reasonable agreement between the calculated and the experimental isotherms. Fig. 5 shows the corresponding calculated and experimental Scatchard plots, where the most significant features observed experimentally, *i.e.* the positive slope and the plateau at higher protein concentration are reproduced. At high Q values, the estimated Q/C values appear to be greater than the experimental values; however, a good fit appears in the

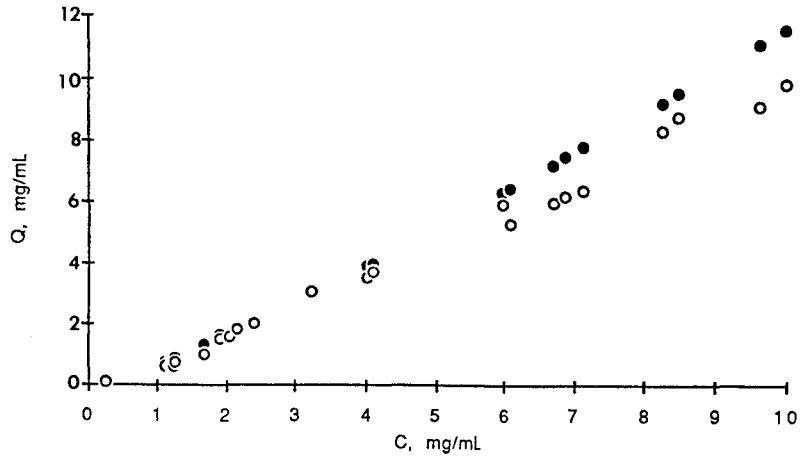

Fig. 4. Comparison of experimental (○) and calculated (●) isotherms of β-lact A. Calculation based on eqn. 17 using parameters $k_A = 0.80$, $k_B = 3.0$, and $K_c = 1.0 \cdot 10^4\ M^{-1}$ obtained from the model. Salt concentration, 1 M $(NH_4)_2SO_4$. Other conditions as in Fig. 1.

low to moderate Q range. The poorer fit at higher protein concentration may be related to the formation of a larger aggregate with weaker strength than the protomer. We briefly examined the adsorption isotherm assuming the formation of a third species ($n = 3$) with weaker binding than the protomer. If the third component is considered in the calculation of Q, as in eqn. 17, the numerical result is qualitatively similar to Figs. 5 and 6; however, a cubic equation results and the precision of the parameters unfortunately does not allow a good estimation of the fit of the experimental data. Nevertheless, the appearance of a third component could be the cause of the poorer fit at high Q values in Fig. 5 (as well as the plateau in Fig. 3).

Eqn. 17 can be further used to simulate the possible shape of isotherms in which the values of the adsorption coefficients and association constants are different from

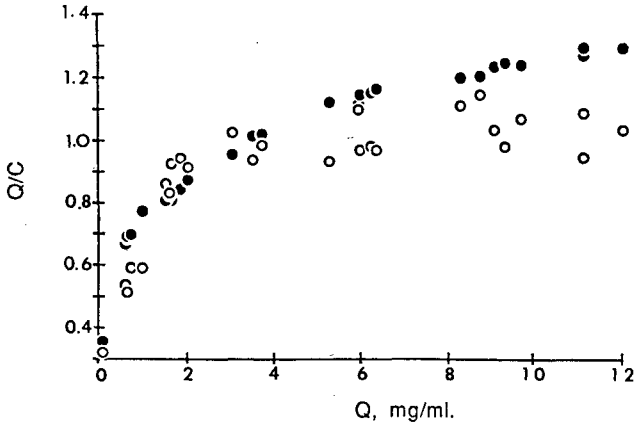

Fig. 5. Scatchard plots derived from the comparison of experimental (○) and calculated (●) isotherms of β-lact A in Fig. 4.

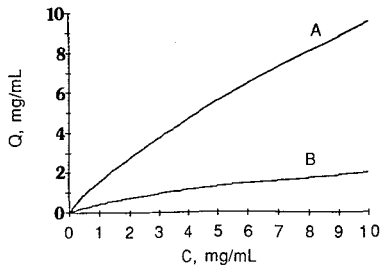

Fig. 6. Calculated isotherms from eqn. 17 for different set of values of adsorption coefficients and equilibrium constants. (A) Protomer (A) more retained than aggregated species (B): $k_A = 3k_B$, $K_e = 1 \cdot 10^4$ M^{-1}. (B) No retention of aggregated species: $k_A = 1.0$, $k_B = 0$, $K_e = 1 \cdot 10^4$ M^{-1}. The protomer and aggregated species are assumed to be in the stoichiometric ratio of 1:2, respectively.

those obtained in this system. For example, curve A in Fig. 6 corresponds to a case in which the association constant has the same value as that observed for β-lact A ($K_e^* = 0.75$ ml/mg, equivalent to $K_e = 1 \cdot 10^4$ M^{-1}) but the protomer A is more adsorbed than the associate B ($k_A = 3k_B$). This behavior corresponds to negative cooperativity, and, interestingly, the isotherm has a Langmuirian shape. Curve B represents the case of zero adsorption of the associate B ($k_B = 0$), calculated with the same association constant as curve A. A Langmuirian shape is also found. From Fig. 6, it can be concluded that associating systems can show adsorption isotherms that follow Langmuirian mathematical behavior in spite of the fact that the system may be far removed from the Langmuir adsorption model.

CONCLUSIONS

It has been demonstrated that a self-associating protein, β-lactoglobulin A, displays positive cooperativity upon adsorption under HIC conditions. This behavior is consistent with the presence in the mobile phase of several aggregated species with different adsorption coefficients. The formation of associates can produce an S-shaped isotherm as a result of the increase with total protein concentration of the relative amount of an associate with a larger adsorption coefficient than the protomer. The observed isotherm can be modeled as a mixed competitive one. This behavior is characteristic of positive cooperativity, where an increase in the analyte concentration results in a greater than linear increase in the amount of protein adsorbed. As already noted, the desorption step does not follow the S-shaped adsorption isotherm, creating a hysteresis loop. Desorption and hysteresis will be discussed in a separate paper.

A conclusion of this work is that protein–protein interaction and the formation of aggregates in preparative scale operation must be considered, even if the protein remains in solution over the whole concentration range of the isotherm. The use of LALLS[21] may prove beneficial in the elucidation of the actual factors causing non-linearity of a peptide-protein adsorption isotherm.

ACKNOWLEDGEMENTS

The authors gratefully acknowledge the support of this work from NIH under GM-15847 and from Merck, Sharp & Dohme Research Laboratories. R. Blanco

thanks CONICIT-UCR and Corte Suprema of Costa Rica for fellowship support. This is contribution number 376 from the Barnett Institute.

REFERENCES

1 J. M. Jacobson, J. H. Frenz and Cs. Horváth, *Ind. Eng. Chem. Res.*, 26 (1987) 43.
2 J. D. Andrade, in J. D. Andrade (Editor), *Surface and Interfacial Aspects of Biomedical Polymers*, Vol. 2, Plenum, New York, 1985, p. 1.
3 T. A. Horbett and J. L. Brash, in J. L. Brash and T. A. Horbett (Editors), *Proteins at Interfaces: Physicochemical Aspects and Biochemical Studies*, American Chemical Society, Washington, DC, 1987, p. 1.
4 W. Norde and J. Lyklema, *J. Colloid Interface Sci.*, 66 (1978) 257.
5 H. P. Jennissen, *J. Colloid Interface Sci.*, 111 (1986) 570.
6 M. E. Soderquist and A. G. Walton, *J. Colloid Interface Sci.*, 75 (1980) 386.
7 J. A. Jonsson and P. Lovkvist, *J. Chromatogr.*, 408 (1987) 473.
8 Y. A. Eltekov and Y. V. Kazakevitch, *J. Chromatogr.*, 395 (1987) 473.
9 H. L. Wang, J. L. Duda and C. J. Radke, *J. Colloid Interface Sci.*, 66 (1978) 153.
10 A. W. Liao, Z. El Rassi, D. M. LeMaster and Cs. Horváth, *Chromatographia*, 24 (1987) 881.
11 G. Guiochon and A. Katti, *Chromatographia*, 24 (1987) 165.
12 E. H. Slaats, W. Markowski, J. Fekete and H. Poppe, *J. Chromatogr.*, 207 (1981) 299.
13 G. Guiochon, S. Golshan-Shirazi and A. Jaulmes, *Anal. Chem.*, 60 (1988) 1856.
14 I. Lundstrom, *Prog. Colloid. Polym. Sci.*, 70 (1985) 76.
15 W. Norde, *Adv. Colloid Interface Sci.*, 25 (1986) 267.
16 J. D. Andrade and V. Hlady, *Adv. Polymer Sci.*, 79 (1986) 1.
17 J. H. Knox and H. M. Pyper, *J. Chromatogr.*, 363 (1986) 1.
18 F. L. deVos, D. M. Robertson and M. T. W. Hearn, *J. Chromatogr.*, 392 (1987) 17.
19 S. N. Timasheff and R. Townsend, *Protides Biol. Fluids*, 16 (1969) 33.
20 N. Grinberg, R. Blanco, D. M. Yarmush and B. L. Karger, *Anal. Chem.*, 61 (1989) 514.
21 H. H. Stuting, R. Blanco, N. Grinberg, I. S. Krull and B. L. Karger, submitted for publication.
22 N. T. Miller, B. Feibush and B. L. Karger, *J. Chromatogr.*, 316 (1984) 519.
23 J. R. Conder, *Adv. Anal Chem. Instrumentation*, Vol. 1(6), Interscience, New York, 1968, p. 209.
24 H. P. Jennissen and G. Botzet, *Int. J. Biol. Macromol.*, 1 (1979) 171.
25 H. P. Jennissen, in I. M. Chaiken, M. Wilchek and I. Parikh (Editors), *Proc. Fifth Int. Symp. Affinity Chromatography and Biological Recognition*, Academic Press, New York, 1983, p. 281.
26 C. H. Giles, D. Smith and A. Huitson, *J. Colloid Interface Sci.*, 47 (1974) 755.
27 J. D. Andrade, in J. D. Andrade (Editor), *Surface and Interfacial Aspects of Biomedical Polymers*, Vol. 2, Plenum, New York, 1985, p. 44.
28 I. M. Klotz, *Quart. Rev. Biophys.*, 18 (1985) 227.
29 F. W. Dahlquist, *Methods Enzymol.*, 48 (1978) 270.
30 K. E. Neet, *Methods Enzymol.*, 64 (1980) 139.
31 H. P. Jennisen, *Adv. Enzyme Regul.*, 19 (1981) 377.
32 J. D. Andrade, in J. D. Andrade (Editor), *Surface and Interfacial Aspects of Biomedical Polymers*, Vol. 2, Plenum, New York, 1985, p. 46.
33 K. Imai, *J. Biol. Chem.*, 249 (1974) 7607.
34 G. Schwarz and S. Stankowski, *J. Biophys. Chem.*, 10 (1979) 173.
35 E. T. Adams, Jr. and H. Fujita, in J. W. Williams (Editor), *Ultracentrifugal Analysis in Theory and Experiment*, Academic Press, New York, 1963, p. 119.

Journal of Chromatography, 482 (1989) 13–22
Elsevier Science Publishers B.V., Amsterdam — Printed in The Netherlands

CHROM. 21 824

CHARACTERIZATION OF NOVEL STEROIDAL ALKALOIDS FROM TUBERS OF *SOLANUM* SPECIES BY COMBINED GAS CHROMATOGRAPHY–MASS SPECTROMETRY

IMPLICATIONS FOR POTATO BREEDING

W. M. J. VAN GELDER*

Present address: Agrotechnological Research Institute ATO, P.O. Box 17, 6700 AA Wageningen (The Netherlands)

L. G. M. TH. TUINSTRA

State Institute for Quality Control of Agricultural Products, RIKILT, P.O. Box 230, 6700 AE Wageningen (The Netherlands)

J. VAN DER GREEF

TNO–CIVO Institutes, P.O. Box 360, 3700 AJ Zeist (The Netherlands)

and

J. J. C. SCHEFFER

Medicinal and Aromatic Plant Science, Agricultural University, P.O. Box 8010, 6700 ED Wageningen (The Netherlands)

(First received March 8th, 1989; revised manuscript received July 25th, 1989)

SUMMARY

Wild *Solanum* species are widely used in potato breeding as a source of valuable germplasm. Together with desired characteristics, toxic steroidal glycoalkaloids (SGAs), including unidentified SGAs, are sometimes transferred from the wild species to the cultivated potato. In this study, steroidal alkaloids (SAs) which originated from unidentified aglycones of SGAs found in tubers of *Solanum* species were characterized using retention indices, gas chromatography–mass spectrometry, high-resolution mass spectrometry (resolution 20 000) and hydrolysis in two-phase systems. All SAs possessed a solanidane skeleton and were probably substituted or dehydrogenated forms of solanidine. Most of these SAs have not been reported before.

Analysis of the SGAs of three wild *Solanum* species and one primitive cultivated subspecies used in potato breeding, showed that the total SGA contents varied widely (403–2228 mg kg^{-1} fresh tuber) as did the concentrations of the individual SGAs within a species. The implications of the results are discussed from the viewpoints of breeding for resistance against pathogens or insects and of food safety of household potatoes.

0021-9673/89/$03.50

INTRODUCTION

Steroidal alkaloids (SAs) are natural toxins of the Solanaceae. They occur in all parts of the plants and are in general glycosidically bound (steroidal glycoalkaloids; SGAs)[1]. Household potatoes contain the solanidine glycosides α-solanine and α-chaconine, usually in concentrations below 150 mg kg^{-1}, which are considered to present no health hazard to the consumer. The occurrence, the genetic and environmental control and the toxicology of the solanidine glycosides have been reviewed[2,3].

Wild *Solanum* species are being used in potato breeding to introduce desired traits, such as disease and pest resistance, into the cultivated potato. The tubers of some of these species contain extremely high concentrations of SGAs which may result in toxic levels in the hybrid progeny[4]. In addition to known SAs, some species contain unidentified compounds, which have been tentatively characterized as the aglycones of SGAs by their response ratios in nitrogen–phosphorus-specific and flame ionization detection (NPD–FID response ratios) after capillary gas chromatography (GC)[4,5].

This paper describes the characterization of these SAs using, amongst other techniques, gas chromatography–mass spectrometry (GC–MS) and high-resolution mass spectrometry (HRMS). A number of novel SAs were characterized. The SA compositions of tubers of three wild *Solanum* species and one primitive cultivated subspecies (ssp.), widely used in potato breeding, are presented. The implications of the results for potato breeding are discussed from the viewpoints of resistance breeding and food safety.

EXPERIMENTAL

Plant material

Tubers of *Solanum chacoense* accession number 8054, *S. leptophyes* 27208 and *S. tuberosum* ssp. *andigena* 1024 were produced by cultural techniques described elsewhere, as were the taxonomic nomenclature and the provenance of the accession numbers[4]. The analyses of *S. sparsipilum* were carried out on an extract prepared earlier from tubers of accession 8206 genotype number 7, which had been grown under different conditions[4].

Chemicals and sample preparation

SA standards, solvents, extraction of the tubers, two-phase hydrolysis, sample clean-up and capillary GC using retention indices and NPD–FID response ratios were as described previously[4–6].

GC–MS and HRMS

A Finnigan 4500 gas chromatograph–mass spectrometer coupled to an Incos data system was used to record the mass spectra of the SAs. The SAs were gas chromatographed using a fused-silica column (25 m × 0.22 mm I.D.) coated with CP-Sil 5 CB, film thickness 0.12 μm (Chrompack, Middelburg, The Netherlands). The temperature programme of the oven was 280°C (held for 20 min), increased at 8°C min^{-1} to 320°C (held for 5 min). The temperature of the injector was 300°C and that of the interface 290°C. Helium was used as carrier gas at a linear velocity of 30 cm s^{-1}.

The injection volume was 2 μl and the splitting ratio 1:50. The conditions of electron impact (EI) ionization were ion source temperature 230°C, emission current 0.25 mA and ion source energy 70 eV, and those of chemical ionization (CI) were ionization gas methane, ion source temperature 180°C, emission current 0.25 mA, ion source energy 100 eV and ionizer pressure 67 Pa. The mass range was monitored from 50 to 500 mass units in the EI mode and from 90 to 450 mass units in the CI mode. The scan rate was 1 scan per 0.5 s.

The peaks of the total ion current (TIC) profile obtained by GC–MS were compared with the peaks of the mass chromatograms recorded at *m/z* 150 and 204, which are specific for the solanidanes, and at *m/z* 114 and 138, which are specific for the spirosolanes[1]. For each tuber extract, the TIC profile and mass chromatograms were compared with the chromatogram of the N-containing compounds, obtained by capillary GC using simultaneous NPD and FID, in order to investigate whether other types of SAs were present. Coelution of components was checked by comparing the TIC profile and mass chromatograms recorded at *m/z* 150 and 204 with mass chromatograms recorded at specific *m/z* values.

HRMS was used for confirmation of the masses obtained by GC–MS, for determination of the exact masses of individual components and for calculation of their elemental compositions. A Finnigan-MAT 711 mass spectrometer coupled to a Tracor TN-1750 multichannel analyser was used. The EI conditions were ion source temperature 240°C, emission current 800 μA, ion source energy 100 eV and acceleration voltage 8 kV. The resolution was 20 000 (10% valley definition), the probe temperature was increased from 50 to 350°C in 500 s and the mass range was fixed. An amount of 1–5 μl of tuber extract was introduced into the mass spectrometer via a direct insertion probe. Only the tuber extracts of *S. chacoense* and *S. sparsipilum* were analysed by HRMS.

RESULTS AND DISCUSSION

Identification and characterization of SAs

The HRMS of the tuber extracts of *S. chacoense* and *S. sparsipilum* showed abundant ions with the exact masses 150.1283 and 204.1752, for which the formulae $C_{10}H_{16}N$ and $C_{14}H_{22}N$, respectively, were calculated. These formulae agree with those of the diagnostic fragments of *m/z* 150 and 204 of the solanidanes[1] (Fig. 1). Exact masses corresponding to the base peaks of other groups of SAs, such as spirosolanes, epiminocholestanes, aminospirostanes and solanocapsines, were not measured.

All the compounds in the tuber extracts of the four *Solanum* species/ssp. that were characterized as SAs by their NPD/FID response ratios showed main ions at *m/z* 150 (base peak) and 204 in the spectra obtained by GC–MS (EI mode). This means that they were all solanidanes with unsubstituted E and F rings[1,7]. Fig. 2 shows the TIC profile (D) and the mass chromatograms at the *m/z* values of the diagnostic ions of the solanidanes (B and C). Base peaks corresponding to other groups of SAs were not detected, as is illustrated for the spirosolanes (Fig. 1) by the mass chromatogram recorded at *m/z* 114 (Fig. 2A).

Substitutions in the steroid skeleton (rings A–D) do not markedly influence the fragmentation patterns[8]. However, a comparison of the EI mass spectra of nine reference compounds showed that differentiation between the saturated SAs (demis-

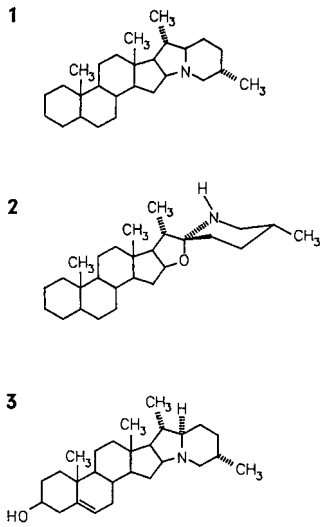

Fig. 1. Structures of the basic skeletons of the solanidanes (1) and spirosolanes (2), and structure of solanidine (solanid-5-en-3β-ol) (3).

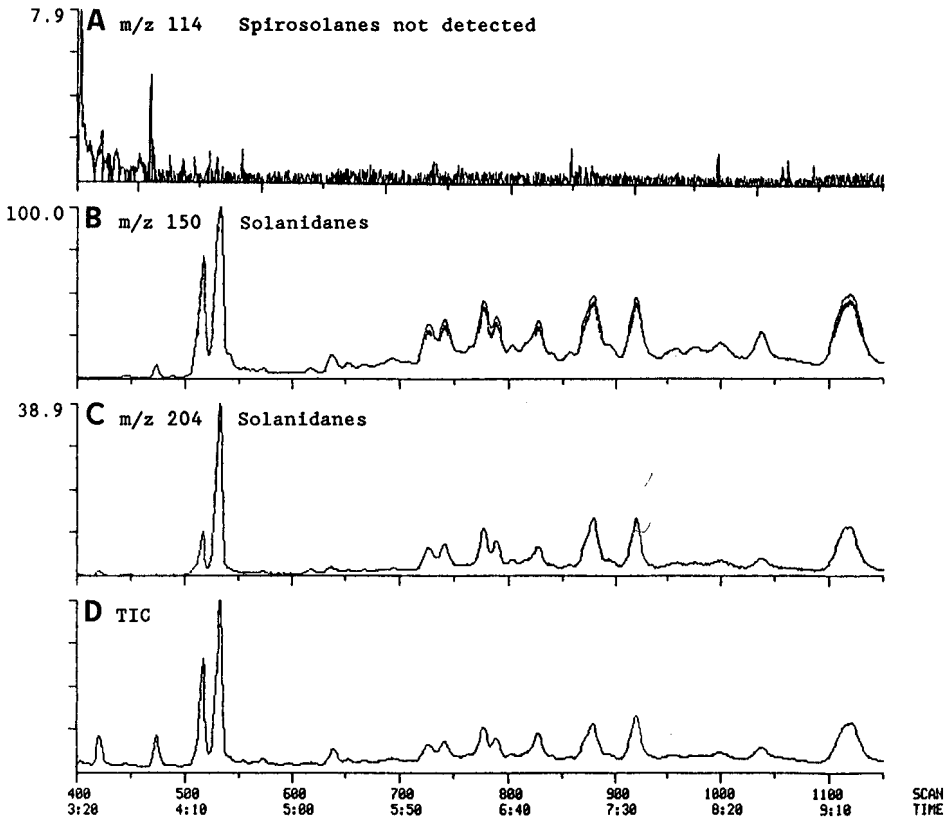

Fig. 2. Mass chromatograms recorded at the diagnostic *m/z* values of spirosolanes [(A) *m/z* 114, base peak] and solanidanes [(B) *m/z* 150, base peak; (C) *m/z* 204] and the total ion current (TIC) profile, obtained by GC–MS (EI mode) analysis of a steroidal alkaloid extract from *S. sparsipilum* tubers.

sidine, soladulcidine and tomatidine), the Δ^5-unsaturated SAs (solanidine, solasodine and tomatidenol) and their 3,5-diene dehydration products (solanthrene, solasodiene and tomatidadiene) was possible by using the ratios of the abudances of the ions at *m/z* 91 and 93, which were about 0.8 for the saturated SAs, 1.3 for the Δ^5-unsaturated compounds and 2.0 for the 3,5-dienes. The same ratios were found for the abundances at *m/z* 105 and 107 for the nine compounds tested.

GC–MS (CI mode) of the SAs showed $(M + 1)^+$ ions with a relative abundance of 30–100%. SAs containing a hydroxyl group showed in addition $(M + 1 - 18)^+$ ions with a relative abundance of 20–50%, due to the loss of water from the protonated molecules (Fig. 3).

On two-phase hydrolysis using chloroform as organic phase, the Δ^5-unsaturated SGAs produce 5-ene-3β-ol aglycones and the corresponding 3,5-diene dehydration products, but using carbon tetrachloride, they produce almost entirely 3,5-dienes[9]. This phenomenon (shift from the concentration of the 5-ene-3β-ol to the concentration of the 3,5-diene) was used for the detection of the enols and the dehydration products by capillary GC. The final identification of each 5-ene-3β-ol and 3,5-diene pair was achieved using the data from EI-mode GC–MS (ratios of the abundances at *m/z* 91:93 and *m/z* 105:107), from CI-mode GC–MS [presence of $(M + 1 - 18)^+$ ions] and from the HRMS (absence of oxygen atoms in the dehydration products and a difference of 18.0105 between the masses of the SAs and their dehydration products).

Table I shows the main physical and chemical data which enabled the SAs to be characterized. Only the naturally occurring SAs are given and not their dehydration products. Compound 1, a solanidadienol, may be dehydrosolanidine according to its retention time and that of its dehydration product $C_{27}H_{39}N$ (exact mass 377.3082), which may be dehydrosolanthrene. Compound 3 is a saturated SA, which contains two hydroxyl groups and is probably an isomer of compound 8. Compounds 4 and 5 are isomers of compound 1. Compound 7 with $M^{+\cdot}$ at *m/z* 427, showed the loss of one molecule of water on hydrolysis (difference in mass of 18.0105 with its dehydration product), an $(M + 1 - 18)^+$ peak in CI-mode GC–MS and an $(M - 31)^+$ peak in the EI mode. Therefore, compound 7 may be methoxysolanidine or hydroxymethyl-solanidine. The data from HRMS revealed the presence of an SA showing the mass 427.3450, which corresponds with the formula $C_{28}H_{45}NO_2$; this supported the above hypothesis. A second compound with $M^{+\cdot}$ at *m/z* 427 was detected by GC–MS, namely compound 6, the mass spectrum of which differed from that of compound 7. HRMS also revealed the presence of a compound with a mass of 427.3086, and consequently it was assumed that this mass corresponded to compound 6, for which the formula $C_{27}H_{41}NO_3$ was calculated. Although the compound contained three oxygen atoms, it lost only one molecule of water on hydrolysis (mass difference 18.0105); it is therefore assumed to be a solanidenol containing no second enol group but more likely keto and/or hydroxy groups. Compound 10 may be methylsolanidine as it produced a dehydration product $C_{28}H_{43}N$ (mass 393.3395), which is probably a methylsolanidadiene (methylsolanthrene). One solanidane-type SA with a molecular mass of 423 was detected by EI-mode GC–MS. This compound (11) could either be $C_{27}H_{37}NO_3$ or $C_{28}H_{41}NO_2$, because exact masses corresponding to both formulae were detected by HRMS. Low intensities of the molecular ions of mass 411.3137 ($C_{27}H_{41}NO_2$) and 425.2930 ($C_{27}H_{39}NO_3$) were also measured by HRMS, but corresponding peaks were not detected by GC–MS; these masses probably correspond to trace compounds.

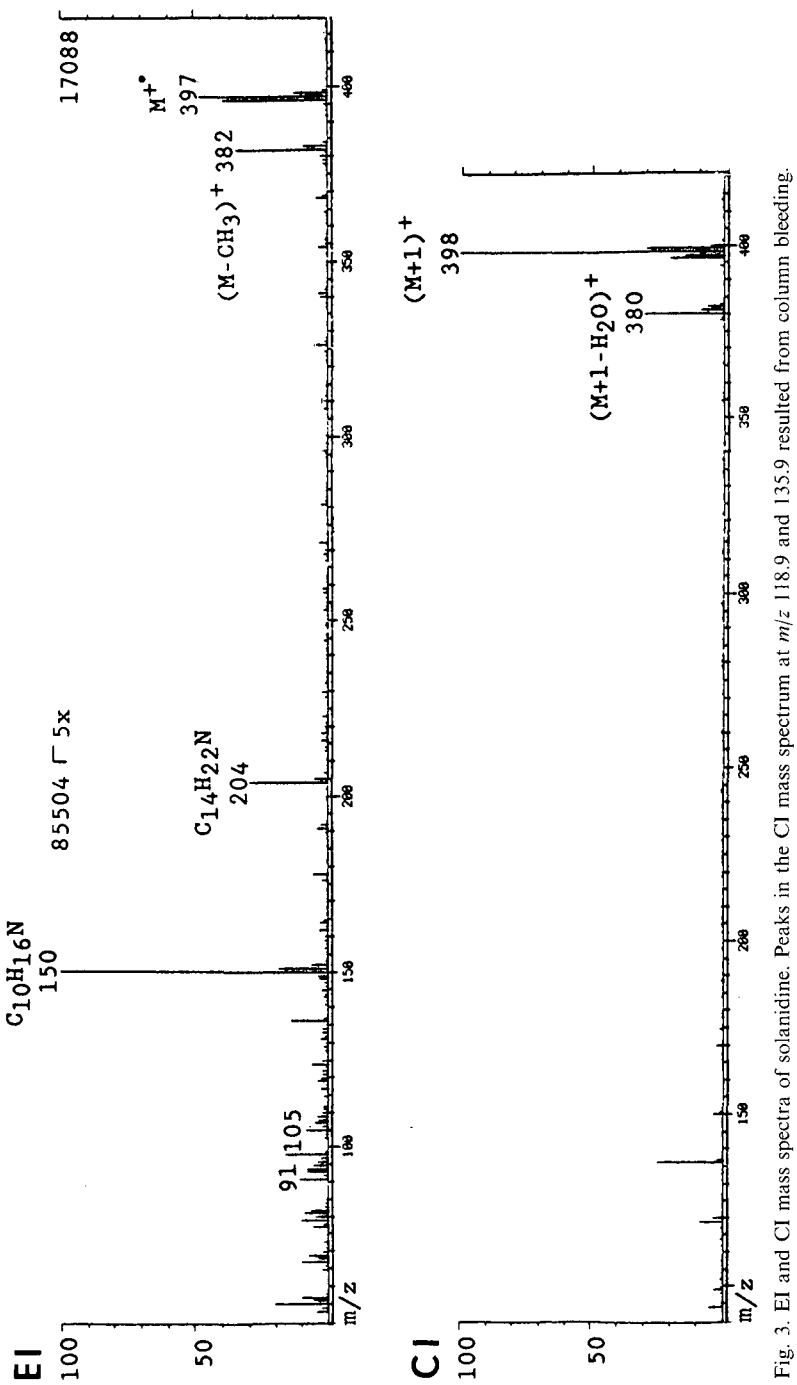

Fig. 3. EI and CI mass spectra of solanidine. Peaks in the CI mass spectrum at *m/z* 118.9 and 135.9 resulted from column bleeding.

TABLE I

STEROIDAL ALKALOIDS (SAs) FROM TUBERS OF *SOLANUM* SPECIES USED IN POTATO BREEDING, CHARACTERIZED BY RETENTION INDICES (*I*), HRMS, GC–MS AND TWO-PHASE HYDROLYSIS

No.	*SA*[a]	$I_{270}^{CP\text{-}Sil\,5\,CB}$	*HRMS*		*GC–MS diagnostic ions (% abundance)*	*Loss of H_2O*	
			Exact mass	*Formula*		*CI*[b]	*Hydrolysis*[c]
1	Solanidadienol	3040	395.3188	$C_{27}H_{41}NO$	150(100), 204(14), 380(2), 395(5)	1	1
2	Solanidine[d]	3130	397.3345	$C_{27}H_{43}NO$	150(100), 204(20), 382(4), 397(5)	1	1
3	Solanidanediol	3143	415.3450	$C_{27}H_{45}NO_2$	150(100), 204(22), 400(2), 415(3)	2	0
4	Solanidadienol	3169	395.3188	$C_{27}H_{41}NO$	150(100), 204(23), 380(5), 395(9)	1	1
5	Solanidadienol	3176	395.3188	$C_{27}H_{41}NO$	150(100), 204(22), 380(6), 395(7)	1	1
6	Substituted solanidenol	3195	427.3086	$C_{27}H_{41}NO_3$	150(100), 204(18), 380(2), 395(2), 396(2), 412(2), 427(3)	nr[e]	1
7	Hydroxymethyl- or methoxysolanidenol	3236	427.3450	$C_{28}H_{45}NO_2$	150(100), 204(28), 380(3), 395(7), 396(4), 412(1), 427(2)	1	1
8	Solanidanediol	3293	415.3450	$C_{27}H_{45}NO_2$	150(100), 204(22), 400(2), 415(5)	2	0
9	Substituted solanidenol	3319	425.3303	$C_{28}H_{43}NO_2$	150(100), 204(14), 410(5), 425(4)	nr	1
10	Methylsolanidenol	3353	411.3501	$C_{28}H_{45}NO$	150(100), 204(20), 396(16), 411(14)	nr	1
			423.2772	$C_{27}H_{37}NO_3$	150(100), 204(19), 394(2), 408(4), 409(4), 423(1)	nr	0
11	Substituted solanidanol	3357	423.3136	$C_{28}H_{41}NO_2$			

[a] Nomenclature according to ref. 1.
[b] $(M + 1 - 18)^+$ resulting from chemical ionization.
[c] Formation of dehydration product on hydrolysis; corresponds to a mass difference of 18.0105.
[d] Solanid-5-en-3β-ol.
[e] nr = CI mass spectrum not recorded.

TABLE II

CONTENTS OF STEROIDAL ALKALOIDS (SAs) OF TUBERS OF *SOLANUM* SPECIES

Steroidal alkaloids expressed as glycosides on a trisaccharide basis in mg kg^{-1} fresh tuber. All SAs possessed a solanidane skeleton.

No.	*SA (glycosidically bound)*	*Solanum chacoense*	*Solanum leptophyes*	*Solanum sparsipilum*	*Solanum tuberosum* ssp. *andigena*
1	$C_{27}H_{41}NO$	30	61	200	19
2	Solanidine	2121	199	255	450
3	$C_{27}H_{45}NO_2$	40	12	35	14
4	$C_{27}H_{41}NO$		30	125	
5	$C_{27}H_{41}NO$			100	
6	$C_{27}H_{41}NO_3$			25	
7	$C_{28}H_{45}NO_2$	5	18	100	12
8	$C_{27}H_{45}NO_2$	15			
9	$C_{28}H_{43}NO_2$		5	40	
10	$C_{28}H_{45}NO$	17	78	200	31
11	$C_{27}H_{37}NO_3$ or $C_{28}H_{41}NO_2$			75	
	Unidentified	tr[a]	tr	140	tr
	Total glycoalkaloids	2228	403	1300	526

[a] tr = Traces.

Implications for potato breeding

A large number of naturally occurring steroidal sapogenins, a well studied class of compounds closely related to the SAs, have been described in a recent review[10]. Among these were methyl-, di- and trihydroxy- and mono- and diketosapogenins, in addition to ene and diene forms. Also, although to a lesser extent, a variety of SAs have been described; up to 1981, more than 80 aglycones had been reported for the genus *Solanum* only[1]. Novel SAs and SGAs are regularly being detected in *Solanum* species, mostly in aerial plant parts[11–13], as a result of studies on pharmacologically interesting compounds. Only few studies on the SA composition of tubers have been carried out, and only occasionally have novel SAs or SGAs been found since 1981[4,14]. So far, six SAs of the solanidane group have been described for *Solanum* species, of which only two, solanidine and demissidine, have been detected in tubers[6].

Table II shows that a variety of minor SAs occurred in the tubers of the *Solanum* species/ssp. used in this study. The detection of these SAs was achieved by the application of capillary GC using simultaneous FID and NPD[5]. In addition to solanidine, at least four of these SAs may be regarded as common minor compounds, as they occurred in species which belong to different series of the genus *Solanum*, namely the series *Commersoniana* (*S. chacoense*) and *Tuberosa*.

The nature of the novel SAs of the *Solanum* species/ssp. studied could be revealed, as was described above. They all belonged to the solanidane group and were probably substituted, dehydrogenated or substituted saturated forms of solanidine (Fig. 1), in which, for instance, a hydrogen has been replaced with a hydroxyl or methyl group. However, their origin remains unclear. In the *S. sparsipilum* sample studied, elevated levels of novel SAs were present. This may have been (partly) the result of the different growing conditions of these tubers[4], as it has been shown that environmental

conditions may affect the biosynthesis of SAs in *Solanum* species in many ways[15]. In *Veratrum* species, solanidine accumulated, or was converted to jervine and veratramine, depending on the illumination[16]. Solanidine, solasodine and tomatidenol, common end-products in the SA biogenesis in *Solanum* species, seemed to be precursors in the biogenesis of camtschatcanidine, hapepunine, anrakorinine and 27-hydroxyspirosolane, which are SAs of *Fritillaria* species[7]. Hence the SAs found in the wild and primitive potato tubers studied might be intermediates in SA metabolism and/or stress metabolites.

Studies on the relationship between (glycosidic-bound) SAs and resistance against pathogens and insects have been reviewed[17,18]. Differences in biological activity between SAs are associated with the structural differences of these SAs, and the sugar moieties may also influence the biological activities. Therefore, in resistance studies, the SGAs or their aglycones should be quantified individually. Preferably, the composition of their sugar moieties should also be determined. Consequently, when the solanidane glycosides that we detected are present in plant samples, they may not be disregarded as being a result of imperfections in the analytical techniques used.

For a complete structure elucidation, the SAs and their glycosides need to be isolated and costly and time-consuming studies by MS, infrared and nuclear magnetic resonance spectroscopy must be carried out. Once the entire structure of the individual compounds is known, information on their toxicity will still be lacking. It is therefore more efficient to investigate whether these compounds either occur normally or are induced by environmental (stress) conditions during cultivation and storage of the tubers. If these compounds do not occur in the current potato cultivars considered safe for consumption, their introduction into future household cultivars should be prevented.

ACKNOWLEDGEMENTS

Thanks are due to Ing. P. G. M. Kienhuis and Mr. L. Gramberg for carrying out the MS analyses.

REFERENCES

1 H. Ripperger and K. Schreiber, in R. G. A. Rodrigo (Editor), *The Alkaloids*, Vol. XIX, Academic Press, New York, 1981, p. 81.
2 S. J. Jadhav, R. P. Sharma and D. K. Salunkhe, *CRC Crit. Rev. Toxicol.*, 9 (1981) 21.
3 S. L. Sinden, L. L. Sanford and R. E. Webb, *Am. Potato J.*, 61 (1984) 141.
4 W. M. J. van Gelder, J. H. Vinke and J. J. C. Scheffer, *Euphytica*, 39S (1988) 147.
5 W. M. J. van Gelder, H. H. Jonker, H. J. Huizing and J. J. C. Scheffer, *J. Chromatogr.*, 442 (1988) 133.
6 W. M. J. van Gelder, in R. F. Keeler and A. T. Tu (Editors), *Handbook of Natural Toxins*, Vol. VI, Marcel Dekker, New York, 1990, in press.
7 K. Kaneko, M. Tanaka, U. Nakaoka, Y. Tanaka, N. Yoshida and H. Mitsuhashi, *Phytochemistry*, 20 (1981) 327.
8 H. Budzikiewics, *Tetrahedron*, 20 (1964) 2267.
9 W. M. J. van Gelder, *J. Sci. Food Agric.*, 35 (1984) 487.
10 A. V. Patel, G. Blunden, T. A. Crabb, Y. Sauvaire and Y. C. Baccou, *Fitoterapia*, 58 (1987) 67.
11 A. K. Chakravarty and S. C. Pakrashi, *Tetrahedron Lett.*, 28 (1987) 4753.
12 C.-N. Lin, M.-I. Chung and S.-Y. Lin, *Phytochemistry*, 26 (1987) 305.
13 A. K. Chakravarty and S. C. Pakrashi, *Phytochemistry*, 27 (1988) 956.
14 S. F. Osman, T. A. Johns and K. R. Price, *Phytochemistry*, 25 (1986) 967.

15 J. Kuc, *Am. Potato J.*, 61 (1984) 123.
16 K. Kaneko, N. Kawamura, T. Kuribayashi, M. Tanaka, H. Mitsuhashi and H. Koyama, *Tetrahedron Lett.*, (1978) 4801.
17 W. M. Tingey, *Am. Potato J.*, 61 (1984) 157.
18 J. G. Roddick, in G. Fuller and W. D. Nes (Editors), *Lipid Interactions Among Plants and Their Pests and Pathogens* (*ACS Symposium Series*, No. 325), American Chemical Society, Washington, DC, 1987, p. 286.

Journal of Chromatography, 482 (1989) 23–34
Elsevier Science Publishers B.V., Amsterdam — Printed in The Netherlands

CHROM. 21 820

ISOLATION OF OFF-FLAVOUR COMPOUNDS IN WATER BY CHROMATOGRAPHIC SNIFFING AND PREPARATIVE GAS CHROMATOGRAPHY

BO LUNDGREN*, HANS BORÉN, ANDERS GRIMVALL and ROGER SÄVENHED
Department of Water and Environmental Studies, Linköping University, S-581 83 Linköping (Sweden)
(Received May 18th, 1989)

SUMMARY

A procedure for the isolation and identification of off-flavour compounds in water was developed. Odorous volatile compounds were enriched by stripping and dichloromethane extraction. The extracts obtained were analysed by chromatographic sniffing and preparative gas chromatography, followed by sensory evaluation of different fractions dissolved in odourless water. The chromatographic sniffing technique was found to be sensitive enough to detect known odorous compounds in concentrations far below their threshold odour concentrations in water. However, in order to quantify the contribution of specific compounds to the off-flavour of the water, preparative gas chromatography and sensory evaluation of dissolved extracts were indispensable. One of the case studies performed showed that the origin of off-flavours in water can be very complex, with contributions from several so far unidentified compounds.

INTRODUCTION

Taste and odour problems in drinking water are primarily caused by naturally produced, volatile organic compounds. So far, research in this field has focused on a relatively small number of compounds. In particular, the occurrence of geosmin and 2-methylisoborneol (MIB) in water has been investigated in detail[1–6]. There is no doubt that these two compounds may cause serious off-flavour problems. However, several results indicate that the origin of objectionable tastes and odours in water involves a much larger group of compounds, many of them so far unidentified. By combining an efficient enrichment method for organics in water with chromatographic sniffing [high-resolution gas chromatography (GC) with sensory detection], one can easily detect 10–30 different odorous compounds in a surface water sample[7–11]. Results obtained by the so-called flavour profile analysis method give further evidence of the complexity of off-flavours in water. Trained panelists have been reported to perceive several different flavours in a single water sample[12].

The complex composition of off-flavours in water calls for a systematic method of establishing cause–effect relationships. A first step in this direction was taken by Lundgren *et al.*[11], who suggested a procedure based on enrichment of odorous organic

0021-9673/89/$03.50

compounds followed by fractionation by preparative GC. The contribution to the off-flavour of the water from different fractions of organic compounds was assessed by redissolving these fractions in odourless water and characterizing the resulting flavour of the water. In this study, this procedure was further developed and tested. Furthermore, the relevance of the chromatographic sniffing technique was evaluated by comparing the odour intensities of the redissolved extracts with those of chromatographic sniffing.

EXPERIMENTAL

Water samples

Water samples from two rivers used as raw water sources for drinking water production were analysed in detail: a moderately eutrophic river, only slightly affected by industrial pollution (Stångå River, Linköping, Sweden), and a eutrophic river affected by discharges from a pulp mill and several municipal sewage treatment plants (Motala River, Norrköping, Sweden). Sampling of the Stångå River was conducted in September 1988 and of the Motala River water in December 1988.

Concentration methods

Volatile organics in samples from the Stångå River and the Motala River were enriched by stripping. In addition, organics in samples from the Motala River were enriched by dichloromethane extraction.

Stripping was performed in an open system as described by Borén and co-workers[13,14]. The sample volume was 1 l, the stripping temperature 60°C and the stripping time 2 h. The carbon filter was extracted with distilled dichloromethane using an on-column syringe. The final volume of the extract was approximately 10 μl, thus giving a concentration factor of $1 \cdot 10^5$.

Enrichment of organics in water by dichloromethane extraction was performed as described by Wigilius *et al.*[15]. The sample volume was 7.5 l and the final volume of the concentrated extract was 75 μl, thus giving a concentration factor of $1 \cdot 10^5$.

Sensory evaluation of extracts redissolved in water

Sensory evaluation of extracts obtained by dichloromethane extraction or stripping was performed by dissolving the extracts in odourless water and characterizing the flavour created. More precisely, 2 μl of the extract were rapidly injected into 200 ml of MilliQ (Millipore) water in a graduated flask. The small droplets thus produced were left to dissolve slowly in the water without stirring. After 1 h the water sample was transferred to an erlenmeyer flask, covered with a watch-glass and heated at 60°C in a water-bath for approximately 15 min. The threshold odour number (TON) of the water with the dissolved extract was determined with triangle tests at 60°C[16]. Odour quality was characterized using the descriptors suggested by Mallevialle and Suffet[12].

Two trained panellists took part in all sensory evaluations of dissolved extracts. The main results were confirmed by a group of four panellists. Odour usually being the most important component of the flavour, the concepts of odour and flavour were used interchangeably.

Losses during dissolution and heating of extracts in water

Losses during dissolution and heating of extracts in water were evaluated with a mixture of fourteen organic compounds with different functional groups and boiling points from 174 to 274°C (see Table I). Aliquots of this mixture (2 μl of dichloromethane containing 5 ng/μl of each compound) were added to 200 ml of Milli-Q water in five different flasks. After dissolution and heating at 60°C in a water-bath for 30 min, the five water samples were combined and analysed by stripping analysis. In a parallel experiment, 10 μl of the test mixture were added directly to the stripping bottle.

GC parameters

The following conditions were used: gas chromatograph, Hewlett-Packard 5880; fused-silica column, DB-1 (0.25 μm), 60 m × 0.32 mm I.D. (J&W); carrier gas, helium at 40 cm/s; temperature programme, 40°C for 5 min, increased at 5°C/min to 230°C, held for 5 min; flame ionization detection (FID).

All extracts were analysed using on-column injection. Surface water extracts were also analysed using splitless injection with the split valve closed for 180 s.

The C_6, C_8, C_{10} and C_{12} 1-chloroalkanes were used as standards, and retention indices (I) were calculated according to

$$I = \frac{t_{R(\text{substance})} - t_{R(Z)}}{t_{R(Z+1)} - t_{R(Z)}} + Z$$

where $t_{R(Z)}$ and $t_{R(Z+1)}$ are retention times for the standards that bracket the substance of interest and $Z = 1$, 2 or 3.

Chromatographic sniffing

The GC capillary column was led through copper tubing to a sniffing funnel outside the chromatograph[9]. A trained observer recorded the retention time and assessed the perceived odour intensity and odour quality of each odorous compound in the column effluent. Assessments of odour intensity were made according to a 6-grade scale, with 1 = weak and 6 = strong.

The sensitivity of the chromatographic sniffing technique was evaluated by two different TON analyses of dichloromethane extracts of known odorous compounds. One of the TON values, TON_{water}, is the ordinary TON value at 60°C of a water sample obtained by dissolving 2 μl of the extract in 200 ml of odourless water (see below). The other, $TON_{GCsniff}$, denotes the largest dilution of the extract giving a detectable odour in chromatographic sniffing (on-column injection, 2 μl). For each of the compounds in Fig. 3, the concentration was adjusted to give a TON_{water} value of 8. The extracts thus obtained were then analysed by chromatographic sniffing at different dilutions with distilled dichloromethane. Perceived odour intensities in chromatographic sniffing were recorded and the $TON_{GCsniff}$ was determined.

When analysing extracts of surface water samples, the concentration factor was $2 \cdot 10^4$. The GC parameters were as above.

Preparative GC

Fractions of the GC effluent were cold-trapped in PTFE tubing (Habia Teknofluor; 20 cm × 1.2 mm I.D.). The device connecting the GC column to the PTFE tubing is shown in Fig. 1. From this device the PTFE tubing was led through the GC oven wall and, thereafter, through a small container of liquid nitrogen. This arrangement guaranteed that the entire GC column had the same temperature, thus eliminating retardation or cold-trapping at the end of the column. Further, this trapping device permitted the fast exchange of PTFE tubing during a chromatographic run.

In order to increase the trapping efficiency, the PTFE tubing was pre-treated with distilled dichloromethane. Several droplets of the solvent (total volume 3 μl) were applied inside the tubing. When the desired fraction had been collected, the tubing was extracted with dichloromethane, giving a final extract volume of 10 μl. The GC parameters were as above.

Instrumental evaluation of GC fractionation

The GC fractionation technique was evaluated instrumentally with the previously mentioned fourteen component mixture (see Tables 1 and 2). A 3-μl volume of this mixture (5 ng/μl of each compound in dichloromethane) was injected on-column. Suitable fractions of the GC effluent were collected as described above, and the recovery was determined by GC with FID. 1-Chloroundecane (50 ng/μl in dichloromethane) was used as an internal standard. The GC parameters were as above.

GC fractionation of extracts of water samples

In order to isolate the fractions giving the largest contribution to the off-flavour of the water, the original extract was split into fractions step by step. Each fraction was dissolved in odourless water, and the fractions creating the highest TON values were further split into smaller fractions. The results of the chromatographic sniffing were used as a guide for the selection of suitable retention time intervals in the fractionation procedure.

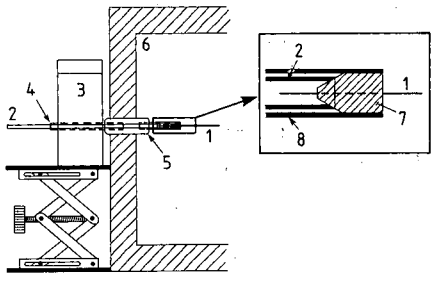

Fig. 1. Device for cold trapping of different fractions of the GC effluent. 1 = GC column; 2 = PTFE tubing for fraction collection; 3 = liquid nitrogen container; 4 = metal tubing through the liquid nitrogen container; 5 = connecting PTFE block; 6 = GC oven; 7 = PTFE plug; 8 = PTFE tubing.

RESULTS

Losses during dissolution and heating of extracts in water

In the standard procedure for dissolving extracts in water, the extract was left to dissolve in cold water for 1 h and then heated for about 15 min at 60°C in a water-bath before sensory evaluation was begun. Losses of different compounds in the fourteen-component mixture after 30 min at 60°C in a water-bath are shown in Table I. For compounds with permanent dipoles, losses from water were normally negligible. Substances with a long hydrocarbon chain, such as methyldecanoate, were exceptions. As expected, the largest losses were obtained for non-polar, volatile compounds. Sensory evaluations of extracts containing such compounds should therefore be performed as quickly as possible.

The loss of dichloromethane during dissolution and heating was determined by dibutyl ether extraction and GC analysis with FID. The results obtained showed that the dichloromethane concentration decreased only slowly at 60°C. After 30 min about 50% of the solvent remained, and after 60 min about 35% remained. The extract-to-water ratio ($1:10^5$) in the standard procedure for dissolving extracts in water was close to the highest ratio permitting sensory evaluation of the extracts without interference from the smell of the solvent.

Instrumental evaluation of the GC fractionation technique

When the solvent elutes from the column, it condenses in the cold trap, thus creating a solvent film on the inside wall of the PTFE tubing. This solvent film, which could also be created by pre-treating the PTFE tubing with small droplets of dichloromethane, proved to have a crucial effect on the recovery of many compounds. The results in Table II show that pretreated tubing gave a recovery of at least 80% for

TABLE I

RELATIVE LOSSES FROM WATER DURING DISSOLUTION AND HEATING (60°C, 30 min) OF 2 μl OF A DICHLOROMETHANE EXTRACT (5 ng/μl OF EACH COMPOUND) IN 200 ml OF WATER

Compound	*b.p. (°C)*	*Relative loss (%)*
n-Decane	174	90
Acetophenone	202	0
1-Chlorooctane	180	75
1-Octanol	194	0
Benzyl acetate	215	0
Naphthalene	218	25
2,6-Dichloroanisole	220	8
3-Phenyl-1-propanol	236	[a]
1,2,3,5-Tetrachlorobenzene	246	43
Methyl decanoate	224	58
2,3,6-Trichloroanisole	240	0
Diphenyl ether	258	0
2-Methoxynaphthalene	274	0
Ethyl cinnamate	272	[a]

[a] Not possible to analyse by stripping analysis.

TABLE II

RECOVERIES OF MODEL COMPOUNDS (5 ng/μl) OF EACH COMPOUND IN DICHLOROMETHANE) AFTER ON-COLUMN INJECTION (3 μl), COLD-TRAPPING IN PTFE TUBING PRETREATED WITH 3 μl OF DICHLOROMETHANE AND EXTRACTION OF THE TUBING WITH 7 μl OF DICHLOROMETHANE

Mean values and standard deviations (n = 5).

Compound	*Recovery (%)*	
	Mean	*Standard deviation*
n-Decane	81	3
Acetophenone	81	5
1-Chlorooctane	83	6
1-Octanol	82	6
Benzyl acetate	82	4
Naphthalene	81	4
2,6-Dichloroanisole	83	4
3-Phenyl-1-propanol	82	5
1,2,3,5-Tetrachlorobenzene	68	8
Methyl decanoate	74	5
2,3,6-Trichloroanisole	74	6
Diphenyl ether	75	5
2-Methoxynaphthalene	69	7
Ethyl cinnamate	73	7

the most volatile compounds in the test mixture. Without pretreatment the recovery of these compounds was less than 50%. The small decrease in the recovery of very high-boiling compounds in Table II may also be related to the solvent film. High-boiling compounds are probably adsorbed on the walls of the PTFE tubing before they reach the solvent film, and may therefore be more difficult to extract.

The average recovery of the fourteen model compounds in Table II was 78%. Additional experiments showed that losses were primarily caused by incomplete recovery of solvent from the PTFE tubing. When this factor was eliminated by calculating recoveries with respect to an internal standard added directly to the solvent in the PTFE tubing, the average recovery for the model compounds increased to 96%.

The feasibility of collecting very small fractions is illustrated by the chromatograms in Fig. 2. The recovery of the selected compound was 66%, and there were no traces of surrounding compounds. The retention time distances to preceding and subsequent peaks were 28 and 29 s, respectively.

Sensitivity of chromatographic sniffing

The results in Fig. 3 demonstrate the high sensitivity of the chromatographic sniffing technique. Let TOC_{water} denote the threshold odour concentration of a certain compound in water (as determined by triangle tests at 60°C) and assume that this compound is concentrated by a factor of 10^5 by the enrichment method used. The lowest concentration in water that can be detected by chromatographic sniffing, $TOC_{GCsniff}$, is then

$$TOC_{GCsniff} = TOC_{water} \cdot TON_{water}/TON_{GCsniff}$$

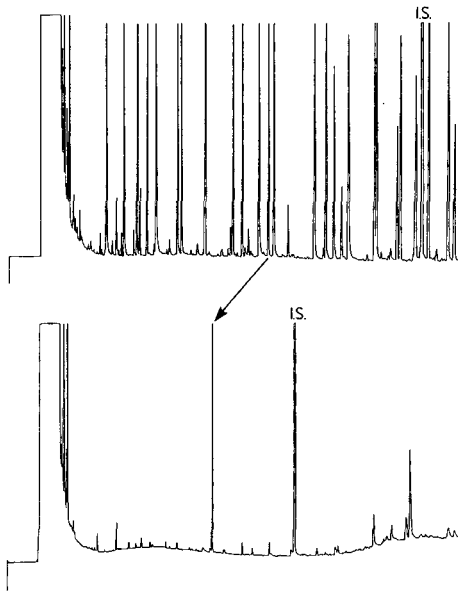

Fig. 2. Cold trapping of one selected compound (1-chlorooctane) in a mixture of organic compounds (5 ng/μl in dichloromethane). On-column injection. PTFE tubing pretreated with 3 μl of dichloromethane. Internal standard added to the extract, 1-chloroundecane.

For all compounds tested, this concentration was at least ten times lower than the TOC_{water}. For compounds such as MIB and 2,4,6-trichloroanisole it was more than 300 times lower.

Artefacts in GC fractionation

Two different injection techniques were used in the GC fractionation. For one of the surface water extracts (obtained by dichloromethane extraction of water from the

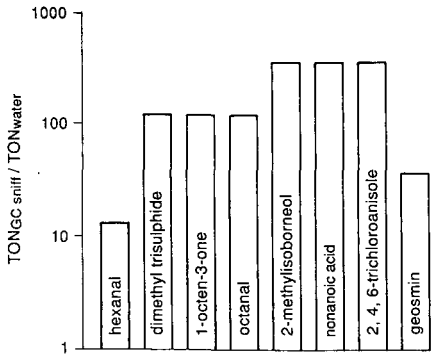

Fig. 3. Ratios of $TON_{GCsniff}$ and TON_{water} for dichloromethane extracts of known odorous compounds. $TON_{GCsniff}$ determined by on-column injection of 2 μl of the extract; TON_{water} determined at 60°C after dissolving 2 μl of the extract in 200 ml odourless water.

Motala River), the choice of injection technique had a marked effect on the sensory properties of the collected GC effluent. When dissolved in water, the effluent from splitless injection created a pungent smell. Using on-column injection, however, the original odour of the river water was recreated. Chromatographic sniffing and GC fractionation confirmed these results. During then first 10 min of the GC run, chromatographic sniffing gave several detections that were much stronger for splitless injection than for on-column injection. Sensory evaluation of GC fractions dissolved in water gave similar results. This strongly indicated that new odorous compounds were formed in the splitless injector, which had a temperature of 250°C.

Case study I: Stångå River

The water from the Stångå River had a TON value of 64. A strong earthy/musty odour indicated, even prior to the GC fractionation, that MIB or geosmin might be present in the water.

When the stripping extract was dissolved in odourless water, the original earthy/musty odour of the river water was recreated with a TON value of 32. This indicated that the compounds making the largest contribution to the off-flavour of the Stångå River water could be enriched by stripping. Further, these compounds were apparently gas chromatographable. A 3-μl volume of the stripping extract was injected, and the whole GC effluent (retention time interval 0–35 min) was collected. When redissolved in water, the extract with this effluent created a flavour of the same intensity and quality as the original stripping extract.

Prior to GC fractionation, the stripping extract was analysed by chromatographic sniffing. At a concentration factor of $2 \cdot 10^4$, twelve odorous compounds, including MIB and geosmin, were detected. The sniffing chromatogram is shown in Fig. 4.

In an attempt to confirm that MIB and geosmin were the two most important off-flavour compounds in the stripping extract, the GC effluent was split into three fractions: a small fraction with MIB, a small fraction with geosmin and a large fraction

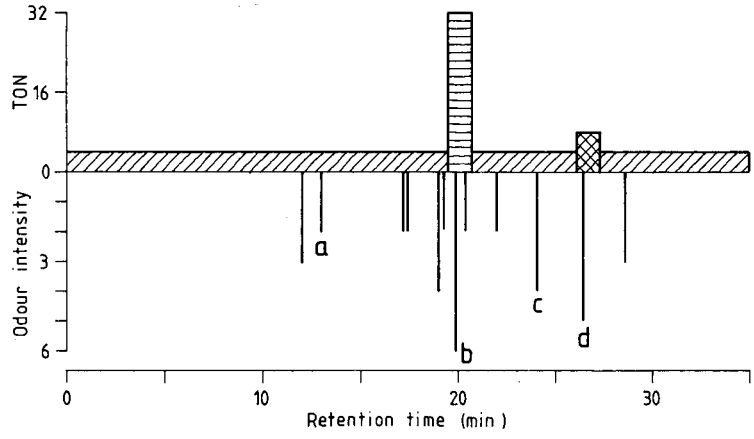

Fig. 4. GC fractionation of a stripping extract of a surface water sample from the Stångå River. TON values of different fractions, dissolved in odourless water, and sniffing chromatogram. a, 1-Octen-3-one; b, 2-methylisoborneol; c, 2,4,6-trichloroanisole; d, geosmin (see text).

covering the remaining parts of the chromatogram (Fig. 4). When dissolved in water, the MIB fraction created the same odour quality and TON value (32) as the original stripping extract. The geosmin fraction gave a TON value of only 8. The third fraction gave nine detections in chromatographic sniffing. However, when dissolved in water, this fraction gave a TON value of only 4. It was concluded that MIB was the most important off-flavour compound in the water from the Stångå River.

Case study II: Motala River

The water from the Motala River had a TON value of 32. The odour quality was described as being more marshy/swampy than earthy/musty.

The off-flavour compounds in the Motala River water were not satisfactorily enriched by stripping. When dissolved in odourless water, the stripping extract of this water created just a faint flavour (TON = 4). Dichloromethane extraction proved to be a more efficient concentration method. The extract obtained by this method was able to recreate a flavour that was difficult to distinguish from that of the original water sample. Provided that on-column injection was used (see above), this odour could also be recreated by the GC effluent of the dichloromethane extract. Actually, the TON value (32) of the water with the dissolved GC effluent was the same as that for the original river water sample. When analysing the dichloromethane extract by chromatographic sniffing, more than twenty detections were made (Fig. 6). The stepwise GC fractionation of this extract and the TON value of each fraction, dissolved in water, are shown in Fig. 5.

Fig. 5 A shows that the first half of the chromatogram (0–21.70 min), including MIB, made only a small contribution (TON = 8) to the odour intensity of the whole

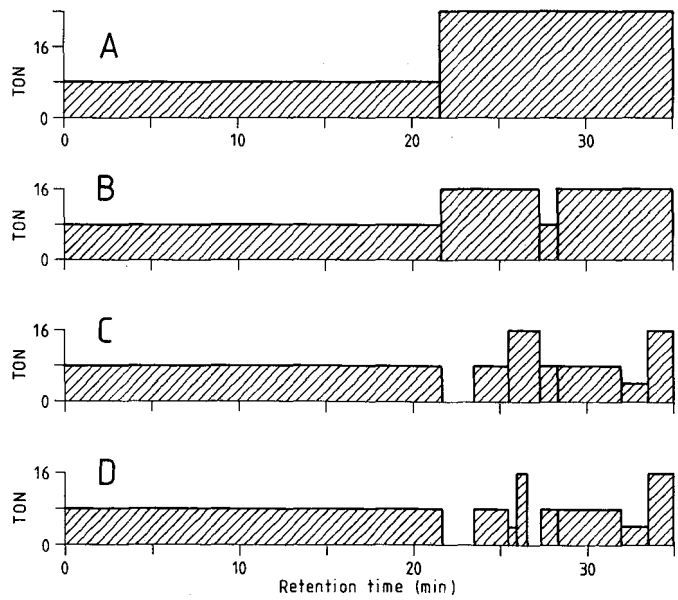

Fig. 5. Stepwise GC fractionation of a surface water sample from the Motala River. Enrichment by dichloromethane extraction. TON values of different fractions dissolved in odourless water.

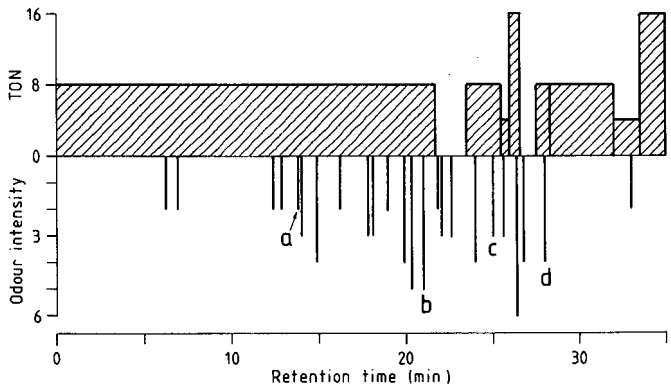

Fig. 6. TON values of different fractions obtained by GC fractionation and sniffing chromatogram. Enrichment by dichloromethane extraction. Water sample from the Motala River. a, 1-Octen-3-one; b, 2-methylisoborneol; c, 2,4,6-trichloroanisole; d, geosmin.

GC effluent. The most important off-flavour compounds were obviously present in the second half of the chromatogram (21.70–35.00 min), which gave a TON value of 16–32. Fractionation of the second half of the chromatogram (Fig. 5B) showed that geosmin, which had a retention time of approximately 28 min, was surrounded by important off-flavour compounds. However, the geosmin fraction alone created a weak flavour (TON = 8), indicating that neither geosmin nor MIB belonged to the more prominent off-flavours in the Motala River water.

On splitting the fraction from 21.70 to 27.25 min into three subfractions, two entirely different flavours were revealed. The last subfraction (25.50–27.25 min) had a musty flavour with TON = 16, while the middle fraction (23.75–25.50 min) had a fragrant flavour with TON = 8 (Fig. 5C). On splitting the fraction from 28.30 to 35.00 min in a similar way, another three flavours, with TON values of 8, 4 and 16, were revealed. The first was described as fragrant and the other two as earthy/musty.

The first fraction with TON = 16 (Fig. 5C) was further split into three subfractions (Fig. 5D). Sensory evaluation of these subfractions, dissolved in odourless water, strongly indicated that the retention time interval 26.00–26.60 min (retention index 3.40–3.51) contained one of the compounds contributing the most to the off-flavour of the Motala River water.

The agreement between the TON values of different fractions and the results of the chromatographic sniffing was partially good and partially less satisfactory (Fig. 6). One of the two fractions having the highest TON value (16) contained the compound having the highest odour intensity in chromatographic sniffing. However, in the other fraction, giving a TON value of 16, chromatographic sniffing gave no detections at all. Further, it is worth noting that, for some fractions that gave no flavour when dissolved in water, column sniffing resulted in several detections.

To summarize, the fractionation performed showed that the Motala River water contained at least six different compounds that were able to give the water a TON value of 8 or higher. Two fractions, each having a TON value of 16, were pointed out as particularly important for the flavour of the water. The compounds causing these off-flavours were present in concentrations too low to permit identification by GC–mass spectrometry.

DISCUSSION

The use of chromatographic sniffing and sensory evaluation of GC fractions dissolved in odourless water has several aspects worth discussing, including technical measures to guarantee optimum performance, relevance of chromatographic sniffing data and application areas of the methods proposed.

Stripping enrichment has been used successfully in several studies of off-flavours in water[2,5,9]. Recently, Lundgren *et al.*[11] observed that certain off-flavours were more efficiently enriched by other concentration methods, *e.g.*, dichloromethane extraction. GC fractionation of extracts of the Motala River water confirmed this observation. However, it also showed that the extracts obtained by solvent extraction were not ideal for GC fractionation. When on-column injection was used, the life of the GC column was markedly shortened by the high-molecular-weight substances in the extract. When splitless injection was used, odorous compounds formed in the injector interfered with the sensory analysis of odorous compounds in the water. Therefore, as long as the flavour of the water sample can be recreated by dissolving the stripping extract in odourless water, stripping is the enrichment technique to be preferred.

Preparative GC has previously been used in several areas[17–19]. This work emphasized the development of a simple device, giving high recoveries of compounds over a fairly wide range of boiling points. Cold trapping in PTFE tubing produced very satisfactory results, provided that the tubing was pretreated with a few droplets of dichloromethane. The last step in the proposed procedure, dissolution of GC fractions in odourless water, worked properly, provided that the extracts were given sufficient time to dissolve in cold water.

Sävenhed *et al.*[9] have previously shown that, for some well known odorous compounds, chromatographic sniffing gives a lower detection limit than FID. This study demonstrated both the strength and the weakness of the chromatographic sniffing technique. The odorous model compounds in Fig. 3 could all be detected by this technique at concentrations far below their threshold odour concentrations in water. However, these results also showed that TON values, as determined by chromatographic sniffing, are of limited value in predicting the contribution of specific compounds to the off-flavour of a water sample. This was further demonstrated by the Motala River case study.

It seems reasonable to assume that, for less volatile compounds, chromatographic sniffing (in combination with an efficient enrichment method) implies higher exposure than direct sensory evaluation of the water. This would explain why compounds such as MIB and 2,4,6-trichloroanisole gave a higher $TON_{GCsniff}$-to-TON_{water} ratio than more volatile compounds such as hexanal. However, there were also indications of high-boiling compounds being trapped in the sniffing device. The sensitivity to geosmin in chromatographic sniffing was surprisingly low, and the last GC fractions from the Motala River extract made a considerable contribution to the flavour of the water, even though these fractions gave few or no detections in chromatographic sniffing.

In summary, this study has shown that chromatographic sniffing is very useful for listing a number of potentially important off-flavour compounds. It can also provide guidance in the selection of suitable retention-time intervals in GC fractionation. However, the relevance of perceived odour intensities in chromatographic

sniffing is difficult to judge, unless this technique is complemented by GC fractionation and sensory evaluation of different fractions dissolved in water.

Studies of the origin of off-flavours in water may have two objectives: to connect the off-flavour to certain activities, processes or organisms, and to identify the substances causing the off-flavour. In both instances, the combined use of chromatographic sniffing and sensory evaluation of GC fractions redissolved in odourless water is a powerful technique. The chromatogram of a surface water sample, analysed by stripping enrichment, high-resolution GC and FID, is normally very complex. The list of candidates of off-flavour substances thus produced may exceed 100 compounds. Still, it is uncertain whether this list will include the compounds making the largest contribution to the off-flavour of the water[9]. Chromatographic sniffing may reduce the list of candidates to 10–30 compounds and increase the probability that the important compounds are included. However, in order to quantify the contribution of specific compounds to the off-flavour of the water, preparative GC and sensory analysis of extracts dissolved in odourless water are indispensable.

ACKNOWLEDGEMENTS

The authors are indebted to Lisbeth Samuelsson for drawing the figures and to Bo Thunér for technical assistance.

REFERENCES

1 G. J. Piet, B. C. J. Zoeteman and A. J. A. Kraayeveld, *Water Treat. Exam.*, 21 (1972) 281.
2 M. J. McGuire, S. W. Krasner, C. J. Hwang and G. Izaguirre, *J. Am. Water Works Assoc.*, 73 (1981) 530.
3 N. Gerber, *Water Sci. Technol.*, 15(6/7) (1983) 115.
4 P.-E. Persson, *Water Sci. Technol.*, 15(6/7) (1983) 1.
5 H. Naes, *Doctoral Thesis*, University of Oslo, 1987.
6 M. Yagi, *Water Sci. Technol.*, 20(8/9) (1988) 133.
7 A. Veijanen, M. Lahtiperä, R. Paukku, H. Kääriäinen and J. Paasivirta, *Water Sci. Technol.*, 15(6/7) (1983) 161.
8 A. Veijanen, J. Paasivirta and M. Lahtiperä, *Water Sci. Technol.*, 20(8/9) (1988) 43.
9 R. Sävenhed, H. Borén and A. Grimvall, *J. Chromatogr.*, 328 (1985) 219.
10 R. Sävenhed, *Doctoral Thesis*, Linköping University, 1986.
11 B. V. Lundgren, H. Borén, A. Grimvall, R. Sävenhed and B. Wigilius, *Water Sci. Technol.*, 20(8/9) (1988) 81.
12 J. Mallevialle and I. H. Suffet, *Identification and Treatment of Tastes and Odors in Drinking Water*, American Water Works Association, Denver, CO, 1987.
13 H. Borén, A. Grimvall and R. Sävenhed, *J. Chromatogr.*, 252 (1982) 139.
14 H. Borén, A. Grimvall, J. Palmborg, R. Sävenhed and B. Wigilius, *J. Chromatogr.*, 348 (1985) 67.
15 B. Wigilius, H. Borén, G. E. Carlberg, A. Grimvall, B. V. Lundgren and R. Sävenhed, *J. Chromatogr.*, 391 (1987) 169.
16 *Annual Book of ASTM Standards, Part 31, Water*, ASTM, Philadelphia, PA, 1980, p. 206.
17 P. Sandra, T. Saeed, G. Redant, M. Godefroot, M. Verstappe and M. Verzele, *J. High Resolut. Chromatogr. Chromatogr. Commun.*, 3 (1980) 107.
18 A.-B. Wassgren and G. Bergström, *J. Chem. Ecol.*, 10 (1984) 1543.
19 J. Roeraade, S. Blomberg and H. D. J. Pietersma, *J. Chromatogr.*, 356 (1986) 271.

Journal of Chromatography, 482 (1989) 35–51
Elsevier Science Publishers B.V., Amsterdam — Printed in The Netherlands

CHROM. 21 856

USE OF A FRAGMENT OF BOVINE SERUM ALBUMIN AS A CHIRAL STATIONARY PHASE IN LIQUID CHROMATOGRAPHY

PER ERLANDSSON*
Department of Technical Analytical Chemistry, Chemical Center, University of Lund, P.O. Box 124, S-221 00 Lund (Sweden)
and
STAFFAN NILSSON[a]
Department of Medical Chemistry 4, University of Lund, P.O. Box 94, S-221 00 Lund (Sweden)
(First received May 18th, 1989; revised manuscript received August 4th, 1989)

SUMMARY

Bovine serum albumin (BSA) was cleaved into fragments by proteolytic degradation. A fragment consisting of the N-terminal half of BSA was isolated and immobilized on a silica column. Compared with BSA-based columns, this column showed a retained stereoselective resolving capability for the enantiomers of oxazepam, benzoin and morpholep, whereas the enantiomers of, *e.g.*, tryptophan and warfarin were not resolved.

INTRODUCTION

A large number of chiral selectors have been used for the direct resolution of enantiomers. Owing to their generality and often high enantioselectivity, a number of protein-based phases have been utilized as chiral selectors in liquid chromatography for the direct resolution of enantiomers[1,2]. A large number of basic drugs have, for instance, been resolved on columns containing α_1-acid glycoprotein (α_1-AGP, orosmucoid)[3]. Bovine serum albumin (BSA) has been studied by Stewart and Doherty[4] and later by Allenmark *et al.*[5] as chiral selector. Allenmark and co-workers managed to immobilize BSA covalently on silica[6], and also to immobilize BSA by cross-linking it on silica[7]. These materials have been used successfully as chiral stationary phases to resolve a variety of compounds. Human serum albumin has been adopted as a chiral additive in the mobile phase by Sébille and Thuaud[8] and by Pettersson *et al.*[9]. Both α_1-AGP- and BSA-based columns are commercially available (α_1-AGP-based columns, EnantioPac from Pharmacia, Uppsala, Sweden, and Chiral-AGP from ChromTech, Stockholm, Sweden; BSA-based column; Resolvosil from Macherey, Nagel & Co., Düren, F.R.G.). Some other proteins, *e.g.*, immunoglobulin G (IgG)[10], ovomucoid[11] and α-chymotrypsin[12], have also been used as chiral selectors in liquid

[a] Present address: Euro-fassel AB, University Site, Ole Römers väg 12, S-223 70 Lund, Sweden.

0021-9673/89/$03.50

chromatography. However, columns based on α_1-AGP and BSA dominate the reported applications. Major drawbacks of proteins as chiral selectors in liquid chromatographic systems are low efficiency, which causes low sensitivity in analytical applications, and low loadability, making these phases less useful in preparative work[13]. The main reason for the low loadability seems to be that for each analyte there is only one or a few stereoselective sites on the large protein molecule, leading to a low concentration of stereoselective sites in the column. Owing to the physical size of some proteins, supports with large pores, *e.g.*, 300 Å silica, are necessary. Such silicas have a lower specific surface area, *ca.* 100 m^2/g for a 300 Å pore size compared with a 300 m^2/g for the "standard" pore size of 100 Å. This limits the amount of chiral selector that can be immobilized per unit amount of silica and consequently also the loadability. A low efficiency may be due to the time needed for conformational changes of the protein in the binding and releasing steps. A smaller mass of the protein would require a shorter time to make the necessary conformational motions. It is also difficult to predict chiral recognition on these phases because the mechanism of interaction is not known on a molecular level.

To the best of our knowledge, only intact protein molecules have been used as chiral selectors in liquid chromatography. However, different immobilization techniques affect the properties of the stationary phase[14], and consequently also the condition of the protein. Different pathways are accessible for modifying the proteins and hopefully for improving their chromatographic performance, such as (a) chemical modifications, *e.g.*, altering the side-chains of the amino acids residues to change charge distribution, hydrophilicy and bulkiness, etc., (b) using biosynthetic analogues, which involves a change in the primary amino acid sequence, *e.g.*, by substituting, inserting or deleting amino acids; this may be done by changing the DNA sequence by genetic engineering or by using the species-dependent variance in the amino acid sequence; (c) selecting specified parts of the protein by chemical or enzymatic cleavage to eliminate parts which do not contribute to chiral recognition; or (d) by peptide synthesis. If sufficiently small proteolytic peptides can be obtained which still show stereoselectivity, synthetic analogues could be produced. Another possibility for producing stereoselective proteins is to carry out "*in vivo* printing", which results in polyclonal or monoclonal antibodies directed towards the chiral substrate[10,15].

The primary aim of this project was to study the mechanism of the chiral selectivity of serum albumins and locate stereospecific binding sites on the protein. This was studied by cleavage of albumin into smaller peptide fragments followed by isolation, characterization and use of these fragments as chiral selectors. Also, owing to the decreased size of the chiral selector, the number of selectors immobilized in a column would be increased, leading to a higher loadability. If albumin fragments that consist of one domain (see Fig. 1) or part of a domain show retained stereoselectivity, these are hopefully sufficiently rigid to allow the determination of the three-dimensional structure by X-ray crystallography. This would provide the possibility of performing molecular modelling of the stereoselective docking of the chiral substrate to serum albumin by computer graphics.

BSA was chosen because it had been used as a chiral selector in liquid chromatography, is easily immobilized on silica, inexpensive, readily available and robust and its amino acid sequence is known. The amino acid sequence of BSA has been

reported by Brown[16]. The BSA molecule is estimated to be 141 Å long and 41 Å in diameter, formed like a cigar (see Fig. 1). It consists of a single peptide chain with 581 amino acids stabilized by 17 disulphide bridges and the molecular weight is approximately 66 500. The molecule is organized in three domains which are very flexible with respect to each other but more rigid internally. Owing to the high flexibility of serum albumin, no unambiguous three-dimensional structure from X-ray crystallography has yet been obtained. The isolation of different fragments from serum albumins and their binding to various ligands has also been reported, and a review of serum albumin has been published by Peters[17].

The purpose of this paper is to show that it is possible to cleave BSA into smaller fragments with retained stereoselectivity and that these fragments may be used as chiral stationary phases in liquid chromatography. Some of these results have been reported previously[18].

EXPERIMENTAL

Materials

Bovine serum albumin (BSA) (A-7030), pepsin porcine (P-6887), *rac*-benzoin, N-benzoyl-DL-alanine, N-benzoyl-D-alanine, N-benzoyl-L-alanine, L-cystine and octanoic acid were obtained from Sigma (St. Louis, MO, U.S.A.), D-tryptophan from United States Biochemical (Cleveland, OH, U.S.A.) and DL-tryptophan and L-tryptophan from Merck (Darmstadt, F.R.G.). *rac*-Warfarin was a gift from Ferrosan (Malmö, Sweden), *rac*-oxazepam from Kabi Vitrum (Stockholm, Sweden) and DL-kynurenine sulphate, L-kynurenine sulphate, *rac*-morpholep, 2,4-dinitrophenyl-DL-glycine and *rac*-mandelic acid from Shalini Andersson (University of Linköping, Sweden).

Proteolytic degradation of BSA

The proteolysis was carried out according by the guidelines given in ref. 19, and was optimized to give a reasonable yield of one large peptide under the condition that no or only a very small amount of BSA remained, as estimated from sodium dodecyl sulphate–polyacrylamide gel electrophoresis (SDS-PAGE) and size-exclusion chromatography.

In procedure I, 3.0 g of BSA was dissolved in 100 ml of buffer A (0.10 *M* Tris–HCl, pH 7.96). L-Cystine (70 mg) was first dissolved in 1.5 ml of 1 *M* NaOH and

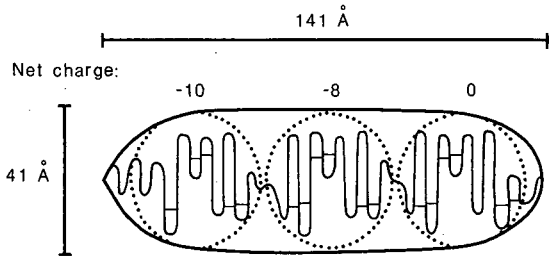

Fig. 1. Model of the serum albumin molecule, based on physical properties. The amino terminus is at the left. The net charges shown above the three domains are for bovine albumin at pH 7. Reprinted from T. Peters, Jr., *Adv. Protein Chem.*, 37 (1985) 161–245, with permission.

then immediately diluted to 140 ml with buffer A. The disulphide bonds of BSA were reduced by mixing the BSA and the cystine solutions and the reaction solution was allowed to stand for 17 h in room temperature (25°C). A 2-ml volume of the BSA–cystine solution was concentrated to approximately 200 μl in a Centricon 30 microconcentrator (Amicon, Danvers, MA, U.S.A.), and the concentrated BSA solution was then diluted with 1.6 ml of buffer B (0.1 *M* ammonium formate in HCl–3.2 m*M* octanoic acid, pH 3.7) and 50 μl of 1 *M* HCl to saturate hydrophobic sites and adjust the pH. A 100-μl volume of 0.5 mg/ml pepsin in buffer B was added and the solution was treated in a ultrasonic bath for 1 min. The reaction vessel was then immersed in a thermostatic water-bath (37°C) with occasional gentle swirling for 30 min. The proteolysis was stopped by adding 300 μl of 2 *M* Tris and 4 ml of water.

Procedure II was identical with procedure I, but all volumes were increased 100-fold and the concentration of the pepsin solution was reduced to 0.2 mg/ml.

Chromatography

Potassium phosphate buffer and ammonium carbonate buffer mobile phases were prepared in Millli-Q grade water obtained by purifying demineralized water in a Milli-Q filtration system (Millipore, Bedford, MA, U.S.A.). In some instances, 1-propanol, analytical-reagent grade (Merck, Darmstadt, F.R.G.) was used as an organic modifier. All mobile phases were degassed and filtered through a 0.45-μm HV Millipore filter prior to use. Unless stated otherwise, the following chromatographic set-up was used; a Philips PU4003 solvent delivery system (Pye Unicam, Cambridge, U.K.) equipped with a Philips PU4025 UV detector with a 1-μl flow-cell. The detector was connected to a Philips PM8252 strip-chart recorder. Samples were injected with a Rheodyne (Cotati, CA, U.S.A.). Model 7520 valve injector equipped with a 0.5-μl internal loop. Larger volumes were injected with a Rheodyne Model 7125 valve injector equipped with external loops of various sizes (10 μl–30 ml). Eluates from the columns were collected by a Gilson (Villiers-le-Bel, France) Model 201 or 203 fraction collector.

The volumes of unretarded solutes used for calculating the capacity factor (k') and separation factor (α) were determined by injection of sodium nitrite or water or by observing the first baseline disturbance. The resolution (R_s) was calculated according to: $R_s = 2(t_{R2} - t_{R1})/(w_1 + w_2)$, where t_R = retention time and w = peak width at baseline[20].

Isolation of peptide

Procedure I. The albumin fragment mixture was first concentrated and desalted on Centricon 30 microconcentrators and then subjected to an anion-exchange separation using a Mono-Q HR 5/5 anion-exchange column (Pharmacia, Uppsala, Sweden). A conductivity meter, Type CDM 2d (Radiometer, Copenhagen, Denmark), was employed to monitor the salt gradient. The conductivity cell, consisting of two platinum capillaries separated by a short plastic tube, was connected to the outlet of the UV detector. The experimental conditions are given in Fig. 4. The fractions of interest were concentrated on a Centricon 30 microconcentrator and further purified by size-exclusion chromatography using a Superose 12 HR 10/30 column (Pharmacia) and the conditions given in Fig. 5.

Procedure II. Procedure I was modified to increase the volumes handled. The

concentration steps were carried out using a 200-ml Amicon stirred ultrafiltration cell with Millipore PLGC (10 000 nominal molecular weight limit) regenerated-cellulose low-binding membranes (Millipore) operated at 0.17 MPa (25 p.s.i.). A larger anion exchange column, Mono-Q HR 10/10, and a larger size-exclusion column (Sephadex) were used for the ion-exchange and size-exclusion steps, respectively. Before use, Sephadex G-75 Superfine gel (Pharmacia) was swollen in 0.05 *M* ammonium hydrogencarbonate solution (pH 7.8) to a thick slurry and then packed into a 100 cm × 5 cm I.D. column according to ref. 21. A Gilson Minipuls 2 peristaltic pump (Gilson) with 0.090-in. I.D. pump tube (Elkay Laboratory Products, Basingstoke, U.K.), an LDC Spectromonitor III UV detector using the reference cell (to reduce the pressure drop across the detector cell) and a Servogor SE 120 strip-chart recorder was used in the chromatographic set-up for the size-exclusion step. The conditions are given in Fig. 8.

Electrophoresis

Electrophoresis equipment suitable for use with precast 5 cm × 5 cm PhastSystem gels from Pharmacia was constructed in cooperation with R. Berglund (Department of Technical Analytical Chemistry, University of Lund, Lund, Sweden). SDS-PAGE[22] in the presence of β-mercaptoethanol was performed as described in ref. 23 with PhastGel SDS buffer strips (Pharmacia). The samples were applied using a PhastGel 8/1 sample applicator (Pharmacia) on a PhastGel 10–25 gel gradient (Pharmacia). The gels were stained with Coomassie Brillant Blue (Carl Roth, Karlsruhe, F.R.G.). Pharmacia LMW calibration kit proteins were used for the molecular weight determination (Phosphorylase b 94 000, BSA 67 000, ovalbumin 43 000, carbonic anhydrase 30 000, trypsin inhibitor 20 100, α-lactalbumin 14 400).

Amino acid sequencing

The amino acid sequences were determined at the Institution for Clinical Chemistry, Malmö General Hospital[24]. A Model 470A gas-phase sequencer from Applied Biosystems was used with on-line determination of PTH-amino acids, utilizing a Model 120A PTH analyser from Applied Biosystems.

Preparation of silica columns

The columns were prepared by packing Nucleosil silica (5 μm, 300 Å) obtained from Macherey, Nagel & Co. (Düren, F.R.G.) into stainless-steel 100 mm × 1.6 mm I.D. Nova-HP tubing (Annel, Stockholm, Sweden), using an descending slurry packing technique. A 0.3-g amount of silica was suspended in chloroform–methanol (2:1) and poured into a 75-ml packing bomb. The slurry was packed into the column at 300 bar using methanol as the displacing medium.

Preparative resolution of benzoin

Optically enriched fractions of benzoin, obtained by chromatography on microcrystalline triacetylcellulose (TAC), were used to determine the elution order of the enantiomers. The general preparative procedure is described in ref. 25. A 1-ml volume of a saturated benzoin solution [< 10 mg/ml in ethanol–water (95:5)] was injected with a Rheodyne 7126 injector equipped with a 5-ml loop on two 600 mm × 10 mm I.D. columns connected in series. The columns were packed with ConbrioTAC, (15–25 μm) obtained from Perstorp Biolytica (Lund, Sweden) and eluted with etha-

nol–water (95:5) using a Beckman (San Ramon, CA, U.S.A.) 110B pump at 1 ml/min. UV-detection was performed with an LKB Uvicord S 2138 detector (Pharmacia) operated at 224 nm and polarimetric detection with a Perkin-Elmer (Norwalk, CT, U.S.A.) Model 241 MC polarimeter operated at 436 nm.

Immobilization of BSA and peptides

The mixture of peptides obtained by proteolytic degradation of BSA, the purified peptide and BSA was immobilized in 100 mm × 1.6 mm I.D. silica columns. Potassium phosphate and phosphoric acid was added to the solution of peptide or BSA to obtain 0.5 *M* phosphate and pH 5.0. The solution was pumped into the column until a breakthrough detected by the UV detector at 280 nm was observed[13].

RESULTS AND DISCUSSION

Proteolytic degradation

The proteolytic degradation produced several peptides of various sizes, as can be seen from SDS-PAGE (Fig. 2) and size-exclusion chromatography (Fig. 3). It was found that experimental conditions such as concentration of pepsin and BSA, the degree of cystination, time for proteolysis, etc., had a great influence on the cleavage pattern. The volume of the reaction vessel also influenced the proteolysis, making a decrease in the concentration of pepsin necessary to retain the cleavage pattern in the scaled-up procedure.

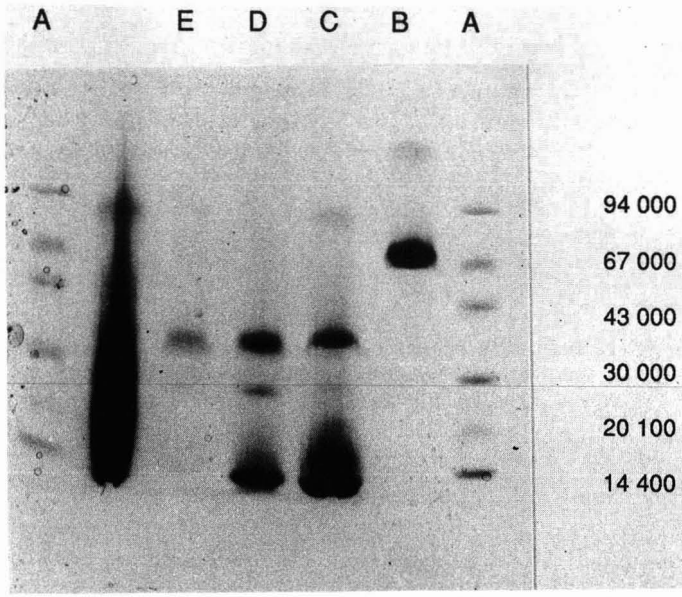

Fig. 2. Electrophoresis separation of samples from different steps of isolation procedure I. Lane A, markers of molecular weight; lane B, intact BSA; lane C, mixture of peptides obtained by proteolysis of BSA (see Fig. 3), these peptides were immobilized on peptide column I; lane D, peptides in the last eluting peak from the anion-exchange column (see Fig. 4); lane E, peptide in the last eluting peak from the size-exclusion step (see Fig. 5), the last peptide was immobilized on peptide column II.

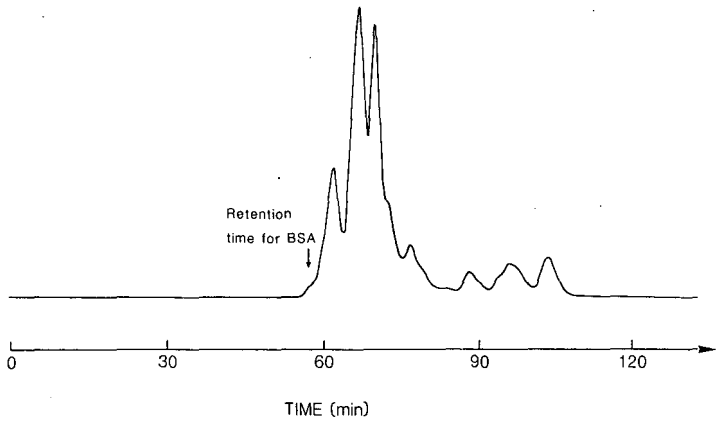

Fig. 3. Size-exclusion chromatography of albumin fragments obtained by proteolytic degradation. Pharmacia Superose 12 HR 10/30 column; eluent, 0.05 *M* NH_4HCO_3 (pH 7.8); flow-rate 0.2 ml/min; UV detection at 280 nm; 0.1 ml injected.

Isolation of peptide

The largest peptide, with an M_r of 38 000, as determined by SDS-PAGE, eluted as the last band during the ion-exchange chromatography according to procedure I (Fig. 4). This indicated that the peptide contained regions with several negative charges. This last band also contained a peptide of M_r 27 000. The larger peptide was further purified by size-exclusion chromatography (Fig. 5), and the results from the

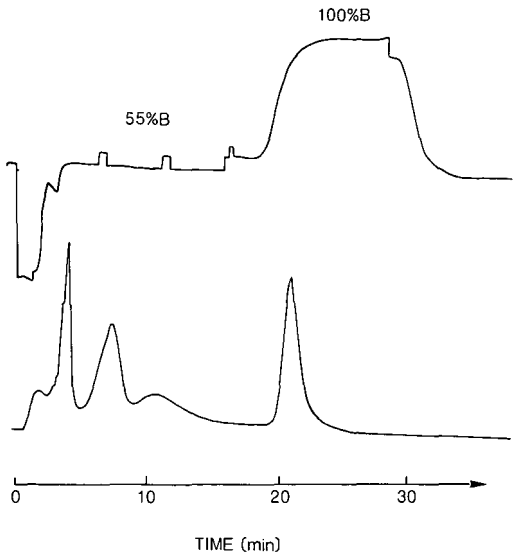

Fig. 4. Ion-exchange separation of albumin fragments according to procedure I. Pharmacia Mono Q HR 5/5 column; eluent A, 0.05 *M* NH_4HCO_3 (pH 7.8); eluent B, 0.05 *M* NH_4HCO_3 (pH 7.8)–0.3 *M* NaCl; flow-rate, 1.0 ml/min; 2 ml injected. The upper trace shows conductimetric detection and the lower trace UV detection at 280 nm.

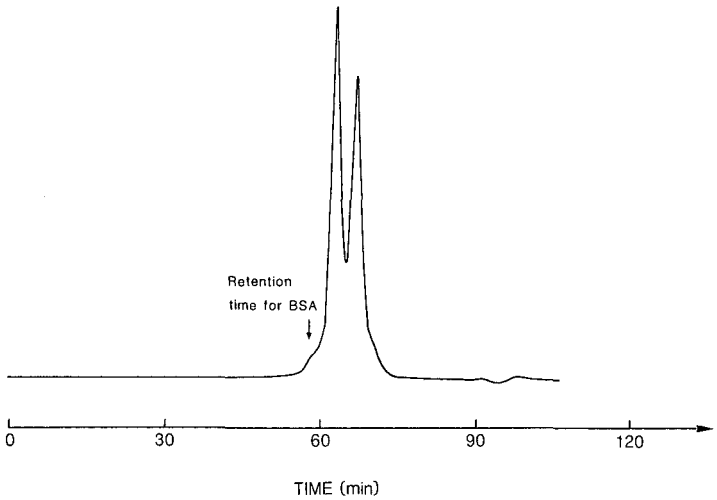

Fig. 5. Size-exclusion chromatography of the last-eluting peak from the ion-exchange separation of albumin fragments according to procedure I (see Fig. 4). Conditions as in Fig. 3. The first peak contained the peptide with M_r 38 000 and the second peak the peptide with M_r 27 000.

amino sequence analysis showed that the peptide consisted of the N-terminal part of BSA starting with amino acid 1 (Asp) (Table I). Owing to the limited accuracy inherent in the electrophoretic analysis, it was not possible to determine exactly the site of cleavage.

The larger anion-exchange and size-exclusion columns used in procedure II showed a lower separation capability (see Fig. 8) than the columns utilized in procedure I. Therefore, the purity of the peptide obtained by procedure II was not as good as that obtained by procedure I.

The amino acid sequence analysis showed that three sequences were present in the peptide solution (Table II). The three peptides are derived from the N-terminal

TABLE I

SEQUENCE ANALYSIS OF THE PEPTIDE SOLUTION OBTAINED BY PROCEDURE I

Amino acid position in BSA	*Identity*	*Yield (nmol)*[a]
1	Asp	0.73
2	Thr	ND
3	His	ND
4	Lys	0.88
5	Ser	ND
6	Glu	0.50
7	Ile	ND
8	Ala	0.76
9	His	0.15
10	Arg	0.15
11	Phe	0.56

[a] ND = Not determined.

TABLE II

SEQUENCE ANALYSIS OF THE PEPTIDES SOLUTION OBTAINED BY PROCEDURE II

Sequence	*Amino acid position in BSA*	*Identity*[a]	*Yield (nmol)*[a]
1	1	Asp	0.20
	2	Thr	0.15
	3	His	0.09
	4	Lys	0.22
	5	Ser	ND
	6	Glu	0.12
	7	Ile	0.13
	8	Ala	0.19
	9	His	0.07
	10	Arg	0.06
	11	Phe	0.12
	12	Lys	0.09
	13	Asp	0.05
	14	Leu	0.08
	15	Gly	0.06
	16	Glu	0.14
2	11	Phe	0.10
	12	Lys	0.03
	13	Asp	0.07
	14	Leu	0.10
3	49	Phe	0.10
	50	Ala	0.16
	51	Lys	0.11
	52	Thr	0.05
	53	ND	ND
	54	Val	0.05
	55	Ala	0.09
	56	Asp	0.04
	57	Glu	0.11
	58	Ser	0.03

[a] ND = Not determined.

half of BSA and contain mainly the same overlapping sequence. Half the amount of the peptides consists of the peptide starting with amino acid 1 (Asp) and the two other peptides starting with amino acid 11 (Phe) and 49 (Phe), representing approximately a quarter each. SDS-PAGE showed that also a small amount (*ca.* 5%) of a larger peptide (M_r 45 000) was present in the peptide solution. The high retention of the peptides on the ion-exchange column is in agreement with the non-uniform distribution of charges of BSA. The calculated net charge at pH 7 decreases from the N-terminal end towards the C-terminal end[17] (see Fig. 1). The isolation of the peptide was very time consuming and difficult to carry out, *e.g.*, owing to time-dependent associations caused by the formation of intermolecular disulphide bonds leading to coelution of different peptides in the size-exclusion step. To increase the loadability of the anion-exchange chromatographic step, attempts were also made to replace the Mono-Q material with cellulose-based ZetaPrep QAE anion exchanger (LKB–Phar-

TABLE III

CHROMATOGRAPHIC DATA FOR PEPTIDE COLUMN I

0.05 *M* phosphate buffers (pH 7.0) were used as mobile phases; 0.05 μg was injected.

Compound	*1-Propanol (%)*	k'_1	k'_2	α	R_s
Tryptophan	0	0.1	0.1	1.0	0
Benzoin	0	0.82	1.6	1.9	1.2
	2	0.61	1.3	2.1	1.5
Oxazepam	2	1.9	3.4	1.8	1.4
Warfarin	2	0.82	0.82	1.0	0

macia). However, the peptides were not as effectively separated as when using the Mono-Q columns. The interactions from the divinylbenzene–polystyrene matrix of the Mono-Q material seemed to promote the selectivity between the peptides.

Evaluation of peptide columns

To confirm that the peptides still had stereoselective properties, the mixture of peptides was immobilized on a silica column (peptide column I), which showed a retained resolving power for benzoin and oxazepam (Table III, Figs. 6, 7). However, the stereoselectivity was lost for tryptophan and warfarin. This showed that one or several peptides had retained stereoselectivity for at least benzoin and oxazepam, and that no intact BSA was responsible for the resolvation of benzoin. The results also indicated that in order to obtain peptides with retained stereoselectivity for, *e.g.*, tryptophan and warfarin, a different cleavage procedure might be necessary, or that such peptides might not have been properly immobilized owing to blockage of the stereoselective sites or not have been immobilized at all on the silica (a small background of UV absorbance was observed during the immobilization procedure).

The peptide obtained by procedure I was immobilized on a silica column (peptide column II). Owing to the limited amount of peptide available, all the peptide injected (*ca.* 10–15 mg) was adsorbed, which means that the column was probably not completely covered. The column showed the same characteristics (Table IV) as that based on the mixture of peptic fragments, *i.e.*, the resolving power for tryptophan and warfarin was lost compared with BSA (see Table V). Benzoin and oxazepam were resolved and showed a better or equal separation (α) compared with intact BSA (Figs. 9, 10). The retention was decreased for all four compounds. The fact that the reten-

TABLE IV

CHROMATOGRAPHIC DATA FOR PEPTIDE COLUMN II

0.05 *M* phosphate buffer (pH 7.0) was used as the mobile phase; 0.05 μg was injected.

Compound	k'_1	k'_2	α	R_s
Tryptophan	0.1	0.1	1.0	0
Benzoin	0.84	2.7	3.1	2.5
Oxazepam	1.6	3.1	1.9	1.2
Warfarin	0.98	0.98	1.0	0

TABLE V

CHROMATOGRAPHIC DATA FOR BSA COLUMN

0.05 *M* phosphate buffers were used as mobile phases; 0.05 μg of benzoin, morpholep, N-benzoylalanine 2,4-dinitrophenylglycine and tryptophan, 0.10 μg of oxazepam, mandelic acid and kynurenine and 2.5 μg of warfarin were injected.

Compound	*pH*	*1-Propanol (%)*	k'_1	k'_2	α	R_s
Benzoin	5.0	0	3.5	6.0	1.7	2.2
	6.0	0	3.0	5.6	1.9	2.4
	7.0	0	2.8	5.7	2.0	2.5
	7.5	0	2.2	3.8	1.7	1.7
	6.0	2	1.2	1.6	1.3	0.9
	7.5	2	1.5	2.1	1.4	1.0
Morpholep	5.0	0	1.0	1.3	1.3	0.8
	6.0	0	0.91	1.1	1.3	0.6
	7.0	0	0.88	1.1	1.2	0.5
	7.5	0	0.54	0.54	1.0	0
	6.0	2	0.46	0.46	1.0	0
	7.5	2	0.47	0.47	1.0	0
Oxazepam	5.0	0	9.0	20.0	2.2	2.1
	6.0	0	8.1	18.7	2.3	2.7
	7.0	0	7.7	15.9	2.0	2.3
	7.5	0	5.3	9.7	1.8	1.9
	6.0	2	3.1	6.4	2.0	2.0
	7.5	2	2.6	5.2	2.0	2.2
N-Benzoylalanine	5.0	0	1.3	2.1	1.6	
	6.0	0	0.63	1.5	2.4	
	7.0	0	0.44	1.7	3.8	
	7.5	0	0.44	1.9	4.4	
	6.0	2	0.53	1.4	2.7	
	7.5	2	0.39	1.3	3.4	
2,4-Dinitrophenylglycine	7.5	0	1.2	4.2	3.6	
	7.5	2	1.1	1.6	1.5	
Mandelic acid	5.0	0	3.0	3.7	1.2	
	6.0	0	0.44	0.62	1.4	
	7.0	0	0.14	0.25	1.8	
	7.5	0	0.12	0.12	1.0	
	6.0	2	0.12	0.12	1.0	
	7.5	2	0.47	0.47	1.0	
Tryptophan	5.0	0	0.29	0.29	1.0	
	6.0	0	0.28	0.32	1.2	
	7.0	0	0.27	0.85	3.2	
	7.5	0	0.32	2.3	7.2	
	6.0	2	0.25	0.31	1.2	
	7.5	2	0.31	1.3	4.3	
Kynurenine	5.0	0	0.24	0.24	1.0	
	6.0	0	0.24	0.32	1.3	
	7.0	0	0.24	1.24	5.2	
	7.5	0	0.29	3.70	13.0	
	6.0	2	0.20	0.20	1.0	
	7.5	2	0.29	2.10	7.3	
Warfarin	5.0	0	51.0	114.0	2.2	
	6.0	0	44.0	60.0	1.4	
	7.0	0	15.0	21.0	1.4	
	6.0	2	3.3	5.0	1.5	
	7.5	2	3.4	5.0	1.5	

TABLE VI

CHROMATOGRAPHIC DATA FOR PEPTIDE COLUMN III

0.05 *M* phosphate buffers were used as mobile phases; 0.05 μg of benzoin, morpholep, N-benzoylalanine, 2.4-dinitrophenylglycine and tryptophan, 0.10 μg of oxazepam, mandelic acid and kynurenine and 2.5 μg of warfarin were injected.

Compound	*pH*	*1-Propanol (%)*	k_1'	k_2'	α	R_s
Benzoin	5.0	0	3.8	6.8	1.8	2.1
	6.0	0	3.0	6.9	2.3	2.3
	7.0	0	2.4	6.3	2.6	2.3
	7.5	0	1.7	4.1	2.4	2.1
	6.0	2	0.66	0.81	1.2	–
	7.5	2	0.82	1.4	1.7	1.0
Morpholep	5.0	0	1.2	1.9	1.6	1.7
	6.0	0	0.75	0.94	1.3	0.4
	7.0	0	0.59	0.59	1.0	0
	7.5	0	0.32	0.32	1.0	0
	6.0	2	0.20	0.20	1.0	0
	7.5	2	0.20	0.20	1.0	0
Oxazepam	5.0	0	10.8	20.4	1.9	1.8
	6.0	0	7.4	5.4	2.1	1.7
	7.0	0	5.7	9.9	1.7	1.2
	7.5	0	3.8	6.0	1.6	0.8
	6.0	2	1.9	2.5	1.3	–
	7.5	2	2.1	3.0	1.5	1.0
N-Benzoylalanine	5.0	0	0.62	0.62	1.0	
	6.0	0	0	0	1.0	
	7.0	0	0	0	1.0	
	7.5	0	0	0	1.0	
	6.0	2	0	0	1.0	
	7.5	2	0	0	1.0	
2,4-Dinitrophenylglycine	7.5	0	0	0	1.0	
	6.0	2	0	0	1.0	
	7.5	2	0	0	1.0	
Mandelic acid	5.0	0	0.41	0.41	1.0	
	6.0	0	0	0	1.0	
	7.0	0	0	0	1.0	
	7.5	2	0	0	1.0	
	6.0	2	0	0	1.0	
Tryptophan	5.0	0	0.35	0.35	1.0	
	6.0	0	0.23	0.23	1.0	
	7.0	0	0.17	0.17	1.0	
	7.5	0	0.17	0.17	1.0	
	7.5	2	0.17	0.17	1.0	
Kynurenine	5.0	0	0.29	0.29	1.0	
	6.0	0	0.24	0.24	1.0	
	7.0	0	0.21	0.21	1.0	
	7.5	0	0.26	0.26	1.0	
Warfarin	5.0	0	30.0	30.0	1.0	
	7.0	0	2.0	2.0	1.0	
	7.5	0	0.71	0.71	1.0	
	7.5	2	0.29	0.29	1.0	
	6.0	2	1.0	1.0	1.0	

tion decreased while the separation was increased or was equal to that with BSA showed that the parts of BSA that gave rise to interactions not contributing to the stereoselectivity had been removed or denatured. It also showed that the proteolytic degradation and the immobilization procedure had not adversely affected the chiral discrimination power for benzoin and oxazepam.

The peptides obtained by procedure II were immobilized on a silica column (peptide column III). The peptide solution contained 0.33 mg/ml of peptide and *ca.* 18 mg were adsorbed. The column showed the same general behaviour as peptide column II (Table VI). The stereoselectivity was lost for all compounds studied except benzoin, oxazepam and morpholep. The separation factors were not as good as those obtained for peptide column II, probably owing to the lower purity of the immobilized peptides.

As a reference, a BSA column was made by immobilizing BSA on a silica column (see Table V, Figs. 11, 12). The BSA solution used contained 0.12 mg/ml of BSA and *ca.* 11 mg of BSA were adsorbed. The elution orders of the benzoin enantiomers on peptide column III and the BSA column were compared by injecting optically enriched fractions of benzoin. The same elution order was observed.

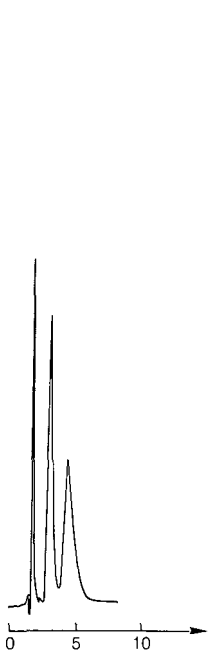

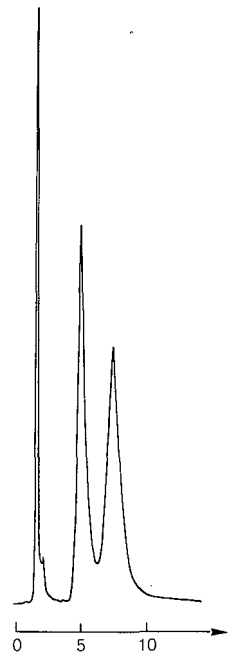

Fig. 6. Resolution of *rac*-benzoin on peptide column I, which contained the mixture of peptides obtained by proteolytic degradation. Column, 100 mm × 1.6 mm I.D.; mobile phase, 0.05 *M* phosphate (pH 7.0); flow-rate 0.1 ml/min; UV detection at 250 nm; 0.05 μg injected in 0.5 μl of methanol. The first peak at the void volume is caused by the injected methanolic solution.

Fig. 7. Resolution of *rac*-oxazepam on peptide column I. Mobile phase, 0.05 *M* phosphate (pH 7.0) containing 2% 1-propanol; flow-rate; 0.1 ml/min; UV detection at 230 nm; 0.05 μg injected in 0.5 μl of methanol.

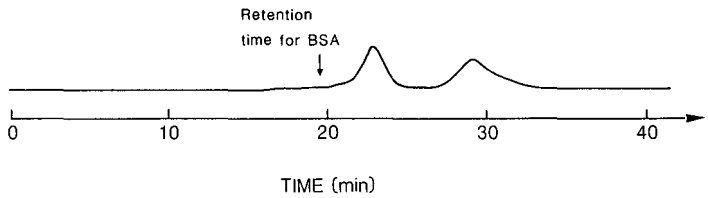

Fig. 8. Size-exclusion chromatography of the last-eluting peak from the ion-exchange separation of albumin fragments according to procedure II. Sephadex G-75 Superfine, 100 × 5 cm column; eluent, 0.05 *M* NH_4HCO_3 (pH 7.8); flow-rate, 0.5 ml/min; UV detection at 280 nm; 12 ml injected. The first peak contained the peptide with M_r 38 000 and the second peak the peptide with M_r 27 000.

A column was also made by immobilizing peptides obtained from procedure II by cross-linking with glutaraldehyde on 3-aminopropylsilica. The results will be reported elsewhere[14].

The binding sites in the immobilized peptide stereoselective to benzoin, oxazepam and morpholep are probably the same as or very similar to those in intact BSA. In theory, although less likely, the cutting of the protein could generate new stereoselective binding sites. The observed loss of steroselectivity for, *e.g.*, tryptophan

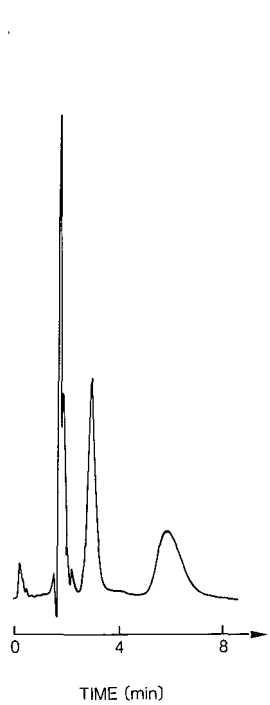

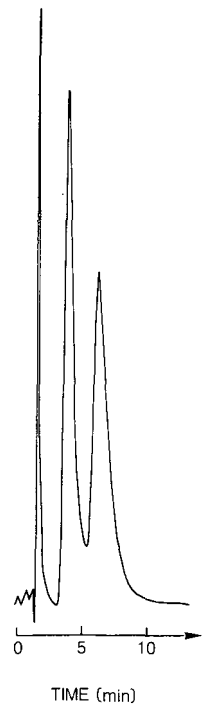

Fig. 9. Resolution of *rac*-benzoin on peptide column II which contained the peptide obtained by isolation procedure I. Conditions as in Fig. 6. A 0.05-μg amount of *rac*-benzoin in 0.5 μl of methanol was injected.

Fig. 10. Resolution of *rac*-oxazepam on peptide column II. Conditions as in Fig. 9. UV detection at 230 nm. A 0.05-μg amount of *rac*-oxazepam in 0.5 μl of methanol was injected.

and warfarin is probably due to removal of the parts of BSA containing the necessary binding sites or due to conformational changes of the immobilized fragment.

The peptide-based columns had a shorter lifetime than the corresponding BSA columns and degraded more rapidly, especially when using 1-propanol as the modifier in the mobile phase. The reason for this instability is not yet known, but may arise from the fact that BSA was cleaved in domain 2, leaving a partial domain which probably disrupts the three-dimensional structure of domain 2 and therefore makes it more susceptible to degradation. Owing to the stability problems encountered, no loadability experiments were performed. The maintained selectivity and decreased retention indicate that a higher productivity should be obtained in preparative resolution of chiral compounds. The time needed to isolate the peptides using procedure I was shorter (weeks) than for procedure II (several months) and the above-mentioned stability problems may have contributed to the lower purity of the peptide obtained by procedure II.

To decrease the amount of peptide needed to cover fully, *e.g.*, a silica column and to reduce the time of the isolation procedure, the use of smaller columns, *e.g.*, packed fused-silica columns with an I.D. of *ca.* 0.2 mm or less, will be used in future work. This will also allow the utilization of small "high-performance" ion-exchange

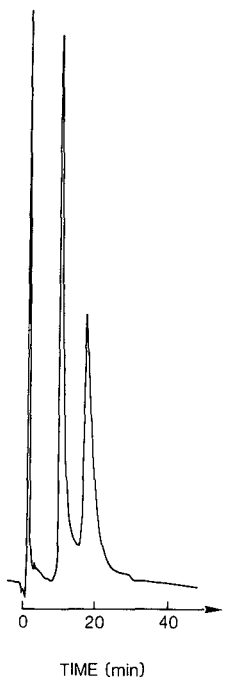

Fig. 11. Resolution of *rac*-benzoin on a 100 mm × 1.6 mm I.D. BSA column. Conditions as in Fig. 6. A 0.05-μg amount of *rac*-benzoin in 0.5 μl of methanol was injected.

Fig. 12. Resolution of *rac*-oxazepam on a 100 mm × 1.6 mm I.D. BSA column. Mobile phase, 0.05 *M* phosphate (pH 7.5); other conditions as in Fig. 10. A 0.10-μg amount of *rac*-oxazepam in 0.5 μl of methanol was injected.

and size-exclusion columns. The preparation of small BSA columns has been suggested[18] and demonstrated by Vindevogel *et al.*[26]. Peptides stereoselective to compounds such as tryptophan and warfarin, which were not successfully resolved by the peptide reported in this paper, may perhaps be isolated from a proteolytic peptide mixture by affinity chromatography. It may also be necessary to cleave the protein in the presence of the ligand in order to protect the binding site during proteolysis.

CONCLUSION

The successful resolution of benzoin, oxazepam and morpholep showed that it is possible to degrade BSA proteolytically into smaller fragments and to immobilize the latter with retained stereoselectivity. Increased or maintained separation factors (α) and decreased capacity factors (k') of the peptide compared with BSA showed that interactions not contributing to the chiral recognition had been removed. It was also concluded that regions stereoselective to benzoin, oxazepam and morpholep should be situated in the N-terminal half of BSA.

ACKNOWLEDGEMENTS

Ingrid Dahlqvist, Malmö General Hospital, is thanked for performing the amino acid sequencing and Roland Isaksson, Division of Organic Chemistry 3, University of Lund, for putting the TAC chromatographic set-up at our disposal. This work was supported by grants from the Crafoord Foundation, Lund, the Lars Hierta Memorial Foundation, the Royal Physiographical Society of Lund and the Swedish Natural Science Research Council.

REFERENCES

1 W. Lindner and C. Pettersson, in I. W. Wainer (Editor), *Liquid Chromatography in Pharmaceutical Development*, Aster, Springfield, OR, 1985, p. 99.
2 S. Allenmark, *Chromatographic Enantioseparation: Methods and Applications*, Ellis Horwood, Chichester, 1988.
3 J. Hermansson, *J. Chromatogr.*, 269 (1983) 71–80.
4 K. K. Stewart and R. F. Doherty, *Proc. Natl. Acad. Sci. U.S.A.*, 70 (1973) 2850–2852.
5 S. Allenmark, B. Bomgren and H. Borén, *J. Chromatogr.*, 237 (1982) 473–477.
6 S. Allenmark, *J. Liq. Chromatogr.*, 9 (1986) 425–442.
7 R. A. Thompson, S. Andersson and S. Allenmark, *J. Chromatogr.*, 465 (1989) 263–270.
8 B. Sébille and N. Thuaud, *J. Liq. Chromatogr.*, 3 (1980) 299–308.
9 C. Pettersson, T. Arvidsson, A.-L. Karlsson and I. Marle, *J. Pharm. Biomed. Anal.*, 4 (1986) 221–235.
10 J. P. Knox and G. Galfre, *Anal. Biochem.*, 155 (1986) 92–94.
11 T. Miwa, T. Miyakawa, M. Kayano, Y. Miyake, *J. Chromatogr.*, 408 (1987) 316–322.
12 P. Jadaud, S. Thelohan, G. R. Schonbaum and I. W. Wainer, *Chirality*, 1 (1989) 38–44.
13 P. Erlandsson, L. Hansson, R. Isaksson, *J. Chromatogr.*, 370 (1986) 475–483.
14 S. Andersson, S. Allenmark, P. Erlandsson and S. Nilsson, *J. Chromatogr.*, 498 (1990) in press.
15 S. Bergqvist, Neurochemical Laboratory, University of Lund, and S. Nilsson, Euro-fassel, Lund, Sweden, personal communication.
16 J. R. Brown, *Fed. Proc. Fed. Am. Soc. Exp. Biol.*, 35 (1976) 2141–2144.
17 T. Peters, Jr., *Adv. Protein Chem.*, 37 (1985) 161–245.
18 P. Erlandsson and S. Nilsson, paper presented at the *11th International Symposium on Column Liquid Chromatography, Amsterdam, 1987.*
19 T. P. King, *Arch. Biochem. Biophys.*, 156 (1973) 509–520.

20 L. R. Snyder and J. J. Kirkland, *Introduction to Modern Liquid Chromatography*, Wiley, New York, 2nd ed., 1979, p. 34.
21 *Gel Filtration, Theory and Practice*, Pharmacia, Uppsala, Sweden, 1981.
22 U. K. Laemmli, *Nature (London)*, 227 (1970) 680–685.
23 *PhastSystem Separation Technique*, File No. 110, Pharmacia, Uppsala, Sweden, 1986.
24 B. Dahlbäck, Å. Lundwall and J. Stenflo, *J. Biol. Chem.*, 261 (1986) 5111–5115.
25 R. Isaksson and J. Roschester, *J. Org. Chem.*, 50 (1985) 2519–2521.
26 J. Vindevogel, J. van Dijck and M. Verzele, *J. Chromatogr.*, 447 (1988) 297–303.

Journal of Chromatography, 482 (1989) 53–64
Elsevier Science Publishers B.V., Amsterdam — Printed in The Netherlands

CHROM. 21 871

NOVEL TRANSPORT DETECTOR FOR LIQUID CHROMATOGRAPHY

I. PRELIMINARY EXPERIMENTS

DAVID J. MALCOLME-LAWES* and PHILIP MOSS
Centre for Research in Analytical Chemistry and Instrumentation, Chemistry Department, King's College London, Strand, London WC2R 2LS (U.K.)
(First received June 12th, 1989; revised manuscript received August 8th, 1989)

SUMMARY

A transport detector mechanism is being developed for the removal of volatile solvents from a chromatographic eluent and the detection of residues using a flame ionization detector. The mechanism employs a number of novel features, which allow close control over solvent removal and permit the detector to be used for relatively volatile sample materials. A number of results obtained using normal phase chromatography are presented, and the characteristics of the experimental system are discussed.

INTRODUCTION

High-performance liquid chromatography (HPLC) has become one of the most widely used techniques for routine analyses[1], and this is due in part to the quality and relatively low cost of many of the commercial chromatographic systems available. Over the past decade the reliability of pumping systems, the efficiency of columns and the sensitivity of detectors have improved considerably, and the wide range of detection systems now available is capable of dealing with the majority of application requirements. However, it is still the case that there is no universal, high sensitivity detector available to compare with the flame ionization detector of gas chromatography (GC). The most popular HPLC detector remains the UV absorption detector[1], with other detectors, such as fluorescence and electrochemical, being used where the sensitivity of absorbance detectors is inadequate. However, for many compounds none of these detectors is suitable, and the only commonly encountered alternative is the refractive index monitor, which tends to operate with rather poor sensitivity.

Many attempts have been made over the past 20 years to utilize the sensitivity of flame ionization detection (FID) in liquid chromatography. The approach has generally involved the deposition of the chromatographic eluent onto a moving chain[2–9], belt[10–18], wire[19–30] or disc[31–38] (the transport mechanism), which may then be heated to evaporate the volatile components of the eluent, leaving any less volatile residue on the support. The problem was then reduced to that of transferring the residue to the detector.

0021-9673/89/$03.50

Haahti and Nikarri[2] used a 1-mm diameter gold chain driven by a synchronous motor at a velocity of 1 mm s^{-1} as the transport mechanism. Solvent was removed by air heated to 120°C and the chain passed directly into an FID flame, *ca.* 2 mm above the jet, with the chain biased to *ca.* 10 V above the jet potential. The system was used for classical chromatography, although quantitative measurements were not successful owing to the loss of components from the chain and the electrical noise generated by the chain mesh. Some of these problems were tackled by Stouffer *et al.*[3], who used a platinum chain that passed vertically through the FID flame, so that the collector electrode was concentric with the chain. Karmen[4,7] used a continuous metal chain from which the eluent was evaporated, followed by strong heating in a nitrogen-filled tube. Volatile vapours and pyrolysis products were swept into a flame ionization detector. This system had difficulties with non-volatile material melting and spreading over the chain, and with crystalline material spattering before pyrolysis. It was really limited to moderately volatile compounds that could be pyrolysed below 250°C.

A major improvement was made by Scott and co-workers[20,24] who employed a nickel wire that passed through the eluent and through a two-stage glass tube, through which argon was passed. The first stage was heated to evaporate the solvent, with the vapour being swept away by the argon. The second stage was heated much more strongly to pyrolyse the eluent residue. The argon pressure forced the pyrolysis products into a flame ionization detector. A subsequent enhancement[25] passed the wire directly into the flame. The device was developed into a commercial product, which became known as the moving wire detector. There were several difficulties with this approach: the relatively small amount of the eluent collected by the wire; the dimensional changes in the wire as it was heated; contamination of one part of the wire by contact with structural components; and the general lack of reliability of the mechanism.

In the more successful disc detectors eluent is deposited on a rotating disc. Owens *et al.*[35] used a rotating perforated metal disc (a 2.5-in. diameter platinum screen) to carry eluent from a gel permeation column into the flame (the disc was insulated at its hub). This system relied on relatively small gel permeation columns (0.01–0.125 in. I.D.) and low flow-rates, and was successfully applied to the detection of polystyrenes separated in THF. Dubsky[36,37] used an 8-in. diameter ceramic disc, heated by an infrared lamp to evaporate solvent prior to passage through a two-part detector (the flame below the disc and the electrodes above), which could also be used as a thermoionization detector by continuously applying an alkaline metal salt to the disc. Szakasits[38] and Szakasits and Robinson[39] used a vertical spinning porous alumina disc, which passed through an oven to evaporate the solvent before the disc itself met a dual-nozzle flame. After passing through the flame, the edge of the disc was cooled by air drawn over the disc by a fan. Fischer and Kohl[40] employed a transport mechanism consisting of a rigid ring coated with a porous ceramic material to transfer eluent from a column to a pyrolysis oven fed by hydrogen (or helium) and nitrogen. The pyrolysis products were swept into a flame ionization detector or mass spectrometer. Dixon and Hall[17] used a quartz-fibre belt mounted at the periphery of a rotating disc, with volatile solvent being allowed to evaporate within the heated housing, leaving any residue on the belt. The belt rotated into flame ionization detector and then into a hydrogen–oxygen "clean-up" flame, before cooling to receive further eluent. The principal difficulty with most of these approaches is that precise control of

evaporation is difficult. The disc needs to be cool to receive eluent and yet pass through the flame to combust the residue. The thermal mass of the disc makes it difficult to accommodate these conflicting requirements.

Transport mechanisms based on metal belts have also been used. Yang *et al.*[18] described a device using a stainless-steel belt that is loaded using thermospray vaporization followed by subsequent pyrolysis (typically at 420°C) in the presence of a carrier gas, such as helium, which sweeps the pyrolysis products into a GC detector (in this case most of the work was carried out using a photoionization detector, although an electron-capture detector was also used). Hoskin[19] has also described a two-part nickel belt onto which discrete droplets of eluent may be loaded, followed by evaporation and pyrolysis. This system forms the basis of a transport detector manufactured by Analink Ltd. With these systems the principal difficulty is the requirement of a limited temperature pyrolysis stage to avoid damage to the belt, coupled with the high thermal conductivity of the belt material.

We have designed a transport mechanism that attempts to overcome the limitations imposed by the continuous "analogue" mechanisms used in the past. By treating the eluent flow as a series of discrete packets of liquid it becomes possible to use a low conductivity support material and yet keep the thermal mass small enough to allow evaporation of the solvent and cooling of the support material to be carried out by controlled-temperature air-flows. In this paper the basic structure of the transport mechanism is described, and the parameters that effect the separation of solvent from sample component are discussed. A number of preliminary results are presented to demonstrate the practical operation of the detector.

DETECTOR

The detector consists of five components: the transport mechanism, the evaporation and cooling air-flow systems, the flame ionization detector, the controlling and data logging microcomputer, and the interface between the computer and the other components. During the design and construction of the detector there was a fairly clear distinction between each of these components, but a description of the system produces an unavoidable overlap between them. A major feature of the design is that the entire operation of the system is under the control of software in the microcomputer —there are no manual controls of any kind on the detector. Thus the transport mechanism is a specific item of hardware but its operation is governed by the computer system, which defines transport parameters to the interface electronics. In describing the system we will discuss each component in turn, even though this must result in aspects of the operation being described before the controlling mechanism has been detailed.

The transport mechanism consists of a two-part disc mounted on the shaft of a stepper motor fixed to the main chassis of the instrument. From the disc protrude a number of 1-mm diameter drawn quartz rods (40 on the experimental system), as shown in Fig. 1. Each rod is 12 cm long, protruding 10 cm from the disc, is located in a groove machined into the lower part of the disc and is held in place by an O-ring located in the upper part. The rods are not treated before use, apart from several passages through the FID flame, and the surface of the rods can be described as smooth but not polished. The stepper motor is operated so that the disc steps around

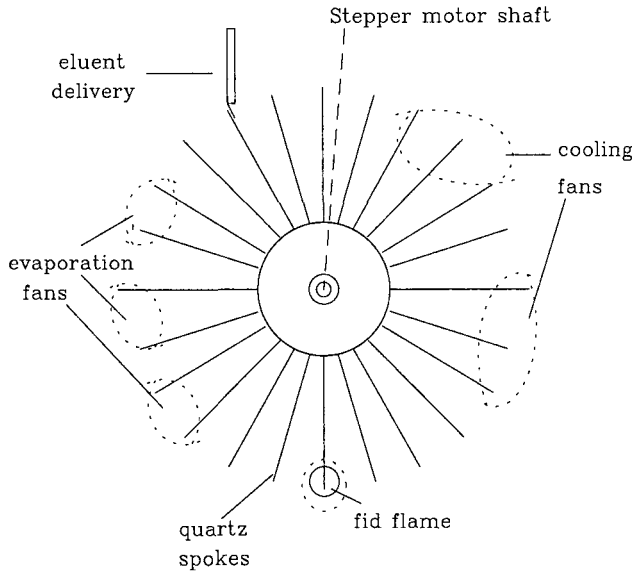

Fig. 1. Quartz rod assembly of the transport mechanism shown in relation to the other major components, the eluent delivery tube, evaporators and coolers.

maintaining one rod under the eluent delivery point, several rods over the evaporation points, one rod in the flame, and several rods over the cooling air-flows. Eluent is deposited on the rod at the delivery point, where the liquid is applied *ca.* 2 mm from the end of the rod. The disc mechanism is positioned at a slight angle from the horizontal (*ca.* 2°), so that the liquid tends to flow towards the end of the rod. While the actual amount of liquid deposited on any rod may be up to *ca.* 20 μl, in normal operation we deposit *ca.* 10 μl per rod. The rate at which the disc steps around may be varied up to about six steps per second, although again in normal operation the rate is likely to be about one step per second.

Once liquid is deposited on a rod, the rod moves over the evaporating air-flow, whose flow-rate and temperature are carefully controlled. In the experimental system three stages of evaporation are used, and different combinations of flow-rates and temperature may be used to evaporate different multicomponent eluents. The rods step from one evaporation stage to the next, remaining in a given stage for three steps. By the end of the third stage, the volatile eluent should have been evaporated. The rod is then stepped into the centre of the flame, where any carbon-containing residue is combusted and current is produced. The rods then step over two stages of cooling air-flow to ensure that they are cool enough to receive another drop of eluent by the time they reach the eluent delivery point again.

The air-flow systems are all based on variable speed fans, with the speed set by the computer. The air-flow system is outlined in side view in Fig. 2. The cooling fans are fixed under the main chassis of the system and blow their air through holes in the chassis. The evaporation fans are mounted at the ends of tubes that contain the mains-powered heating elements, and the heated air is also blown through holes in the chassis. Temperature sensors located in the evaporation air-flows ensure that the

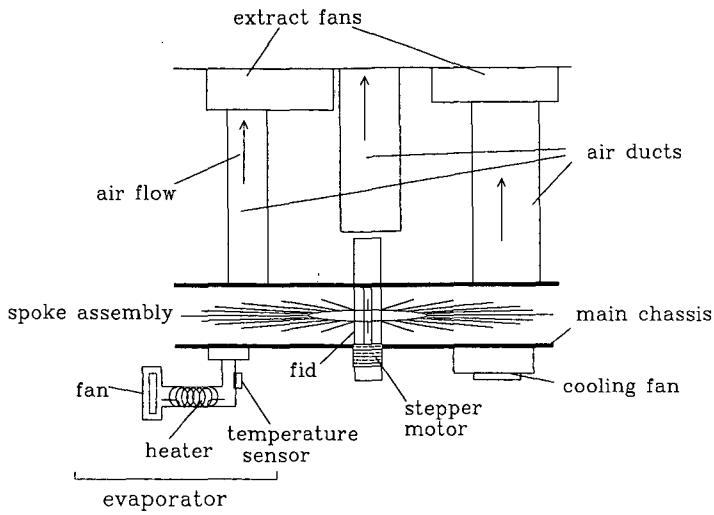

Fig. 2. Side view showing position of evaporator and cooler fans on the mounting plate.

forced-air temperature is maintained as required. Air-flows from the evaporation and cooling stages are kept separated from one another and from the ambient air in the instrument's housing; this prevents solvent-laden air from being drawn into the detector. The separation is maintained by allowing blown air to pass through holes in a baffle plate and then into tubes, which are maintained at a slight negative pressure by a pair of pressure balance exhaust fans mounted in the cabinet roof. The experimental system uses three evaporators, two coolers and two pressure balance fans, so that seven fan speeds and three evaporator temperatures must be specified by the computer during operation.

The FID system is shown in Fig. 3. Essentially the detector is a conventional one, *ca.* 70 × 15 mm I.D., with a slot cut in the outer wall to allow the rods to pass into the flame *ca.* 8 mm above the base of the flame. In the experimental system the collector consists of a 6-mm diameter platinum mesh held *ca.* 10 mm above the FID jet by a length of stainless-steel tubing. The hydrogen is brought into the detector through similar tubing, insulated from the support brackets and operated at a potential of *ca.* 300 V. The outer wall of the detector is mounted on a small plate, which slides under the rod path through a cut-out in the chassis using a drawer arrangement. The outer wall is grounded electrically. The collector current is passed to a transresistance amplifier, which generates a voltage signal that is digitized using a dynamic analog input interface to the computer.

The computer system controls all aspects of the detector's operation and the flow-rate of the chromatographic eluent (this avoids the risk of flammable eluents being accidentally pumped into a box containing mains-powered heaters!). The software is required to adjust the stepper motor's stepping rate to suit the user-specified eluent flow-rate, to adjust the evaporation temperatures and air flow-rates to suit the eluent composition and its flow-rate, and to adjust the pressure balance fans to ensure that the evaporation and cooling areas of the detector are operating under a negative pressure. The software also collects the detector signal data.

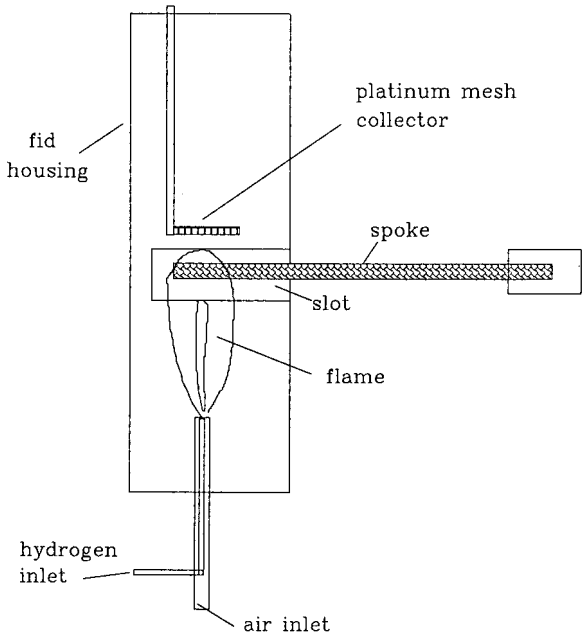

Fig. 3. Detector assembly, showing a spoke in position at the tip of the flame.

Because the detector operates in a sequential mode (*i.e.* one rod at a time is passed into the flame) the signal (at least when a component is eluting) actually consists of a series of rapidly changing peaks, each caused by a single spoke entering the flame, its residue starting to combust, and then combustion reaching completion. While the many ways of handling such data can become complex, they all require that the computer samples the signal at specified times after the rod enters the flame. Thus the computer must synchronize the signal readings with the stepping of the stepper motor. The computer must also display the chromatogram, and it is desirable to have this carried out in real time. Our software also provides facilities for plotting the chromatograms on a graphics plotter, although this is usually carried out after the chromatogram has been collected; the chromatograms reported below were produced in this way by plotting onto a laser printer. Finally, as the detector consists of a large box containing mains-powered heaters and a flame, and into which is passing flammable eluent and hydrogen gas, the computer system must monitor various safety aspects of the system and be able to take appropriate action in the event of a problem. In the experimental system the computer monitors the hydrogen flame (using a temperature sensor mounted in the detector chimney) and can shut off the hydrogen supply if the flame goes out. It also monitors the movement of the rods and can turn off the HPLC pump if the rods cease to move. Several other eventualities are catered for, and in response to most of these the heaters are all turned off while the fans speeds are all set to maximum and appropriate warning bleeps are delivered.

Although the detector's working is simple in principle, it will be clear that there are a number of parameters that are specified, monitored or controlled by the computer during operation. In designing the computer–detector interface it became

clear that either the computer could do everything (send the pulses to the stepper motor, monitor the evaporator temperatures and adjust the heater power several times a second, read the signal, etc.) or that some of these activities must be handled by purpose-designed electronics. We chose the latter approach, and an outline diagram of the control system is shown in Fig. 4.

An initial study has been undertaken to obtain an indication of the range of hydrocarbons to which the experimental version of the detector responds. It is difficult to present preliminary results without the reader arriving at incorrect conclusions, but it must be emphasized that the result reported below were obtained by selecting operating conditions that seemed reasonable. No attempt has been made to optimize the operating conditions (*i.e.* temperatures and air flow-rates), and the range of application would be reasonably expected to be increased by such optimization.

EXPERIMENTAL

A diagram showing the major components of the experimental detector is shown in Fig. 5. The chromatographic system consisted of a Knauer pump, a Rheodyne Model 7125 injection valve fitted with a 20-μl loop, and a 150 × 4.6 mm I.D. column packed with Partisil 5 μm. The sample materials consisted of pyrene (SLR, Aldrich) and in some cases hydrocarbon standards provided by BP Sunbury Research Centre. All were used without further purification. Apart from pyrene, samples are identified by carbon number, *e.g.* C12 is dodecane.

Samples of 20 μl of test compounds diluted in hexane were loaded onto the column and eluted with hexane–dichloromethane (3:1, v/v) at a flow-rate of 0.6 ml

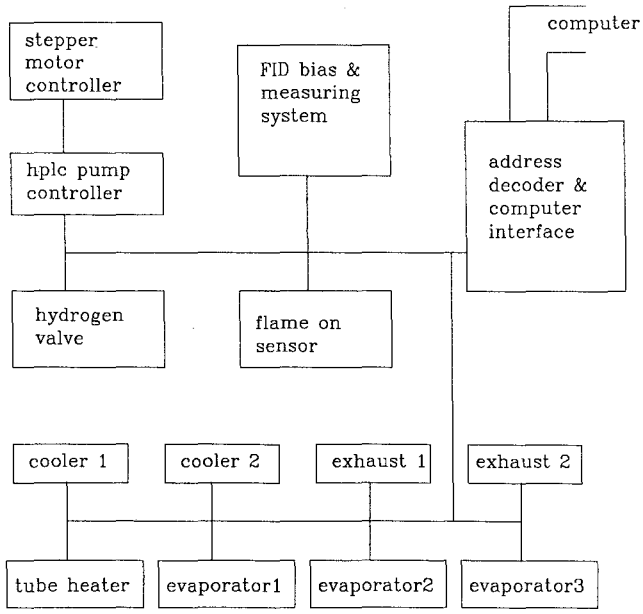

Fig. 4. Block diagram of major elements of the control system used to operate the transport detector under computer control.

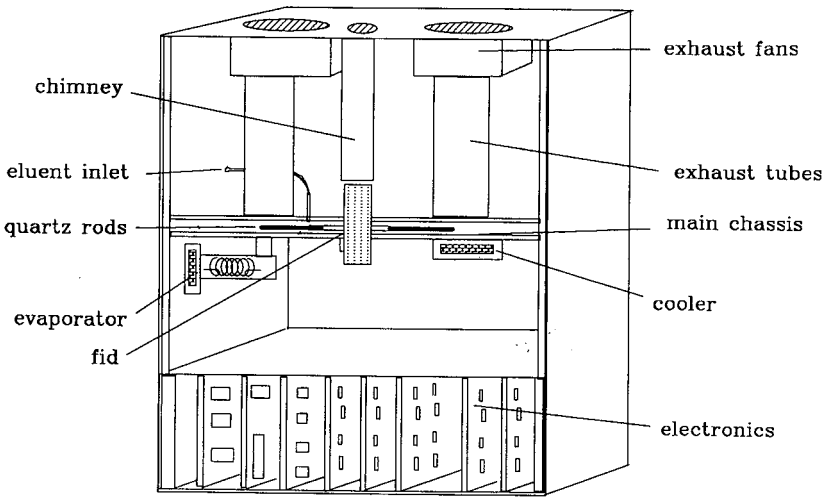

Fig. 5. Outline of the prototype detector showing the major components of the detector system.

min^{-1}. The detector was operated with the following parameters: eluent temperature, 55°C; evaporator 1: speed, 98%; temperature, 120°C; evaporator 2: speed, 68%; temperature, 130°C; evaporator 3: speed, 56%; temperature, 130°C; detector jacket temperature, 110°C; step speed, *ca.* 1 s/spoke; detector amplifier gain, 33.

RESULTS AND DISCUSSION

The results presented represent initial studies of certain areas of interest associated with a transport detector system. The first question asked of any detector concerns its reproducibility, and results typical of many we have obtained are illustrated in Fig. 6. In this case the peaks arise from four samples each of 10 μg of

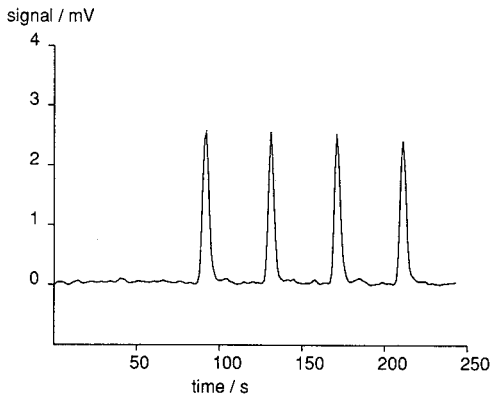

Fig. 6. Chromatographic signals recorded from four successive samples, each containing 10 μg of pyrene in hexane, eluted with hexane–dichloromethane (3:1, v/v).

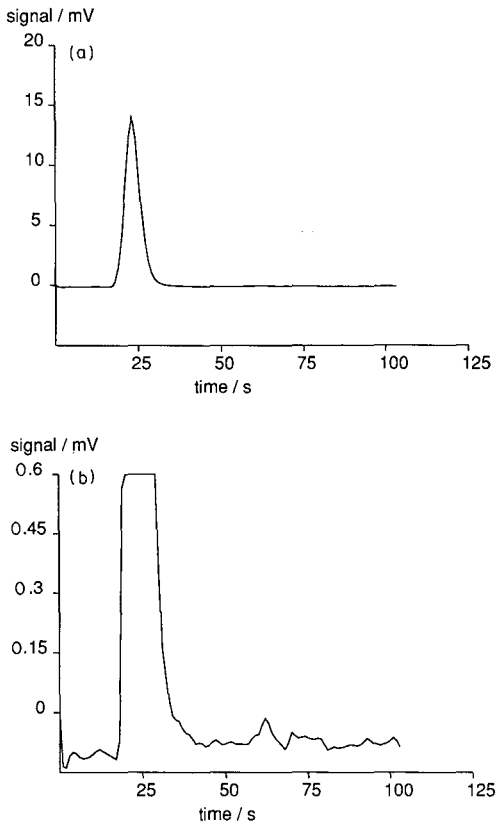

Fig. 7. Demonstration of the minimal carry-over exhibited by the detector. (a) The response from a large sample of Arab heavy oil tar injected directly into the detector (no column). (b) The same record expanded 33-fold: the small carry-over peak is seen at 65 s.

pyrene, and the variance of the peaks shown is better than 2% (and better than 1% for the first three peaks).

Carry-over (*i.e.* material from one component appearing a second time when the spoke re-enters the flame) is another important characteristic of a transport mechanism. Fig. 7 shows the results of injecting a relatively concentrated solution of Arab heavy oil tar (actual concentration unknown, but estimated to result in an injected mass of *ca.* 100 μg). In this case no column was used! Fig. 7a shows the "chromatogram" recorded, and Fig. 7b shows the same data scaled up by a factor of 33. The very small degree of carry-over is shown by the peak at *ca.* 65 s, representing a carry-over of less than 0.5%.

Linearity of response was examined by injecting samples containing 20.8, 10.4, 5.0, 2.6, and 1.04 μg of pyrene. The chromatographic responses are shown in Fig. 8a, and a plot of peak height *vs.* sample mass is shown in Fig. 8b. We believe that 20 μg is sufficient to overload the detector, so the 20-μg point has been ignored in drawing the solid line in Fig. 8b. The correlation coefficient for the solid line drawn was 0.998.

Carbon number response is of particular interest for a detection system based on

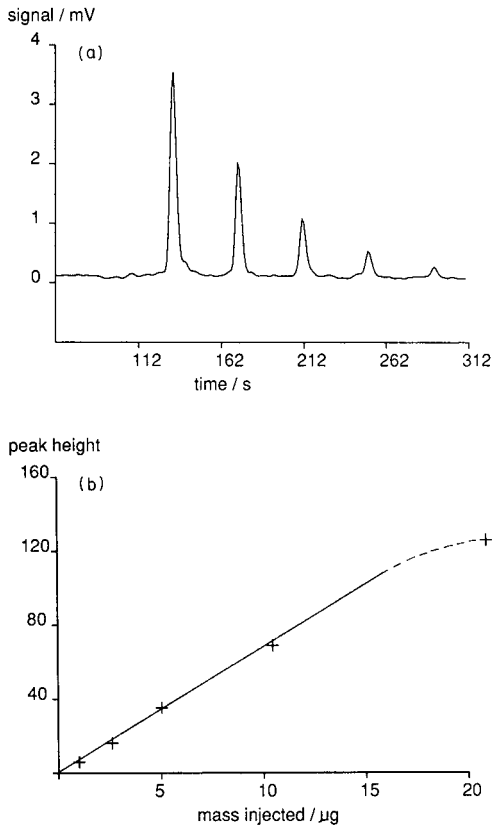

Fig. 8. Linearity of response illustrated by responses from samples containing 20.8, 10.4, 5.0, 2.6, and 1.04 μg of pyrene (eluted as described for Fig. 6): (a) the chromatographic responses; (b) a plot of the peak heights as a function of sample mass.

FID, and this aspect of the performance was examined by injecting 10-μg samples of C12, C14, C16, C20, C24, C28, C32, C36 and C40. The results in Fig. 9 indicate that, under the conditions chosen for this preliminary study, the response is essentially flat down to *ca.* C22, and then falls steadily down to C12. It must be noted that changing the evaporation conditions (fan speeds and temperatures) significantly modifies this response curve, and the one presented does not represent an optimum response curve. Thus we have routinely used the detector for detecting C10 using a hexane eluent under the following detector conditions: eluent temperature, 55°C; evaporator 1: speed, 98%; temperature, 80°C; evaporator 2: speed, 68%; temperature, 90°C; evaporator 3: speed, 56%; temperature, 95°C; detector jacket temperature, 110°C; step speed, *ca.* 1 s/spoke; detector amplifier gain, 33.

As the results of Fig. 7 indicated, we also expect the detector to function with hydrocarbons of substantial molecular weight.

Fig. 10 illustrates a typical chromatogram recorded with the detector. In this case the sample consists of 10 μg each of C36 and pyrene. Analysis of this and similar

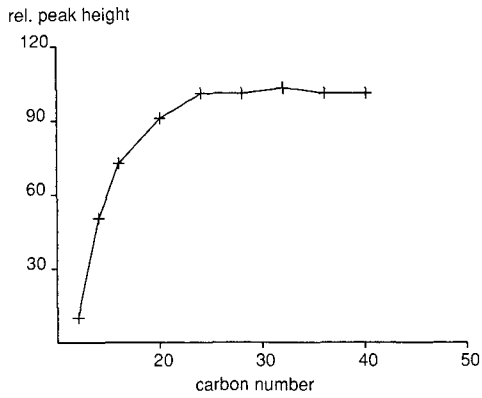

Fig. 9. Response as a function of sample carbon content: the variation of peak height as a function of sample carbon number for 10-μg samples of C12, C14, C16, C20, C24, C28, C32, C36 and C40, all eluted as described for Fig. 6.

chromatograms leads to a preliminary estimate of the limit of detection of the order of 100 ng for either component.

The detector has been in operation for several months and we are confident that the major aspects of the design are sound. We have demonstrated that the detector functions reliably, results in acceptable sensitivity and linearity of response with sample size, exhibits minimal carry-over, and can deal with a useful range of carbon-number samples. There remains a considerable amount of work to be carried out to optimize the detector's performance in relation to the air flow-rates and temperature. However, with the precise control of these parameters available through the use of direct computer control, we hope to demonstrate that the design offers significant advantages over earlier designs of transport detector.

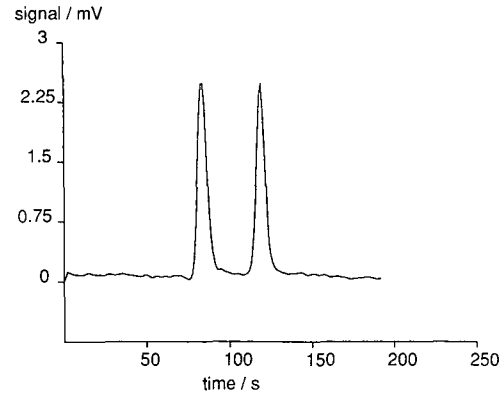

Fig. 10. Typical chromatogram record with the transport detector. Sample of 10 μg each of C36 and pyrene, eluted as described for Fig. 6.

ACKNOWLEDGEMENTS

This work has been supported by BP Sunbury Research Centre, and the authors are grateful for the assistance and encouragement provided by Drs. M. Tricker, I. Roberts, and D. Westlake, DJM-L thanks the Royal Society for support. Patent protection has been sought for some aspects of the instrument described above. Commercial versions of a transport detector similar to that described in this paper are available from Applied Chromatography Systems Ltd., The Arsenal, Heapy Street, Macclesfield, Cheshire SK11 7JB, U.K.

REFERENCES

1 M. T. Gilbert, *High Performance Liquid Chromatography*, Wright, Bristol, 1987.
2 E. Haahti and T. Nikarri, *Acta Chem. Scand.*, 17 (1963) 2565.
3 J. E. Stouffer, T. E. Kersten and P. M. Kruger, *Biochim. Biophys. Acta*, 93 (1964) 191.
4 A. Karmen, *Anal. Chem.*, 38 (1966) 286.
5 E. Haahti, T. Nikarri and J. Karkkainen, *J. Gas Chromatogr.*, 4 (1966) 12.
6 J. E. Stouffer, P. L. Oakes and J. E. Schlatter, *J. Gas Chromatogr.*, 4 (1966) 89.
7 A. Karmen, *Sep. Sci.*, 2 (1967) 287.
8 R. H. Stevens, *J. Gas Chromatogr.*, 6 (1968) 375.
9 E. Foster and A. H. Weiss, *J. Chromatogr. Sci.*, 9 (1971) 266.
10 S. Lieberman, *U.S. Pat.* 3 128 619 (1964).
11 H. W. Johnson Jr., E. E. Seibert and F. H. Stross, *Anal. Chem.*, 40 (1968) 403.
12 A. Karmen, L. D. Kane, M. Karasek and B. Lapidus, *J. Chromatogr. Sci.*, 8 (1970) 439.
13 I. M. Savinov, Y. I. Yashin, V. I. Zhigalev and V. G. Berezkin, *U.S.S.R. Pat.*, 366 410 (1973); *C.A.*, 78 (1973) 606.
14 N. P. Burnev, A. A. Balaukin, B. G. Vtorov, V. I. Kalmanovskii, I. S. Katashin, G. K. Klimeshov, I. I. Frolov, A. V. Shernov, V. P. Chernokozhin and Y. I. Yashin, *U.S.S.R. Pat.*, 368 542 (1973); *C.A.*, 79 (1973) 572.
15 A. A. Balaukin, B. G. Vtorov, V. I. Kalmanovski and V. P. Chernokozhin, *U.S.S.R. Pat.*, 370 520 (1973); *C.A.*, 79 (1973) 693.
16 A. Stolyhwo, O. S. Privett and W. L. Erdahl, *J. Chromatogr. Sci.*, 11 (1973) 263.
17 J. B. Dixon and R. C. Hall, *U.S. Pat.* 4 271 022 (1981).
18 L. Yang, G. J. Fergusson and M. L. Vestal, *Anal. Chem.*, 54 (1984) 2632.
19 M. Thorpe, W. J. Hoskin and L. Brown, *U.K. Pat.*, 2 184 033 (1986).
20 A. T. James, J. R. Ravenhill and R. P. W. Scott, *Chem. Ind.*, (1964) 746.
21 A. Karmen, *Anal. Chem.*, 36 (1964) 1416.
22 N. G. Anderson and R. H. Stevens, *U.S. Pat.* 3 419 359 (1965).
23 A. Karmen, *J. Gas Chromatogr.*, 3 (1965) 336.
24 R. P. W. Scott, *U.K. Pat.* 998 107 (1965).
25 R. P. W. Scott, *U.K. Pat.* 1 045 801 (1966).
26 T. E. Young and R. J. Maggs, *Anal. Chim. Acta*, 38 (1967) 105.
27 R. P. W. Scott, *J. Chromatogr. Sci.*, 8 (1970) 65.
28 G. Nota and R. Palombari, *J. Chromatogr.*, 62 (1971) 153.
29 B. M. Lapidus and A. Karmen, *J. Chromatogr. Sci.*, 10 (1972) 03.
30 J. H. van Dijk, *J. Chromatogr. Sci.*, 10 (1972) 31.
31 V. Pretorius and J. F. J. van Rensburg, *J. Chromatogr. Sci.*, 11 (1973) 355.
32 K. Slais and M. Krejci, *J. Chromatogr.*, 91 (1974) 181.
33 K. Aitzemuller, *J. Chromatogr. Sci.*, 13 (1975) 454.
34 T. Cotgreave, *Chem. Ind.*, (1966) 689.
35 E. G. Owens II, H. H. Gill, W. E. Hatton and J. G. Cobler, *U.S. Pat.* 3 376 694 (1968).
36 H. Dubsky, *J. Chromatogr.*, 71 (1972) 395.
37 H. Dubsky, *U.S. Pat.* 3 744 973 (1973).
38 J. J. Szakasits, *U.S. Pat.* 3 788 479 (1974).
39 J. J. Szakasits and R. E. Robinson, *Anal. Chem.*, 46 (1974) 1648.
40 D. Fischer and E. G. Kohl, *Ger. Offen.* 2 424 985 (1975).

Journal of Chromatography, 482 (1989) 65–73
Elsevier Science Publishers B.V., Amsterdam — Printed in The Netherlands

CHROM. 21 883

MICROCYLINDER ELECTRODES AS SENSITIVE DETECTORS FOR HIGH-EFFICIENCY, HIGH-SPEED LIQUID CHROMATOGRAPHY

JOHN E. BAUR[a] and R. MARK WIGHTMAN*,[a]
Department of Chemistry, Indiana University, Bloomington, IN 47405 (U.S.A.)
(First received May 16th, 1989; revised manuscript received August 14th, 1989)

SUMMARY

A carbon fiber microcylinder electrode ($r = 3.5$ μm) is used as a detector for high-efficiency and high-speed liquid chromatography. The microcylinder has a detection volume of a few picoliters, and can be placed directly at the outlet frit of the column. With proper positioning equipment, the electrode can be placed at the region of the outlet frit where the separation efficiency is highest. Such selective sampling results in greatly increased measured efficiency over a conventional electrochemical detector when short (4 cm) columns of conventional diameter (3.2 mm) are used. The microcylinder detector is sensitive and subpicomole detection limits are obtained in less than 30 s for norepinephrine. The need for expensive positioning equipment is eliminated by mounting the electrode into a fitting which can be mated directly with the column.

INTRODUCTION

In situations such as microdialysis experiments where large numbers of chemically labile samples are collected in a short time, very rapid separation and analysis of these samples is desirable. In order to achieve these high-speed separations, high-efficiency columns with small volumes are required[1–5]. In addition to the decreased analysis time, columns with small volumes result in reduced mobile phase consumption and increased sensitivity because the solutes are not diluted to the extent they would be in a conventional column. However, in order to realize the potential of high-speed separations, detectors with very low detection volumes and very rapid response times are required. In this paper we report the use of 4 cm × 3.2 mm I.D. analytical cartridge columns to achieve rapid separations while meeting the detector requirements with carbon-fiber electrodes.

Microelectrodes have several advantages that make them ideal detectors for such high-speed separations. As a consequence of their small dimensions (μm),

[a] Present address: Department of Chemistry, University of North Carolina at Chapel Hill, Chapel Hill, NC 27599-3290, U.S.A.

0021-9673/89/$03.50

detection volumes are very small. The diffusion layer (δ) for a microcylinder electrode under quasi-steady-state conditions is given by

$$\delta = r_0 \ln [2(D_m t)^{\frac{1}{2}}/r_0]$$

where r_0 is the electrode radius (3.5 μm in this experiment), D_m is the diffusion coefficient for the analyte (*ca.* $5 \cdot 10^{-6}$ cm^2 s^{-1}) and t is the time of the experiment[6]. For a 5-s peak, the dimension of the solution sampled is *ca.* 15 μm, thus, for a 50-μm long cylindrical electrode, the detection volume is 35 pl. Additionally, the microelectrode can be directly mated with the column outlet, eliminating any extra-column band broadening from connecting tubing. This advantage has been exploited by Jorgensen and others in capillary liquid chromatography[7–13]. If the microelectrode is much smaller than the outlet of the column, the region of highest efficiency can be selectively sampled, increasing the measured efficiency[14]. Noise for electrochemical detectors is related to the electrode capacitance which is directly proportional to the area[15–17]. Therefore, even though small electrodes result in small currents, less noise is expected as well. The low capacitance also leads to a rapid detector response time. Finally, microelectrodes are less sensitive to flow variations than conventional electrochemical detectors[18].

In this paper we demonstrate that single carbon-fiber electrodes are useful for the detection of catecholamines following rapid separation. Liquid chromatography with electrochemical detection has become the major method for the determination of catecholamines and related compounds[19–23]. The combination of the spatial selectivity and high sensitivity of the carbon-fiber microcylinder with high-speed chromatography increases the usefulness of this technique. Here we report the determination of trace amounts of catecholamines in under 1 min.

EXPERIMENTAL

Chromatographic system

A syringe pump (Model μLC-500, Isco, Lincoln, NE, U.S.A.) was used to deliver the mobile phase to the system through a pneumatically actuated loop injector with a 10-μl internal loop (Model 3XL, Scientific Systems, State College, PA, U.S.A.). An old 4-cm column placed before the loop injector was used as an in-line filter. Analytical cartridge columns with 3-μm RP-18 packing were obtained from Brownlee Labs. (Santa Clara, CA, U.S.A.). The detector was either a carbon-fiber microcylinder electrode placed directly at the exit frit of the column with a micropositioner[14], or a microcylinder electrode permanently mounted into a plastic fitting (see below). For comparison, a commercially available thin-layer amperometric detector was employed with a 5-ml spacer (Model TL8A, Bioanalytical Systems, West Lafayette, IN, U.S.A.) and connected to the column with 4 cm of 0.01-in. I.D. tubing.

An IBM personal computer with a Labmaster board (Scientific Solutions, Solon, OH, U.S.A.) was used to collect data and to open and close the loop injector. In order to inject a symmetrical bolus of solute, the loop injector was returned to the "load" position before the entire sample passed through the loop. The injection time was adjusted so that 7 μl were injected regardless of flow-rate. Chromatographic

figures of merit were evaluated with statistical moments using the exponentially modified Gaussian model[24].

The potentiostat used was of local design and construction. In order to measure subpicoampere currents required for low concentrations with the microcylinder electrode an AD 310J varactor bridge operational amplifier (Analog Devices, Norwood, MA, U.S.A.) was used in the current-to-voltage convertor. The feedback resistor was a 1 GΩ, 1% precision resistor, and the potentiostat time constant was 180 ms. For curent measurements with the thin-layer detector, a potentiostat with a 1 MΩ feedback resistor and 35 ms time constant was used. Detection limits were defined as signal-to-noise (S/N) = 3. Measurements were taken at 0.7 or 0.8 V *vs.* the saturated sodium chloride electrode (SSCE).

Electrodes

Microelectrodes were prepared by aspirating carbon fibers into glass capillaries and pulling the glass around the fibers with a capillary puller (Narisige, Tokyo, Japan). The fibers were then sealed with epoxy (Epon 828 with metaphenylenediamine as crosslinking agent, Miller-Stephenson, Canbury, CT, U.S.A.)[6]. Electrodes were either *ca.* 50 or 100 μm in length with a nominal radius of 3.5 or 5 μm, respectively. The electrodes were electrochemically pre-treated daily by applying a potential of 1.8 V *vs.* SSCE for 30 s.

Permanently mounted microcylinder

The center of a Mini-tight fitting (Upchurch Scientific, Oak Harbor, WA, U.S.A.) was enlarged to accommodate a microcylinder electrode (1.2 mm O.D.) with a drill bit large enough to allow passage of eluent around the electrode walls (Fig. 1). A hole perpendicular to the fitting axis was drilled from the fitting grip to the center hole into which was inserted a 1/16-in. tubing to serve as the drain to waste. Perpendicular to this, another hole was drilled into which the platinum wire auxiliary electrode was placed. The central hole was expanded from the top of the fitting to the perpendicular exit hole so that tubing with an I.D. equal to the electrode O.D. could be

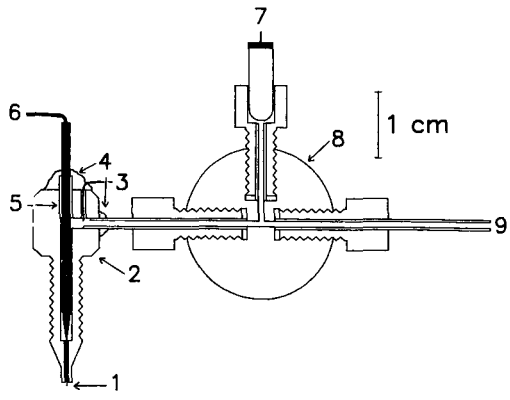

Fig. 1. Permanently mounted microcylinder detector: 1 = microcylinder carbon-fiber working electrode; 2 = minitight end fitting; 3 = platinum wire auxiliary electrode; 4 = clear silicone sealant; 5 = guide/seal tube; 6 = hook-up wire for working electrode; 7 = SSCE reference electrode; 8 = tee; 9 = tubing to waste.

placed. This tubing served both as a guide for inserting the electrode into the fitting and as a seal, forcing flow out of the exit hole. Electrodes and tubing were held in place and sealed with clear silicone sealant (General Electric, Waterford, NY, U.S.A.). The reference electrode was placed in a tee through which the eluent flowed.

Reagents

All chemicals were used as received from commercial sources. Except where noted, the mobile phase consisted of 0.1 m*M* disodium EDTA, 1.0 m*M* octyl sodium sulphate, and 0.2 *M* monobasic sodium phosphate. All solutions were prepared in doubly distilled, deionized water and filtered with 0.45-μm paper (Gelman Sciences, Ann Arbor, MI, U.S.A.). Samples were stored in 0.1 *M* perchloric acid and dilutions were carried out so that the final perchloric acid concentration was 0.001 *M*. Test compounds included norepinephrine (NE), epinephrine (E), and 3,4-dihydroxybenzylamine (DHBA). Bovine adrenal medullary chromaffin cells were used as a test system for biological applications of this system. The cells were prepared and cultured using published procedures[25].

RESULTS AND DISCUSSION

Column characterization

The calculated and the experimentally determined radial concentration distributions of the 4-cm column are shown in Fig. 2. As before[14] a large deviation of the experimental from the theoretical concentration distribution is observed, indicative of an uneven distribution of solutes onto the column. However, there is less evidence of channeling at this column than at the 10-cm column studied previously.

Similar to the findings reported for the 10-cm column, the efficiency for the 4-cm column is greatest at the column center (h = 1.9) and decreases substantially as the wall is approached (h = 4.2 at 1.0 mm from the center). Also, the retention time is 5% greater near the column wall than at the column center. Most significantly, the regions

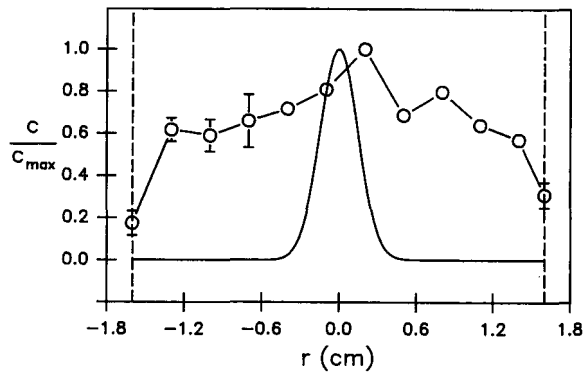

Fig. 2. Radial concentration distribution (normalized by maximal concentration, c_{max}) of DHBA on 4-cm column. Open circles, experimentally determined distribution; solid line, calculated concentration distribution for point injection (σ_r = 0.15 mm). The walls of the column are denoted by the vertical dashed lines. Flow-rate, 0.4 ml/min.

of highest efficiency, fastest flow, and highest concentration occur near the same radial position.

As the electrode was raised above the column frit, the observed efficiency at the center of the 4-cm column was nearly constant for a distance of 0.6 mm. Thus, as with a 10-cm column[14], a 0.6-mm fiber could be used without loss of efficiency. With a longer fiber, however, the increase in electrode area and the accompanying electrochemical noise have been found to offset the advantage of increased faradaic current.

The dependence of the reduced axial plate height on the reduced linear velocity for a 4-cm column is shown in Fig. 3. The open circles are the response of the centrally located microcylinder electrode and the closed circles are the response of the thin-layer detector. The data show that the thin-layer detector is clearly unsatisfactory at optimum chromatographic flow-rates because it acts as a mixing chamber. The optimum reduced velocity of *ca.* 2.6 using the microcylinder electrode (corresponding to a volume flow-rate of 0.2 ml min^{-1}) falls within the expected range ($2 < v < 10$)[28]. The minimum reduced axial plate height of 3.2 observed using the microcylinder electrode indicates that the column is well packed at its center.

Fast, high-efficiency chromatography

To investigate the possibility of achieving fast separations with high efficiency, a reduced linear velocity of 20 was chosen as a reasonable compromise between separation time and efficiency. This velocity corresponds to a flow-rate of 0.6 ml min^{-1}, and the column volume is passed in *ca.* 13 s. The maximum pressure required at this relatively moderate flow-rate for the columns studied is *ca.* 1600 p.s.i. (Note that this includes the pressure drop across the inline filter.) Therefore, the conditions required for these separations are easily attained with simple equipment.

Fig. 4A shows the separation of 70 pmol of each of eight compounds, with baseline resolution of all (except DHBA and homovanillic acid) in less than 50 s. The feature on the dopamine peak is unique to this test mixture and is observed to vary with radial position. For comparison, the chromatogram of the same mixture on the same column with the thin-layer detector is shown in Fig. 4B.

Conventional detectors sample the entire eluate exiting the column, giving a weighted average of the individual efficiencies across the column outlet[14]. The microelectrode, however, can be placed at the region of the column where the efficiency is highest, discarding the fraction of the eluate in which the solute is most dispersed.

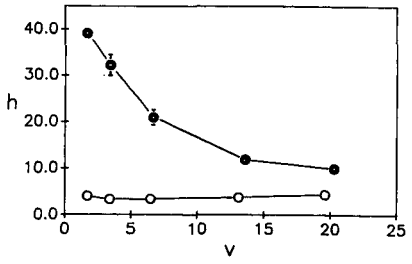

Fig. 3. Dependence of reduced axial plate height on reduced linear velocity at the center of the outlet of a 4-cm column for 70 pmol NE. (○) microcylinder electrode; (●) thin-layer electrochemical detector.

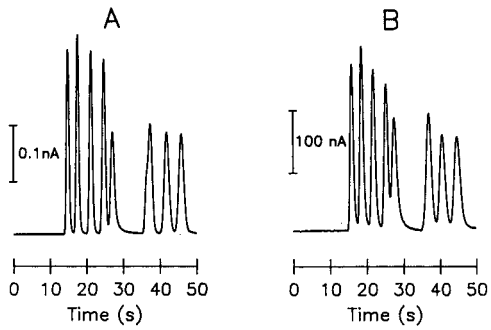

Fig. 4. Chromatogram of 70 pmol each of L-3,4-dihydroxyphenylalanine, 3,4-dihydroxyphenylacetic acid, epinephrine, DHBA, homovanillic acid, dopamine, metanephrine, and epinine (in order of elution) with (A) centrally located microcylinder electrode, (B) thin-layer electrochemical detector. Flow-rate, 0.6 ml min^{-1}.

Shown in Table I are the improvements in measured efficiency for a centrally located microelectrode over a thin-layer amperometric detector for three different compounds. The improvement is especially dramatic at this moderate linear velocity due to the dead volume of the thin-layer amperometric detector. When compared to the results previously reported for the 10-cm column[14], it is apparent that the microelectrode provides greater increase in efficiency over the thin-layer detector in applications which involve short retention times.

Analytical use of the microcylinder

It is because of their extremely small size relative to the chromatographic column that microcylinders can be used to probe spatial heterogeneities at the column outlet. This is also the reason low detection limits can be obtained even though only a very small fraction of the eluate is sampled by the electrode. For electrodes of all size, the amount of noise generated is proportional to the electrode area, yet the current signal for microelectrodes is proportional only to the radius of the electrode[15]. The signal-to-noise ratio, then, increases with decreasing electrode size. With the ability to measure very small current (subpicoampere) therefore comes the ability to detect small amounts of material (subpicomole).

As shown in Fig. 5, subpicomole detection limits can be obtained using microcylinders at the center of the outlet of 4-cm columns (open squares). Comparable

TABLE I

COMPARISON OF NUMBER OF THEORETICAL PLATES (PER METRE) FOR A CENTRALLY LOCATED MICROCYLINDER ELECTRODE AND A THIN-LAYER ELECTROCHEMICAL DETECTOR

Column, 4 cm × 3.2 mm I.D., flow-rate, 0.6 ml min^{-1}.

Compound	*Microcylinder*	*Thin layer*	*Increase (%)*
NE	172 000	55 300	210
E	176 000	61 600	190
DHBA	171 000	56 400	200

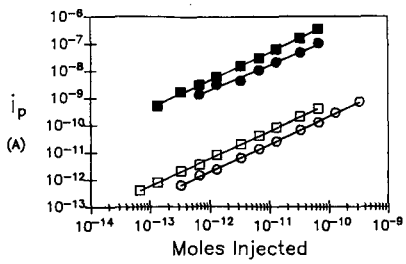

Fig. 5. Calibration curve for NE. Squares, 4-cm column; circles, 10-cm column; filled symbols, thin-layer amperometric detector; open symbols, centrally located microcylinder electrode.

detection limits are also obtained with the thin-layer detector (filled squares). Detection limits with the 4-cm column are nearly an order of magnitude lower than with a 10-cm column of the same diameter[14] because the solute is diluted to a lesser extent as it elutes. Additionally, the efficiency and concentration maxima occur at the same radial position for the 4-cm column, unlike the 10-cm column where the concentration and efficiency maxima are widely separated[14].

An example of the utility of this technique is shown in Fig. 6. Here catecholamines released from bovine chromaffin cells following 5-min nicotine stimulation have been determined with the system described in this paper (Fig. 6A) and compared to a conventional separation system consisting of a thin-layer electrochemical detector and a 25-cm reverse-phase column (Biophase, Bioanalytical Systems, West Lafayette, IN, U.S.A.) (Fig. 6B). The 4-cm column allows separation and quantitation within 30 s whereas separation of the same mixture on the 25-cm column requires 6 min. As a consequence of the small internal volume of the 4-cm column, injections of large amounts of acid (0.1 *M* $HClO_4$ as is typically used to lyse the cells) can have detrimental effects on the peak shapes of eluting compounds. It has been found that this effect can be avoided when volumes less than 7 μl of the sample are injected onto the column.

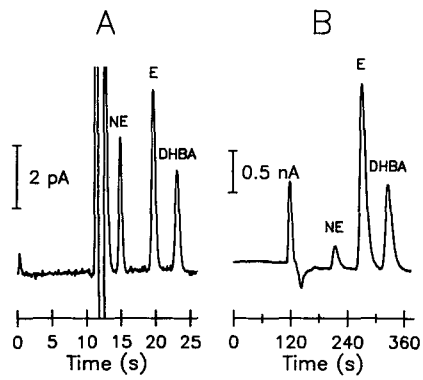

Fig. 6. Separation of total catecholamines in bovine chromaffin cells following 5-min nicotine stimulus: (A) 4-cm column with centrally located microelectrode, flow-rate = 0.6 ml min^{-1}; (B) 25-cm column flow-through electrochemical detector, flow-rate = 1.15 ml min^{-1}, mobile phase 0.1 *M* citric acid–10% methanol–0.6 m*M* sodium octyl sulfate–0.1 m*M* disodium EDTA, adjusted to pH 4.2 with NaOH.

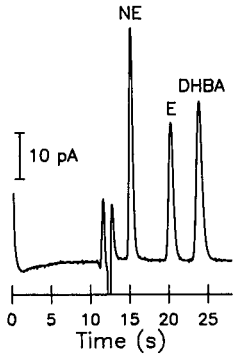

Fig. 7. Chromatogram of 7 pmol each of NE, E, and DHBA with permanently mounted microcylinder electrode. Flow-rate, 0.6 ml min^{-1}.

Permanently mounted microcylinder

The positioning equipment required to make the measurements described in this paper is costly and not available in many laboratories. Therefore, it is desirable to combine the advantages offered with the microcyliner with the ease of a one-piece detector. Such a detector is shown in Fig. 1. A microelectrode is permanently mounted inside a Mini-tight connector that has been drilled out to accommodate moble-phase flow past the electrode barrel. The eluent then flows by the auxiliary electrode and the reference electrode to waste. The electrode extends past the Mini-tight connector so that the tip of the electrode is suspended just above the frit at the center of the column. Recall that the electrode can be placed 0.6 mm from the column frit without significant losses in measured efficiency. Solutes that elute near the edge of the column, where efficiency is less, do not reach the electrode surface, and, thus, do not contribute to the band broadening observed at this detector.

Fig. 7 shows a chromatogram recorded using the permanently mounted microcylinder electrode. The efficiency evaluated in plates per metre was twice that found with the conventional detector. This detector out-performs the thin-layer detector because of the low detection volume and selective placement of the microcylinder. However, the efficiency is not as good as measured with the electrode positioned with micromanipulators. This is because the permanently mounted electrode cannot be placed exactly at the position where the efficiency is the highest.

CONCLUSIONS

The major advantages of coupling microcylinder electrodes with liquid chromatography are spatially selective sampling and the extremely small dead volume of the electrode. Yet even though a very small fraction of the eluate is sampled, subpicomole detecton limits can be attained because of the low noise of the electrode. This means that when microelectrodes are coupled with short columns and relatively fast flow-rates, complex mixtures can be separated in less than 1 min. The need for expensive positioning equipment can be eliminated by permanently mounting the microelectrode into an end-fitting that easily can be coupled with any liquid chromatography column. With smaller columns and better control of the separation,

even faster high-efficiency separations are possible. In addition, electrochemical techniques used with conventional electrodes (pulsed techniques, multiple electrodes, and reductive potentials, etc, see ref. 29 for an overview) may be used with the miniaturized detector to extend these advantages to analytes other than catecholamines.

ACKNOWLEDGEMENTS

The authors thank Jeff Jankowski for providing the bovine chromaffin sample. The research was supported by the National Institutes of Health (PHS R01-NS15841).

REFERENCES

1 L. R. Snyder and J. J. Kirkland, *Introduction to Modern Liquid Chromatography*, Wiley, New York, 2nd ed., 1979, Ch. 5.
2 J. J. Kirkland, W. W. Yau, J. J. Stoklosa and C. H. Dilks, Jr., *J. Chromatogr. Sci.*, 15 (1977) 303–316.
3 N. H. C. Cooke, B. G. Archer, K. Olsen and A. Berick, *Anal. Chem.*, 54 (1982) 2277–2283.
4 J. F. Reinhard, Jr. and J. A. Perry, *J. Liq. Chromatogr.*, 7 (1984) 1211–1220.
5 M. E. Dwyer and P. R. Brown, *J. Liq. Chromatogr.*, 10 (1987) 1769–1787.
6 R. M. Wightman and D. O. Wipf, in A. J. Bard (Editor), *Electroanalytical Chemistry*, Marcel Dekker, New York, 1988, vol. 16.
7 L. A. Knecht, E. J. Guthrie and J. W. Jorgenson, *Anal. Chem.*, 56 (1984) 479–482.
8 J. G. White and J. W. Jorgenson, *Anal. Chem.*, 58 (1986) 2992–2995.
9 J. G. White, R. L. St. Claire III and J. W. Jorgenson, *Anal. Chem.*, 58 (1986) 293–298.
10 R. T. Kennedy, R. L. St. Claire III, J. G. White and J. W. Jorgenson, *Mikrochim. Acta*, 1987 (II) (1988) 37–45.
11 M. D. Oates and J. W. Jorgenson, *Anal. Chem.*, 61 (1989) 432–435.
12 R. T. Kennedy and J. W. Jorgenson, *Anal. Chem.*, 61 (1989) 436–441.
13 M. Goto and K. Shimada, *Chromatographia*, 21 (1986) 631–634.
14 J. E. Baur, E. W. Kristensen and R. M. Wightman, *Anal. Chem.*, 60 (1988) 2334–2338.
15 S. G. Weber and J. T. Long, *Anal. Chem.*, 60 (1988) 903A–913A.
16 S. G. Weber and W. C. Purdy, *Anal. Chim. Acta*, 100 (1978) 531–544.
17 R. M. Wightman, *Science (Washington, D.C.)*, 240 (1988) 415–420.
18 W. L. Caudill, J. O. Howell and R. M. Wightman, *Anal. Chem.*, 54 (1982) 2532–2535.
19 I. J. Mefford, *J. Neurosci. Meth.*, 3 (1981) 207–224.
20 P. T. Kissinger, *Anal. Chem.*, 49 (1977) 447A–456A.
21 P. T. Kissinger, C. J. Refshauge, R. Dreiling and R. N. Adams, *Anal. Lett.*, 6 (1973) 465–477.
22 P. T. Kissinger, *Anal. Chem.*, 54 (1982) 1417A–1434A.
23 A. M. Krstulovic and H. Colin, *Trends Anal. Chem.*, 2 (1983) 42–49.
24 J. P. Foley and J. G. Dorsey, *Anal. Chem.*, 55 (1983) 730–737.
25 S. P. Wilson and O. H. Viveros, *Exp. Cell. Res*, 133 (1981) 159–169.
26 J. H. Knox, G. R. Laird and P. A. Raven, *J. Chromatogr.*, 122 (1976) 129–145.
27 C. H. Eon, *J. Chromatogr.*, 149 (1978) 29–42.
28 P. A. Bristow and J. H. Knox, *Chromatographia*, 10 (1977) 279–289.
29 D. C. Johnson, S. G. Weber, A. M. Bond, R. M. Wightman, R. E. Shoup and I. S. Krull, *Anal. Chim. Acta*, 180 (1986) 187–250.

Journal of Chromatography, 482 (1989) 75–85
Elsevier Science Publishers B.V., Amsterdam — Printed in The Netherlands

CHROM. 21 872

PARTICLE BEAM LIQUID CHROMATOGRAPHY–ELECTRON IMPACT MASS SPECTROMETRY OF DYES[a]

JEHUDA YINON*[,b], TAMMY L. JONES and LEON D. BETOWSKI
U.S. Environmental Protection Agency, Environmental Monitoring Systems Laboratory, P.O. Box 93478, Las Vegas, NV 89193-3478 (U.S.A.)
(First received April 4th, 1989; revised manuscript received June 9th, 1989)

SUMMARY

A liquid chromatograph was interfaced with a triple quadrupole mass spectrometer by means of a particle beam-type interface. The system was used for the analysis and characterization by electron impact mass spectra of a series of commercial dyes. The pure dyes were separated from their impurities with a reversed-phase C_{18} column using methanol–water as the mobile phase. Detection limits were determined using the system as a single quadrupole mass spectrometer. Sensitivity for dyes was found to be two to three orders of magnitude worse than with thermospray ionization using a wire repeller. Characterization of the azo dyes could be achieved by observing typical fragment ions formed by cleavage of the N–C and C–N bond on either side of the azo linkage and/or cleavage of the N=N double bond with transfer of two hydrogen atoms to form an amine.

INTRODUCTION

Dyestuffs are of major environmental interest because of their widespread use as colorants in a variety of products, such as textiles, paper, leather, gasoline and foodstuffs. Synthetic intermediates, byproducts and degradation products of these dyes could be potential health hazards owing to their toxicity and/or carcinogenicity.

Several methods have been developed for the identification and determination of these dyes in order to monitor environmental contamination. Thermospray high-performance liquid chromatography–mass spectrometry (TSP-LC–MS) has been found to be a suitable technique for the analysis of the non-volatile dyes[1–7]. It is sensitive, specific and the ionization process is soft. One of the drawbacks of TSP-LC–MS is that one obtains mainly molecular and adduct ions and this information

[a] Although the research described in this paper was supported by the U.S. Environmental Protection Agency, it has not been subjected to Agency review and, therefore, does not necessarily reflect the views of the Agency, and no official endorsement should be inferred. Mention of trade names or commercial products does not constitute endorsement or recommendation for use.

[b] EPA Visiting Scientist. On sabbatical leave from the Weizmann Institute of Science, Rehovot, Israel (present address).

0021-9673/89/$03.50

AZO CLASS

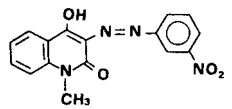

1. Disperse Yellow 5
C.I. 12790

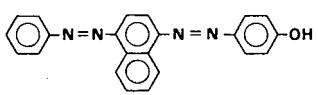

2. Disperse Orange 13
C.I. 26080

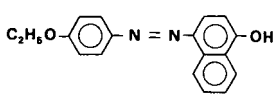

3. Solvent Red 3
C.I. 12010

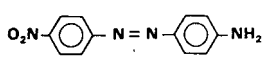

4. Disperse Orange 3
C.I. 11005

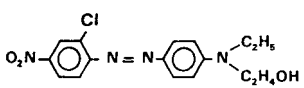

5. Disperse Red 13
C.I. 11115

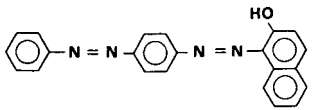

6. Solvent Red 23
C.I. 26100

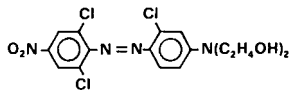

7. Disperse Brown 1
C.I. 11152

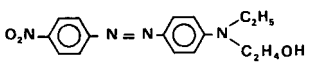

8. Disperse Red 1
C.I. 11110

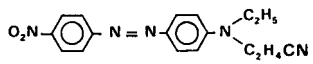

9. Disperse Orange 25
C.I. 11227

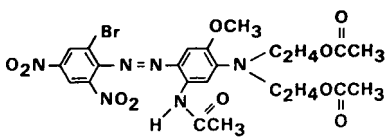

10. Disperse Blue 79
C.I. None

ARYLMETHANE CLASS

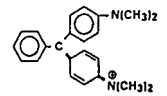

11. Basic Green 4
C.I. 42000

ANTHRAQUINONE CLASS

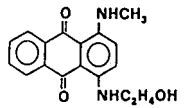

12. Disperse Blue 3
C.I. 61505

COUMARIN CLASS

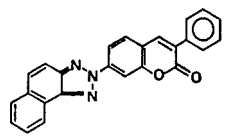

13. Fluorescent Brightener 236
C.I. None

XANTHENE CLASS

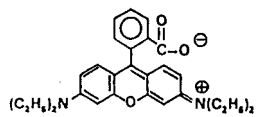

14. Solvent Red 49
C.I. 45170.1

may not be sufficient for structural elucidation of dyes of unknown structure. While tandem mass spectrometry (MS–MS) has been used to deconvolute fully the structural information contained in the TSP mass spectra of dyes[1,3], it would be of great utility to analyze dyes with a single quadrupole LC–MS system and obtain structural information.

In order to assess the characteristics of such a system, we have interfaced a liquid chromatograph by means of an Extrel ThermaBeam LC–MS interface to a Finnigan quadrupole mass spectrometer. The ThermaBeam is a particle beam-type interface, using a solute transport–enrichment technique, between the chromatograph and the mass spectrometer (PB-LC–MS)[8]. In the ThermaBeam interface, a thermal concentric nebulizer is used which combines nebulization and desolvation. While the nebulization process serves to increase the surface area per unit mass of the liquid effluent, the desolvation process serves to evaporate the volatile solvent components in the effluent, while leaving the solute components in the particulate state. The resulting aerosol is accelerated through two stages of pressure reduction and axial nozzles, to produce a solvent-depleted particle beam, exploiting the momentum differences in the expanding aerosol beam.

The PB-LC–MS system was used for the analysis of a series of commercial dyes, including detection limits and electron impact (EI) mass spectra. The system was mostly used as a single quadrupole mass spectrometer.

EXPERIMENTAL

Materials

The following dyestuffs, identified by their Color Index (C.I.), name and number, were obtained from the sources indicated and were used without further purification: 1–6, 8, 9, 11 and 14 (Aldrich, Milwaukee, WI, U.S.A.); 7, 10 and 13 (Sandoz Colors and Chemicals, Charlotte, NC, U.S.A.); and 12 (Ciba Geigy Dyestuffs and Chemicals Division, Greensboro, NC, U.S.A.).

Dyes were dissolved in an appropriate solvent prior to analysis: dyes 1, 3–5, 7, 9 and 14 in acetonitrile–water (50:50), 2, 8, 10 and 11 in methanol, 6 and 12 in acetonitrile and 13 in methylene chloride–acetonitrile (50:50).

Instrumentation

The mass spectrometer was a Finnigan-MAT Triple Stage Quadrupole (TSQ) equipped with a 4510 EI source. The PB-LC–MS interface was an Extrel Corporation ThermaBeam interface, fitted to the ion source by a laboratory-made adaptor as shown in Fig. 1. This heatable adaptor, made mainly of Vespel (DuPont) and partly

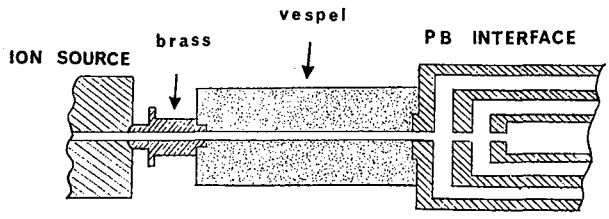

Fig. 1. PB-LC–MS interface adapter.

of brass, was heated to 200–250°C. The ion source was operated at 240°C. The filament emission current was 0.3 mA, electron energy 70 eV and electron multiplier voltage 1600 V. The preamplifier sensitivity was set at 10^{-8} A/V. The ThermaBeam nebulizer temperature was 210–240°C; this temperature varied with the composition of the mobile phase gradient. The ThermaBeam expansion chamber temperature was 95°C. The HPLC system consisted of a Spectra-Physics SP8700XR solvent-delivery system with a Rheodyne Model 7125 injector valve fitted with a 10-μl sample loop. A Varian MicroPak MCH-5-N-CAP C_{18} column (15 cm × 4 mm I.D.) was used. The chromatograph was operated in the gradient mode, starting at a mobile phase of methanol–water (50:50), changing within 5 min to 100% methanol and staying at that level for 10 min. The flow-rate was 0.9 ml/min.

RESULTS AND DISCUSSION

Because the commercial dyes were not pure, each was injected separately into the HPLC system in order to separate the pure dye from the impurities. The limits of detection were obtained by recording the mass chromatograms of characteristic ions of the dyes under full-mass scan, with a signal-to-noise ratio of at least 3:1. Table I presents the detection limits for each dye and their reported commercial purity levels. These detection limits were not corrected for the pure dye content of the materials analyzed and should therefore be regarded as an upper limit that can be obtained for commercial dyestuffs.

The sensitivity of the system was checked by analyzing caffeine. The detection limit was found to be 5 ng, which is in accordance with the Extrel ThermaBeam LC–MS specifications.

Fig. 2–7 show examples of mass chromatograms of some of the dyes. Table II presents a list of the ions observed in the EI mass spectra of the pure dues. Several fragmentation patterns were observed, thus forming characteristic ions: cleavage of

TABLE I

DETECTION LIMITS FOR COMMERCIAL DYES

Dye	*Structure*	*Mol.wt.*	*Dye content(%)*	*Detection limit(μg)*
Disperse Yellow 5	1	324	~30	0.5
Disperse Orange 13	2	352	~15	5.5
Solvent Red 3	3	292	100	0.2
Disperse Orange 3	4	242	~20	0.05
Disperse Red 13	5	348	~25	4.4
Solvent Red 23	6	352	~85	0.5
Disperse Brown 1	7	432	~25	2.7
Disperse Red 1	8	314	~30	0.25
Disperse Orange 25	9	323	~20	0.5
Disperse Blue 79	10	624	100	0.3
Basic Green 4	11	329	~98	0.7
Disperse Blue 3	12	296	~20	0.8
Fluorescent Brightener 236	13	389	100	0.6
Solvent Red 49	14	442	~97	0.5

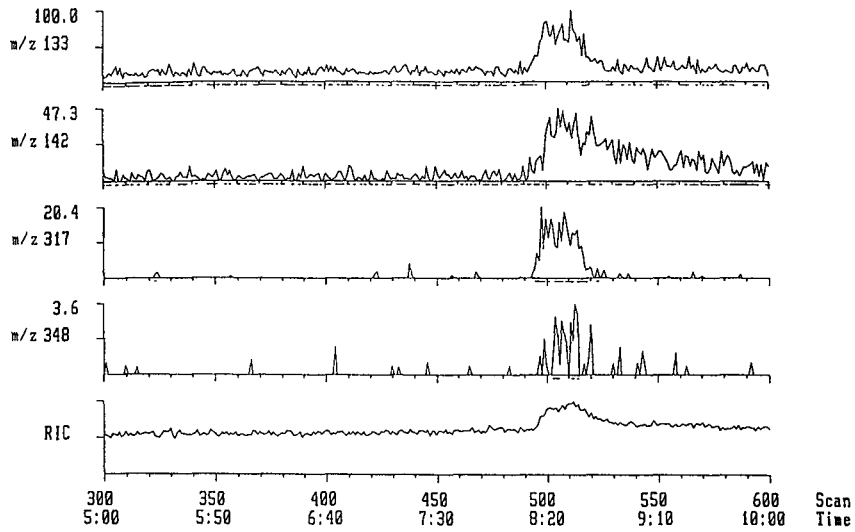

Fig. 2. Reconstructed mass chromatograms and reconstructed total ion current chromatogram (RIC) of Disperse Red 13. Amount injected into the LC–MS system, 4.4 μg. Solvent, acetonitrile–water (50:50).

the double bond between the two N atoms of the azo linkage with transfer of two hydrogen atoms to form an amine. Such cleavage with transfer of one hydrogen atom was reported previously in the secondary ion mass spectra (SIMS) of azo dyes[9], and with transfer of two hydrogen atoms in the EI mass spectrum of 2-methoxyazoben-

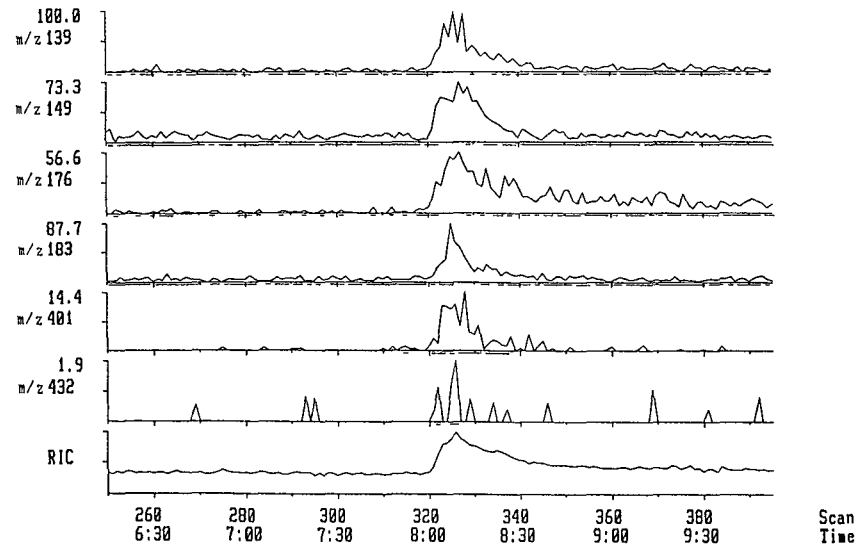

Fig. 3. Reconstructed mass chromatograms and RIC of Disperse Brown 1. Amount injected into the LC–MS system, 10 μg. Solvent, acetonitrile–water (50:50).

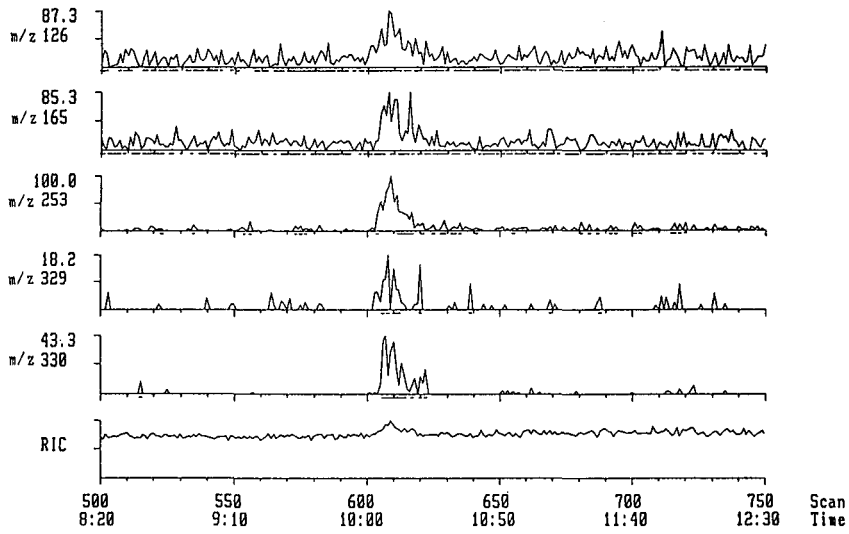

Fig. 4. Reconstructed mass chromatograms and RIC of Basic Green 4. Amount injected into the LC–MS system, 1.4 μg. Solvent, methanol.

zene[10] and in the EI mass spectra of azo dyes[11]. Formed by this process are the ion at *m/z* 138 in Disperse Yellow 5, the ion at *m/z* 93 in Disperse Orange 13, the ion at *m/z* 142 in Disperse Red 13, the ions at *m/z* 197 and 120 in Solvent Red 23, the ions at *m/* 206 and 176 in Disperse Brown 1, the ions at *m/z* 149 and 108 in Disperse Red 1 and the ions at *m/z* 189, 149, and 108 in Disperse Orange 25. Other characteristic frag-

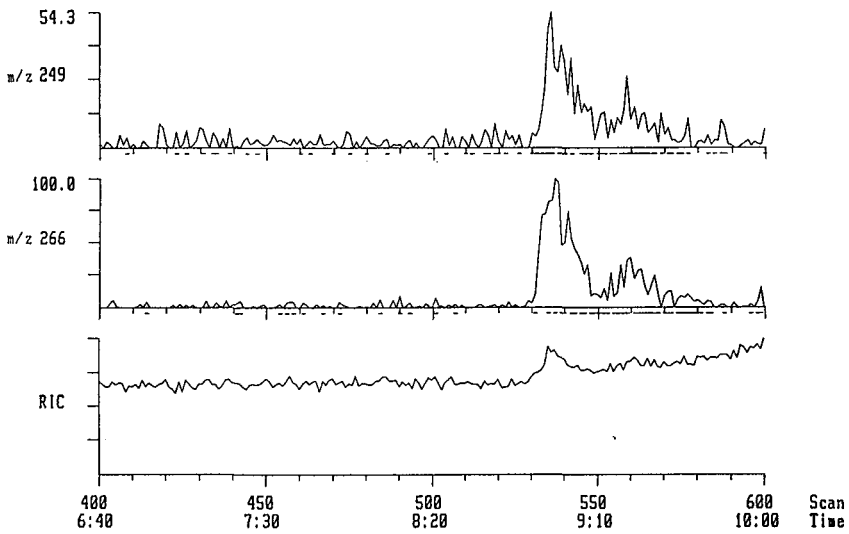

Fig. 5. Reconstructed mass chromatograms and RIC of Disperse Blue 3. Amount injected into the LC–MS system, 0.8 μg. Solvent, acetonitrile.

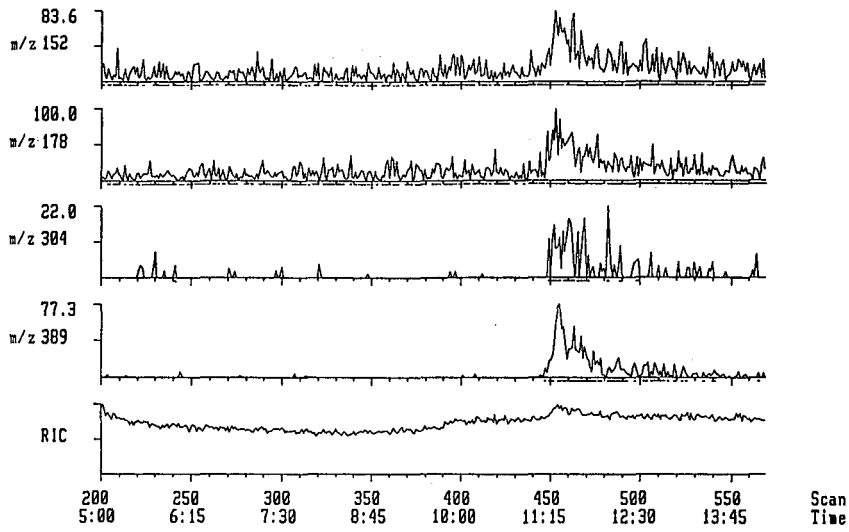

Fig. 6. Reconstructed mass chromatograms and RIC of Fluorescent Brightner 236. Amount injected into the LC–MS system, 0.6 μg. Solvent, methylene chloride–acetonitrile (50:50).

mentations observed in azo dyes were cleavage of the azo C–N bond and the N–C bond on either side of the azo linkage. Both these cleavages were previously observed in azo dyes[11] and in substituted azobenzenes[11,12]

An interesting mass spectrum was observed for Basic Green 4, a cationic dye (Fig. 7). The EI mass spectrum includes an ion at m/z 329 which is the molecular

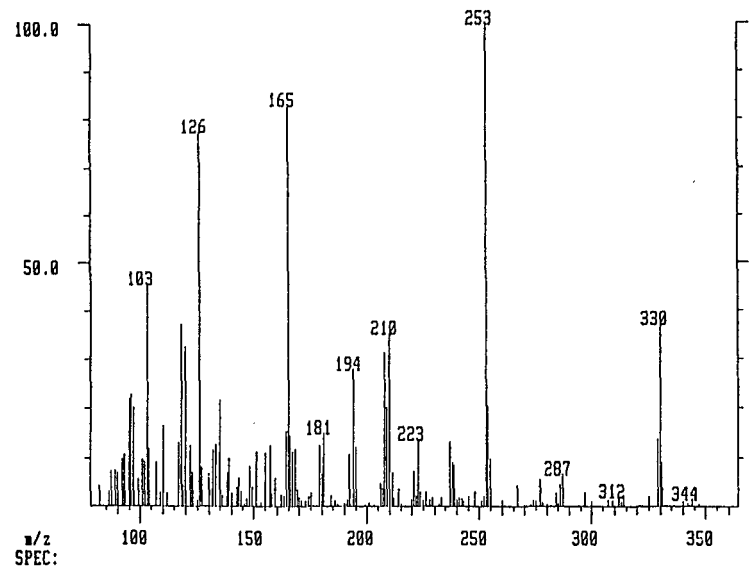

Fig. 7. EI mass spectrum of Basic Green 4, obtained by PB-LC–MS. Amount injected, 1.4 μg. Solvent, methanol. The spectrum was obtained by taking average of sums of spectra of scans 603–612 in the RIC in Fig. 4.

TABLE II

PARTICLE BEAM EI MASS SPECTRA OF DYES

Dye	*Mol.wt.*	*m/z of ions observed (% relative abundance)*
Disperse Yellow 5	324	324(1); 295(1.5); 202(3); 174(7); 138(9); 108(100); 92(17)
Disperse Orange 13	352	352(2); 247(10); 142(26); 115(22); 109(22); 93(100)
Solvent Red 3	292	292(17); 263(3); 235(4); 171(6); 149(9); 143(100); 121(48); 115 (36); 108(18)
Disperse Orange 3	242	242(3); 213(4); 212(10); 120(55); 92(100)
Disperse Red 13	348	317(22); 287(20); 154(17); 144(25); 142(28); 134(25); 133(100); 126(40); 120(30); 105(50); 104(50); 99(20); 92(32); 90(40)
Solvent Red 23	352	352(4); 267(1.5); 197(20); 143(30); 120(46); 115(32); 108(11); 93 (40); 92(100)
Disperse Brown 1	432	432(1.5); 403(15); 402(5); 401(17); 359(5.5); 357(7); 313(5); 214 (15); 208(17); 206(36); 185(40); 183(78); 176(39); 167(32); 149 (77); 139(100); 124(49); 104(82); 90(48)
Disperse Red 1	314	314(4); 297(2); 283(34); 267(11); 253(19); 237(8); 207(9); 180(15); 168(18); 149(15); 147(18); 133(100); 120(49); 108(63); 105(55); 103(47)
Disperse Orange 25	323	323(1); 293(12); 283(7); 253(26); 240(9); 224(3); 189(3); 173(10); 149(20); 133(35); 120(62); 108(31); 105(19); 104(20); 93(18); 92 (100)
Disperse Blue 79	624	87(100)
Basic Green 4	329	330(38); 329(13); 287(8); 255(10); 254(21); 253(100); 237(13); 223 (12); 210(35); 209(20); 208(32); 194(29); 181(15); 165(82); 135 (22); 126(78); 120(32); 118(37); 103(45); 95(22)
Disperse Blue 3	296	267(12); 266(100); 249(49); 234(28); 220(22); 204(11); 194(10); 181(8); 180(9); 165(17); 164(13); 152(22); 139(12); 124(15); 110 (13); 104(19)
Fluorescent Brightener 236	389	390(29); 389(100); 361(19); 333(11); 304(19); 207(75); 206(28); 195(38); 181(26); 180(18); 179(43); 178(82); 165(18); 152(78); 151 (47); 139(35); 127(35); 114(21); 105(30); 102(57)
Solvent Red 49	442	399(18); 398(34); 397(26); 327(18); 326(100); 282(18); 199(20); 184(40); 177(23); 170(23); 163(20); 162(18); 156(32); 149(48); 142 (20); 105(16); 91(19)

cation. The ion at m/z 330, $(M')^+$, is the ion representing the leuco compound, that is, the reduced neutral form of the cationic dye generated by the addition of a hydride ion to the cation. The two ions at m/z 165 and 126 are the doubly charged ions M'^{2+} and $[M' - C_6H_6]^{2+}$, respectively. This was substantiated by recording the collision activated dissociation (CAD) spectra of these two ions. The CAD spectrum of the ion at m/z 165 produces a single ion at m/z 126, which can be explained by the loss of C_6H_6 from the doubly charged M'^+ ion. The CAD spectrum of the ion at m/z 126 is shown in Fig. 8. The most intense daughter ion is at m/z 118. The loss of eight apparent mass units can be explained only by both ions being doubly charged, and therefore the ion at m/z 118 is due to the loss of CH_4 (16 mass units), thus forming the $[M' - C_6H_6 - CH_4]^{2+}$ ion.

The EI mass spectra of dyes obtained with the PB-LC–MS system are similar to the EI spectra obtained by a solid probe in the contents of the fragment ions, but not necessarily in their relative intensities. An example is shown in Figs. 9 and 10, which

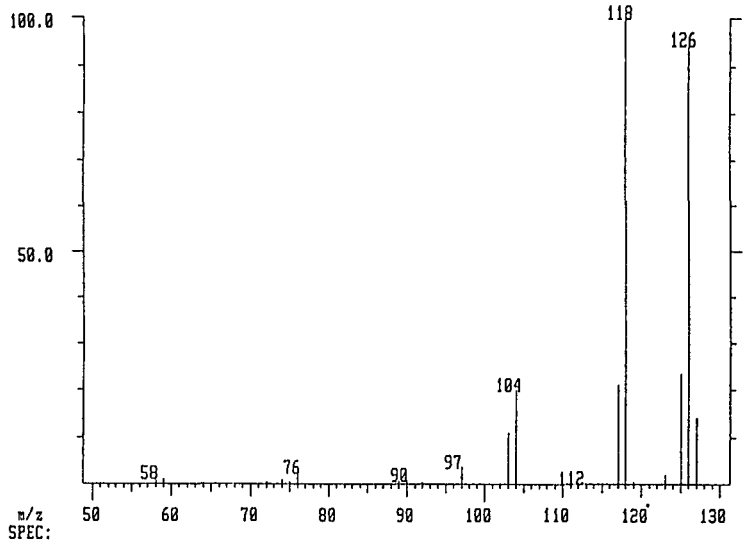

Fig. 8. CAD spectrum of the ion at m/z 126 in Basic Green 4.

show the EI mass spectra of Solvent Red 3 obtained by PB-LC–MS and with the solid probe, respectively. In PB-LC–MS the dye was injected through the HPLC column and therefore the EI mass spectrum obtained was of the pure compound. When using the solid probe, the sample included the dye in addition to the impurities. The mass spectrum therefore does not include the lower mass range because of the impurity background.

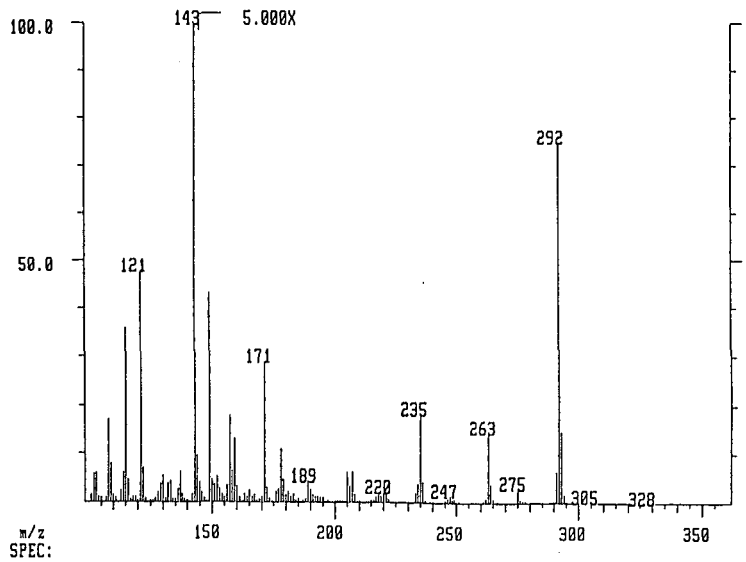

Fig. 9. PB-LC–MS EI mass spectrum of Solvent Red 3. Amount injected, 3.6 μg. Solvent, acetonitrile–water (50:50).

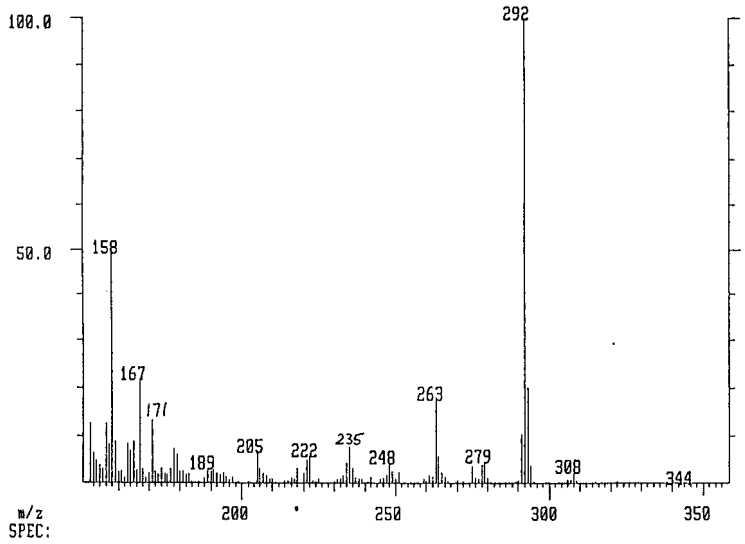

Fig. 10. Solid probe EI mass spectrum of Solvent Red 3.

CONCLUSIONS

It has been demonstrated that structural information on dyes can be obtained by recording their EI mass spectra with an LC–MS system, using a PB interface. However, the sensitivity for dyes was about two to three orders of magnitude worse than in TSP ionization with a wire repeller[7]. This difference in sensitivity is probably due to the two pumping stages in the PB interface where part of the sample is being pumped away. Also, whereas in TSP ionization most of the ion intensity is concentrated in a single ion, usually the MH^+ ion, in PB-EI ionization the ion intensity is divided amongst a large number of fragment ions.

Characteristic EI fragmentations in azo dyes included cleavages of the N–C and C–N bonds on either side of the azo linkage and cleavage of the N=N double bond with transfer of two hydrogen atoms to form an amine. The mass spectra of most azo dyes contained a small molecular ion or none at all. With all the azo dyes no fragmentation resulting from ring cleavage was observed.

The sensitivity for Disperse Orange 3 was better than that for the other dyes, probably beause of its amino group. Fragmentation of other dyes involved first a rearrangement to form such an amino group.

The mass spectrum of Basic Green 4, which is a cationic dye belonging to the arylmethane class, included a molecular ion and an $(M+H)^+$ ion, generated by the addition of a hydride ion to the cation. Two major doubly charged fragment ions were observed in the mass spectrum of this dye.

ACKNOWLEDGEMENT

One of us (J.Y.) thanks the U.S. Environmental Protection Agency, Office of Research and Development, for financial support under Cooperative Agreement Grant No. CR-815425-01-2.

REFERENCES

1 L. D. Betowski and J. M. Ballard, *Anal Chem.*, 56 (1984) 2604.
2 R. D. Voyksner, *Anal. Chem.* 57 (1985) 2600.
3 J. M. Ballard and L. D. Betowski, *Org. Mass. Spectrom.*, 21 (1986) 575.
4 D. A. Flory, M. M. McLean, M. L. Vestal and L. D. Betowski, *Rapid. Commun. Mass Spectrom.*, 1 (1987) 48.
5 L. D. Betowski, S. M. Pyle, J. M. Ballard and G. M. Shaul, *Biomed. Environ. Mass. Spectrom.*, 14 (1987) 343.
6 J. Yinon, T. L. Jones and L. D. Betowski, *Rapid Commun. Mass Spectrom.*, 3 (1989) 38.
7 J. Yinon, T. L. Jones and L. D. Betowski, *Biomed. Environ. Mass Spectrom.*, 18 (1989) 445.
8 *ThermaBeam LC/MS Operators Manual*, Extrel, Pittsburgh, PA, 1988.
9 S. M. Scheifers, S. Verma and R. G. Cooks, *Anal. Chem.*, 55 (1983) 2260.
10 J. H. Bowie, G. E. Lewis and R. G. Cooks, *J. Chem. Soc. B*, (1967) 621.
11 T. E. Beukelman, in K. Venkataraman (Editor), *The Analytical Chemistry of Synthetic Dyes*, Wiley, New York, 1977, Ch. 9.
12 J. C. Gilland, Jr. and J. S. Lewis, *Org. Mass Spectrom.*, 9 (1974) 1148.

Journal of Chromatography, 482 (1989) 87–97
Elsevier Science Publishers B.V., Amsterdam — Printed in The Netherlands

CHROM. 21 828

CHARACTERIZATION OF THE METAL COMPOSITION OF METALLOTHIONEIN ISOFORMS USING REVERSED-PHASE HIGH-PERFORMANCE LIQUID CHROMATOGRAPHY WITH ATOMIC ABSORPTION SPECTROPHOTOMETRIC DETECTION

MARK P. RICHARDS
U.S. Department of Agriculture, Agricultural Research Service, Nonruminant Animal Nutrition Laboratory, Beltsville Agricultural Research Center, Beltsville, MD 20705 (U.S.A.)
(Received June 7th, 1989)

SUMMARY

Reversed-phase high-performance liquid chromatography (RP-HPLC) was used to separate metallothionein (MT) isoforms and on-line atomic absorption spectrophotometric (AAS) detection was used to quantitatively determine their metal content. With this coupled system (HPLC–AAS), it was possible to determine the zinc, cadmium and copper content of individual horse kidney MT isoforms. When rabbit liver MT and the purified isoforms (MT-1 and MT-2) were subjected to RP-HPLC and the zinc content determined by AAS, it was possible to assign each of the two major zinc-containing peaks of the MT sample to MT-1 or MT-2. HPLC–AAS was used to identify zinc-induced MT in heat-treated cytosol from turkey hen liver, thereby demonstrating its application to the analysis of crude tissue extracts. A standard curve was established using turkey liver MT for the quantitative determination of the zinc content of MT isoforms. There was excellent linear correlation between the μg of zinc bound to MT injected onto the column (ranging from 0.34 to 3.43 μg of MT-bond zinc) and the integrated peak area of the atomic absorbance for zinc. Using this standard curve, it was possible to quantitate the amount of MT-bound zinc in cytosol extracts of cultured turkey embryo hepatocytes exposed to varying levels of supplemental zinc in the culture medium.

INTRODUCTION

Metallothionein (MT) is a low-molecular-weight, heavy-metal-binding protein that is generally characterized by several distinctive features including: (1) a single polypeptide chain comprised of 61–63 amino acids, (2) an abundance of cysteine residues (30%), (3) an absence of aromatic amino acids, (4) a high metal content and (5) a highly conserved structure which, because of the positioning of the cysteine residues, gives rise to two distinct metal-binding domains[1,2]. Another unique feature of MT is that it is a metal-inducible protein such that the metals that bind to the protein (thionein) also induce its synthesis. This observation has been cited as evidence

0021-9673/89/$03.50

indicative of its function in basic cellular metal metabolism[3]. MT has been proposed to play a role in the detoxification of heavy metals such as cadmium and mercury as well as in the homeostasis of essential nutrient metals such as copper and zinc[4–7].

Multiple forms (isoforms) of MT have been isolated and characterized from the tissues of a number of eukaryotic species[1,2]. Generally, these isoforms have been designated as two types, MT-1 and MT-2, based on their order of elution from an anion-exchange column. The MT-1 and MT-2 isoforms differ in their amino acid composition and net negative charge at neutral pH[8]. Sequence analysis of purified MT isoforms revealed the existence of microheterogenity (*i.e.*, the existence of additional isoforms)[1,2] which has subsequently been confirmed and extended using molecular cloning techniques to identify and characterize the individual genes coding for distinct MT isoforms[9,10]. In addition, there is another form of heterogenity characteristic of MT that arises not from genetically determined changes in the primary structure of the thionein polypeptide chain, but from differences in its metal composition[1,2]. MTs that differ in their metal composition but not in their amino acid sequence have been referred to as metalloforms[11].

Several techniques have been developed for the isolation and characterization of MT isoforms from tissue extracts. These include a combination of gel permeation and ion-exchange column chromatography[1,2,4], gel electrophoresis[12] and high-performance liquid chromatography (HPLC)[13–19]. Because of its high metal content, the detection and quantitation of MT in tissues is often performed by measuring the amount of metal bound to the isolated protein. Suzuki[16] first introduced a detection technique for MT based on a gel permeation HPLC separation of MT coupled with atomic absorption spectrophotometric (AAS) detection of the bound metals. The ability of this technique to separate MT isoforms was based on the combination of gel permeation and weak cationic-exchange properties of the column used (TSK gel SW 3000; Toyo Soda, Tokyo, Japan). Since that initial report, the technique of HPLC coupled with AAS (HPLC–AAS) has been modified and extended to include anion-exchange and reversed-phase columns and the combination of gel permeation and ion-exchange columns coupled by means of column switching resulting in a higher degree of resolution in the separation of MT isoforms[17,18]. Lehman and Klaassen[19] have utilized the HPLC–AAS combination with a prior cadmium displacement treatment to detect and quantitate rat liver MT isoforms based on their ability to bind the exogeneous cadmium. Although ion-exchange columns are capable of resolving MT-1 and MT-2, such columns generally do not resolve all of the isoform subspecies. Reversed-phase HPLC (RP-HPLC) has proven to be an efficient method for the complete separation and quantitation of individual MT isoforms[13–15]. However, RP-HPLC may not distinguish between different metalloforms of MT, unless the metal composition affects their elution characteristics. Therefore, the purpose of these studies was to determine the feasibility of coupling RP–HPLC with AAS in order to characterize the metal content of individual MT isoforms and to determine the applicability of such a coupled system to the quantitation of MT-bound metal.

EXPERIMENTAL[a]

Preparation of samples for HPLC–AAS

Rabbit liver MT and the purified isoforms (MT-1 and MT-2) and horse kidney MT were purchased from Sigma (St. Louis, MO, U.S.A.). Stock solutions (1 mg/ml) were prepared gravimetrically in 10 m*M* sodium phosphate buffer, pH 7.0. Turkey hen liver was obtained 24 h after the second of two intraperitoneal injections of zinc (10 mg/kg body weight, as $ZnSO_4 \cdot 7H_2O$ injected at 24-h intervals) to induce the synthesis and accumulation of MT. A soluble extract was prepared by homogenizing turkey hen liver tissue in one volume of 10 m*M* Tris–HCl, pH 8.6 with a Polytron device set at 3/4 speed for 60 s, followed by heating the homogenate at 60°C for 10 min and centrifugation at 105 000 *g* for 90 min at 4°C. The resulting supernatant (heat-treated cytosol) was filtered through a 0.22-μm membrane and stored at −20°C prior to HPLC–AAS analysis. Purification of the MT-2 isoform (*i.e.*, the predominant MT species present in turkey liver) involved a two-step column chromatographic fractionation of liver cytosol not subjected to prior heat treatment: (1) gel permeation chromatography was performed on a column (60 × 5.0 cm I.D.) of Sephadex G-75, eluted with 10 m*M* Tris–HCl, pH 8.6. Fractions of 10 ml were collected and analyzed for zinc using AAS to detect the MT peak. (2) Those fractions comprising the MT peak from the gel permeation separation were pooled and applied to a column (20 × 2.6 cm I.D.) of DEAE Sephadex A25 and eluted with a linear gradient of 10–300 m*M* Tris–HCl, pH 8.6. Fractions of 5 ml were collected and analyzed using AAS to detect a zinc peak corresponding to the MT-2 isoform. Those fractions containing MT-2 were pooled, dialyzed extensively against deionized water and lyophilized.

HPLC and AAS apparatus

A Waters (Milford, MA, U.S.A.) liquid chromatograph equipped with dual M6000A pumps, a WISP 710 autosampler, a Model 720 system controller and a Model 730 data module (plotter–integrator) was used to perform the separation of MT isoforms. UV absorbance (214 nm) was monitored with a Model 441 fixed-wavelength monitor. The column used was a μBondapak C_{18} cartridge (10 cm × 8 mm I.D., 10-μm particle size) in a Z-module radial compression device. Buffer A consisted of 10 m*M* sodium phosphate, pH 7.0 and buffer B consisted of 60% acetonitrile in buffer A. MT was eluted with a two-step, linear gradient consisting of 0–10% B for 0–5 min followed by 10–25% B from 5–20 min. The column was maintained at ambient temperature and run at a flow-rate of 3.0 ml/min. To determine the metal content of separated MT isoforms, the effluent from the column was fed directly into the nebulizer of a Model 5000 atomic absorption spectrophotometer (Perkin Elmer, Norwalk, CT, U.S.A.) set to accept a flow-rate of 3.0 ml/min. An air–acetylene flame was used and the spectrophotometer was set to 213.9, 228.8 and 324.8 nm for the determination of zinc, cadmium and copper, respectively. A 1-V output signal from the atomic absorption spectrophotometer was used for peak area integration.

---

[a] Mention of a trade name, proprietary product or specific equipment does not constitute a guarantee or warranty by the U.S. Department of Agriculture and does not imply its approval to the exclusion of other suitable products.

Quantitation of MT–zinc

MT–zinc quantitation was based on peak area integration of the atomic absorbance for zinc (213.9 nm). Purified turkey hen liver MT-2 was used to construct a standard curve. A stock solution (34.3 μg zinc per ml) was gravimetrically prepared in 10 m*M* sodium phosphate, pH 7.0 (buffer A). The stock solution was diluted with buffer A to yield 100-μl aliquots containing 0.34, 0.86, 1.71, 2.57 and 3.43 μg of MT-bound zinc. Each of the 100-μl aliquots was injected onto the column and eluted as described above. The integrated peak area of the atomic absorbance for zinc was plotted against μg of MT-bound zinc injected onto the column and linear regression analysis was used to establish the relationship.

Quantitation of MT–zinc in cultured hepatocytes

Turkey embryo hepatocytes were prepared as described previously[20]. Briefly, primary monolayer cultures of hepatocytes were prepared from the livers of 16 day-old embryos by digestion with collagenase (0.05%). The isolated cells were plated in medium 199 (M199, Gibco, Grand Island, NY, U.S.A.) containing 10% fetal bovine serum and 0.5 μg/ml bovine insulin. After 16 h, the culture medium was replaced with M199 containing 0–50 μ*M* zinc without serum supplementation. At the end of the exposure period, each plate was washed twice with ice-cold phosphate buffered saline and the monolayer harvested by scraping with a rubber policeman into 2 ml of deionized water. The cell suspensions were sonicated and the protein content determined using a dye-binding procedure (Bio Rad Labs., Richmond, CA, U.S.A.). A soluble fraction of the cell sonicates was prepared by centrifugation (105 000 *g* for 30 min at 4°C) and subjected to HPLC–AAS as described above. MT–zinc was quantified using integrated peak area and extrapolated from the turkey hen liver MT-2 standard curve. Values were expressed as μg MT–zinc per mg cell protein.

RESULTS AND DISCUSSION

Detection of MT-bound metals

RP-HPLC has proven to be an efficient method for the isolation and quantitation of MT isoforms[13–15]. This study confirms the fact that RP-HPLC can be adapted to include AAS detection of the metals bound to the separated MT isoforms. Fig. 1 depicts the separation of horse kidney MT isoforms using RP-HPLC with AAS detection of zinc, cadmium and copper bound to each of the isoform species. Cadmium and zinc, the two most abundant metals bound, gave essentially identical patterns of isoform species, with two predominant peaks (MT-1 and MT-2) and a number of additional less abundant peaks. This pattern of MT isoform peaks is similar to that determined by monitoring UV absorbance at 214 nm[15]. Copper was detected, although at a much reduced level compared to cadmium or zinc. Moreover, the isoform pattern detected by monitoring the atomic absorbance for copper was markedly different from that observed for either cadmium or zinc. The majority of the copper appears to be bound to the MT-2 isoform species with less bound to the MT-1 isoform and the less abundant peaks. The significance of this apparent preferential binding of copper by the MT-2 isoform remains to be explained.

Fig. 2 (MT) depicts the separation of rabbit liver MT on RP-HPLC with AAS detection of the bound zinc. Like horse kidney MT, a complex pattern is demonstrated

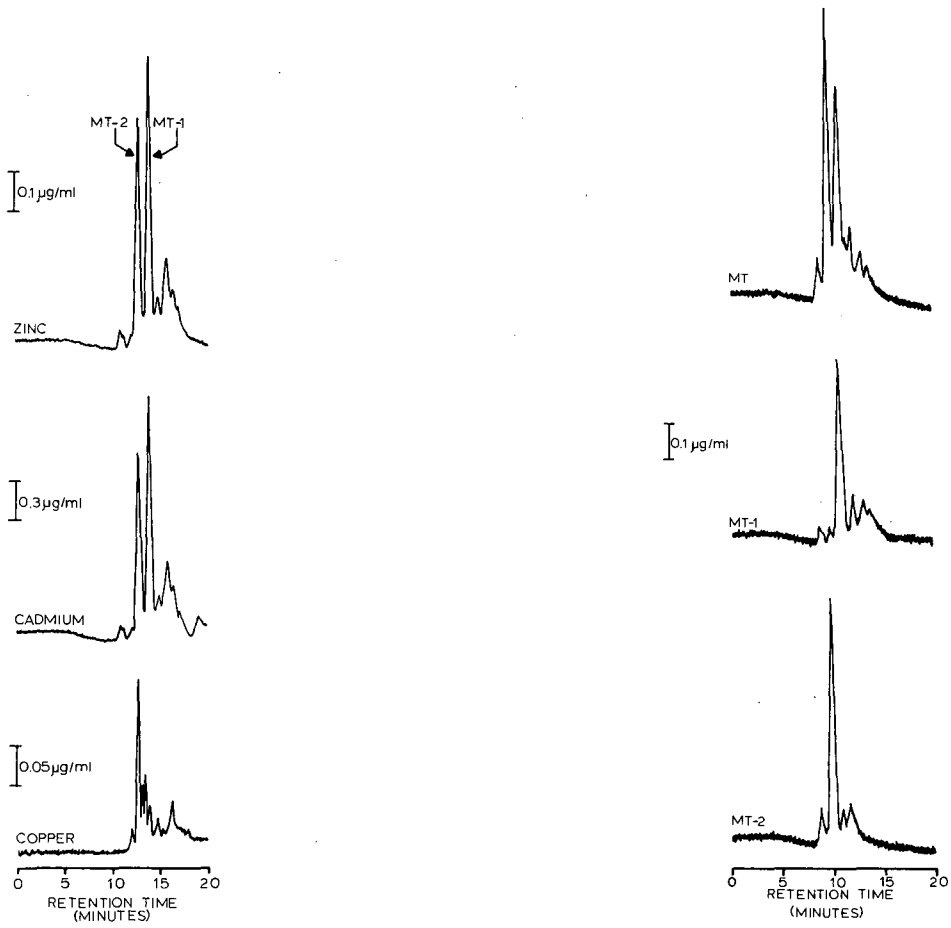

Fig. 1. Horse kidney MT separated using RP-HPLC with on-line monitoring of the atomic absorbances at 213.9 nm (zinc), 228.8 nm (cadmium) and 324.8 nm (copper). The separation of individual MT isoforms was performed with a µBondapak C_{18}, radially-compressed cartridge column eluted with a two-step, linear gradient of 0–6% (0–5 min) and 6–15% (5–20 min) acetonitrile in 10 m*M* sodium phosphate, pH 7.0 at ambient temperature with a flow-rate of 3.0 ml/min. The column effluent was fed directly into the nebulizer of an atomic absorption spectrophotometer for the detection of metals. A separate injection of 100 µg of MT in 100 µl of 10 m*M* sodium phosphate, pH 7.0 was made for the determination of each metal. The vertical bars represent the atomic absorbance level for the indicated concentration of the appropriate aqueous metal standard. The two major MT isoform species are denoted as MT-1 and MT-2.

Fig. 2. Rabbit liver MT and purified MT isoforms (MT-1 and MT-2) subjected to RP-HPLC with on-line monitoring of the atomic absorbance for zinc at 213.9 nm. Separate injections consisted of 100 µg each of MT, MT-1 and MT-2 in 100 µl of 10 m*M* sodium phosphate, pH 7.0. The separation conditions were the same as described in the legend to Fig. 1. The vertical bar represents the level of atomic absorbance for an aqueous standard at a concentration of 0.1 µg zinc per ml.

by the occurrence of 6–7 distinct peaks exhibiting zinc-binding. Furthermore, if purified MT-1 and MT-2 isoform species are subjected to RP-HPLC (Fig. 2, MT-1 and MT-2), it is possible to determine which of the two major zinc-binding peaks observed

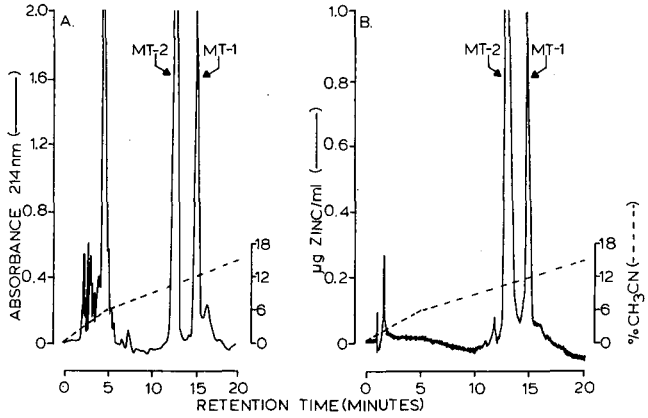

Fig. 3. Turkey hen heat-treated cytosol from birds which had received two consecutive intraperitoneal injections of zinc (10 mg/kg body weight) subjected to RP-HPLC with on-line detection for UV absorbance at 214 nm (A) and atomic absorbance for zinc at 213.9 nm (B). The separation conditions were the same as described in the legend for Fig. 1 with the dashed line denoting the two-step linear acetonitrile gradient used to elute the samples. A separate injection of 100 μl of cytosol was made for monitoring UV and atomic (zinc) absorbances. Two MT species are designated as MT-1 (eluting at 14.83 min) and MT-2 (eluting at 12.93 min).

for MT is classified as MT-1 and which is MT-2. The pattern of peaks for MT and both of the purified isoforms is similar to that observed when UV absorbance was monitored at 214 nm[15].

It is possible to resolve MT isoforms from crude extracts of tissue using RP-HPLC[13-15]. Fig. 3 depicts a comparison of two methods for the detection of MT in heat-treated cytosol from turkey hen liver after its induction by two successive intraperitoneal injections of zinc. The separation of MT from the heat-treated cytosol revealed the presence of two peaks of UV absorbance eluting at 12.93 and 14.83 min which have been designated as MT-2 and MT-1, respectively (Fig. 3A). When AAS detection for zinc was used, a similar pattern of MT peaks was observed indicating that both putative MT species contained zinc (Fig. 3B). It is clear from both chromatograms that the MT species designated as MT-2 is the predominant one which is consistent with what has been reported previously for turkey liver MT[15]. Moreover, the ratio of MT-2 to MT-1 was found to be 4.2 and 4.6 based on the integrated peak areas of UV and atomic absorbances, respectively. The occurrence of two species for turkey liver MT is somewhat curious, since chicken MT has been shown to exist as a singular isoform[21–23]. Although an amino acid analysis of the putative MT-1 and MT-2 species indicated that both were cysteine-rich polypeptides[15], further analysis such as sequencing of the peptides is required to confirm that these species are indeed true MT isoforms. Also it must be emphasized that the turkey liver was obtained from birds that received two large consecutive doses of zinc. It is possible that the additional MT species (MT-1) is present in appreciable quantities only under conditions of maximal induction. Others have reported the existence of at least two forms of MT in quail[18,24,25] and chickens[25] in response to induction by toxic heavy metals or large doses of zinc. Under non-induced conditions, avian MT has been reported to occur as

a singular form[25]. Heterogeneity in chicken MT can arise from differences in the metal composition (*i.e.*, the formation of distinct MT metalloforms), despite the fact that the protein (thionein) portion of the molecule is identical[26]. Moreover, it is possible to separate two different metalloforms of chicken MT using anion-exchange column chromatography[26]. Whether the two forms of turkey liver MT isolated in this study represent distinct isoforms or metalloforms is not known. A similar situation has been reported for rat and mouse MTs. Despite the fact that only two functional MT genes have been identified for rodents[10], a third isoform (a subspecies of MT-2) has been isolated using anion-exchange HPLC[27,28] and RP-HPLC[13]. Suzuki *et al.*[27] have speculated that the third "isoform" may in fact be identical to MT-2 in its amino acid sequence but differ with respect to the state of enzymatically labile functional groups. Clearly, the exact nature of the observed heterogeneity in turkey liver MT remains to be defined. However, RP-HPLC and HPLC–AAS should prove to be useful analytical techniques for the isolation and characterization of heterogeneous MT species.

Quantitation of MT–zinc

In order to investigate the ability of HPLC–AAS to quantitate MT-bound metal, a standard curve was established using zinc-induced MT-2 derived from turkey liver. This particular source of MT affords an excellent standard because it is easily purified and because it is comprised of a singular species[15]. In addition, a standard curve has previously been derived from turkey liver MT-2 for the quantitative determination of MT by monitoring UV absorbance at 214 nm[15]. Varying amounts of MT-2 were

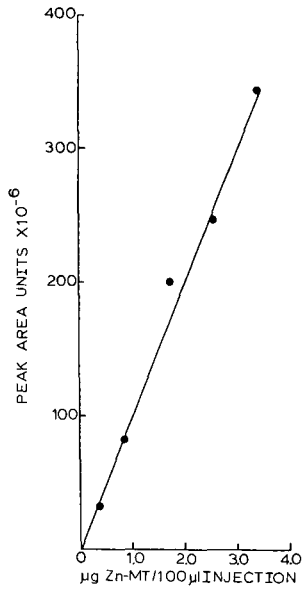

Fig. 4. Turkey hen liver MT-2 standard curve for RP-HPLC with atomic absorbance detecton of zinc at 213.9 nm. Aliquots of MT-2 containing from 0.34 to 3.43 μg zinc in 100 μl of 10 m*M* sodium phosphate, pH 7.0 were injected onto the column and separated as described in the legend to Fig. 1. The μg of zinc bound to MT-2 (Zn–MT) is plotted against the integrated peak area units of the atomic absorbance for zinc at 213.9 nm. Linear regression analysis was used to fit the line to the data points.

prepared gravimetrically in sodium phosphate buffer (pH 7.0) such that a 100-μl aliquot contained 0.34–3.43 μg of zinc. Fig. 4 demonstrates the linear relationship ($r=0.991$) between the μg of zinc bound to MT-2 injected onto the column and the integrated peak area of the atomic absorbance for zinc. It is possible to accurately detect as little as 0.1 μg of zinc injected onto the column. This agrees well with a detection limit of 1 μg of MT (assuming that 1 μg of MT fully saturated with zinc would bind about 0.07 μg) determined by monitoring UV absorbance at 214 nm[15]. Furthermore, the recovery of MT-2-bound zinc from RP-HPLC has been estimated to be 97%[15]. Considering the detection limit of HPLC–AAS (1 μg MT), it is clear that the application of this technique is well suited to the detection and quantitation of MT-bound metal in tissues containing considerable amounts of this protein but not to fluids such as serum and urine in which MT levels can be 2–5 orders of magnitude less than typical tissue levels.

Although zinc was the only metal determined quantitatively in this study, it is reasonable to expect that the technique of RP-HPLC coupled with AAS detection could be applied to the quantitation of MT-bound cadmium as well. There have been a number of reports concerning the detection of cadmium following an HPLC separation of MT isoforms[16–19]. Horse kidney MT isoforms were found to contain substantial amounts of this metal (Fig. 1) and, with the appropriate standard, undoubtedly could have been quantitatively determined. Lehman and Klaassen[19] have described a quantitative analytical technique for MT isoforms. This involves an anion-exchange HPLC separation with on-line determination of cadmium by AAS. Previous reports in which HPLC–AAS was employed to detect MT isoforms utilized aqueous metal solutions for quantitation whereas, Lehman and Klaassen[19] were the first to introduce MT isoform standards saturated with cadmium *in vitro*. However, their technique assumes that cadmium completely displaces all of the bound metal on MT which may not always be the case, especially for copper[8]. This study employed a homologous MT standard for which the metal was incorporated into the protein *in vivo*. The use of an MT standard *versus* an aqueous one takes into account any effects that protein-binding might have on the detection and subsequent quantitation of the metal following RP-HPLC. Moreover, it may be possible to use the same MT standard containing more than one metal to quantitate MT-bound zinc, cadmium and perhaps copper. For example, commercially available MTs, such as those from horse kidney or rabbit liver used in this study, contain both zinc and cadmium as well as traces of copper (Fig. 1). Alternatively, since MT can be depleted of its metals *in vitro* by reducing the pH and can be reconstituted with zinc or cadmium upon raising the pH in the presence of either metal, it may be possible to produce MT standards of any desired metal content or combination for subsequent use as standards for the quantitation of MT-bound metal using HPLC–AAS. Moreover, RP-HPLC may be useful for the isolation of singular MT isoform or metalloform species to be used as standards. It has been suggested previously that individual heterologous MT isoforms may be useful as internal standards for the quantitation of MT in tissue extracts[15]. Further studies are required to assess the feasibility of these approaches.

One limitation of HPLC–AAS that has been encountered concerns the detection of copper-induced or copper-enriched MTs. Hunziker and Kagi[29] have found as we[30] have that MT isoforms containing substantial amounts of copper cannot adequately be separated and detected using RP-HPLC at neutral pH. Given the fact that these

species are inherently unstable, readily oxidizable and require anaerobic conditions for their isolation, this finding is not really surprising. Although the reasons for the inability of RP-HPLC to resolve copper–MTs remain to be determined, this observation should be considered when attempting to analyze MTs containing copper. Suzuki *et al.*[18,31] have demonstrated the feasibility of HPLC–AAS for the detection of MT-bound copper using gel permeation and ion-exchange columns to perform the separation of MT isoforms. However, when copper is not the predominant metal bound, as is the case for many naturally occurring MTs isolated from vertebrate animal species, it may be possible to detect as well as quantitate this particular metal using RP-HPLC. Glennas *et al.*[32] have reported that RP-HPLC was well suited for the resolution and detection of cadmium- and zinc-containing MT but was inappropriate for aurofin-induced, gold-containing MT from cultured human epithelial cells. It has

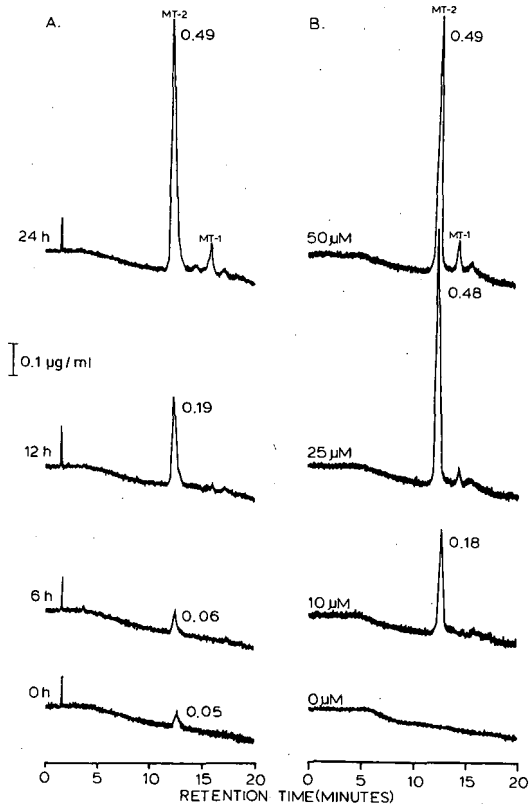

Fig. 5. Cytosol extracts from turkey embryo hepatocytes cultured under serum-free conditions subjected to RP-HPLC with atomic absorbance detection of zinc (213.9 nm). The separation conditions were the same as described in the legend to Fig. 1. The vertical bar represents the level of atomic absorbance for an aqueous standard at a concentration of 0.1 µg zinc per ml. Individual MT species are designated as MT-1 and MT-2. (A) Hepatocytes were cultured in the presence of 50 μM supplemental zinc in the medium and analyzed at 0, 6, 12 and 24 h after exposure. (B) Hepatocytes were cultured in the presence of 0, 10, 25 and 50 μM supplemental zinc in the medium for 24 h. The numbers next to the MT-2 pak represent the amount (µg) of zinc bound per mg of total cellular protein.

been suggested that zinc and cadmium stabilize thionein against degradation[33] and this may, in part, explain our ability to detect copper in the sample of horse kidney MT (Fig. 1). Clearly, more work needs to be done to explore the many possibilities for the application of RP-HPLC with AAS detection to the quantitative determination of MT-bound metals.

Quantitation of MT–zinc in cultured Hepatocytes

One of the advantages of using HPLC to isolate, characterize and quantitate MT and MT-bound metals is that only a small amount of sample is required for such an assay. Therefore, the application of the HPLC–AAS method to the determination of MT-bound zinc in turkey embryo hepatocytes was investigated. Fig. 5A depicts the separation of cytosol extracts from hepatocytes cultured in the presence of 50 μM zinc for up to 24 h using RP-HPLC with detection of zinc by AAS. The amount of zinc bound to the MT-2 species increased from 0.05 to 0.49 μg/mg cell protein by 24 h. Also at 24 h a second zinc-containing peak was detected, although its level was too low to accurately quantitate. This species has been designed MT-1. Similarly, hepatocytes exposed to varying levels of supplemental zinc (0–50 μM) in the culture medium for 24 h exhibited an increase in MT-2-bound zinc from an undetectable level to 0.49 μg/mg (Fig. 5B). In hepatocytes exposed to 25 or 50 μM supplemental zinc, the putative MT-1 species was again detected, although at levels which did not permit an accurate assessment of the amount of bound zinc. The detection of the species designated MT-1 only in the two highest zinc exposure groups (25 and 50 μM) is consistent with its occurrence only under conditions of maximal induction. A similar finding was observed concerning the occurrence of this species in livers from zinc injected chicks[15]. Recently, Klasing and Laurin[34] working with an avian macrophage cell line have reported that two MT species are induced in response to supplemental zinc in the culture medium.

CONCLUSIONS

This study demonstrates that RP-HPLC can be coupled with AAS for the detection and quantitative determination of MT-bound metals. This technique combines the efficiency of RP-HPLC in completely resolving MT isoforms with AAS detection in order to determine the metal content of individual MT isoforms. Moreover, because this technique requires considerably less sample than classical chromatographic techniques, it can readily be applied to pure or partially pure samples of MT or to cytosol extracts from small pieces of tissue or cultured cells. With appropriate standards, it is possible not only to characterize the metals bound to individual MT isoforms, but also to quantitate them. HPLC–AAS represents a useful analytical tool with which to study the metal composition of individual MT isoforms. Furthermore, it may also prove useful in the isolation and characterization of distinct metalloforms of MT.

REFERENCES

1 J. H. R. Kagi and M. Nordberg (Editors), *Metallothionein*, Birkhauser Verlag, Basel, 1979.
2 J. H. R. Kagi and Y. Kojima (Editors), *Metallothionein II*, Birkhauser Verlag, Basel, 1987.
3 M. A. Dunn, T. L. Blalock and R. J. Cousins, *Proc. Soc. Exp. Biol. Med.*, 185 (1987) 107.

4 M. Webb, in M. Webb (Editor), *The Chemistry, Biochemistry and Biology of Cadmium*, Elsevier/North Holland, New York, 1979, Ch. 6, p. 195.
5 R. J. Cousins, *Physiol. Rev.*, 65 (1985) 238.
6 I. Bremner, in J. H. R. Kagi and Y. Kojima (Editors), *Metallothionein II*, Birkhauser Verlag, Basel, 1987, p. 81.
7 M. P. Richards, *J. Nutr.*, 119 (1989) 1062.
8 J. H.R. Kagi and A. Schaffer, *Biochemistry*, 27 (1988) 8509.
9 D. H. Hamer, *Annu. Rev. Biochem.*, 55 (1986) 913.
10 R. D. Palmiter, in J. H. R. Kagi and Y. Kojima (Editors), *Metallothionein II*, Birkhauser Verlag, Basel, 1987, p. 63.
11 I. Bremner, *J. Nutr.*, 117 (1987) 19.
12 L.-Y. Lin and C. C. McCormick, *Comp. Biochem. Physiol.*, 85C (1986) 75.
13 S. Klauser, J. H. R. Kagi and K. J. Wilson, *Biochem. J.*, 209 (1983) 71.
14 P. E. Hunziker and J. H. R. Kagi, *Biochem. J.*, 231 (1985) 375.
15 M. P. Richards and N. C. Steele, *J. Chromatogr.*, 402 (1987) 243.
16 K. T. Suzuki, *Anal. Biochem.*, 102 (1980) 31.
17 K. T. Suzuki, H. Sunaga, Y. Aoki and M. Yammamura, *J. Chromatogr.*, 281 (1983) 159.
18 K. T. Suzuki, H. Sunaga and T. Yajima, *J. Chromatogr.*, 303 (1984) 131.
19 L. D. Lehman and C. D. Klaassen, *Anal. Biochem.*, 153 (1986) 305.
20 M. P. Richards and N. C. Steele, in L. S. Hurley, C. L. Keen, B. Lonnerdal and R. B. Rucker (Editors), *Trace Elements in Man and Animals 6*, Plenum Press, New York, 1988, p. 625.
21 D. Wei and G. K. Andrews, *Nucleic Acids Res.*, 16 (1988) 537.
22 L. P. Fernando, D. Wei and G. K. Andrews, *J. Nutr.*, 119 (1989) 309.
23 C. C. McCormick, C. S. Fulmer and J. S. Garvey, *Proc. Natl. Acad. Sci. U.S.A.*, 85 (1988) 309.
24 M. Yamamura and K. T. Suzuki, *Comp. Biochem. Physiol.*, 77B (1984) 101.
25 K. T. Suzuki, in J. H. R. Kagi and Y. Kojima (Editors), *Metallothionein II*, Birkhauser Verlag, Basel, 1987, p. 365.
26 C. C. McCormick and L.-Y. Lin, in L. S. Hurley, C. L. Keen, B. Lonnerdal and R. B. Rucker (Editors), *Trace Elements in Man and Animals 6*, Plenum Press, New York, 1988, p. 39.
27 K. T. Suzuki, H. Uehara, H. Sunaga and N. Shimojo, *Toxicol. Lett.*, 24 (1985) 15.
28 S. Kobayashi and J. Sayato-Suzuki, *Biochem. J.*, 251 (1988) 649.
29 P. E. Hunziker and J. H. R. Kagi, in J. H. R. Kagi and Y. Kojima (Editors), *Metallothionein II*, Birkhauser Verlag, Basel, 1987, p. 257.
30 M. P. Richards, unpublished results.
31 K. T. Suzuki and T. Maitani, *Biochem. J.*, 199 (1981) 289.
32 A. Glennas, P. E. Hunziker, J. S. Garvey, J. H. R. Kagi and H. E. Rugstad, *Biochem. Pharmacol.*, 35 (1986) 2033.
33 K. Cain and D. E. Holt, *Chem.-Biol. Interact.*, 28 (1979) 91.
34 K. C. Klasing and D. E. Laurin, *FASEB J.*, 3 (1989) A1078.

Journal of Chromatography, 482 (1989) 99–106
Elsevier Science Publishers B.V., Amsterdam — Printed in The Netherlands

CHROM. 21 836

PREPARATIVE PURIFICATION OF *PLASMODIUM FALCIPARUM* CIRCUMSPOROZOITE PROTEIN SYNTHETIC POLYPEPTIDES BY DISPLACEMENT CHROMATOGRAPHY

GIUSEPPE C. VISCOMI*, ALESSANDRA ZIGGIOTTI and ANTONIO S. VERDINI
Laboratory of Peptide Synthesis, SCLAVO SpA, 00015 Monterotondo, Rome (Italy)
(First received October 7th, 1988; revised manuscript received May 8th, 1989)

SUMMARY

Displacement chromatography was used for the preparative purification of a synthetic polypeptide that is a promising malaria vaccine. It was prepared by solid-phase synthesis and contains two important epitopes of circumsporozoite (CS) protein of *Plasmodium falciparum* sporozoite. With apparatus typically employed in analytical high-performance liquid chromatography (HPLC) and on a 250 × 4.6 mm I.D. reversed-phase column, up to 50 mg of crude polypeptide were purified in a single run and with a yield higher than 95%. The results demonstrate that displacement chromatography is suitable for the isolation of several milligrams of a pure polypeptide from a complex mixture that is difficult to separate even by analytical HPLC. In such a preparative application, displacement appears to be superior to elution chromatography as used traditionally.

INTRODUCTION

Numerous studies have demonstrated that reversed-phase high-performance liquid chromatography (RP-HPLC) is a powerful technique for polypeptide analysis[1]. Concomitantly, reversed-phase chromatography has been the main method used for the preparative separation of synthetic and natural peptides[2].

In approaching preparative chromatography, if the amount of injected sample is kept low, it may be possible to maintain the separation obtained on the analytical scale by using similar chromatographic conditions[3]. Neverthless, as the loading is increased, the retention times become strongly dependent on the sample concentration and the peak shapes become so distorted that the recovery may be significantly reduced[4]. Displacement chromatography has been demonstrated to be able to overcome such high loading problems, because the separation of feed components in the displacement mode takes place when the concentrations of the components are sufficiently high to be in the non-linear range of their absorption isotherms[5].

In practice displacement chromatography is carried out in the following steps. First, the column is conditioned with the carrier solution, which permits a subsequent complete absorption of the feed on the stationary phase. Second, a relatively large sample is loaded on the column. Third, a solution containing the displacer, which is

0021-9673/89/$03.50

absorbed more strongly than any of the feed components on the stationary phase, is passed through the column. During the third stage, the feed components begin to be displaced by the displacer, moving down the column, and because of their competitive absorptions they become separated in adjacent bands of pure components[5]. After each displacement run, the displacer is washed out with a suitable regenerant to permit the reuse of the columns[6].

Recently, applications of displacement chromatography in the isolation of peptide hormones obtained from extractions procedures have been reported[7–9]. The successful results prompted us to apply this technique to the purification of biologically active synthetic peptides.

RI-$(NANP)_3NA$ is a 29-amino acid residue polypeptide, whose sequence is shown in Fig. 1; it elicits a high-titre antibody response in mice and the IgGs produced react specifically with *Plasmodium falciparum* sporozoites of infected mosquitoes, which are responsible for malaria infection. This synthetic peptide, which combines two epitopes of *P. falciparum* CS protein, was designed to overcome the genetically restricted response of $(NANP)_n$ sequences[10].

```
H-Lys-Pro-Lys-His-Lys-Lys-Leu-Lys-Gln-Pro-Gly-Asp-Gly
  1           5                10

-Asn-Pro-Asn-Ala-Asn-Pro-Asn-Ala-Asn-Pro-Asn-Ala-Asn-Pro
   15              20                25

-Asn-Ala-OH
   29
```

Fig. 1. RI-$(NANP)_3NA$ sequence.

EXPERIMENTAL

Material

The RI-$(NANP)_3NA$ polypeptide was synthesized by solid-phase synthesis on a polyamide matrix[11], as reported elsewhere[12]. Benzyldimethyldodecylammonium bromide (BDMDA), trifluoroacetic acid (TFA) and triethylamine were supplied by Fluka (Buchs, Switzerland); the last two compounds were distilled prior to use. Methanol and acetonitrile (HPLC grade) were purchased from Merck (Darmstadt, F.R.G.). Water was purified with a Milli-Q system (Millipore, Bedford, MA, U.S.A.). CM-52 cellulose ion-exchange resin was obtained from Whatman (Clifton, NJ, U.S.A.).

All the chromatographic eluents were filtered on a 0.45-μm Millipore filter and degassed by purging with helium.

Apparatus and procedures

Displacement chromatography was carried out on an Aquapore RP-18 (7 μm, 300 Å) column (250 × 4.6 mm I.D.) (Brownlee Labs., Santa Clara, CA, U.S.A.), installed in an HPLC system composed of two Model 303 pumps for the carrier and displacer solution, a Model 802C manometric module, a Model 811 dynamic mixer and an Apple II-Plus gradient controller (Gilson, Villiers-le-Bel, France), a Model

7125 injector (Rheodyne, Cotati, CA, U.S.A.) with a 3-ml loop, a PU 4025 UV detector (Pye Unicam, Cambridge, U.K.) and a Model 2210 recorder (LKB, Bromma, Sweden). The column effluent was collected in 0.1-ml fractions by a Model 2070 Ultrarack II (LKB).

The apparatus for preparative elution chromatography consisted of a Model 590 programmable HPLC pump (Waters Assoc., Milford, MA, U.S.A.), an axial compression column (250 × 20 mm I.D.) (ISA Jobin Yvon, Longjumeau, France), packed with 40 g of LiChroprep RP-18 (25–40 μm; Merck), a PU 4025 UV detector (Pye Unicam) and a Model 2210 recorder (LKB). The flow-rate was 8 ml/min and the eluent, collected in 12-ml fractions by a Model 2070 Ultrarack II (LKB), was monitored at 225 nm.

HPLC of the crude material and chromatographic fractions was performed on a Vydac 201TP54 C_{18} (5 μm, 300 Å) column (250 × 4.0 mm I.D.) (Separation Group, Hesperia, CA, U.S.A.) and using an HPLC system assembled from two Model 114M pumps, a System Organizer, a Model 165 UV detector and a Model 450 Data/System Controller (Beckman, Fullerton, CA, U.S.A.) and a Model BD-41 recorder (Kipp & Zonen, Delft, The Netherlands).

The presence of the displacer in the collected fractions of the displacement runs was checked by HPLC on a LiChrosorb-DIOL column (250 × 4 mm I.D.; Merck) under isocratic conditions with 25 m*M* triethylammonium trifluoroacetate solution as eluent.

RESULTS AND DISCUSSION

The peptide mixture from the synthesis was passed through a CM-52 cellulose column and in Fig. 2 the results of ion-exchange chromatography are depicted. The

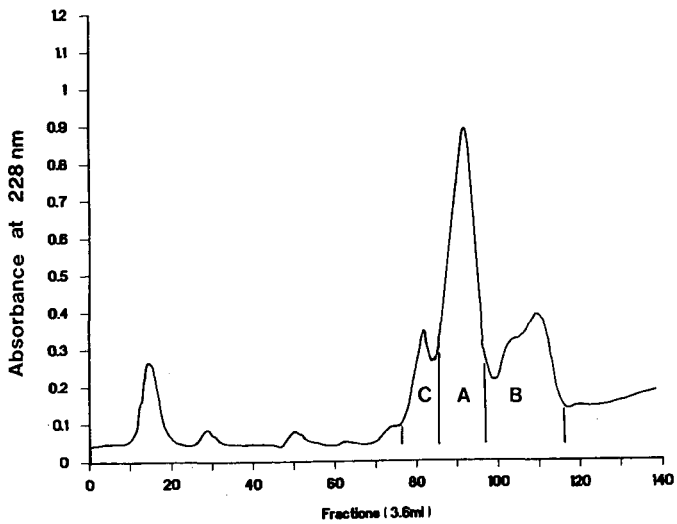

Fig. 2. Ion-exchange chromatography of RI-$(NANP)_3$NA mixture. Column, 450 × 25 mm I.D. CM-52 cellulose; eluent, linear gradient from 0.1 to 0.5 *M* ammonium acetate; pH, 6.1; flow-rate, 36 ml/h; amount of sample loaded, 400 mg of crude mixture.

three main peaks (A, B and C) were collected separately. The amino acid analyses of these fractions were very similar as well as the HPLC profiles shown in Fig. 3A–C. The fused peaks around t_R = 7.1 min (Fig. 3) represented peptide material, while the large peak at t_R = 5.5 min was a chromatographic artefact also present in blank runs.

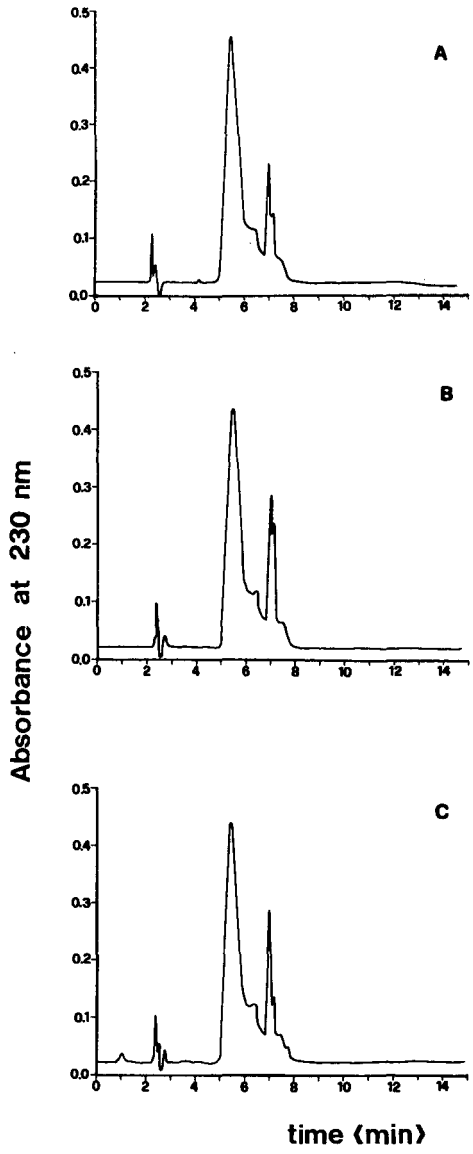

Fig. 3. Analytical chromatograms of Fractions A, B and C. Column, 5-μm Vydac 201 TP54 C_{18} (250 × 4.0
Fig. 4. Displacement chromatography of A. Column, Aquapore RP-18 (7 μm, 300 Å) (250 × 4.6 mm I.D.); carrier, 0.1% TFA; displacer, 50 m*M* BDMDA in 0.1% TFA; flow-rate, 0.1 ml/min; temperature, 23°C.

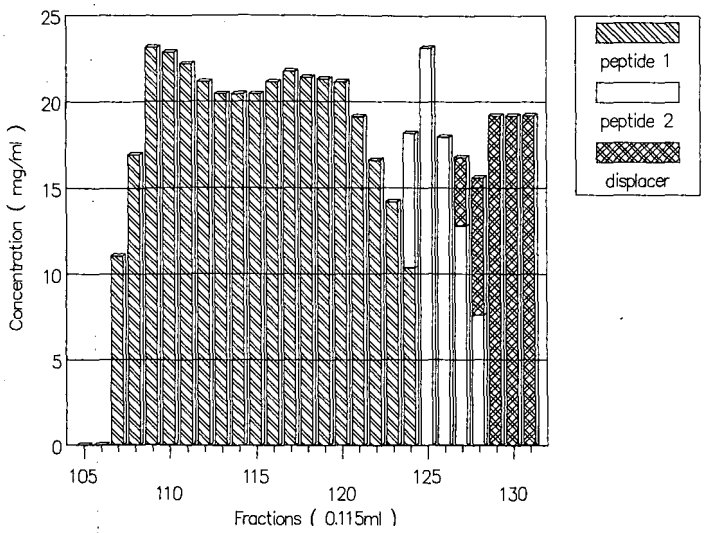

Fig. 4. Displacement chromatography of A. Column, Aquapore RP-18 (7 μm, 300 Å) (250 × 4.6 mm I.D.); carrier, 0.1% TFA; displacer, 50 m*M* BDMDA in 0.1% TFA; flow-rate, 0.1 ml/min; temperature, 23°C.

Attempts to find isocratic eluents suitable for preparative elution chromatography were unsuccessful. When 20 mg of A were loaded on a 250 × 20 mm I.D. LiChroprep RP-18 (25–40 μm) column with 0.1% TFA as the eluent containing 0.1% TFA and 2% acetonitrile they were eluted unresolved at the void volume of the column.

The purification of 45 mg of A by displacement chromatography, using BDMDA as the displacer and 0.1% TFA solution as the carrier, is shown in Fig. 4. The histogram depicted represents the quantitative RP-HPLC analysis of the collected fractions, carried out in the following manner. A 5-μl volume of each fraction was diluted with 100 μl of water and the solution was analysed under the same conditions as

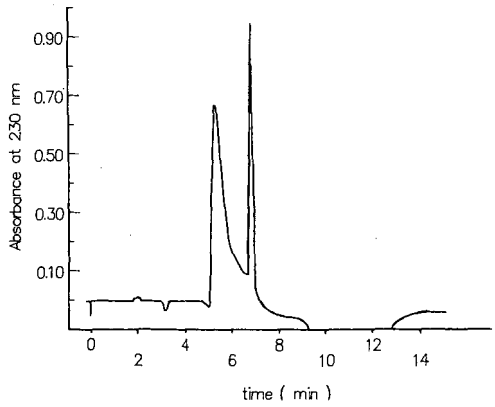

Fig. 5. Typical analytical chromatogram of a fraction containing pure peptide 1. Column, 5-μm Vydac 201 TP^{54} C_{18} (250 × 4.0 mm I.D.); eluent, 0.1% TFA with a linear gradient of acetonitrile from 0 to 20% in 15 min; flow-rate, 1.5 ml/min; sample size, 20 μl; detection, UV absorbance at 230 nm.

TABLE I

AMINO ACID ANALYSES OF PEPTIDES 1 AND 2 ISOLATED BY DISPLACEMENT CHROMATOGRAPHY

Amino acid	*Residues per mol*		
	From RI-(NANP)$_3$NA sequence	*Peptide 1*	*Peptide 2*
Aspartic acid	9	8.80	7.96
Glutamic acid	1	1.09	1.20
Proline	6	6.46	6.21
Glycine	2	1.89	2.00
Alanine	4	3.80	4.04
Leucine	1	1.09	1.00
Histidine	1	0.99	0.98
Lysine	5	4.56	4.50

in Fig. 3. A typical RP-HPLC profile of a fraction containing pure peptide 1 is shown in Fig. 5.

Fractions 107–123 were pooled and lyophilized; 34.5 mg of pure product (peptide 1) were recovered. Its retention time in RP-HPLC was 7.1 min and the amino acid analysis, reported in Table I, gave the corrected amino acid ratios of the desired peptide. A 5.4-mg amount of a product with a retention time of 7.3 min (peptide 2), was recovered from fractions 125–126. Its amino acid analysis (Table I) showed that it was a peptide missing an Asx residue relative to peptide 1. In this purification, 97% of the total amount of RI-(NANP)$_3$NA present in the crude mixture (calculated as the sum of pure collected material plus the peptide present in the zones overlapping with the impurities) was recovered in pure form.

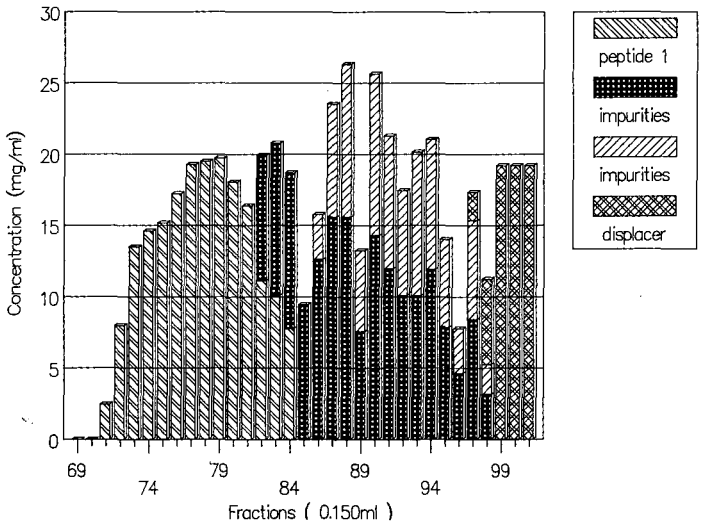

Fig. 6. Displacement chromatography of B. Conditions as in Fig. 4.

Under the same chromatographic conditions as in Fig. 4, 40 mg of B were purified and the relative histogram is shown in Fig. 6. The pooled fractions 71–81 gave 24.5 mg of peptide 1, with a yield of 85%; the impurities, which were collected as unresolved products from fractions 85–88, had retention times close to 7.3 min. Coelution analysis, carried out by injecting under the same conditions as in Fig. 3 a mixture of this fraction pool with pure peptide 2 (1:1), indicated that none of the major peaks of the pool coincided with that of peptide 2.

An increase in the amount of sample loaded to 100 mg of B caused complete saturation of all the stationary phase and part of peptide 1 started to elute at the void volume of the column as a gaussian peak, purified through a frontal chromatographic mechanism, and part as a square band typical of a displacement mechanism, during the displacer run.

In a first attempt to purify C, 60 mg of the material were loaded under the same displacement chromatographic conditions as applied to both A and B but, in contrast with the previous results the products were eluted close to the void volume rather than displaced. The low recovery of peptide material (20 mg) indicated that C was rich in salts. When this peptide material, made free from major amounts of salts in the first attempt to purify, was rerun under the previous conditions, separation of the products by displacement chromatography occurred (Fig. 7) and 2.52 mg of pure peptide 1 were obtained from fractions 92–93. The unresolved peptide impurities collected from fractions 94–98 were different from those of B, even though the retention times were very close.

After each displacement run, the column was washed with 25 ml of pure methanol at a flow-rate of 1.5 ml/min and reconditioned with the 0.1% TFA carrier solution; no reduction of the column efficiency was detected after the regeneration procedures.

The purification of synthetic peptides is a challenge, because in the course of synthesis they are frequently contaminated by very closely related by-products. An

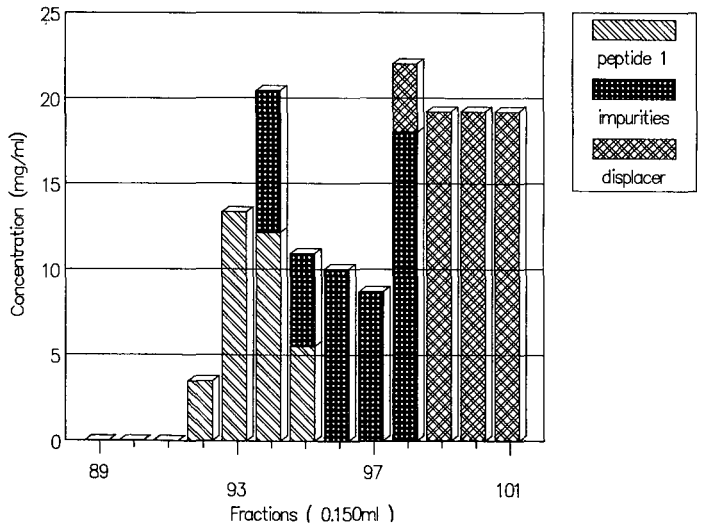

Fig. 7. Displacement chromatography of C. Conditions as in Fig. 4.

indication of this aspect can be deduced from Fig. 2, where fractions A, B and C of the RI-$(NANP)_3$NA mixture, isolated by ion-exchange chromatography, show similar amino acid analyses and HPLC profiles, and from Fig. 3A–C, where the retention time of the desired peptide is so close to those of the impurities that it is impossible to separate them efficiently by reversed-phase preparative elution chromatography. In spite of this, the reported purifications (Figs. 4, 6 and 7) by displacement chromatography clearly demonstrate the potential of this technique in preparative liquid chromatography.

The choice of BDMDA as the displacer was based on the consideration that, as the peptide products were separated in gradient runs always starting from 0% of organic solvent, a mixed hydrophobic–hydrophilic interaction is probably responsible for the retention of these products. Under such conditions, for a compound to be a proper displacer it should be absorbed on the stationary phase more strongly than any feed components in both hydrophobic and hydrophillic interactions, reacting with the C_{18} chains and with the free silanol groups still present in the reversed stationary phase. Tetraalkyl halides with long alkyl chains have these properties. Indeed, it has been reported that they work as hydrophobic displacers of peptides in the reversed-phase mode[7–9] and as hydrophilic displacers of polar compounds in the normal-phase mode[13].

CONCLUSION

The high level of purity required for biopharmaceutical products has substantial ly increased the importace of preparative liquid chromatography in purification and isolation processes. In this respect, the purification of synthetic peptides, which are important therapeutically, has received particular emphasis. The remarkable properties of displacement chromatography compared with the elution mode, namely a high ratio of the amount of sample loaded to the amount of stationary phase (20 mg per gram of stationary phase), the reduced volume of eluent per milligram of purified material (1 ml/mg), the collection of concentrated pure peptide (20 mg/ml) and the use of the same equipment and columns employed in HPLC, make this technique a powerful tool for the purification of peptides at levels of several milligrams, which are usually obtained in solid-phase synthesis.

REFERENCES

1 M. J. O'Hare and E. C. Nice, *J. Chromatogr.*, 171 (1979) 209.
2 J. Rivier, R. McClintock, R. Galyean and H. Anderson, *J. Chromatogr.*, 288 (1984) 303.
3 G. Cretier and J. L. Rocca, *Chromatographia*, 21 (1986) 143.
4 G. Guiochon and A. Katti, *Chromatographia*, 24 (1987) 165.
5 Cs. Horváth, A. Nahum and J. H. Frenz, *J. Chromatogr.*, 218 (1981) 365.
6 J. H. Frenz and Cs. Horváth, *J. Chromatogr.*, 282 (1983) 249.
7 H. Kalasz and Cs. Horváth, *J. Chromatogr.*, 215 (1981) 295.
8 Gy. Vigh, Z. Varga-Puchony, G. Szepesi and M. Gazdag, *J. Chromatogr.*, 386 (1987) 353.
9 G. C. Viscomi, S. Lande and Cs. Horváth, *J. Chromatogr.*, 440 (1988) 157.
10 A. Pessi, F. Bonelli, G. Del Giudice, G. Corradin, H. D. Engers, P. Lambert and A. S. Verdini, in T. Shiba and S. Sakakibara (Editors), *Peptide Chemistry*, Protein Research Foundation, Osaka, 1988, p. 781.
11 E. Atherton, L. J. Logan and R. C. Sheppard, *J. Chem. Soc., Perkin Trans. 1*, (1981) 538.
12 A. Bernardi, F. Bonelli, A. Pessi and A. S. Verdini, *Ital. Pat. Appl.*, 21144, 1986.
13 F. Cardinali, A. Ziggiotti and G. C. Viscomi, *J. Chromatogr.*, 499 (1990) in press.

Journal of Chromatography, 482 (1989) 107–115
Elsevier Science Publishers B.V., Amsterdam — Printed in The Netherlands

CHROM. 21 837

CHROMATOGRAPHIC METHOD FOR THE PREPARATION OF APO-CELLULAR RETINOL-BINDING PROTEIN AND APO-CELLULAR RETINOIC ACID-BINDING PROTEIN FROM THEIR HOLO-TYPES

FUMIO FUKAI*, HIROYUKI SUZUKI and TAKASHI KATAYAMA
Department of Patho-Physiology, Faculty of Pharmaceutical Sciences, Science University of Tokyo, 12 Ichigaya Funagawara-Machi, Shinjuku-ku, Tokyo 162 (Japan)
(First received March 7th, 1989; revised manuscript received June 20th, 1989)

SUMMARY

A chromatographic method is described for the preparation of apo-cellular retinol-binding protein (CRBP) and apo-cellular retinoic acid-binding protein (CRABP) from their corresponding holoproteins. Elimination of retinoids from either purified CRBP or CRABP holoprotein complex could be performed quantitatively by DEAE-cellulose chromatography without any alteration in the inherent properties of the native proteins. In contrast, the usual methods, involving UV irradiation or acetone precipitation, resulted in some modification of these binding proteins. This chromatographic method was also applicable to the preparation of apo-fatty acid-binding protein (FABP) from FABP–palmitic acid holoprotein complex.

INTRODUCTION

In addition to circulating retinol-binding protein (so-called RBP)[1], some retinoid-binding proteins exist in tissues, including cellular retinol-binding protein (CRBP) and cellular retinoic acid-binding protein (CRABP)[2,3]. These binding proteins are distributed in various organs with relatively high concentrations and play a role in transporting their corresponding ligands to appropriate intracellular locations[3]. It has been presumed that interaction of retinoids with CRBP and CRABP would be a prerequisite for the storage or metabolism of retinoids and for the expression of retinoid action[2–4]. For the correct understanding of such interactions, it would be necessary first to obtain both apo- and holo-types of these retinoid-binding proteins having their inherent properties.

The purification of specific binding proteins, including CRBP and CRABP, is usually performed after occupying their binding sites with the corresponding ligands, as these proteins are generally unstable when free from ligands. Accordingly, in order to obtain their apoproteins, it is necessary to purify holoproteins and then to strip the ligands from them. CRBP and CRABP apoproteins have previously been prepared from their holo-types by acetone precipitation[5] and UV irradiation[5,6] methods, but there is little information about whether or not apoproteins prepared by these methods

0021-9673/89/$03.50

still maintain their own properties. In the acetone precipitation method, the proteins may be denatured in acetone solution. And also in the UV irradiation of holoproteins, some possible modifications of the proteins by decomposition products of retinoids are suspected. We describe here a method for the preparation of apo-CRBP and apo-CRABP from their corresponding holoproteins wihout their denaturation. A comparison of this method with the previous method is reported.

EXPERIMENTAL

Materials

[11,12(*n*)-^{3}H]Vitamin A, free alcohol (60 Ci/mmol), was purchased from Amersham International and [11,12-^{3}H(N)]retinoic acid (52.5 Ci/mmol) from New England Nuclear. All-*trans*-retinol and all-*trans*-retinoic acid were obtained from Sigma. DEAE-cellulose (DE 52) was purchased from Whatman.

Purification of CRBP, CRABP and FABP holoproteins

Purification of CRBP and CRABP holoproteins from rat testes cytosol was carried out according to the method of Ong and Chytil[7,8]. During purification, CRBP and CRABP were labelled with [^{3}H]retinol and [^{3}H]retinoic acid, respectively, instead of non-radioactive retinoids. Purification of the fatty acid-binding protein (FABP)–[^{3}H]palmitic acid holoprotein complex was performed as described previously[9]. Each purified holoprotein was shown to be apparently homogeneous as judged by sodium dodecyl sulphate polyacrylamide gel electrophoresis.

Preparation of CRBP and CRABP apoproteins

CRBP and CRABP free from retinoids were prepared using three different methods, as follows.

Chromatographic method using a DEAE-cellulose column. A 1-ml volume of the purified holoprotein solution at a concentration of 6 μM in 20 mM Tris–HCl buffer (pH 7.4) containing 10% glycerol (TG buffer) was applied to a DEAE-cellulose column (2 × 0.5 cm I.D.) equilibrated with TG buffer. The column was washed successively with 4 ml each of 10%, 20% and 50% ethanol in TG buffer, and then washed with the opposite series of ethanol concentrations in TG buffer. After washing further with 5 ml of TG buffer, the protein was eluted with 0.2 M sodium chloride in TG buffer and then dialysed with 20 mM potassium phosphate buffer (pH 7.4) containing 0.15 M sodium chloride (phosphate-buffered saline; PBS).

UV-irradiation method. UV irradiation was carried out as reported previously[5,6]. Each purified preparation of the holoproteins at a concentration of 6 μM in PBS was exposed to glass-filtered UV light (365 nm; intensity 0.5 $\mu W/cm^2$; UV lamp, Tokyo Kohgaku) below 4°C for over 12 h. Destruction of retinoids was assessed by monitoring the disappearance of the intrinsic absorption at 350 nm and fluorescence (excitation 350 nm, emission 480 nm) of these holoproteins[6–9]. The irradiated sample was subjected to gel filtration on a Sephadex G-25 column (9.5 × 1.5 cm I.D.) in PBS and the protein fractions were pooled.

Acetone precipitation method. This method was performed as reported by MacDonald and Ong[5]. A 1-ml volume of the purified holoprotein solution at a concentration of 6 μM in PBS was added dropwise to 20 ml of acetone at −20°C in an

acetone–dry-ice bath. After stirring for 10 min, the precipitated protein was recovered by centrifuging at 5000 rpm (3000 *g*) for 5 min. The supernatant was discarded and the pellet was resuspended in 8 ml of acetone at −20°C. Following centrifugation, the precipitate was carefully dried under a gentle stream of argon. The pellet was dissolved in 1 ml of PBS and subjected to gel filtration on a Sephadex G-25 column as described above.

The protein concentration in each preparation was determined by the method of Lowry *et al.*[10].

Apparent binding activity of CRBP and CRABP

Each sample containing 100–150 n*M* protein in PBS (1-ml volume) was incubated with 300 n*M* of tritium-labelled retinoid ([^{3}H]retinol or [^{3}H]retinoic acid) at 4°C for 3 h in the dark. The sample mixture was then subjected to gel filtration as described above. Radioactivity in the protein fraction was measured as the total binding activity. To measure the non-specific binding activity, parallel incubations were carried out in the presence of a 100-fold molar excess of the corresponding non-radioactive retinoids. The specific binding activity was calculated by subtracting the non-specific binding activity from the total binding activity.

Dissociation constant

Apoprotein solution was incubated with the corresponding tritium-labelled retinoids at concentrations from $1 \cdot 10^{-8}$ to $1 \cdot 10^{-6}$ *M* in the presence or absence of a 100-fold molar excess of non-radioactive retinoids. After the incubation, each sample was subjected to gel filtration (Sephadex G-25 column, 9.5 × 1.5 cm I.D.) as described above. Binding data were plotted according to Scatchard[11].

RESULTS

Purified CRBP–[^{3}H]retinol holoprotein complex adsorbed quantitatively on the DEAE-cellulose column at pH 7.4. When the column was washed with increasing concentrations of ethanol (10–50% in TG buffer), most of the applied radioactivity was eluted (Fig. 1). As protein was not detected in this eluate, it was considered that only retinol was released from the column, leaving the protein on the gel. After washing off the ethanol with TG buffer, about 80% of the applied CRBP, which was nearly free from retinol, could be recovered by eluting with 0.2 *M* sodium chloride in TG buffer (Fig. 1 and Table I). Similarly, the preparation of apo-CRABP from the CRABP–[^{3}H]retinoic acid holoprotein complex was achieved in the same way with over 80% yield as protein. Whether or not these apoproteins maintain their inherent properties was analysed as described below.

The spectral properties were examined (Fig. 2). The original holo-CRBP revealed a dominant absorption peak at 350 nm due to bound retinol. After the DEAE-cellulose chromatography, the peak at 350 nm almost disappeared. This absorption peak reappeared in holo-CRBP reconstituted by incubating the apoprotein with retinol. The ratio of the absorbance at 350 nm to that at 280 nm (A_{350}/A_{280}) in the reconstituted holo-CRBP (1.68) was higher than that in the original holo-CRBP (1.62). The absorption spectrum of the reconstituted holo-CRABP was similar to that of the original holoprotein, and the A_{350}/A_{280} values for the original and reconstituted

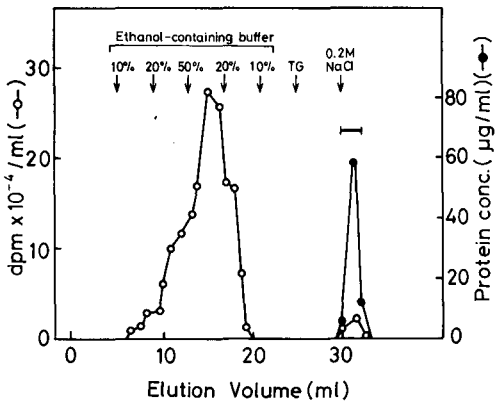

Fig. 1. Preparation of apo-CRBP from CRBP-[^{3}H]retinol holoprotein complex by DEAE-cellulose chromatography. Purified preparation (1 ml) of the holoprotein (6 μM) was applied to a DEAE-cellulose column (2 × 0.5 cm I.D.) equilibrated with TG buffer, and the column was washed with 4 ml each of the indicated concentrations of ethanol solution in TG buffer. After further washing with 5 ml of TG buffer, elution was carried out with TG buffer containing 0.2 M sodium chloride. Eluates were examined for (○) radioactivity and (●) protein concentration. Fractions eluted with 0.2 M sodium chloride were pooled (solid bar) as the preparation of apo-CRBP.

holo-CRABP were 1.72 and 1.76, respectively. These results indicate that the conformational changes of these binding proteins during the chromatography may be negligible.

The binding characteristics of these apoproteins were next examined. The binding activity of the apo-CRBP with retinol increased apparently up to 1.5 times that of the original holo-CRBP (Table I). Such an increase in apparent binding activity was also observed with the apo-CRABP obtained by the chromatographic method, and its

TABLE I

COMPARISON OF METHODS FOR THE PREPARATION OF CRBP AND CRABP APOPROTEINS

Method	*Apoprotein*	*Radioactivity (dpm · 10^{-4})*		
		Original holoprotein	*After treatment*[a]	*Reconstituted holoprotein*[b]
DEAE-cellulose chromatography	CRBP	133.8	3.8	202.0 (151%)[c]
	CRABP	68.5	2.1	90.4 (132%)
UV irradiation	CRBP	133.8	18.7	61.4 (46%)
	CRABP	68.5	10.3	28.0 (41%)
Acetone precipitation	CRBP	133.8	1.8	22.7 (17%)
	CRABP	68.5	1.2	17.1 (25%)

[a] Radioactivity remaining after the treatment.

[b] Apparent binding activity as determined by incubation of each apoprotein with 300 nM of the corresponding tritium-labelled retinoids as described under Experimental.

[c] Recovery of binding activity through the treatment expressed as a percentage of that of the original holoprotein is given in parentheses.

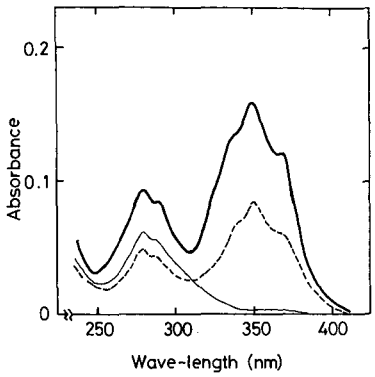

Fig. 2. Absorption spectra of CRBP. Bold line, original holo-CRBP; thin line, CRBP after the chromatography; dotted line, reconstituted holo-CRBP. Each sample was subjected to gel filtration on a Sephadex G-25 column and absorption spectra of the protein fractions were measured.

binding activity with retinoic acid was about 130% of the original value for holo-CRABP (Table I). As mentioned above, with both CRBP and CRABP the A_{350}/A_{280} value of the original holoprotein was smaller than that of the reconstituted holoprotein. Therefore, the increase in the apparent binding activity might be attributed to both original holoproteins not being fully saturated by their corresponding ligands. To assess the recovery of binding activity in the chromatographic method more quantitatively, Scatchard analysis was then performed (Fig. 3). Apo-CRBP obtained with our method showed a dissociation constant ($K_d = 1.6 \cdot 10^{-9}$ M) of the same order as that of apo-CRBP in rat testes cytosol ($2.5 \cdot 10^{-9}$ M). The total binding sites in the preparation after the chromatography were calculated by extrapolation of the linear plot to be about 5 μM. As the protein concentration of this preparation was about 5 μM as CRBP, the results indicate that most of the protein was

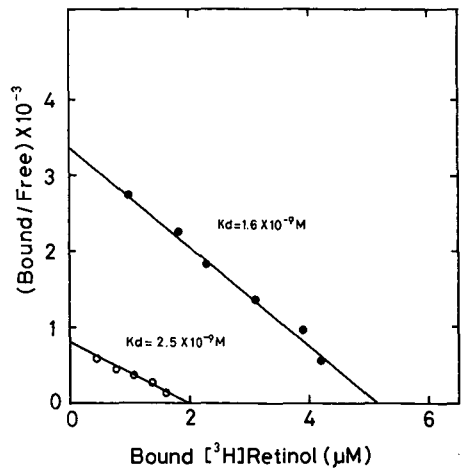

Fig. 3. Scatchard analysis of binding of retinol with CRBP. (○) Rat testes cytosol; (●) apo-CRBP obtained by the chromatographic method.

recovered as an active protein that displays a high affinity toward retinol. On the other hand, binding of the apo-CRBP with [^{3}H]retinol was interrupted by a 100-fold molar excess of non-radioactive retinol, but not by retinoic acid (Fig. 4). Apo-CRABP obtained by our method also retained its own binding affinity and specificity (data not shown). In addition, the molecular parameters of both CRBP and CRABP (Stokes radius 17 Å, sedimentation coefficient 2.3S) were not changed after the chromatography. It was therefore concluded that either CRBP or CRABP apoprotein could be prepared by the chromatographic method without the loss of their own characteristics.

In this chromatographic method, an increase in the ethanol concentration of the washing buffer caused a decrease in binding activity. For example, the binding activity of apo-CRBP prepared using 80% ethanol solution was 65% of that in the standard method. Utilization of another organic solvent having a lower polarity, such as a 50% solution of isopropanol or acetone, also resulted in some decrease in their binding activities (data not shown). In contrast, ethylene glycol was shown to have the ability to dissociate retinol from holo-CRBP. Apo-CRBP could be obtained quantitatively with the chromatographic method by utilizing 50% ethylene glycol solution instead of ethanol. However, elimination of retinoic acid from holo-CRABP by this solution was hardly detectable. On the other hand, DEAE-cellulose could be used as an adsorbent in this method instead of a hydroxyapatite gel. Both CRBP and CRABP adsorbed on the gel, and retinoids were removed effectively with the ethanol-containing buffer in the same manner. However, the recoveries of both proteins were very low (20–40% of the applied protein).

Our chromatographic method was also applicable to the preparation of apo-FABP from the FABP–[^{3}H]palmitic acid holoprotein complex. As FABP has a basic p*I* (8.5), as reported previously[12], it was necessary to carry out the DEAE-cellulose chromatography at pH 9.5. Elimination of the ligand and elution of the resulting apo-FABP could be performed as described above. The binding activity of apo-FABP thus obtained was about 90% of that of the original holoprotein. The Stokes radius (16 Å) and sedimentation coefficient (2.3S) did not change after the chromatography.

The usual methods for the preparation of apo-CRBP, with either UV irradiation

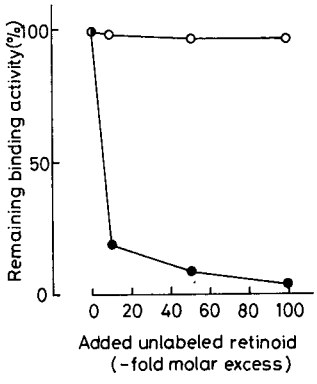

Fig. 4. Binding specificity of apo-CRBP prepared by the chromatographic method. Aliquots of the apo-CRBP preparation were incubated with 300 n*M* of [^{3}H]retinol with the addition of the indicated molar excess of (●) retinol or (○) retinoic acid.

or acetone precipitation, were compared with our chromatographic method. When purified CRBP–[^{3}H]retinol holoprotein complex was exposed to long-wavelength UV light, the characteristic absorption peak at 350 nm decreased in size and had almost completely disappeared after irradiation for over 12 h. However, a considerable amount of radioactivity still remained in the protein fraction (12% of the original) (Table I). The apparent binding activity of the protein with retinol was less than 50% of that of the original holo-CRBP (Table I). Neither the radioactivity remaining in the protein nor the binding activity was altered even when the irradiation was prolonged. The remaining radioactivity could not be released by extraction with *n*-hexane. Some decomposition products of retinol might bind covalently to the protein. Similarly, the absorption at 350 nm of holo-CRABP disappeared on irradiation, and the treatment was accompanied by loss of its binding activity with retinoic acid (Table I). Some radioactivity (about 15% of the original) also remained in the preparation (Table I).

In contrast to the UV-irradiation method, the radioactivity of retinoids was effectively removed from the holoproteins by acetone precipitation (Table I). However, treatment with acetone caused a considerable decrease in their binding activities (Table I). Apo-CRBP prepared by this method retained only 17% of the binding activity of the original holo-CRBP, although nearly 80% of the protein was recovered. This means that about 80% of the recovered protein was inactivated during the treatment. When holo-CRBP reconstituted by relabelling the protein with [^{3}H]retinol was subjected to sucrose density gradient centrifugation analysis, most of the radioactivity migrated to the bottom of the centrifuge tube (over 10S). The results show clearly that CRBP was aggregated by treatment with acetone. Acetone precipitation of CRABP also resulted in a marked decrease in its binding activity (Table I) and in aggregation of the protein.

DISCUSSION

A chromatographic method utilizing a DEAE-cellulose column for the preparation of CRBP and CRABP apoproteins was established. This method enabled both apoproteins to be obtained quantitatively without any loss of their inherent properties. The principle of this method is substantially similar to that of the acetone precipitation method, *i.e.*, both methods are based on the fact that hydrophobic ligands are easily released from binding with protein in an organic solvent. In the utilization of these methods, protein denaturation should therefore be taken into account. Indeed, acetone precipitation resulted in denaturation of CRBP and CRABP. As in our method the proteins are bound to DEAE-cellulose and retinoids can be eliminated by relatively low concentrations of ethanol (less than 50%), denaturation of the proteins may be avoided. The similarity of the spectral properties of the holoproteins prior to and after passage through a DEAE-cellulose column supports the assumption that the conformational changes of the proteins may be kept to a minimum in our method.

Retinoid-binding proteins free from retinoids have been prepared exclusively by the UV-irradiation method, taking advantage of the photo-lability of retinoids[6,13]. We tried to examine this method. The characteristic absorption peak at 350 nm of holo-CRBP or holo-CRABP disappeared on UV irradiation, indicating degradation of the retinoids. However, the binding activity had also decreased by about half after

the irradiation. Ong and Chytil[6] reported that retinol bound to CRBP could be destroyed by long-wavelength UV light (intensity 0.5 $\mu W/cm^2$) for 10–15 h without detectable damage to the protein. Their irradiation conditions were almost the same as those in this work. In contrast, MacDonald and Ong[5] treated CRBP and CRBP II holoproteins with UV light for only 25 min to obtain the corresponding apo-proteins[5]. The reduction in binding activity in our experiment may be related to the prolonged time of UV irradiation. However, the fact that considerable amounts of radioactivity were bound covalently to the proteins after the irradiation would be meaningful for assessing this method. In any case, the UV-irradiation method is suitable only for removing photo-labile ligands.

On examination of the washing buffer conditions in our chromatographic method, a unique phenomenon was observed. Elimination of retinol from holo-CRBP could also be achieved with 50% ethylene glycol solution, extended to retinoic acid was not dissociated from holo-CRABP under these conditions. Although the mechanism of this specific effect of ethylene glycol remains unclear, it may be possible that ethylene glycol specifically affects the interaction between CRBP and retinol. On the other hand, we adopted DEAE-cellulose as the adsorbent of the retinoid-binding proteins, but another adsorbent such as CM-cellulose or hydroxyapatite could be employed, depending on the characteristics of the desired protein. For instance, both CRBP and CRABP were adsorbed quantitatively on a hydroxyapatite gel and removal of the retinoids could be carried out effectively by washing the gel with an ethanol-containing buffer, although the proteins could not be eluted in good yields.

Recently, Gordon and co-workers[14–16] reported a comparison of the tertiary structures of FABP and CRBP II by X-ray diffraction. To obtain FABP and CRBP II apoproteins without denaturation, they expressed these apoproteins genetically in *Escherichia coli* and purified them from cell lysate. Our chromatographic method was shown to be applicable to the preparation of apo-FABP from the FABP–palmitic acid holoprotein complex by DEAE-cellulose chromatography at pH 9.5[9,12]. Similarly, apo-CRBP II may be obtained by the chromatographic method. Hence it can be expected that our chromatographic method will be widely applicable to the preparation of various apoproteins including other retinoid-binding proteins and also steroid hormone receptors if appropriate chromatographic conditions are chosen.

ACKNOWLEDGEMENT

The authors thank Dr. Sukeo Onodera, Science University of Tokyo, for his valuable suggestions.

REFERENCES

1 D. S. Goodman and W. S. Blander, in M. B. Sporn, A. B. Roberts and D. S. Goodman (Editors), *Biosynthesis, Absorption, and Hepatic Metabolism of Retinol, Vol. 2, The Retinoids*, Academic Press, New York, 1984, pp. 1–39.
2 J. C. Saari and A. H. Bunt-Milam, in M. I. Sherman (Editor), *Retinoids and Cell Differentiation*, CRC Press, Boca Raton, FL, 1986, pp. 1–15.
3 F. Chytil and D. E. Ong, *Fed. Proc. Fed. Am. Soc. Exp. Biol.*, 38 (1979) 2510.
4 A. M. Jetten and M. E. Jetten, *Nature (London)*, 278 (1979) 180.
5 P. N. MacDonald and D. E. Ong, *J. Biol. Chem.*, 262 (1987) 10550.

6 D. E. Ong and F. Chytil, *Methods Enzymol.*, 67 (1980) 288.
7 D. E. Ong and F. Chytil, *J. Biol. Chem.*, 253 (1978) 828.
8 D. E. Ong and F. Chytil, *J. Biol. Chem.*, 253 (1978) 4551.
9 F. Fukai, T. Kase, T. Shidotani, T. Nagai and T. Katayama, *Biochem. Biophys. Res. Commun.*, 147 (1987) 899.
10 O. H. Lowry, N. J. Rosebrough, A. L. Farr and R. J. Randall, *J. Biol. Chem.*, 193 (1951) 265.
11 G. Scatchard, *Ann. N. Y. Acad. Sci.*, 51 (1949) 660.
12 F. Fukai, T. Kase, T. Shidotani, T. Nagai and T. Katayama, *Biochem. Int.*, 18 (1989) 1101.
13 Y. Takahashi, T. Nakajima, M. Washitake, T. Anmo, M. Sugiura and H. Matsumaru, *Chem. Pharm. Bull.*, 27 (1979) 12.
14 E. Li, B. Locke, N. C. Yang, D. E. Ong and J. I. Gordon, *J. Biol. Chem.*, 262 (1987) 13773.
15 J. C. Sacchettini, D. S. Khausen, E. Li, L. J. Banazak and J. I. Gordon, *J. Biol. Chem.*, 262 (1987) 15756.
16 E. Li, C. A. Demmer, D. A. Sweetser, D. E. Ong and J. I. Gordon, *Proc. Natl. Acad. Sci. U.S.A.*, 83 (1986) 5779.

Journal of Chromatography, 482 (1989) 117–123
Elsevier Science Publishers B.V., Amsterdam — Printed in The Netherlands

CHROM. 21 829

TSK-TOYOPEARL GELS FOR THE PREPARATIVE SEPARATION OF STEROL CARRIER PROTEIN$_2$ FROM RAT LIVER[a]

TORU OEDA*, AIZAN HIRAI, TOSHIAKI BAN, YASUSHI TAMURA and SHO YOSHIDA
Division of Endocrinology and Metabolism, Second Department of Internal Medicine, School of Medicine, Chiba University, 1-8-1 Inohana, Chiba 280 (Japan)
(First received November 28th, 1988; revised manuscript received April 28th, 1989)

SUMMARY

The application of TSK-Toyopearl gels to the preparative separation of a basic and low-molecular-weight protein, sterol carrier protein$_2$ (SCP$_2$), was studied. SCP$_2$ was purified from 105 000 *g* supernatant of rat liver (S_{105}) by ion-exchange chromatography on CM-Toyopearl 650M and gel permeation on Toyopearl HW60S. Separation of S_{105} by CM-Toyopearl 650M was carried out at a high flow-rate in the presence of 10% (v/v) glycerol, a stabilizer of the protein. Toyopearl HW60S showed a significant ion-exchange effect on the elution of SCP$_2$. Using an elution buffer of ionic strength of 45 m*M*, a highly efficient purification of SCP$_2$ on HW60S was achieved. SCP$_2$ was purified approximately 5000-fold to apparent homogeneity with an overall yield of 69%.

INTRODUCTION

Sterol carrier protein$_2$ (SCP$_2$), also designated non-specific lipid transfer protein (nsL-TP), is a basic and low-molecular-weight protein[1,2] and has been shown to play an important role in intracellular transfer of both cholesterol and phospholipids and to participate in cholesterol metabolism in the liver[3,4] and various extrahepatic tissues[5–8].

Purification of SCP$_2$ has been reported by several laboratories[9–11]. However, the procedures were complicated and time-consuming, with low yields. The exact physiological role of SCP$_2$ in both the liver and extrahepatic tissues does not seem to have been fully explored as yet. In addition, the amount of tissues available is not always sufficient. Therefore, a simpler procedure for the purification of SCP$_2$ with a high yield is required.

TSK-GEL Toyopearl, a semi-rigid hydrophilic polymer, has been shown to provide high resolution of protein mixtures and good recoveries on a preparative scale[12,13]. Among Toyopearl gel derivatives, TSK-GEL ion exchanger is reported to

[a] Preliminary data were presented at the 8th International Congress of Endocrinology held in Kyoto, in July, 1988.

0021-9673/89/$03.50

be suitable for large-scale and high-speed resolution. Gel permeation on Toyopearl HW60 is said to have a small but significant ion-exchange effect on the separation of low-molecular-weight proteins[12]. This investigation was performed to study the application of Toyopearl gels to the preparative separation of SCP_2. We have established a simple and highly efficient method for the purification of SCP_2 using CM-Toyopearl 650M ion exchanger and Toyopearl HW60S for gel permeation. We describe here the application of TSK-Toyopearl gels to the chromatographic separation of SCP_2 and some properties of the protein obtained.

EXPERIMENTAL

Reagents

7-Dehydrocholesterol was purchased from Aldrich (Milwaukee, WI, U.S.A.) and NADPH from Oriental Yeast (Osaka, Japan). TSK-GEL Toyopearl CM-650M and Toyopearl HW60S were obtained from Tosoh (Tokyo, Japan). All of the reagents for amino acid analysis were obtained from E. Merck (Darmstadt, F.R.G.). Other chemicals were of analytical-reagent grade and obtained from Wako (Osaka, Japan).

Sample preparation

Adult male Sprague–Dawley rats (300–350 g) were killed by decapitation. The lievers were washed with ice-cold 15 m*M* potassium phosphate buffer (pH 6.8) containing 250 m*M* sucrose, 1 m*M* EDTA and 1 m*M* dithiothreitol and homogenized in two volumes of the same buffer. The supernatant obtained after centrifugation at 20 000 *g* was centrifuged twice at 105 000 *g* at 4°C for 60 min. The resulting supernatant (S_{105}) and buffer-washed microsomes were used for the purification of SCP_2 and the assay of SCP_2 activity, respectively.

Assay of SCP_2 activity

SCP_2-activity was determined by measuring the activation of 7-dehydrocholesterol reductase [E.C. 1.3.1.21] according to the method of Noland *et al.*[9] with minor modifications. Each assay mixture contained 50 μM 7-dehydrocholesterol, microsomes (2 mg of protein), 0.5 m*M* NADPH, SCP_2 in various concentrations, 15 m*M* potassium phosphate buffer (pH 6.8) containing 5 m*M* 2-mercaptoethanol and 10% (v/v) glycerol in a total volume of 1 ml. After a preincubation for 6 min, the reaction was started by the addition of 7-dehydrocholesterol and maintained under a nitrogen atmosphere at 37°C for 1 h. After the reaction had been terminated by the addition of 1 ml of 30% (w/v) potassium hydroxide solution and 2 ml of ethanol, sterols were extracted twice with 4 ml of light petroleum. The solvent was evaporated and the residue was dissolved in 750 μl of cyclohexane. The concent of 7-dehydrocholesterol was determined by three-wave quantitative calculation at 276, 282 and 290 nm, using a Hitachi Model 220A double-beam spectrophotometer.

Chromatography

All procedures were carried out at 0–4°C. The S_{105} from rat liver (460 ml) was diluted with the same volume of 15 m*M* potassium phosphate buffer (pH 6.8) containing 5 m*M* 2-mercaptoethanol and 10% (v/v) glycerol and then applied to a CM-

Toyopearl 650M column (20 × 8 cm I.D.) equilibrated with the same buffer. The flow-rate was 100 ml/min. The column was washed with 2 l of the same buffer and the protein was eluted with 3 l of 60 m*M* potassium phosphate buffer (pH 6.8) containing 5 m*M* 2-mercaptoethanol and 10% (v/v) glycerol. The eluate was concentrated to 250 ml using a Lab Cassette system equipped with eight cassettes of PT-10 000 membrane (Millipore, Bedford, MA, U.S.A.), and further concentrated to 50 ml using an Amicon ultrafiltration cell with a YM-5 membrane (Amicon, Danvers, MA, U.S.A.).

The concentrated fraction from the CM column was separated by gel permeation chromatography using Toyopearl HW60S. The effect of the ionic strength of the buffer on the separation and the recovery of SCP_2 was examined using 15, 30, 45 and 60 m*M* potassium phosphate buffer (pH 6.8) containing 5 m*M* 2-mercaptoethanol and 10% (v/v) glycerol. The concentrated fraction from the CM column (3 ml) was applied to a Toyopearl HW60S column (40 × 2 cm I.D.) equilibrated with eluting buffer as mentioned above. The flow-rate was 0.45 ml/min and 1.8-ml fractions were collected and the SCP_2 activity of each fraction was assayed. The UV absorption of column effluent was monitored at 280 nm.

For the preparative scale, the concentrated fraction (50 ml) was applied to a Toyopearl HW60S column (100 × 4 cm I.D.) equilibrated with 45 m*M* potassium phosphate buffer (pH 6.8) containing 5 m*M* 2-mercaptoethanol and 10% (v/v) glycerol. The flow-rate was 2.8 ml/min. The column was eluted with the same buffer and 15-ml fractions were collected. The UV absorption of the collected fractions was measured at 220 nm. The fractions containing SCP_2 activity were pooled and concentrated to 2 ml using an Amicon ultrafiltration cell with a YM-5 membrane.

Protein analysis

Size-exclusion high-performance liquid chromatography was performed on a Shodex Protein WS-802.5F column (600 × 8 mm I.D.) with a pre-column (50 × 6 mm I.D.) (Showa Denko, Tokyo, Japan) using 50 m*M* potassium phosphate buffer (pH 6.5) containing 150 m*M* potassium sulphate, 5 m*M* 2-mercaptoethanol and 10% (v/v) glycerol as the mobile phase. The flow-rate was 0.5 ml/min. Sodium dodecyl sulphate polyacrylamide gel electrophoresis (SDS-PAGE) was performed according to the method of Laemmli[14] using a slab gel consisting of 10–20% gradient separating gel. Molecular weight marker proteins, a mixture of monomer and polymers of cytochrome C (Oriental Yeast), were used. Gels were stained using Coomassie Brilliant Blue R-250. Analytical isoelectric focusing was performed using a LKB Ampholine polyacrylamide gel plate (pH 3.5–9.5). p*I* determinations were made with an isoelectric focusing p*I* calibration kit, pH 3–10 (Pharmacia, Piscataway, NJ, U.S.A.). For amino acid analysis, the sample was injected into a reversed-phase HPLC system equipped with a Nucleosil $5C_{18}$ octadecylsilica (250 × 4.6 mm I.D.) (Ishizu, Osaka, Japan) for removing 2-mercaptoethanol, glycerol and potassium phosphate buffer. The sample was hydrolyzed with 3 *N* mercaptoethanesulphonic acid at 110°C for 44 h. The hydrolysate was analysed on a Hitachi Model 835 amino acid analyser. Protein concentrations were determined by the method of Bradford[15] with bovine γ-globulin as a standard.

RESULTS AND DISCUSSION

Ion-exchange chromatography on CM-Toyopearl 650M

A 460-ml volume of S_{105} was processed on a CM-Toyopearl 650M column. SCP_2 was eluted from the column with 60 m*M* phosphate buffer. In contrast to soft gel ion exchangers such as CM-cellulose, CM-Toyopearl 650M is applicable to the high-speed separation of viscous samples such as S_{105} containing 10% (v/v) glycerol, and thereby seems to be suitable for the first step of the purification. In this study, a high flow-rate (100 ml/min) was achieved even in the presence of 10% (v/v) glycerol and the original supernatant was processed successfully within 1 h. The eluate from the CM column was concentrated to 50 ml. Thus, SCP_2 was purified 16-fold with 129% recovery in the initial step.

Gel permeation chromatography on Toyopearl HW60S

Fig. 1 shows the effect of the ionic strength of eluting buffer on the elution profile and the recovery of SCP_2 from the Toyopearl HW60S column. There was no significant effect of ionic strength on the retention of the protein peak at 280 nm. In contrast, the retention time of SCP_2 activity was increased as the molarity of the buffer was reduced from 60 to 15 m*M*. Baseline separation of SCP_2 activity from the protein peak at 280 nm was achieved at less than 30 m*M*. On the other hand, the recovery of SCP_2 activity was decreased on reducing the ionic strength of the buffer. The recovery of SCP_2 activity at 60, 45, 30 and 15 m*M* were 94.7, 68, 51.4 and 30.6%, respectively. A concentration of 45 m*M* was chosen for the eluting buffer in order to optimize the separation and recovery of the protein.

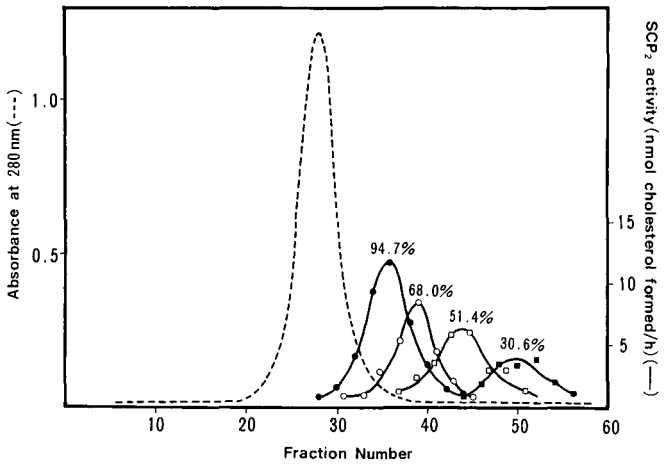

Fig. 1. Effect of buffer ionic strength on elution profile and recovery of SCP_2. A 3-ml volume (33.6 mg of protein) of the concentrated fraction from CM-Toyopearl 650M was applied onto a Toyopearl HW60S column (40 × 2 cm I.D.) equilibrated with (●) 60, (○) 45, (□) 30 and (■) 15 m*M* potassium phosphate buffer (pH 6.8) containing 5 m*M* 2-mercaptoethanol and 10% (v/v) glycerol. The column was eluted with the same buffer at a flow-rate of 0.45 ml/min and 1.8-ml fractions were collected. Dashed line, absorbance at 280 nm; solid lines, SCP_2 activity. Percentage values indicate the recovery of SCP_2 activity using each ionic strength of elution buffer.

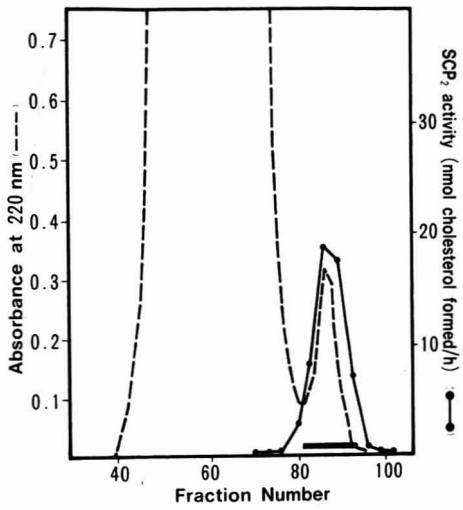

Fig. 2. Elution profile on Toyopearl HW60S. A 50-ml volume (1340 mg of protein) of the concentrated fraction from CM-Toyopearl 650M was applied to a Toyopearl HW60S column (100 × 4 cm I.D.) equilibrated with 45 m*M* potassium phosphate buffer (pH 6.8) containing 5 m*M* 2-mercaptoethanol and 10% (v/v) glycerol. The column was eluted with the same buffer at a flow-rate of 2.8 ml/min and 15-ml fractions were collected. Dashed line, absorbance at 220 nm; solid line, SCP_2 activity. The marker bar indicates the fractions which were pooled for the following step.

For the preparative separation of SCP_2, the concentrated fraction (50 ml) from the CM column was injected on to the preparative Toyopearl HW60S column (100 × 4 cm I.D.). As shown in Fig. 2, SCP_2 was eluted as a small and symmetrical peak and was separated from a large protein peak. The pooled fractions were concentrated to 2 ml with an Amicon ultrafiltration cell with a YM-5 membrane. There was a 303-fold purification and 54% recovery in this step. Table I shows the results for the specific activities and recoveries during the purification of the protein. The protein was purified 4969-fold with a 69% yield.

Properties of the purified protein

The final preparation of the protein eluted as a single and symmetrical peak on high-performance gel permeation, which coincided exactly with the SCP_2 activity.

TABLE I

PURIFICATION OF STEROL CARRIER PROTEIN$_2$ FROM RAT LIVER

Sample	*Volume (ml)*	*Total activity (units)*[a]	*Total protein (mg)*	*Specific activity (nmol cholesterol formed/h/mg protein)*	*Yield (%)*	*Purification factor (fold)*
S_{105}	460	27 123	22 310	1.216	100	1
CM-Toyopearl 650M	50	34 951	1755	19.9	129	16
Toyopearl HW60S	2.1	18 714	3.1	6037	69	4969

[a] One unit of SCP_2 activity is defined as the activity that causes an increment of 1 nmol/h in the conversion of 7-dehydrocholesterol to cholesterol.

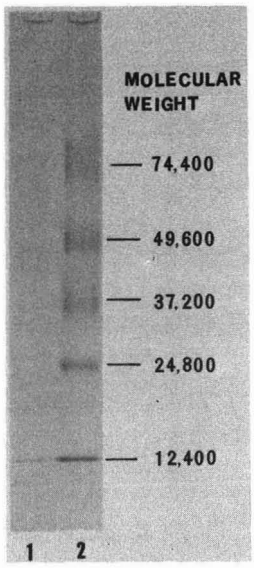

Fig. 3. SDS-PAGE of the purified protein (lane 1) and standard proteins (lane 2).

The protein also gave a single protein band on SDS-PAGE (Fig. 3). These results indicate that the purified protein was homogeneous. The molecular weight of the purified protein was 12 300 as determined by SDS-PAGE. The protein had a p*I* of 9.1 as determined by analytical isoelectric focusing. The most abundant amino acid was lysine which accounted for 16.5 mol-%. The protein contained no arginine or tyrosine and only small amounts of histidine and tryptophan. The correlation coefficient of the amino acid composition was 0.996 between the purified protein and SCP_2 reported by Noland *et al.*[9]. Hence, the purified protein is thought to be identical with SCP_2 as purified by Noland *et al.*[9]. The UV spectrum of the protein showed a low absorbance at 280 nm, as expected from the low tyrosine and tryptophan contents. The maximum absorbance occurred at 216 nm. Therefore, monitoring effluent at *ca.* 220 nm, as opposed to 280 nm, appears to give a more exact approximation during gel permeation chromatography.

ACKNOWLEDGEMENTS

The authors thank Dr. Masao Tachibana of Central Research Laboratory, Eisai (Tsukuba, Japan), for amino acid analyses and the Prof. Masamiti Tatibana of Chiba University for valuable suggestions and comments during the preparation of manuscript. This study was supported in part by a Grant-in-Aid from the Ministry of Health and Welfare and a research grant (63570522) from the Scientific Research Fund of the Ministry of Education, Japan.

REFERENCES

1 T. J. Scallen, M. V. Srikantaiah, B. Seetharam, E. Hansbury and K. L. Gavery, *Fed. Proc.*, 33 (1974) 1733–1746.
2 B. Bloj, M. E. Hughes, D. B. Wilson and D. B. Zilversmit, *FEBS Lett.*, 96 (1978) 87–89.
3 H. Seltman, W. Diven, M. Rizk, B. J. Noland, R. Chanderbhan, T. J. Scallen, G. Vahouny and A. Sanghvi, *Biochem. J.*, 230 (1985) 19–24.
4 K. L. Gavey, B. J. Noland and T. J. Scallen, *J. Biol. Chem.*, 256 (1981) 2993–2999.
5 G. V. Vahouny, P. Dennis, R. Chanderbhan, G. Riskum, B. J. Noland and T. J. Scallen, *Biochem. Biophys. Res. Commun.*, 122 (1984) 509–519.
6 R. Chanderbhan, B. J. Noland, T. J. Scallen and G. V. Vahouny, *J. Biol. Chem.*, 257 (1982) 8928–8934.
7 G. V. Vahouny, R. Chanderbhan, B. J. Noland, D. Irwin, P. Dennis, J. D. Lambeth and T. J. Scallen, *J. Biol. Chem.*, 258 (1983) 11731–11737.
8 A. Kharroubi, J. A. Wadsworth, R. Chanderbhan, P. Wiesenfeld, B. Noland, T. Scallen, G. V. Vahouny and L. Gallo, *J. Lipid Res.*, 29 (1988) 287–292.
9 B. J. Noland, R. E. Arebalo, E. Hansbury and T. J. Scallen, *J. Biol. Chem.*, 255 (1980) 4282–4289.
10 J. M. Trzaskos and J. L. Gaylor, *Biochem. Biophys. Acta*, 751 (1983) 52–65.
11 B. J. H. M. Poorthuis, J. F. C. Glatz, R. Akeroyd and K. W. A. Wiltz, *Biochim. Biophys. Acta*, 665 (1981) 256–261.
12 J. Germershausen and J. D. Karkas, *Biochem. Biophys. Res. Commun.*, 99 (1981) 1020–1027.
13 Y. Kato, K. Komiya, T. Iwaeda, H. Sasaki and T. Hashimoto, *J. Chromatogr.*, 206 (1981) 135–138.
14 U. K. Laemmli, *Nature (London)*, 227 (1970) 680–685.
14 M. M. Bradford, *Anal. Biochem.*, 72 (1976) 248–254.

Journal of Chromatography, 482 (1989) 125–132
Elsevier Science Publishers B.V., Amsterdam — Printed in The Netherlands

CHROM. 21 853

DYE LIGAND CHROMATOGRAPHY AND TWO-DIMENSIONAL ELECTROPHORESIS OF COMPLEX PROTEIN EXTRACTS FROM MOUSE TISSUE

PETER JUNGBLUT and JOACHIM KLOSE*
Institut für Humangenetik, Institut für Toxikologie und Embryonal-Pharmakologie, Freie Universität Berlin, Garystrasse 5, D-1000 Berlin 33 (F.R.G.)
(First received January 14th, 1988; revised manuscript received August 2nd, 1989)

SUMMARY

A complex protein fraction of mouse brain was subjected to dye ligand chromatography with various dye ligands. The proteins that were bound by the dye–gel matrix and also the non-binding proteins were separated by high-resolution two-dimensional electrophoresis. The protein patterns obtained were compared. The results show that a large number of different protein species bind to dye ligands and do not occur in the eluate. Red A was the most efficient dye in isolating an individual protein class from a complex tissue extract. Moreover, we found that many of the binding proteins did not cross-react among different types of dye ligands. Orange A and Blue B were the most unrelated dyes among those compared. Our investigation shows that dye ligand chromatography can be used as a means (among others employed previously) of fractionating and classifying the enormous number of different protein species in a mammalian tissue when combined with high-resolution two-dimensional electrophoresis.

INTRODUCTION

In an attempt to analyse mouse proteins systematically, our strategy is to fractionate the proteins according to biological[1–3] or chemical[4] criteria and to separate the protein fractions by two-dimensional electrophoresis[5,6]. In this study, we tried to reveal, by using dye ligand chromatography of mouse brain proteins, classes of proteins characterized by their ability to bind to distinct dye ligands. This method uses sulphonated triazinyl dyes[7,8] as ligands. The most common dye used is Cibacron Blue 3GA (Ciba-Geigy), here referred to as Blue A (Amicon).

The mechanism of binding proteins to Blue A has been studied[9–12] and reviewed[13–16] by several investigators. Proteins that showed biospecific interactions with dyes are, in principle, enzymes that have negatively charged substrates, in particular phosphorylated substrates[15]. Enzymes using ATP, NAD and some other purine nucleotides have proved to be particularly strongly adsorbed by Blue A[17]. Stellwagen[9], studied the binding mechanism of lactate dehydrogenase and phosphoglycer-

0021-9673/89/$03.50

ate kinase and also the Blue A affinity of 43 other proteins and proposed the concept of nucleotide-fold specificity. However, other investigations have shown in a number of instances that proteins without a nucleotide-binding-fold bind to Blue A (data cited by Dean and Watson[13]). According to Miribel *et al.*[16], the fractionation of proteins by dye ligand chromatography results from different effects, such as ion exchange, diffusion–exclusion, pseudo-ligand affinity or hydrophobicity. This suggests that Blue A is a general ligand that interacts with several types of proteins. However, the binding specificity can be influenced by the conditions used to perform chromatography[11,18].

We performed dye ligand chromatography at a high pH, used short and wide columns and started with low ionic strength. Under these conditions, the total binding effect of the dye ligand may be decreased, while the relative portion of nucleotide-fold proteins that binds to Blue A may be increased.

EXPERIMENTAL

Preparation of solubilized cell proteins

Mice of the inbred strain DBA/2J (Jackson Laboratory, Bar Harbor, ME, U.S.A.) were used as experimental animals. Investigations were carried out on 10–14-week-old females. Solubilized cell proteins (water-extractable proteins) were prepared from the brain. Ten brains were used for one preparation and two preparations were made. The method used for the preparation was the same as described earlier[2,4]. The frozen brains were thawed and homogenized (five up and down strokes, 250 rpm) in half a volume of deionized water. The homogenized tissue was centrifuged in a Beckman Ti-50 rotor for 40 min at 225 000 *g*. All of the fluid supernatant (including the thick and the clear layers) was removed and centrifuged again as above. The clear supernatant was considered as an extract that contains all protein species solubilized in the brain tissue. The extract was subjected to fractionation by heparin–Sepharose Cl-6B chromatography[4]. The proteins that did not bind to the heparin–Sepharose column were further subfractionated by dye ligand chromatography.

Dye ligand chromatography

Five dye ligand media were purchased from Amicon (Lexington, MA, U.S.A.): Blue A, Red A, Orange A, Green A and Blue B, coupled (by the triazine ring) to agarose as a supporting media. Prepacked columns (3.2 cm × 0.9 cm I.D.), available as a dye matrix screening kit, were used. The bed volume was 2 ml.

Before use, each matrix gel was regenerated with urea. A 12-ml volume of 8 *M* urea was added to each column, allowed to drain and stored overnight. The regenerated columns were equilibrated with 12 ml of a 50 m*M* Tris–HCl (pH 7.3) buffer (running buffer).

When Blue A, Red A or Green A was used, solutions containing 4.4 mg of protein were applied to the column; when Orange A or Blue B was used, 6.6 mg of protein were applied. The protein concentration was measured by the method of Lowry *et al.*[19] as modified by Peterson[20]. After an incubation time of 30 min, the column was washed with 15 ml of running buffer. Elution was achieved with a running buffer containing 1.5 *M* sodium chloride. The flow-rate of the solution was maintained at 5 ml/h. Fractions of 1.4 ml were collected. Two to three fractions of the

peaks absorbing at 280 nm were pooled. As a result, two pools were obtained, the binding and non-binding proteins of the sample. The pool containing the binding proteins was desalted and concentrated by Centricon (Amicon) ultrafiltration. The sodium chloride concentration was thereby reduced to about 1 m*M*, and the final protein content was in the range 4–12 mg/ml. The pool containing the non-binding proteins was concentrated in the same way. The final protein concentration was 4–16 mg/ml. For each dye type used, chromatography was performed twice.

The possibility that proteins are bound selectively to the ultrafiltration membrane (YM 10) of the Centricon tubes was investigated by comparing 2-DE patterns from unfiltered samples with those from diluted and reconcentrated aliquots of the same sample. The differences were negligible (0.3% of the spots showed qualitative changes and 3.8% of the spots showed quantitative changes).

Two-dimensional electrophoresis

The high-resolution two-dimensional electrophoresis technique developed by Klose[5] and modified by Klose and Feller[6] was used for final protein separation. This method combines isoelectric focusing in polyacrylamide gels containing urea and mercaptoethanol (first dimension) with electrophoresis in polyacrylamide gels containing sodium dodecyl sulphate (SDS) (second dimension).

Protein samples were prepared from the pooled and concentrated fractions of the binding and non-binding proteins obtained by dye ligand chromatography. The protein fractions were mixed with urea, mercaptoethanol and ampholytes (pH 5–7) (Serva, Heidelberg, F.R.G.) to yield concentrations of 9 *M*, 5% (v/v) and 2% (m/v), respectively. The resulting mixture was stirred for 40 min at room temperature. Up to 60 μl of the sample containing about 150–220 μg of protein were applied to the gel. The samples prepared from the binding and non-binding protein fractions of the same dye column and separated by two-dimensional electrophoresis in parallel contained equal amounts of protein.

Isoelectric focusing (first dimension) was performed in a pH gradient generated by one part of Ampholine of pH 3.5–10 (LKB, Bromma, Sweden) and two parts of Servalyt of pH 5–7 (Serva). SDS gel electrophoresis (second dimension) was performed in 15% polyacrylamide slab gels. The size of the gels was 6.5 cm (running direction) × 7.4 cm × 0.31 cm. The proteins were stained with Serva Blue R250.

RESULTS

Evaluation of two-dimensional electrophoresis patterns

The protein patterns obtained by two-dimensional electrophoresis were compared with regard to the protein spot composition, *i.e.*, the positions of the spots of different patterns were compared. To facilitate this matching procedure, marker proteins were added to the protein sample. The following marker proteins were used: bovine serum albumin (Sigma), bovine β-lactoglobulin (Sigma, St. Louis, MO, U.S.A.), chicken conalbumin (Serva), bovine carbonic anhydrase (Serva) and horse myoglobin (Serva). A detailed description of the visual matching procedure was presented by Jungblut and Klose[4].

For each protein class investigated, two or three two-dimensional electrophoresis patterns were produced to ascertain the reproducibility of the spot number and

spot position. One of these patterns was used for evaluation and the repeat patterns were considered in cases of critical spots (*e.g.*, weak spots).

The two-dimensional electrophoresis protein patterns were evaluated with the aim of determining for each type of dye ligand chromatography performed the protein species unique to the binding proteins, unique to the non-binding proteins or common to both fractions. We then considered the binding proteins and compared the two-dimensional electrophoresis patterns of these proteins pair-wise. The two-dimensional electrophoresis patterns of each pair differed in the type of dye ligands from which they were deduced.

Binding proteins and non-binding proteins

The binding and non-binding protein fractions obtained by dye ligand chromatography using different dyes (Blue A, Red A, Orange A, Green A and Blue B) were separated by two-dimensional electrophoresis (Fig. 1). The patterns of the binding and non-binding proteins were compared. The protein spots common to both the binding and non-binding proteins were registered (Table I). The results show that Red A was the most efficient dye in isolating an individual protein class from the total protein sample. At best, the binding protein fraction contained only about 10% of proteins which also occurred in the non-binding fraction. In contrast, Blue B was the most inefficient dye for fractionating proteins. The portion of Blue B binding proteins that did not bind completely amounted to 34%.

When a complex protein mixture is fractionated by column chromatography into a binding and a non-binding fraction and the fractions are compared by two-dimensional electrophoresis, a general problem arises because these two fractions usually contain different amounts of proteins. The two protein samples used for two-dimensional electrophoresis can then be prepared from the binding and non-binding fractions in such a way that they contain (i) equal amounts of proteins or (ii) protein amounts differing in the same proportions as the protein amounts of the two fractions obtained from the column. We assume that the larger amount of proteins in the non-binding fraction compared with the binding fraction results from a larger number of protein species in that fraction rather than from a small number of protein species present in very high concentrations. If so, the excess of protein species in the non-binding fraction would result from protein species that do not bind completely (100%) to the column (protein species specific for the non-binding fraction). The number of protein species that do not bind completely to the column and, therefore, also occur in the non-binding fraction, is necessarily the same in the binding and non-binding fractions. However, common protein species may be distributed over these two fractions in different proportions, *e.g.*, 50% binding–50% non-binding; 90% binding–10% non-binding; 10% binding–90% non-binding. The consequence is that protein spots present in concentrations below the detection level in one two-dimensional electrophoresis pattern but above this level in the other would be wrongly classified as specific proteins. This error cannot be avoided or minimized, regardless of the quantitative proportions in which the proteins are applied to the two-dimensional electrophoresis. In contrast, in order to reveal the protein species, specific for the binding and non-binding fractions, in the same numerical proportions in the two-dimensional electrophoresis patterns as present in the unfractionated protein mixture, the protein content in the samples used for two-dimensional electrophoresis

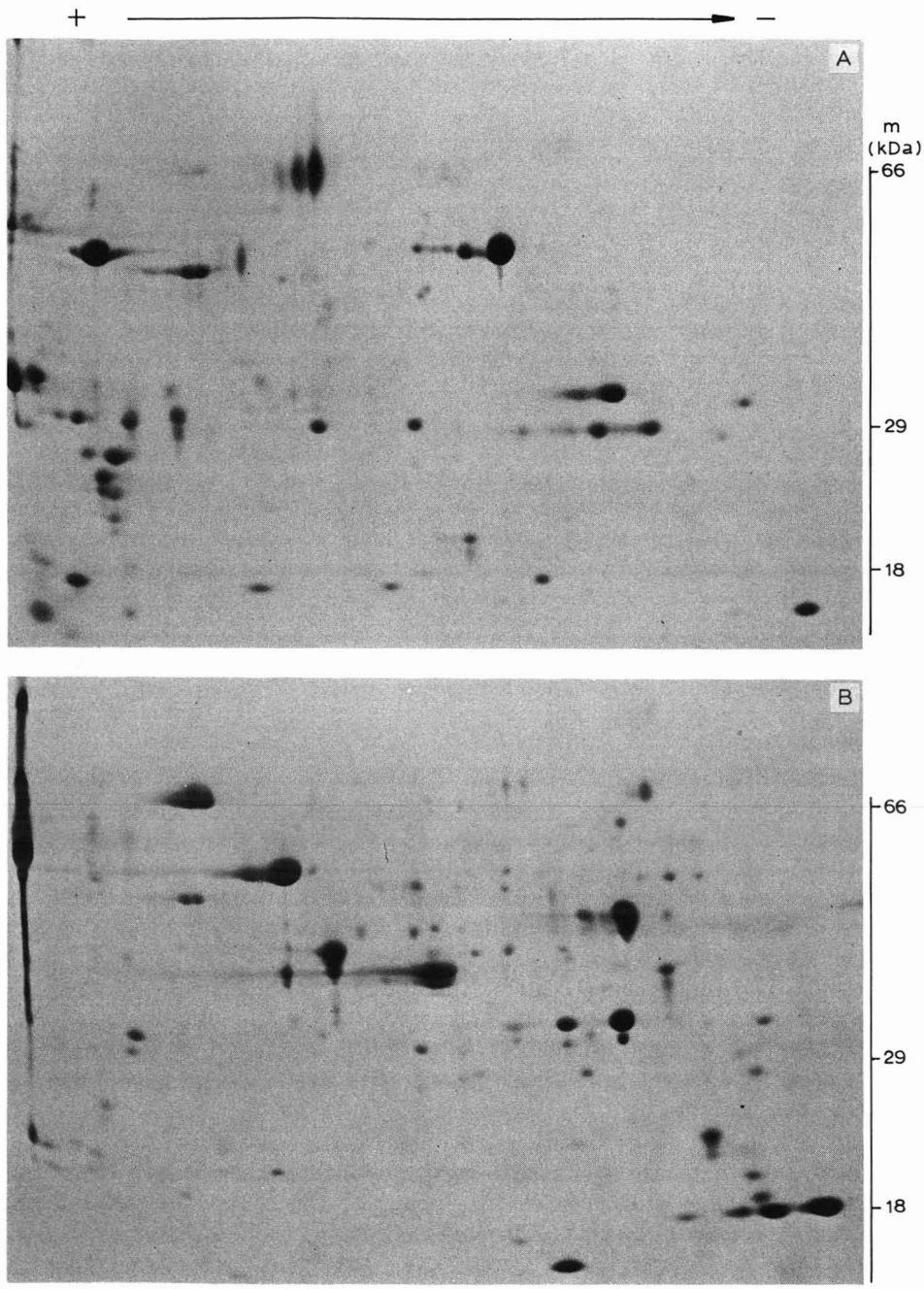

Fig. 1. Two-dimensional electrophoretic protein patterns from chromatographic fractions of mouse brain proteins. The solubilized brain proteins were subjected to heparin–Sepharose chromatography and the non-binding proteins were further fractionated by dye ligand chromatography using Red A. The protein fractions obtained were separated by two-dimensional electrophoresis. (A) Red A non-binding proteins; (B) Red A binding proteins. Small gels [6.5 cm (running direction) × 7.4 cm × 0.31 cm] were used for electrophoretic separation and Serva Blue R250 for protein staining. The patterns show considerable differences between the binding and non-binding proteins. m = Molecular weight; kDa = kilodaltons.

TABLE I

COMPARISON OF BINDING AND NON-BINDING PROTEINS (POLYPEPTIDE SPOTS) FROM MOUSE BRAIN OBTAINED BY DYE LIGAND CHROMATOGRAPHY FOLLOWED BY TWO-DIMENSIONAL ELECTROPHORESIS

Dye	*No. of binding proteins*[a]	*No. of non-binding proteins*[a]	*No. of proteins common to both fractions*[b]
Red A	287 (66.3)[c]	116 (26.8)[c]	30 (10.5)[c]
Green A	176 (47.6)	163 (44.1)	31 (17.6)
Blue A	173 (51.6)	137 (40.9)	25 (14.5)
Orange A	141 (29.7)	308 (64.8)	26 (18.4)
Blue B	156 (21.7)	510 (70.9)	53 (34.0)

[a] Sum of the number of binding, non-binding and common proteins = 100%.
[b] Number of binding proteins = 100%.
[c] Percentages in parentheses.

should differ correspondingly. In our experiments, the protein content in the sample prepared from the binding fraction was too low when the proportion with respect to the protein content of the non-binding protein fraction was maintained, and hence did not reveal a representative number of protein spots in the two-dimensional electrophoresis patterns. Therefore, we increased the protein content in the binding fraction to the protein level in the non-binding fraction. In this way, a maximum number of completely binding proteins could be detected in the two-dimensional electrophoresis patterns, and the number of common protein species in relation to the number of binding protein species could be used as a characteristic value on the basis of which the capacity of the different dye ligands for binding proteins specifically could be compared.

Whereas our aim was to use dye ligand chromatography as a method to obtain individual protein classes, other investigators may be interested in using this method for protein purification. In this respect Blue B may be preferred, because this dye bound the smallest portion of the protein sample applied. If the protein species to be isolated is among the binding proteins of Blue B, the purification effect is greater than in cases in which other dyes were used.

Binding proteins from different dye ligands

Let us consider whether each of the different types of dye ligand tested separates its own protein class from the total protein sample, or whether the proteins bound by the different dye ligands consist, more or less, of the same protein species. This question was investigated by comparing the two-dimensional electrophoresis patterns of the binding proteins from different dyes. A precondition for such a comparison is that the amount of proteins applied to the two-dimensional electrophoresis corresponds to the amount of binding proteins in the original protein extract. If the proportion of the amount of binding proteins to the amount of non-binding proteins is nearly the same for the two dyes compared, this precondition can be fulfilled by applying for each of the two dyes equal amounts of proteins to the two-dimensional electrophoresis. Under these conditions we were able to compare the following dyes: Red A–Green A, Red A–Blue A, Green A–Blue A and Orange A–Blue B. Among these, the most unrelated dyes were Orange A and Blue B. The Orange A-binding proteins

revealed 141 spots in the two-dimensional electrophoresis pattern and the Blue B-binding proteins 156 spots. Of these, 57 spots were common to both patterns. Thus, more than 60% of the protein spots of these two-dimensional electrophoresis patterns were different. These results show that different dyes bind different protein species, and that this is true for a large number of proteins. This suggests that different dyes act by different binding mechanisms and, therefore, may be used as one criterion among others for classifying the enormous number of unknown cell proteins.

CONCLUSION

Dye ligand chromatography and column chromatography in general are used to separate and purify single protein species or a few closely related protein species from a pool of other proteins[13,21]. The sample subjected to chromatography is usually already the result of preceding fractionation procedures. The investigation presented here demonstrates a basically different concept in the application of chromatography. Complex protein extracts were subjected to chromatographic fractionation and the aim was to isolate from the pool a particular protein class rather than a single protein species. Electrophoretic techniques were then used to characterize the separated protein fraction as an individual protein class. In this way, the investigation showed that dye ligands are able to bind a large number, possibly hundreds, of different protein species. Most of the binding proteins were not detected in the eluate and many of these did not show cross-reactions among different types of dye ligands. This suggests that proteins which bind to a certain type of dye ligand form a distinct class of proteins characterized by their binding mechanism(s). Studies on this mechanism would be of great interest. If this mechanism is a biospecific binding mechanism, the protein species of the class in question may also be characterized by common functional features. However, such studies may also reveal that a certain class of binding proteins consists of several subclasses characterized by biospecific and non-biospecific bindings. The use of other criteria to characterize protein classes[1–4] may help to elucidate these subclasses.

ACKNOWLEDGEMENTS

The authors are indebted to Mrs. Marina Schüssler for technical assistance. This work was supported by grants from the Deutsche Forschungsgemeinschaft, awarded to Projekt Kl 237/3-2 ("Systematic Analysis of Cell Proteins").

REFERENCES

1 J. Klose and M. Feller, *Biochem. Genet.*, 19 (1981) 859–870.
2 J. Klose, *J. Mol. Evol.*, 18 (1982) 315–328.
3 P. Jungblut and J. Klose, *Biochem. Genet.*, 23 (1985) 227–245.
4 P. Jungblut and J. Klose, *Biochem. Genet.*, 24 (1986) 925–939.
5 J. Klose, *Humangenetik*, 26 (1975) 231–243.
6 J. Klose and M. Feller, *Electrophoresis*, 2 (1981) 12–24.
7 *Dye-Ligand Chromatography*, Amicon, Lexington, MA, 1980.
8 R. K. Scopes, *J. Chromatogr.*, 376 (1986) 131–140.

9 E. Stellwagen, *Acc. Chem. Res.*, 10 (1977) 92–98.
10 R. S. Yon, *Biochem. J.*, 161 (1977) 233–237.
11 E. Gianazza and P. Arnaud, *Biochem. J.*, 203 (1982) 637–641.
12 I. Lascu, H. Porumb, T. Porumb, I. Abrudan, C. Tarmure, I. Petrescu, E. Presecan, I. Proinov and M. Telia, *J. Chromatogr.*, 283 (1984) 199–210.
13 P. D. G. Dean and D. H. Watson, *J. Chromatogr.*, 165 (1979) 301–319.
14 S. Subramanian, *CRC Crit. Rev. Biochem.*, 16 (1984) 169–205.
15 R. K. Scopes, *Anal. Biochem.*, 165 (1987) 235–246.
16 L. Miribel, E. Gianazza and P. Arnaud, *J. Biochem. Biophys. Methods*, 16 (1988) 1–16.
17 D. Watson, M. Harvey and P. Dean, *Biochem. J.*, 173 (1978) 591–596.
18 S. Hjertén, *J. Chromatogr.*, 87 (1973) 325–331.
19 H. Lowry, N. J. Rosebrough, A. L. Farr and R. J. Randall, *J. Biol. Chem.*, 193 (1951) 265–275.
20 G. L. Peterson, *Anal. Biochem.*, 83 (1977) 346–356.
21 C. R. Lowe, S. J. Burton, J. C. Pearson, Y. D. Clonis, *J. Chromatogr.*, 376 (1986) 121–130.

Journal of Chromatography, 482 (1989) 133–144
Elsevier Science Publishers B.V., Amsterdam — Printed in The Netherlands

CHROM. 21 850

ION-EXCHANGE CHROMATOGRAPHY OF PROTEINS

THE EFFECT OF NEUTRAL POLYMERS IN THE MOBILE PHASE

KRISTIN H. MILBY[a], SA V. HO[b] and JAY M. S. HENIS
Monsanto Company, Corporate Research Laboratories, St. Louis, MO 63146 (U.S.A.)
(First received February 14th, 1989; revised manuscript received August 2nd, 1989)

SUMMARY

The addition of neutral water-soluble polymers such as polyethylene glycol to the eluent of standard ion-exchange chromatography systems affects the separations of proteins in a useful and predictable manner. The relative effects of various polymers are predictable on the basis of their hydrophobicities. Protein retention times are increased, especially for larger and/or more hydrophobic proteins, as predicted by the same order as protein precipitation by neutral polymers. Therefore, this "polymer enhanced chromatography" technique can be particularly useful for the separation of proteins or other biopolymers with the same isoelectric points but different sizes. Examples would include the separation of monomers from dimers and higher order aggregates, or of intact proteins from fragments. Examples of applications with model proteins and the separation of bovine somatotropin monomer and dimer are presented.

INTRODUCTION

In designing a chromatographic separation system for complex molecules such as proteins, the traditional approach has been to choose a single factor on which to base the separation and then minimize the other possible effects. For a separation on the basis of size, for example, measures are taken to avoid ionic and hydrophobic interactions between the solutes and the solid phase. When one step is insufficient, a series of separations based upon size, charge or hydrophobicity is carried out. In order to have high selectivity in a single step, multiple control factors must be combined. Affinity chromatography provides this combination as a natural biochemical interaction. Such selective control of separations is also being explored in the new multimodal approaches to chromatography. This paper presents a novel approach to multimodal chromatography that allows for control of a separation on the basis of charge, size, and possibly hydrophobicity, in a single step. Standard ion-exchange

[a] Present address: Kinetek Systems, Inc., St. Louis, MO 63146, U.S.A.
[b] Present address: Eastman Kodak Co., Bioproducts Division, Rochester, NY 14652, U.S.A.

0021-9673/89/$03.50

columns and chromatography equipment are used with the addition of neutral polymers to the eluent.

Neutral water-soluble polymers such as polyethylene glycol (PEG) and dextran have been used for decades in biochemical separations. They have been used for the "salting out" or precipitation of macromolecules[1–6], crystallization of proteins from polyethylene glycol solutions[7,8], and in two-phase aqueous extraction systems[9]. Their use is not only safe for maintaining biological activity, but can actually provide added stability[3,5,7]. In "polymer enhanced precipitation," neutral polymers were used to improve the yield and selectivity of protein purification with ionic polymers[10,11]. The technique presented here is related to these in the prediction of the selectivity available and has been termed "polymer enhanced chromatography."

EXPERIMENTAL

The following items were purchased from Sigma (St. Louis, MO, U.S.A.): bovine transferrin, bovine hemoglobin, horse heart myoglobin, bovine pancreas alpha chymotrypsinogen A, ascorbic acid, citric acid, and the polyethylene glycol fractions of various molecular weights. Dextran (15 000–20 000) was purchased from Polysciences (Warrington, PA, U.S.A.), and the polyvinylpyrrolidone (PVP, 40 000) from Kodak (Rochester, NY, U.S.A.).

All separations were carried out at ambient temperature. For the work with model proteins a Spectra-Physics (Houston, TX, U.S.A.) 8100 System with pump and autosampler and integrator was used with a Spectoflow 757 absorbance detector from Kratos Analytical (Ramsey, NJ, U.S.A.) operating at 280 nm. For the study of effects of different polymers on the four model proteins, the column was a TSK-Gel DEAE-5PW column 7.5 cm × 7.5 mm I.D. purchased from P.J. Cobert Assoc. (St. Louis, MO, U.S.A.). The column used for the separation of myoglobin and hemoglobin with added PEG was a SynChropak SAX 25 cm × 4.6 mm I.D. from Synchrom (Lafayette, IN, U.S.A.). In both cases the columns were run isocratically at 1 ml/min with 50 m*M* sodium phosphate buffer with or without added polymer, pH 7.5. To insure that the addition of polymers to the eluents did not alter the pH, the appropriate weight-to-volume amount of polymer was dissolved in the buffer, then the pH was adjusted and the solution filtered. Protein solutions were approximately 1 mg/ml in eluent buffer (not containing polymer).

For work on the separation of bovine somatotropin monomer and dimer, a fast-protein liquid chromatography (FPLC) pump system, manual injector, and MonoQ HR 5 cm × 5 mm I.D. column, all from Pharmacia (Piscataway, NJ, U.S.A.) were used with an HM Holochrome detector from Gilson (Middleton, WI, U.S.A.) operating at 280 nm. The eluent was 20 m*M* Tris, pH 10 with a 30-min gradient from 0.10 to 0.25 *M* sodium chloride. The PEG 3350 level was held constant during the gradient. Somatotropin monomer only, dimer only, and monomer/dimer mixture were provided by S.B. Storrs of the Monsanto Agricultural Company, Animal Sciences Division.

RESULTS

The molecular weights and isoelectric points of the model proteins are given in

TABLE I

MOLECULAR WEIGHTS AND ISOELECTRIC POINTS OF THE FOUR MODEL PROTEINS

Protein	*Molecular weight*	*pI*
Myoglobin	16 900	6.8
Chymotrypsinogen A	25 000	9.0
Hemoglobin	64 500	7.0
Transferrin	76 000–80 000	5.2

Table I. These four model proteins and five types of water-soluble polymers were tested. The results are presented as the effect of the polymer type on a given protein in Figs. 1–4. The graphs represent retention time in minutes *versus* the percentage (w/v) of polymer in the eluent. These results are presented in Table II as capacity factors for each model protein under all the conditions tested. Myoglobin, the smallest of the proteins tested, is relatively unaffected by the polymers when shown on the same scale as the other proteins (see Fig. 1). However data in Table II does show that as the concentration of polymer increased, the capacity factor also increased. For transferrin, the largest of the proteins tested, some data points are not included because no peak was detected by 30 min at the higher polymer concentrations. For each polymer, the increases in retention time and capacity factor were greater for the more hydrophobic polymers (as discussed below) and increased as the concentration of the polymer increased.

To illustrate how a polymer affected each protein, Figs. 5 and 6 show the data for PEG 1450 and PEG 3350. Again the graphs represent retention time in minutes *versus* the percentage (w/v) of polymer in the eluent.

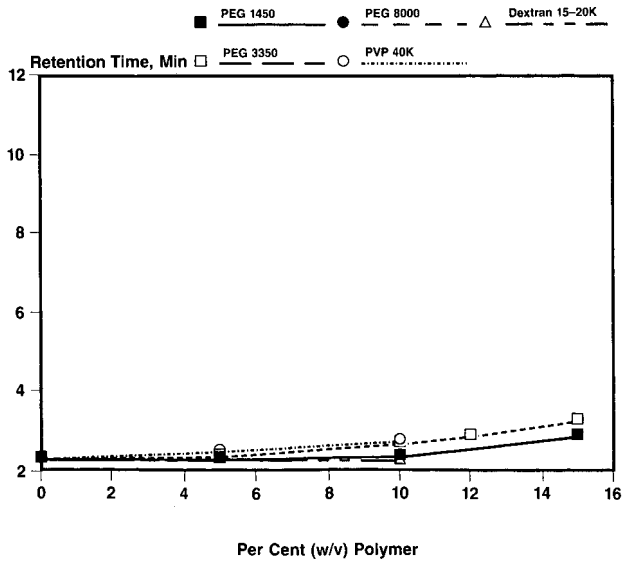

Fig. 1. Effect of type and concentration of neutral polymers in the eluent of an anion-exchange high-performance liquid chromatography (HPLC) system on the retention time of myoglobin.

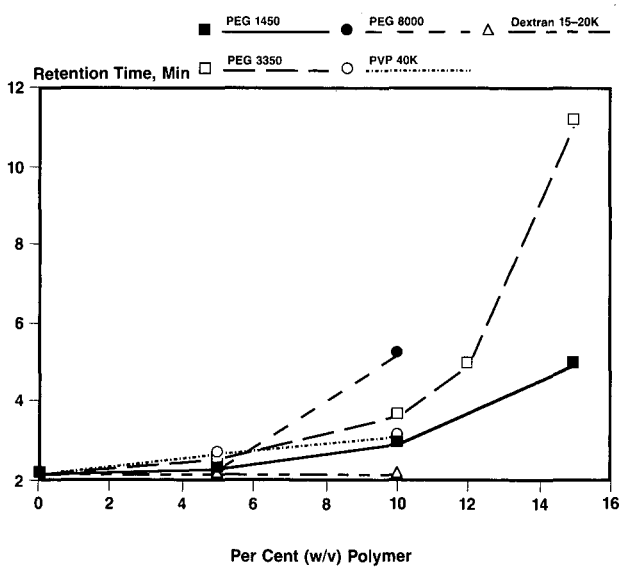

Fig. 2. Effect of type and concentration of neutral polymers in the eluent of an anion-exchange HPLC system on the retention time of hemoglobin.

Under the same conditions as those used for the model proteins, citric acid and ascorbic acid were tested as representative small molecules. They were retained in the absence of polymer with a capacity factor of 0.8. When various concentrations and molecular weights of neutral water-soluble polymers were included in the eluent, the retention times of these small acids were unaffected.

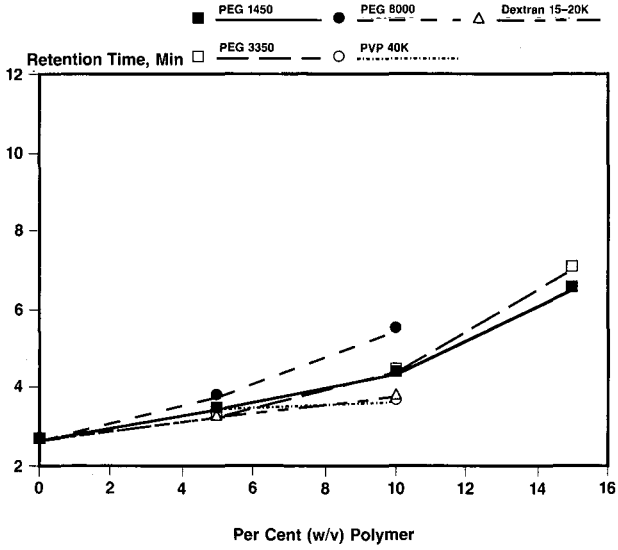

Fig. 3. Effect of type and concentration of neutral polymers in the eluent of an anion-exchange HPLC system on the retention time of chymotrypsinogen A.

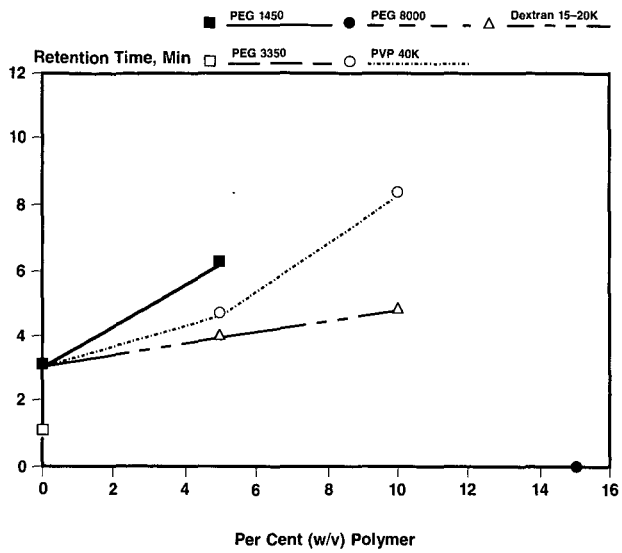

Fig. 4. Effect of type and concentration of neutral polymers in the eluent of an anion-exchange HPLC system on the retention time of transferrin.

To illustrate applications of these concepts, the separation of myoglobin and hemoglobin on an ion-exchange column was tested. The chromatograms in Fig. 7 illustrate how the separation was affected by the presence of PEG in the mobile phase. Under the conditions chosen, the hemoglobin appeared as a shoulder on the unretained myoglobin peak when no polymer was present in the eluent. With PEG

TABLE II

EFFECT OF THE TYPE AND CONCENTRATION OF POLYMER ON THE CAPACITY FACTORS OF MODEL PROTEINS

Conditions: TSK-Gel DEAE-5PW column, 50 m*M* sodium phosphate buffer, pH 7.5, isocratic at 1 ml/min with constant level of polymer in the eluent.

	Myoglobin	*Chymotrypsinogen*	*Hemoglobin*	*Transferrin*
No polymer	0.01	0.20	0.00	0.39
Dextran 15-20K, 10%	0.01	0.70	0.03	1.19
PVP 40 K, 5%	0.12	0.53	0.19	1.08
10%	0.22	0.65	0.42	2.75
PEG 1450, 5%	0.02	0.57	0.02	1.79
10%	0.07	0.94	0.30	[a]
15%	0.30	1.95	1.18	
PEG 3350, 5%	0.08	0.47	0.14	[a]
10%	0.20	0.98	0.62	
12%	0.26		1.21	
15%	0.45	2.15	3.96	
PEG 8000, 5%	0.01	0.70	0.03	[a]
10%	0.08	1.43	1.32	

[a] Peak not detected.

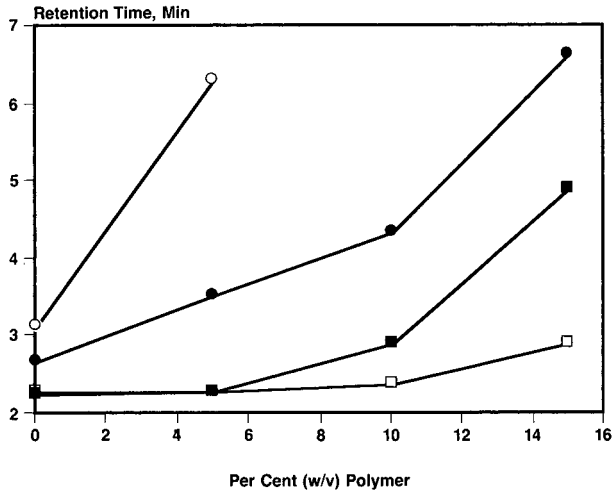

Fig. 5. Effect of PEG 1450 in the eluent of an anion-exchange HPLC system on the retention times of four model proteins. ■ = Hemoglobin; ● = chymotrypsinogen A; □ = myoglobin; ○ = transferrin.

added, however, the retention time of both proteins, especially the hemoglobin, were increased to the point of complete resolution. The results are summarized in Table III as retention times, resolution, and pressure. Both the molecular weight and the (w/v) concentration of the PEG had an effect on the separation. The system pressure was also seen to increase with the addition of PEG to the eluent. Depending upon the equipment used, increased pressure is a potential disadvantage to this technique and did cause limitations to the concentrations of polymer that could be tested in this work. Fortunately, resolution enhancement was observed at low polymer concentrations where the pressure increase was not a concern.

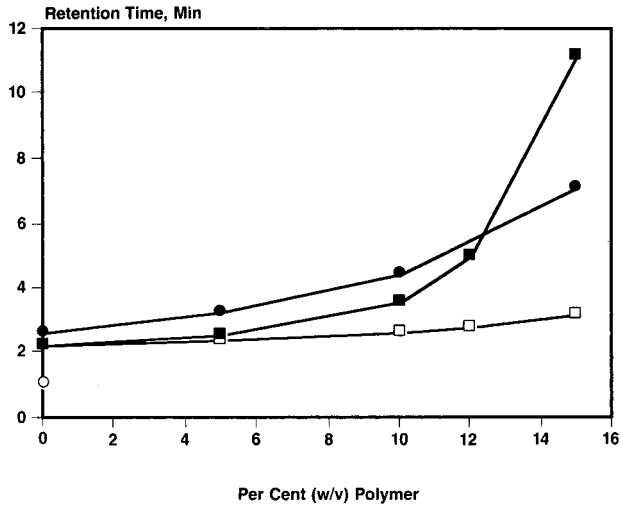

Fig. 6. Effect of PEG 3350 in the eluent of an anion-exchange HPLC system on the retention times of four model proteins. For key to symbols, see Fig. 5.

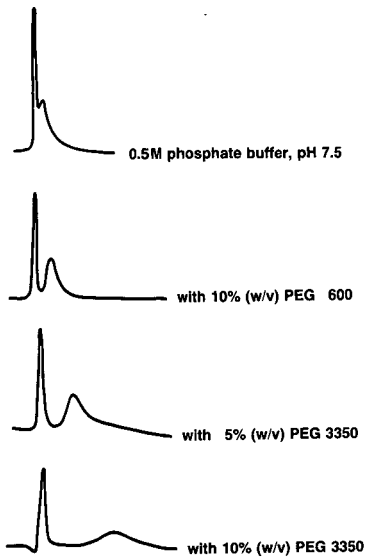

Fig. 7. Separation of myoglobin and hemoglobin on a SynChrom SAX column, 50 m*M* phosphate buffer, pH 7.5, 1 ml/min. The concentration and molecular weight of PEG added to the eluent were varied.

In another application, the influence of PEG 3350 on the separation of bovine somatotropin monomer and dimer is shown in Fig. 8. Without PEG, neither the monomer nor the dimer was retained under the conditions chosen. The retention times of both somatotropin species, especially the dimer, were increased by an increase in the level of PEG in the eluent. A summary of the results for these separations in included in Table IV.

DISCUSSIONS

The precipitation of proteins by neutral polymers is a complex event. While there exists numerous experimental data and theoretical treatments[1–8,12–14], a com-

TABLE III

SEPARATION OF MYOGLOBIN AND HEMOGLOBIN

Conditions: SynChrom SAX column, 50 m*M* phosphate buffer, pH 7.5, isocratic, 1 ml/min. The eluent contained PEG as listed in the first column.

Eluent	*Retention time (min)*		*Resolution*	*Pressure (p.s.i.)*
	Myoglobin	*Hemoglobin*		
0.05 *M* phosphate buffer, pH 7.5	2.24	2.73	0.25	1100
with 10% (w/v) PEG 600	2.25	3.54	0.56	1500
with 5% (w/v) PEG 3350	2.92	5.10	0.70	1460
with 10% (w/v) PEG 3350	2.91	9.12	1.7	2460

TABLE IV

SEPARATION OF BST MONOMER AND DIMER

Conditions: Pharmacia MonoQ column, 20 m*M* Tris, pH 10, with a 30 min gradient from 10 m*M* to 25 m*M* NaCl. PEG 3350 concentration in eluent was held constant during the separation. na = Data not available.

PEG 3350 (%, w/v)	*Retention times (min)*		*Pressure (p.s.i.)*
	Monomer	*Dimer*	
0	3	3	250
1	4	5	na
2.5	6.5	8	300
5	9	13	360
7	11	14.5	420
10	13	38	450

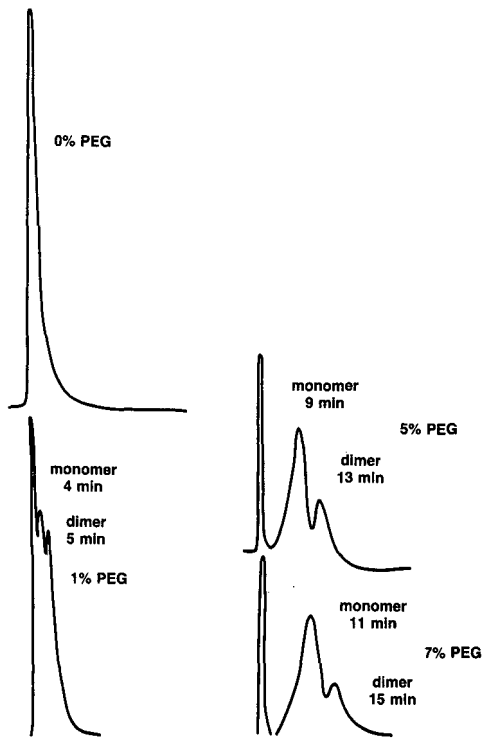

Fig. 8. Separation of bovine somatotropin monomer and dimer on a Pharmacia MonoQ column. The eluent was 20 m*M* Tris, pH 10, with a 30 min gradient from 10 m*M* to 25 m*M* NaCl with 0–7% PEG 3350 which was constant during the gradient.

plete understanding of the phonemenon has not been obtained. It is generally agreed, however, that the observed effects of PEG and other neutral polymers on protein precipitation can be qualitatively explained by the excluded volume theory. According to this theory, water-soluble polymers in aqueous solutions are able to interact with a large number of water molecules, resulting in reduction of the solvating power of water for the protein. The major parameter here is the size (molecular weight) of the polymer: the larger the polymer, the more effective it is as precipitant.

Lee and Lee[7] and Arakawa and Timasheff[14] obtained some evidence for a secondary effect that they termed "preferential interaction" between PEG and the proteins studied. This interaction is proposed to be hydrophobic in nature[14] to explain the opposite effect of PEG on RNase A and β-lactoglobulin. Thus, an important parameter here is the chemical nature (*i.e.*, hydrophobicity) of the protein, which is not considered in the excluded volume theory.

Empirically, the controlling protein parameter is size (volume), with hydrophobicity and charge being secondary. As with salting out, larger proteins precipitate at lower polymer concentrations than smaller ones. The controlling polymer parameter is hydrophobicity as determined by its composition and molecular weight. More hydrophilic polymers are more selective but less efficient than more hydrophobic ones. For the related phenomenon of two-phase aqueous systems, Albertsson has proposed a ranking of the hydrophobicities of water soluble polymers (Fig. 9); in addition, for certain types of polymers such as PEG, hydrophobicity increases as molecular weight increases[9]. The region of aqueous polymer systems is a narrow band within the range from the aqueous salts to the non-polar solvents. This is an unexplored region for applications to chromatographic elution.

In polymer-enhanced precipitation[10,11], a combination of a charged polymer and a neutral polymer is used to selectively precipitate protein(s) of interest. The charged polymer is used to form a charge complex with the appropriate protein(s). The role of the neutral polymer is less straightforward and is probably two-fold. First, it enhances the precipitation of the protein–charged polymer complex, very likely as a result of the excluded volume effect. Secondly the appropriate choice of the neutral polymer appears to enhance the selectivity of the charged polymer, probably through the hydrophobic interactions between the neutral polymer and proteins in solution.

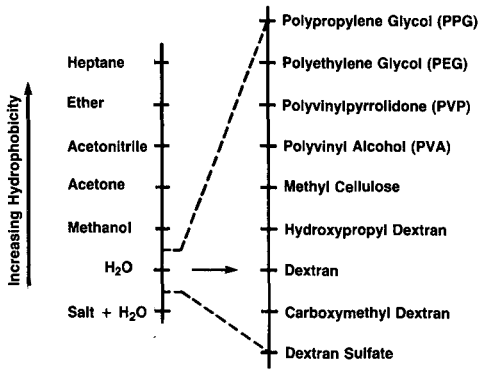

Fig. 9. The hydrophobic ladder as modified from ref. 9. Ether = Diethyl ether.

Fig. 10 shows the important properties for the protein and each polymer. For the protein and the neutral polymer, the same factors have the same qualitative influence as in polymer-induced precipitation. The data presented here can also be explained by these control factors. The neutral polymers decrease the solvating power of the eluent. This shifts the equilibrium of the level of solute in the mobile phase *versus* on the solid phase, so the interaction between the protein and the solid phase is increased. Because this technique uses an immobilized ion exchange support instead of a soluble charged polymer, it has been given the related name of "polymer enhanced chromatography."

If the mechanism of polymer enhanced chromatography is indeed related to protein precipitation and the excluded volume theory, the above results should be qualitatively explained in the same way. If the excluded volume theory is applicable to our observation, it predicts selectivity in how polymers affect protein chromatography. Larger and/or more hydrophobic proteins should be more readily effected than smaller and/or more hydrophilic ones. Furthermore, the effectiveness of a polymer is determined by its hydrophobicity. The series of experiments with model proteins and different polymer types verifies these predictions. In general, the protein retention time increased as the concentration of polymer was increased. As predicted, the effect was greater for more hydrophobic polymers. For a given concentration of PEG, the effect increased as the average molecular weight of the PEG increased. Dextran, the least hydrophobic of the polymers tested, had very little effect on the protein retention. PVP is ranked between dextran and PEG on the hydrophobicity scale (Fig. 9). The particular sample of PVP tested was higher in molecular weight than the PEGs but was still less effective in shifting the protein retention.

Myoglobin, the smallest of the model proteins, was least influenced by the added polymers (Fig. 1). However Table II does show that at 10–15% polymer, there was an increase in capacity factor. Hemoglobin is a protein similar in charge and hydrophobicity to myoglobin, but approximately four times larger (see Table I). As predicted by the excluded volume theory, hemoglobin was more strongly influenced by the presence of polymers than the myoglobin. Transferrin, the largest of the proteins tested, was the most strongly affected by the polymers (Fig. 4). In this case, several of the concentrations of polymers used increased and/or broadened the peak to the point of being undetectable. Chymotrypsinogen is between myoglobin and hemoglobin in size (see Table I) yet was more strongly influenced by the presence of

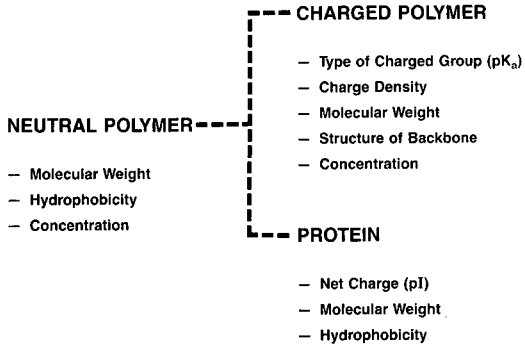

Fig. 10. Controlling factors in polymer-enchanced precipitation[10,11].

polymers (see Table II and Figs. 5 and 6). It is possible that in addition to size, a protein's hydrophobicity may play an important role in the extent its solubility is affected by the presence of the polymer. Also note that at the pH used (7.5) chymotrypsinogen with a p*I* of 9.0 has an overall positive charge, although net charge alone is insufficient to explain protein retention in ion-exchange chromatography[15]. Fig. 6 shows a crossover of the lines for hemoglobin and chymotrypsinogen that may represent the point at which size becomes more dominant than hydrophobic and ionic effects. Further exploration of the effects of pH and ionic strength on polymer enhanced chromatography is needed to obtain a better understanding of these interactions.

Fig. 7 and Table III show enhanced resolution of myoglobin and hemoglobin by the addition of PEG to the eluent of an anion-exchange system. Hemoglobin is an oligomer made up of four polypeptide chains, each of which is similar to the single chain of myglobin. Thus the isoelectric points and the hydrophobicities of these two proteins are very similar, but hemoglobin is approximately four times larger than myoglobin. The presence of PEG in the eluent increased the retention times of the proteins, especially the larger hemoglobin. The effect was greater when the higher molecular weight, and therefore more hydrophobic PEG was used. Peaks were significantly broadened although peak areas were relatively constant, indicating consistant recovery is possible. The broadening is likely due to the heterogeneous nature of the interaction between the protein surface and the solid phase. Using a gradient of the polymer should decrease the peak broadening, but this has not yet been tested.

Fig. 8 shows how the separation of bovine somatotropin (BST) monomer and dimer is affected by the addition of PEG 3350 to the mobile phase of an ion-exchange system. This separation is a real life example which is ideally suited to polymer enhanced chromatography. Because of the need to separate the BST from other contaminants it is necessary to carry out an ion-exchange step at this point of the purification. It is desired to minimize the level of dimer in the final product. The monomer and dimer are obviously very much alike in every way but size. Polymer enhanced chromatography allows the ion-exchange step to also separate monomer from dimer. The retention times of both species are increased, but that of the larger dimer is more affected than the monomer. Just 5% PEG 3350 increased the resolution of the two components from 0.25 to 0.70 without a dramatic increase in pressure. Note that peak broadening is not as significant as in the myoglobin–hemoglobin separation, perhaps because a salt gradient was used in this case.

CONCLUSIONS

The addition of neutral water-soluble polymers to the eluent of ion-exchange chromatography systems selectively increases the retention times of protein solutes. It could be argued that the polymer alters the solid phase in some manner or blocks the pores in the solid support. This does not seem likely because any blocking of charges or pores should act to decrease, rather than increase, retention times. Furthermore, the retention times of small molecules (ascorbic and citric acid) were unaffected by the polymer. It might also be hypothesized that the polymer leads to protein self-association, although this has not been detected in studies of polymer-induced precipitation[2,6].

The observed increased retention times are most probably due to an increased protein–solid phase interaction. That is, the protein is less soluble in eluent containing the polymer and is therefore more likely to interact with the solid phase.

The effect of polymers on the ion-exchange retention of proteins can be predicted qualitatively by the excluded volume theory which is also invoked to explain neutral polymer-induced precipitation of proteins. According to this concept, polymer competes with the protein for water. In the extreme case, the protein becomes dehydrated enough to precipitate. In this application to chromatography, polymer added to the eluent shifts the equilibrium of the protein from solution in the mobile phase to interaction with the solid phase.

For the combination of ion-exchange chromatography with neutral polymers presented here, the greatest power of the technique is when the proteins to be separated have very similar charge properties but different sizes. Two such applications have been presented: the separation of myoglobin and hemoglobin, and the separation of bovine somatotropin monomer and dimer. While these separations are achievable by other chromatographic methods, ion exchange is preferred for preparative separation because of its high loading capacity and its use of aqueous rather than organic eluents. The presence of a neutral polymer in the product is not necessarily a complication since it may improve the product stability or be required in the final formulation.

Based upon the results and hypothesis presented here, neutral polymers would increase the interaction between biopolymers and chromatographic supports in general. Other potential applications of polymer-enhanced chromatography include separating intact molecules from fragments or breakdown products, or separating antibody–antigen complexes from the free components. It is likely that this technique will be applicable to the separations of nucleotides, cellular fragments, etc., in the same manner that polymer-induced precipitation and two-phase aqueous systems have been extended to these areas. Extension of this work may also include hydrophobic interaction chromatography using decreasing gradients of neutral polymers rather than salts.

REFERENCES

1 T. C. Laurent, *Biochem. J.*, 89 (1963) 253.
2 P. H. Iverius and T. C. Laurent, *Biochim. Biophys. Acta*, 133 (1967) 371.
3 P. R. Foster, P. Dunnill and M. D. Lilly, *Biochim. Biophys. Acta*, 317 (1983) 505.
4 W. Honig and M-R. Kula, *Anal. Biochem.* 72 (1976) 502.
5 K. C. Ingham, *Arch. Biochem. Biophys.*, 184 (1977) 59.
6 K. C. Ingham, *Arch. Biochem. Biophys.*, 186 (1978) 106.
7 J. C. Lee and L. L. Y. Lee, *J. Biol. Chem..*, 256 (1981) 625.
8 A. McPherson, *Methods Enzymol.*, 114 (1985) 120.
9 P-A. Albertsson, *Partition of Cell Particles and Macromolecules*, Wiley-Interscience, New York, 2nd ed., 1971.
10 S. V. Ho, *US Pat.*, 4,645,829 (1987).
11 S. V. Ho, *Presented at the 1987 AICHE National Meeting, November 15–20, New York.*
12 I.R.M. Juckes, *Biochim. Biophys. Acta*, 229 (1971) 535.
13 J. C. Lee and L. L. Y. Lee, *Biochemistry*, 18 (1979) 5518.
14 T. Arakawa and S. N. Timasheff, *Biochemistry*, 24 (1985) 6756.
15 W. Kopaciewicz, M. A. Rounds, J. Fausnaugh and F. E. Regnier, *J. Chromatogr.*, 266 (1983) 3.

Journal of Chromatography, 482 (1989) 145–154
Elsevier Science Publishers B.V., Amsterdam — Printed in The Netherlands

CHROM. 21 848

THEORETICAL CONSIDERATIONS ON THE APPEARANCE OF SAMPLE AND SYSTEM PEAKS IN ION CHROMATOGRAPHY WITH PHOTOMETRIC DETECTION

ATSUSHI YAMAMOTO*, AKINOBU MATSUNAGA, MIKIYA OHTO and EIICHI MIZUKAMI
Toyama Institute of Health, Kosugi-machi, Toyama 939-03 (Japan)
and
KAZUICHI HAYAKAWA and MOTOICHI MIYAZAKI
Faculty of Pharmaceutical Sciences, Kanazawa University, Kanazawa 920 (Japan)
(First received August 9th, 1988; revised manuscript received April 27th, 1989)

SUMMARY

A general model is proposed for interpreting the appearance of sample and system peaks in ion-exchange chromatography with photometric detection. In this theory, a changed fraction of organic acid in the mobile phase resulting from the ion-exchange process with a sample ion migrates through the column from plate to plate in accordance with the ionic and partition equilibria. This perturbation of UV-detectable components yields the sample and system peaks. Simulation of this theory by computer accounts well for the sample peaks observed in real ion chromatography. An equation expressing the sample response–capacity factor relationship at low mobile phase pH was derived.

INTRODUCTION

In the determination of inorganic and organic anions by high-performance liquid chromatography with photometric detection, both reversed-phase and ion-exchange columns have been used. It was observed in the reversed-phase mode with a light-absorbing modifier in a mobile phase that a "system peak" appeared and that the direction of the sample peak changed in relation to it. The closer the sample peak eluted to the system peak, the larger the peak area became. It is generally considered that a system peak appears in liquid chromatography when the mobile phase contains more than one component[1–8]. Recently, Schill and co-workers[9–12] derived a theoretical equation for the interpretation on this phenomenon.

In the ion-exchange mode, in which a light-absorbing organic acid solution at neutral pH was usually used, a system peak was not observed and the direction of the sample peak was always negative[13]. A system peak appeared on decreasing the pH of the mobile phase. When an organic acid solution at acidic pH was used as a mobile phase on a column packed with a hydrophilic material-based anion exchanger, the direction of the sample peak was positive prior to the system peak and negative after it.

0021-9673/89/$03.50

These results were similar to those in the reversed-phase mode as described above. However, neither the formation of sample and system peaks nor the direction and area of the sample peak have been studied theoretically in ion-exchange chromatography with photometric detection, especially at low pH. In this paper, we proposed a general model for the formation of sample and system peaks and derive a theoretical equation for the response of a sample peak with a mobile phase low pH. The present theory explains well the phenomenon described above.

THEORY

In a column packed with hydrophilic material-based ion exchanger, there is a small interaction between an organic acid in the mobile phase and the unfunctionalized region of the packing material[1]. Only the undissociated form has been thought to be adsorbed. The following equilibrium is assumed to hold for mobile phase organic acid in the column: where [EH] and [E^-] are the undissociated and dissociated forms of the mobile phase organic acid, respectively, K_{ae} is its acid dissociation constant, K_D is the ratio of the fractions of the undissociated acid in the two phases and the subscripts m and s represent existence in the mobile and the stationary phase, respectively.

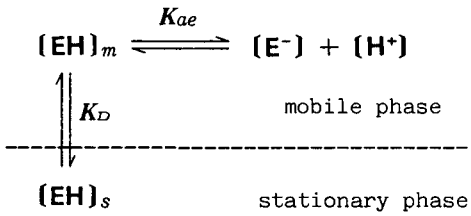

It is assumed that the hydrophilic sample ions are retained on the separation column only by an ion-exchange process. The concentration of sample ion in the mobile phase, [S^-], is deduced from

$$K_{as} = [S^-][H^+]/[SH]$$

$$[ST] = [S^-] + [SH]$$

Therefore,

$$[S^-] = K_{as}[ST]/(K_{as} + [H^+]) \quad (1)$$

where K_{as} is the acid dissociation constant of the sample and [ST] and [SH] are the concentrations of total and undissociated samples in the mobile phase, respectively.

Similarly, [E^-] is deduced from

$$[ET] = [E^-] + [EH]_s + [EH]_m$$

$$K_{ae} = [E^-][H^+]/[EH]_m$$

$$K_D = [EH]_s/[EH]_m$$

Therefore,

$$[E^-] = K_{ae}[ET]/\{K_{ae} + (K_D + 1)[H^+]\} \quad (2)$$

where [ET] is the concentration of total organic acid. From the charge balance, the following equation holds:

$$[H^+] + [Na^+] = [E^-] + [S^-] + [OH^-]$$

where $[Na^+]$ is the concentration of sodium ion as a counter ion. Substitution of eqns. 1 and 2 into this equation gives

$$[H^+] = K_{ae}[ET]/\{K_{ae} + (K_D + 1)[H^+]\} + K_{as}[ST]/(K_{as} + [H^+]) + \\ + K_w/[H^+] - [Na^+] \quad (3)$$

where K_w is ionic product of water. The equilibrium proceeds in all the theoretical plates in the column to satisfy eqn. 3 accompanied by a difference in the concentrations of the sample and mobile phase acid.

The system peak observed in ion chromatography (IC) with an acidic mobile phase is considered to appear as a result of the elution of adsorbed mobile phase acid from the column[1,2]. Its capacity factor (k'_e) is the ratio of the changed fractions between the undissociated acid adsorbed on the stationary phase and the total acid in the mobile phase:

$$k'_e = [dEH]_s/([dEH]_m + [dE^-]) \quad (4)$$

When the sodium ion is free in the mobile phase, as $[E^-] = [H^+]$, eqn. 4 can be rewritten as

$$k'_e = 2[E^-]K_D/(2[E^-] + K_{ae}) \quad (5)$$

Eqn. 5 indicates that k'_e is constant despite the difference in sample species and the K_D value can be determined experimentally.

By applying this constant k'_e, the behaviours of the sample and mobile phase acid in the column under conditions with free sodium ions are calculated based on a Craig-type repetitive distribution[14]. The ideal transfer of sample through a Craig-type repetitive distribution instrument can be described by

$$[ST]^{n,p} = [S]_m^{n,p} + [S]_s^{n,p} = [S]_m^{n-1,p-1} + [S]_s^{n-1,p}$$

where $[S]_m^{n,p}$ is the fraction of sample in the mobile phase that is in contact with plate p when the nth plate has been equilibrated. Similarly, $[S]_s^{n,p}$ is the fraction of sample in the stationary phase and $[ST]^{n,p}$ is the sum of both fractions. The following relationship holds between k'_s and the distribution equilibrium of the sample:

$$k'_s = [S]_s^{n,p}/[S]_m^{n,p}$$

By using this equation, a general equation is deduced:

$$[ST]^{n,p} = (n - 1)!\, k_s^{n-p}/(p - 1)!\,(n - p)!\,(1 + k_s')^{n-1}$$

The organic acid in the mobile phase is substituted quantitatively by the sample ion according to a mechanism of one-to-one ion exchange. Similarly, by using $[dE]_m^{n,p}$ and $[dE]_s^{n,p}$, the fractions of the excess or deficiency of organic acid in the mobile phase and in the stationary phase, respectively, $[dET]^{n,p}$, the sum of both fractions, can be described as follows:

$$[dET]^{n,p} = [S]_s^{n,p} - [S]_s^{n-1,p} + [dE]_m^{n-1,p-1} + [dE]_s^{n-1,p}$$

where $[dE]_s = [dEH]_s$ and $[dE]_m = [dEH]_m + [dE^-]$. By using eqn. 4, a general equation is deduced:

$$[dET]^{n,p} = (n - 1)!\, k_e'^{n-p} k_s'/(p - 1)!\,(n - p)!\,(1 + k_e')^{n-1}\,(k_s' - k_e') -$$

$$(n - 1)!\,(1 + k_e')\,k_s'^{n-p+1}/(p - 1)!\,(n - p)!\,(1 + k_s')^n\,(k_s' - k_e')$$

Now, consider the quantitative ratio between the sample and the changed organic acid in the mobile phase:

$$[dE]_m^{n,p}/[S]_m^{n,p} = \{k_e'^{n-p}(1 + k_s')^n/k_s'^{n-p}(1 + k_e')^n - 1\}k_s'/(k_s' - k_e')$$

$[S]_m^{n,p}$ has its maximum at $n = p(1 + k_s')$:

$$[dE]/[S]_{max} = \{k_e'^{pk_s'}(1 + k_s')^{p(1+k_s')}/k_s'^{pk_s'}(1 + k_e')^{p(1+k_s')} - 1\}k_s'/(k_s' - k_e')$$

In a real system, a large value for p is required for the separation of the peaks:

$$\lim_{p\to\infty} [dE]/[S]_{max} = k_s'/(k_e' - k_s') \qquad (k_e' \neq k_s') \tag{6}$$

The concentration of the mobile phase organic acid in the sample zone can be calculated by eqn. 6. If the sample amounts are equal, the relative peak area (A_s/A_t) of a given sample (S) to the standard sample (T) is expressed by the following equation:

$$A_s/A_t = k_s'(k_e' - k_t')/k_t'(k_e' - k_s') \tag{7}$$

EXPERIMENTAL

The ion chromatographic system included a Shimadzu (Kyoto, Japan) LC-6A pump, a Rheodyne (Cotati, CA, U.S.A.) Model 7125 injector, a Shimadzu SPD-2A UV detector and a Shimadzu C-R3A Chromatopac calculator. The anion-exchange columns used were a Tosoh (Tokyo, Japan) TSK gel IC-Anion-PW (5 cm × 4.6 mm I.D., polyacrylate based, particle size 10 μm), a Tosoh TSK gel IC-Anion-SW (5 cm × 4.6 mm I.D., silica, 5 μm) and a Shimadzu Shim-pack IC-A1 (10 cm × 4.6 mm I.D.,

polyacrylate, 12.5 μm). Mobile phases were prepared by dissolving salicylic acid, *o*-nitrobenzoic acid (ONB), phthalic acid and sulphanilic acid individually in distilled, deionized water. Sodium hydroxide solution was used for pH adjustment, if necessary.

The elution behaviour of samples in ion chromatography (IC) was confirmed by the analysis of samples in eluate fractions. Acetic and formic acids were determined by gas chromatography–mass spectrometry (GC–MS) and phosphoric acid was determined by the method of Baba *et al.*[15]. GC–MS was performed with a Shimadzu QP-1000 gas chromatograph–mass spectrometer. The operating conditions were as follows: column, Gasukuro Kogyo (Tokyo, Japan) Gaskuropack 54 (1.6 m × 3 mm I.D.); column temperature, 170°C; carrier gas, Helium at a flow-rate of 30 ml/min; separator and source temperature, 250°C; and ionization energy, 70 eV. The UV spectra were measured with a Hitachi (Tokyo, Japan) UV-2000 spectrophotometer.

Adsorption isotherms were prepared using the unfunctionalized IC-Anion-PW packing material (30–60 μm) provided by Tosoh, to which the bulk solutions were added. After equilibration for 6 h at 25±1°C, the decrease in concentration was measured.

Calculations were made on an NEC (Tokyo, Japan) PC-9801 UX personal computer.

RESULTS AND DISCUSSION

In the stoichiometric study of chromatographic processes, photometric detection has the great advantage over conductivity detection that the absorbance difference between the mobile phase and sample is constant when samples are not light absorbing, whereas the conductance difference is affected by changes in the sample species. A sample response model for photometric detection with a mobile phase of neutral pH has been proposed[13,16], but it is inapplicable at other pH values. Fig. 1 shows a typical chromatogram of five organic acids by using acidic sulphanilic acid solution as the mobile phase. Two characteristic features were observed. The first was that sample zones of acetic and laevulinic acids eluting prior to the system peak formed

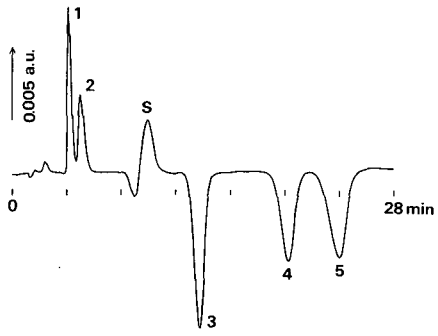

Fig. 1. Ion chromatogram for a system with an organic acid solution at low pH as the mobile phase. Column, TSK gel IC-Anion-PW; mobile phase, 0.5 m*M* sulphanilic acid (pH 3.5); flow-rate, 0.8 ml/min; column temperature, 40°C; wavelength of UV detection, 271 nm; injection volume, 10 μl. Peaks: 1 = acetate (0.7 m*M*); 2 = laevulinate (0.25 m*M*); S = system peak; 3 = lactate (0.25 m*M*); 4 = formate (0.25 m*M*); 5 = succinate (0.25 m*M*).

positive peaks, whereas sample zones of lactic, formic and succinic acids eluting after the system peak gave negative peaks, despite the formation of negative peaks with all of these samples using a sulphanilic acid mobile phase of neutral pH. A similar phenomenon was observed on combination of other anion-exchange columns with hydrophilic packing materials and other organic acids tested as mobile phases in the work. The second feature was that the area of the sample zone increased as its elution time became closer to that of the system peak.

In order to detect the elution of samples directly, GC–MS and spectrophotometry were used. Fig. 2 shows that the total amount of a sample injected is restricted to the corresponding positive peak. As these sample ions show no absorption at the detection wavelength of 310 nm, the positive peaks indicate that sample ions were eluted from the column accompanied by light-absorbing mobile phase organic acid. In this instance, the system peak became negative to compensate for the deficit of the mobile phase organic acid coeluted with sample ions.

At acidic pH, both dissociated and undissociated forms of the mobile phase organic acid coexist. Fig. 3 shows adsorption isotherms for organic acids used as mobile phases on the unfunctionalized IC-Anion-PW packing material of the separation column. In contrast to non-adsorption of the dissociated acids in the presence of high bulk solution concentrations of sodium chloride[17], neutral acids were substantially adsorbed according to the Langmuir model. As these adsorption isotherms might be considered to be straight lines below the mobile phase concentration and were not affected by the coexistence of samples, Scheme I has been found to hold and K_D can be considered to be constant.

The behaviour of sample ions in an ion-exchange column can be considered on the basis of the theory of Gjerde *et al.*[18]. If the sample ions are retained on the column only by an ion-exchange process, there is a constant relationship between the concentration of the eluting solution and the capacity factor of the sample. Plots of the logarithm of salicylate ion concentration in the mobile phase *vs.* log k'_s for four anions

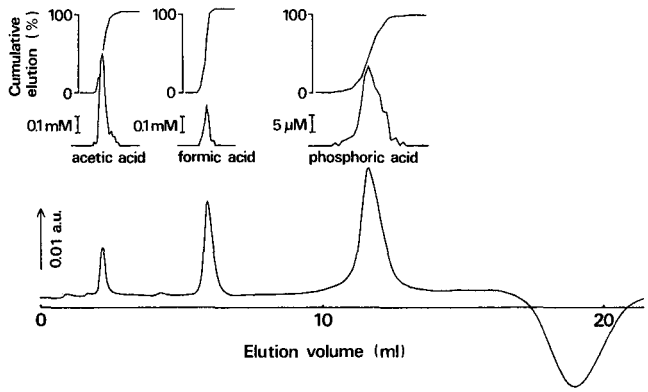

Fig. 2. Verification of the correspondence of sample elutions (upper) to the positive peaks in the ion chromatogram (lower). Sample elutions were analysed by GC–MS (acetic and formic acids) and by spectrophotometry using a molybdenum reagent (phosphoric acid). Mobile phase, 0.5 m*M* salicylic acid; column temperature, ambient; wavelength of UV detection, 310 nm. Samples: acetic acid (6 m*M*), formic acid (2 m*M*) and phosphoric acid (2 m*M*). Other conditions as in Fig. 1.

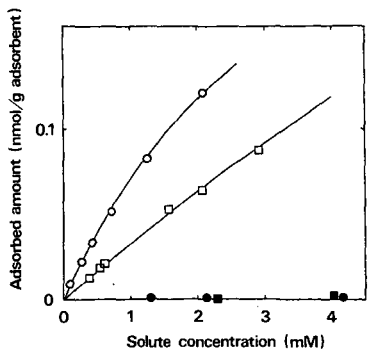

Fig. 3. Adsorption isotherms for mobile phase organic acids on unfunctionalized IC-Anion-PW packing material. Conditions: salicylic acid at pH < 0.7 (○) and at pH > 7 and $Na^+ = 0.2\ M$ (●); phthalic acid at pH < 0.7 (□) and at pH > 7 and $Na^+ = 0.2\ M$ (■).

on IC-Anion-PW are shown in Fig. 4. As these sample ions and salicylate act as monovalent anions, the slopes of these lines must be -1, a deviation from -1 indicating that the ratio of the retention on the column by the ion-exchange process to that by adsorption is decreased. It is clear from the results of adsorption experiments that chloride is not adsorbed on the packing material at all but other sample acids are adsorbed slightly. Consequently, sample ions that follow the theory of Gjerde *et al.* result in chromatograms compatible with our theory.

The simulation of a chromatogram was performed on the basis of a Craig-type repetitive distribution[14] to satisfy eqn. 3 in the column and by considering the acid equilibrium with the delocalized sample in the column effluent[19]. Fig. 5 shows the results of the simulation for 1 mM salicylic acid as the mobile phase. The lower chromatogram was simulated by the K_D of salicylic acid, which was determined from eqn. 4 (upper chromatogram). The two chromatograms are in good agreement.

The simulations made by altering the pH of the mobile phase were performed by

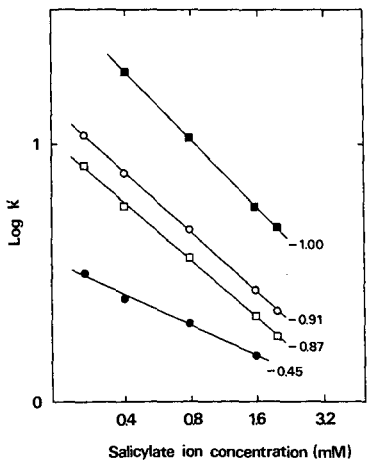

Fig. 4. Log (ionic concentration of salicylic acid) *vs.* log (capacity factor) at pH 3.6 on IC-Anion-PW. ■ = Chloride; ○ = formate; □ = lactate; ● = acetate. The numbers on the lines represent the slopes.

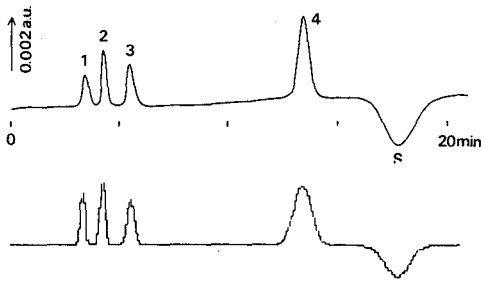

Fig. 5. Comparison between actual (upper) and computer-simulated (lower) chromatograms. Conditions for the actual chromatogram: mobile phase, 1 m*M* salicylic acid; wavelength of UV detection, 319 nm; other conditions as in Fig. 1. Peaks: 1 = lactate (0.5 m*M*); 2 = formate (0.5 m*M*); 3 = pyroglutamate (0.5 m*M*); 4 = chloride (0.2 m*M*); S = system peak. The lower trace represents the elution of mobile phase simulated by using $K_D = 31.0$ and $K_w = 10^{-14}$ in eqn. 3.

use of this K_D value. In this instance, the pK_a values of organic acids were assumed not to be affected, as the local variation of the ionic strength is small. For chloride and lactate, a comparison of the peak areas in the actual and simulated chromatograms is shown in Fig. 6. The solid lines represent the calculated peak areas and the open and closed circles are the actual peak areas of chloride and lactate, respectively. The ordinate indicates the relative peak areas in relation to that of chloride in a mobile phase of neutral pH. The results show clearly that their peaks are positive at low pH (less than *ca.* 3.5), that they reverse with increase in pH and finally converge under standardized conditions[13,16].

In a divalent mobile phase, the charge balance is indicated by

$$[H^+] + [Na^+] = [EH^-] + 2[E^{2-}] + [S^-] + [OH^-]$$

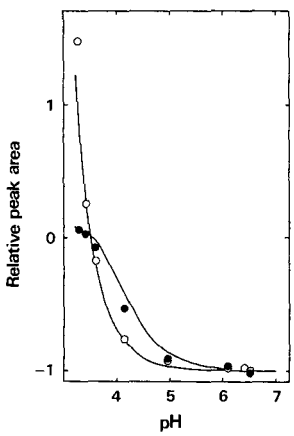

Fig. 6. Comparison of relative peak areas simulated by eqn. 3 (solid lines) with actual values for (○) chloride and (●) lactate with 1 m*M* salicylate as the mobile phase on IC-Anion-PW.

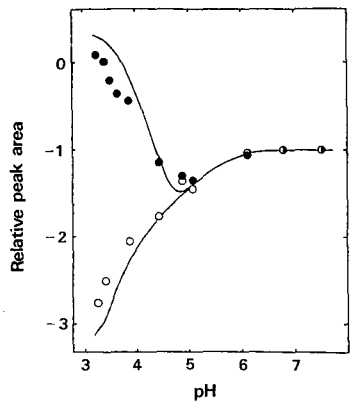

Fig. 7. Comparison of relative peak areas simulated by eqn. 8 with actual values with 1 m*M* phthalate as the mobile phase on IC-Anion-PW. Symbols as in Fig. 6.

Therefore,

$$[H^+] = (K_{ae1}[ET]\,[H^+] + 2K_{ae1}K_{ac2}[ET])/\{K_{ae1}K_{ac2} + K_{ae1}[H^+] + \\ + (K_D + 1)\,[H^+]^2\} + K_{as}[ST]/(K_{as} + [H^+]) + K_w/[H^+] - [Na^+] \quad (8)$$

where K_{ae1} and K_{ae2} represent the first and second acid dissociation constants, respectively, of the mobile phase.

Similarly, the K_D value in 1 m*M* phthalic acid as the mobile phase was determined and simulation of the chromatogram based on eqn. 8 was carried out. The result obtained are illustrated in Fig. 7. Chloride gives a negative peak at all pH values and lactate shows an inversion of peak shape as the pH increases. Their behaviour was elucidated well in this simulation. The discrepancies below pH 4 suggest that the fraction of divalent phthalate in the stationary phase is larger than the calculated value, and this will be investigated in the future.

TABLE I

COMPARISON OF EXPERIMENTAL, COMPUTER-SIMULATED AND CALCULATED SAMPLE PEAK AREAS WITH 1 m*M* ONB AS MOBILE PHASE ON IC-ANION-PW

Sample	*k'*	*Relative peak area (chloride = −1)*		
		Experimental	*Simulated by eqn. 3*	*Calculated by eqn. 7*
Acetate	1.61	0.04	0.15	0.15
Lactate	3.54	0.32	0.37	0.43
Formate	5.60	0.87	0.92	1.02
Pyroglutamate	7.29	2.02	1.85	2.26
System peak	9.71	–	–	–
Phosphate	15.6	−1.32	−1.60	−1.99
Bromate	33.7	−1.03	−1.03	−1.05
Chloride	39.0	−1	−1	−1

In a mobile phase with free sodium ions, the relative peak area is calculated by eqn. 7. The comparison of the experimental results with simulated and calculated values is shown in Table I. The calculated results are in agreement with the experimental values in a similar manner to the simulated values, although small deviations are observed. Consequently no troublesome simulations are required under these conditions.

Eqn. 6 most closely resembles the response–capacity factor relationship of Schill and co-workers[9–11] in reversed-phase liquid chromatography, despite the difference in retention mechanisms. It seems that similar interactions between the sample and components of the mobile phase occur in the column.

The results indicate that new acid and partition equilibria arised in the column between the sample and the mobile phase organic acid if the sample is retained and eluted only by an ion-exchange process in IC. This perturbation of the light-absorbing mobile phase organic acid gives the sample and system peaks.

REFERENCES

1 J. S. Fritz, D. L. DuVal and R. E. Barron, *Anal. Chem.*, 56 (1984) 1177.
2 P. E. Jackson and P. R. Haddad, *J. Chromatogr.*, 346 (1985) 125.
3 S. Levin and E. Grushka, *Anal. Chem.*, 59 (1987) 1157.
4 J. J. Stranahan and N. Deming, *Anal. Chem.*, 54 (1982) 1540.
5 B. A. Bidlingmeyer and F. V. Warren, Jr., *Anal. Chem.*, 54 (1982) 2351.
6 T. Takeuchi and D. Ishii, *J. Chromatogr.*, 393 (1987) 419.
7 M. Denkert, L. Hackzell, G. Schill and E. Sjögren, *J. Chromatogr.*, 218 (1981) 31.
8 S. Banerjee and M. A. Castrogivanni, *J. Chromatogr.*, 396 (1987) 169.
9 G. Schill and J. Crommen, *Trends Anal. Chem.*, 6 (1987) 111.
10 J. Crommen, G. Schill and P. Herné, *Chromatographia*, 25 (1988) 397.
11 E. Arvidsson, J. Crommen, G. Schill and D. Westerlund, *J. Chromatogr.*, 461 (1989) 429.
12 E. Arvidsson, L. Hackzell, G. Schill and D. Westerlund, *Chromatographia*, 25 (1988) 430.
13 H. Small and T. E. Miller, Jr., *Anal. Chem.*, 54 (1982) 462.
14 L. C. Craig and D. Craig, in A. Weissberger (Editor), *Techniques of Organic Chemistry*, Vol. III, Part I, Wiley–Interscience, New York, 2nd ed., 1956, p. 150.
15 Y. Baba, N. Yoza and S. Ohashi, *J. Chromatogr.*, 348 (1985) 27.
16 D. R. Jenke, *Anal. Chem.*, 56 (1984) 2468.
17 F. F. Cantwell and S. Puon, *Anal. Chem.*, 51 (1979) 623.
18 D. T. Gjerde, G. Schmuckler and J. S. Fritz, *J. Chromatogr.*, 187 (1980) 35.
19 E. Papp, *J. Chromatogr.*, 402 (1987) 211.

Journal of Chromatography, 482 (1989) 155–163
Elsevier Science Publishers B.V., Amsterdam — Printed in The Netherlands

CHROM. 21 874

BENZENEPOLYCARBOXYLIC ACID SALTS AS ELUENTS IN ANION CHROMATOGRAPHY

YASUYUKI MIURA[a] and JAMES S. FRITZ*
Ames Laboratory–USDOE and Department of Chemistry, Iowa State University, Ames, IA 50011 (U.S.A.)
(First received April 13th, 1989; revised manuscript received August 11th, 1989)

SUMMARY

Several benzenepolycarboxylate salts were used as eluents for separating common inorganic anions on a highly efficient anion-exchange column. Eluents containing a −3-charged benzenetricarboxylate (BTA) anion or a −4 pyromellitate anion gave better separations than −2 phthalate eluents of samples containing both −1 and −2 anions. Compared with phthalate, a lower concentration of BTA or pyromellitate is used in the eluent, with a consequent improvement in the sensitivity of detection by indirect spectrophotometry. With BTA and pyromellitate eluents, sulfate elutes much earlier than nitrate and other monovalent anions than it does with phthalate. However, this effect may depend partly on the type and capacity of the ion-exchange resin in addition to the eluent.

INTRODUCTION

A number of eluents have been used for the ion-chromatographic separation of anions[1]. Almost all eluents utilized to date have contained displacing anions with a −1 or −2 charge. In general, eluent anions of −2 charge are more effective for late-eluting sample anions than eluent anions of −1 charge. Jardy *et al.*[2] found salts of 1,2,4,5-benzenetetracarboxylic acid (pyromellitic acid) to be effective for eluting several sample anions. Pyromellitate can assume various charges up to −4, depending on the pH at which the eluent is buffered.

The purpose of this work was to evaluate aromatic compounds that form −3 and −4 anions as eluents for ion chromatography and to compare these with the widely used phthalate eluents. The new eluents were found to provide excellent resolution of anion mixtures with better sensitivity than eluents containing displacing anions of lower charge. They also showed some interesting effects with regard to the order of elution of sample anions.

[a] Present address: Department of Chemistry, Faculty of Science, Tokai University, Hiratsuka, Kanagawa 259-12, Japan.

0021-9673/89/$03.50

EXPERIMENTAL

Apparatus

The ion-chromatographic system consisted of the following components: a Milton-Roy mini-pump (Laboratory Data Control, Rivera Beach, FL, U.S.A.), a Rheodyne Model 7000 injection value (Ranin, Waburn, MA, U.S.A.) equipped with 20-, 100- and 500-μl sample loops, a Milton-Roy pulse damper (Laboratory Data Control) placed between the pump and sample injector, a model 970 A variable-wavelength detector (Tracor Instruments, Austin, TX, U.S.A.), a Model 213 conductivity detector (Wescan Instruments, Santa Clara, CA, U.S.A.), a Curkin recorder (Curkin Scientific, Hawleyville, CA, U.S.A.) and glass-lined stainless-steel columns (15 cm × 4 mm I.D. and 25 cm × 4 mm I.D.) (Scientific Glass Engineering, Austin, U.S.A.). A Shandon high-performance liquid chromatographic column packer (Shandon Southern Instruments, Bason, PA, U.S.A.) was used to pack the resin into the columns at a packing pressure of 3500 p.s.i.

Resins

A 4.2-μm spherical non-porous polystyrene resin and a 0.09-μm latex suspension 76% functionalized with quaternary ammonium groups were supplied by Rohm and Haas (Spring House, PA, U.S.A.). The latex was coated onto the polystyrene resin from an aqueous slurry containing sodium chloride by a published procedure[3]. The coated resin had an exchange capacity of 0.027 mequiv./g. The coated resin was packed into the columns as described above.

Reagents and solutions

1,3,5-Benzenetricarboxylic acid (BTA) (97%, Aldrich) and pyromellitic acid (96%, Aldrich) were purified as follows. A saturated solution in boiling water was filtered rapidly through a 0.2-μm membrane filter with suction. On cooling, the precipitate was filtered by suction and washed. All other chemicals were of analytical-reagent grade and were used without further purification. Distilled, deionized water was used throughout.

Aqueous solutions of phthalate, BTA and pyromellitate were prepared by dissolving the acid in water and adjusting the pH to the desired value with 0.1 *M* ammonia solution. These eluents were then filtered through a 0.2-μm membrane filter and vacuum degassed. Stock solutions of sample anions were prepared from the sodium or potassium salts and diluted as required.

RESULTS AND DISCUSSION

Selection of eluent acids

o-Phthalic acid has pK_a values of $pK_1 = 2.95$ and $pK_2 = 5.41$, which means that in an eluent containing phthalic acid, buffered to pH *ca.* 6 or above, mostly the -2 phthalate anion is present. The equivalent conductance of -2 phthalate is sufficiently lower than that of most common anions for use in single-column ion chromatography with a conductivity detector. Phthalate eluents absorb fairly strongly in the UV spectral region so that indirect spectrophotometric detection of common ions is also feasible.

Salts of a number of other aromatic acids with multiple acidic groups were evaluated as eluents for ion chromatography. Of those tested, salts of 1,3,5-benzenetricarboxylic acid (BTA) and pyromellitic acid were selected for further study. BTA has pK_a values of $pK_1 = 3.01$, $pK_2 = 3.71$ and $pK_3 = 4.49$ and pyromellitic acid has values of $pK_1 = 1.92$, $pK_2 = 2.87$, $pK_3 = 4.49$ and $pK_4 = 5.63$. Thus, when buffered at pH 6–7, BTA eluents exist as the -3 anion and pyromellitate eluents primarily as the -4 anion.

Comparison of ion chromatograms using eluents of different charge

Effect of eluent concentration. The exchange reaction in ion chromatography between an eluent anion, E, of charge a and a sample anion, A, of charge b can be written as

$$bR_aE + aA \rightleftharpoons aR_bA + bE \quad (1)$$

where R represents an exchange site in the ion-exchange resin. By manipulation of eqn. 1, it can easily be shown[4] that the adjusted retention time (t'_R) or the capacity ratio (k') of a sample anion is proportional to the concentration of the eluent anion, E. A plot of either log t'_R, or log k' *versus* log [E] should have a slope of $-b/a$.

Several common inorganic anions were separated chromatographically on an anion-exchange column using various eluents. The pH of each eluent was adjusted so that the eluent anion would attain its maximum charge of -2 for phthalate, -3 for BTA and -4 for pyromellitate. Retention times were measured and the logarithm of the adjusted retention time for each ion was plotted against the logarithm of the eluent concentration. All of the plots were linear, as shown in Fig. 1 for TBA eluent.

In every instance the plot of log t'_R against log [E] was very close to the theoretical line. The theoretical slope for phthalate ($E = -2$) is $-1/2$ for monovalent anions and -1 for divalent anions. The theoretical slope for BTA ($E = -3$) is $-1/3$ for A^- and $-2/3$ for A^{2-}. The theoretical slope for pyromellitate ($E = -4$) is $-1/4$ for A^- and $-1/2$ for A^{2-}.

Comparison of eluents. The three eluents, phthalate, BTA and pyromellitate, were compared by separating mixtures of several common anions on an efficient anion-exchange column. The concentration of each eluent was adjusted to give optimum resolution for the anion mixture. Indirect spectrophotometric detection of the sample anions was used in each case.

Fig. 2 shows a typical chromatogram obtained with a phthalate eluent. The low eluent concentration required to resolve the early eluting anions causes the retention times of the nitrate and sulfate to be long.

Fig. 3A shows the separation of the same anions except phosphate with a BTA eluent. Fig. 3B shows the separation of all seven anions on a longer column. The time required for the separation is much shorter than in Fig. 2. The peaks are much sharper and higher even though the concentrations of the sample anions are lower than in Fig. 2. The -3 BTA anion is a more powerful eluent than -2 phthalate so that a much lower concentration is needed for the separation (0.2 mM BTA compared with 1.2 mM phthalate).

Fig. 4 depicts the separation of the same anions as in Fig. 3 using a pyromellitate eluent. The anions are fairly well resolved, although not as well as in Fig. 3 with

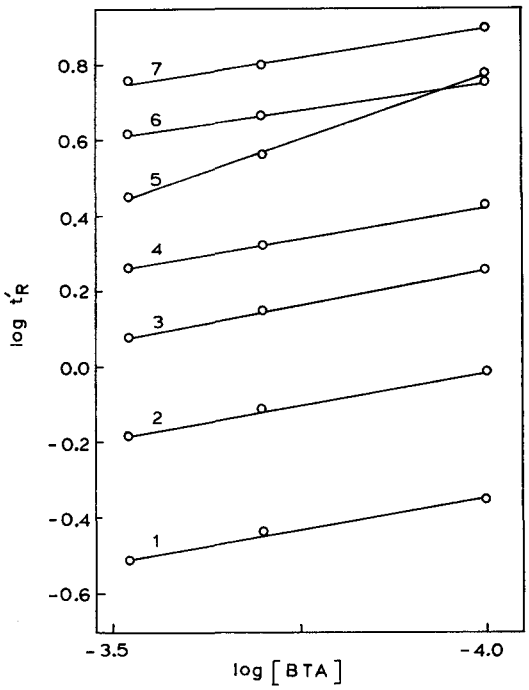

Fig. 1. Logarithm of adjusted retention times of anions *vs.* logarithm of different concentrations of BTA (pH 6.0). Flow-rate, 0.5 ml/min; detection at 250 nm; 20-μl sample; 25-cm column. 1 = F^-; 2 = $H_2PO_4^-$; 3 = Cl^-; 4 = NO_2^-; 5 = SO_4^{2-}; 6 = Br^-; 7 = NO_3^-.

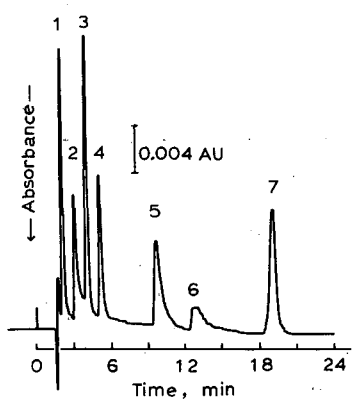

Fig. 2. Separation of seven anions with 1.2 m*M* phthalate eluent (pH 6.0), flow-rate 0.5 ml/min, detection at 272 nm, 20-μl sample and 15-cm column. Peaks: 1 = F^- (5 ppm); 2 = $H_2PO_4^-$ (40 ppm); 3 = Cl^- (10 ppm); 4 = NO_2^- (10 ppm); 5 = Br^- (25 ppm); 6 = NO_3^- (15 ppm); 7 = SO_4^{2-} (20 ppm).

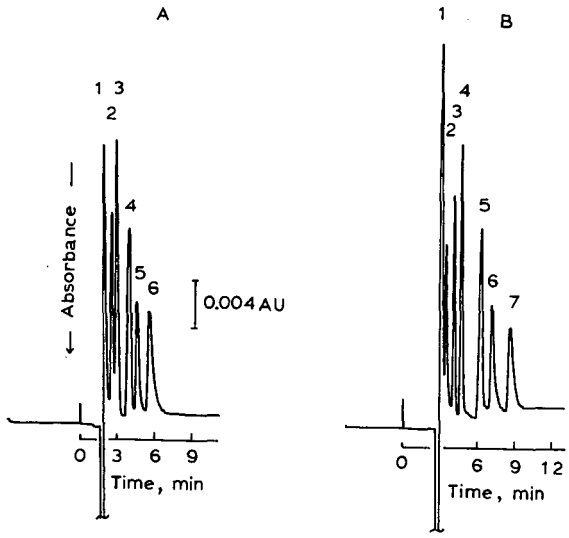

Fig. 3. Separation of anions with 0.2 m*M* BTA eluent (pH 6.0) and detection at 250 nm. (A) 15-cm column: 1 = F^- (5 ppm); 2 = Cl^- (5 ppm); 3 = NO_2^- (10 ppm); 4 = SO_4^{2-} (10 ppm); 5 = Br^- (10 ppm); 6 = NO_3^- (10 ppm); (B) 25-cm column: 1 = F^-; 2 = $H_2PO_4^-$ (20 ppm); 3 = Cl^-; 4 = NO_2^-; 5 = SO_4^{2-}; 6 = Br^-; 7 = NO_3^-.

the BTA eluent. The −4 pyromellitate is a more powerful eluent than either of the previous eluents. The very low concentration of the pyromellitate needed for the separation (0.02 m*M*) permits an excellent detection of the sample anions, even at very low concentrations. Jardy *et al.*[2] also obtained extremely low detection limits for several anions using pyromellitate eluents with indirect spectrophotometric detection.

With each of the three benzenepolycarboxylate eluents, indirect spectrophotometric detection of the sample anions was always better than with a conductivity detector. With BTA eluent, both fluoride and phosphate gave peaks of lower conductance whereas the other anions gave peaks of higher conductance than the background. At the very low concentration levels used in Fig. 4 with pyromellitate eluent, no sample peaks were obtained with a conductivity detector.

Effect of eluent on anion retention times. Comparison of the chromatograms in Figs. 2–4 shows that sulfate elutes earlier than chloride as the charge on the eluent anion increases. The retention times of several anions with the various eluents are compared in Table I. The separation factors (α) are larger for the early eluting anions as the charge on the eluent anion becomes larger. However, the drastic change in the retention of sulfate with respect to nitrate is undoubtedly the most interesting result in Table I. It is worth noting that Jardy *et al.*[2] reported that sulfate eluted *after* bromide and nitrate using pyromellitate at pH 4. However, the exchange capacity of their resin and the concentration of the eluent were different from those used in this work.

The selectivities of commercial ion-chromatographic columns for various anions should be similar to those obtained with the columns used in this work. However, with any column the retention times of divalent anions are more affected by changes in resin capacity and eluent concentration than the retention times of mono-

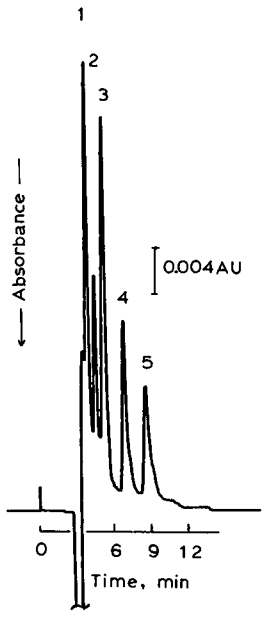

Fig. 4. Separation of anions with 0.02 m*M* pyromellitate eluent (pH 7.0), detection at 220 nm, 25-cm column. Peaks: 1 = Cl^- (1.25 ppm); 2 = NO_2^- (2 ppm); 3 = SO_4^{2-} (2 ppm); 4 = Br^- (2 ppm); 5 = NO_3^- (2 ppm). F^- and $H_2PO_4^-$ were eluted earlier than Cl^-.

valent anions. Therefore, the position of divalent anions relative to monovalent anions may change.

Applications of benzenepolycarboxylate eluents

Determination of nitrate. Nitrate pollution of drinking water and water supplies has become a matter of increasing concern. A high detector sensitivity setting is often necessary to detect low concentrations of nitrate in water. However, nitrate elutes between chloride and sulfate in conventional ion chromatography, and the large

TABLE I

RELATIVE RETENTION TIMES (Cl^- = 1.00) AND SEPARATION FACTORS (α) WITH DIFFERENT ELUENTS

Ion(s)	*Parameter*	*Phthalate, 1.2 mM*	*BTA, 0.2 mM*	*Pyromellitate, 0.1 mM*
NO_2^-	t_R	1.42	1.56	1.61
Br^-		3.21	3.60	4.25
NO_3^-		4.35	4.92	5.65
SO_4^{2-}		6.96	3.00	1.78
NO_2^-/Cl^-	α	1.42	1.56	1.61
Br^-/NO_2^-		2.26	2.31	2.70
NO_3^-/Br^-		1.36	1.37	1.30
SO_4^{2-}/NO_3^-		1.60	0.61	0.32

chloride and sulfate peaks at a high sensitivity setting may obscure the smaller nitrate peak. By using a BTA or pyromellitate eluent, nitrate is eluted after both chloride and sulfate as a well resolved peak. As a very low concentration of either of these eluents can be used, the detection sensitivity of nitrate is also very good.

Figure 5 shows a chromatogram for the determination of small amounts of nitrate in drinking water. Almost all drinking-water samples contain much more chloride and sulfate than nitrate, yet the nitrate peak is well resolved. The baselines of this and other water samples were initially very curved in the early part of the chromatogram. This was believed to be caused by the high concentrations of hydrogencarbonate in the hard-water samples. Treatment of the samples with acid, followed by sonication or purging with an inert gas to remove most of the carbon dioxide, gave chromatograms with a better baseline. Results for determination of nitrate in various water samples are summarized in Table II.

Determination of organic acids. The ability of BTA eluents to achieve fast and complete separations of inorganic anions suggested the use of this eluent to separate

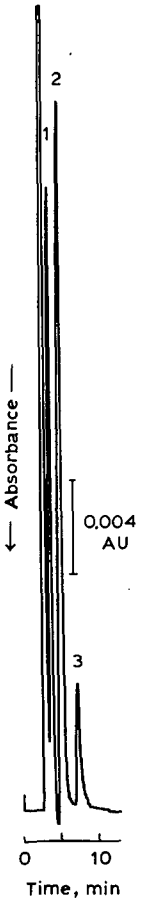

Fig. 5. Chromatogram of Des Moines tap water (diluted 50-fold) with 0.02 m*M* pyromellitate eluent (pH 7.0) and detection at 240 nm. Peaks = Cl^-; 2 = SO_4^{2-}; 3 = NO_3^-.

TABLE II

DETERMINATION OF NITRATE CONCENTRATION IN WATER SAMPLES

Conditions: coated 25-cm columns; 0.03 m*M* pyromellitate (pH 7.0); flow-rate 0.5 ml/min; spectrophotometric detector, 240 nm.

Sample	*Dilution (fold)*	*Injection volume (µl)*	*Found in original sample (ppm)*[a]
Ames tap water (A)	10	100	0.45
Ames tap water (B)	20	500	0.60
Pella tap water	10	100	12.3
Amana tap water	400	500	13.2
Des Moines River	50	100	7.15
Des Moines tap water	50	100	18.0
Skunk River	50	100	9.85
Squaw Creek River	100	100	26.8
George, Iowa City, well 14	100	100	59.4

[a] Average of two determinations.

anions of organic acids. Fig. 6 shows a good separation of four organic acids with excellent detection sensitivity using a BTA eluent. At the detection wavelength used (250 nm), ascorbic acid absorbs more strongly than the eluent and appears as a positive peak (increased absorbance). The other acid anions appear as negative peaks (decreased absorbance) owing to exchanging with the more highly absorbing BTA anion.

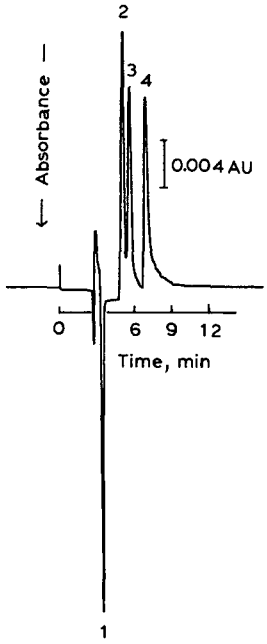

Fig. 6. Separation of four organic anions under the same conditions as in Fig. 3B. peaks 1 = ascorbate (10 ppm); 2 = malonate (20 ppm); 3 = tartrate (20 ppm); 4 = oxalate (20 ppm).

ACKNOWLEDGEMENTS

The authors gratefully acknowledge the assistance of Linda Warth in preparing and packing the chromatographic columns. They also thank John Naples of the Rohm & Haas for preparing and supplying the polystyrene resins and the quaternized latexes. This work was performed at the Ames Laboratory. Ames Laboratory is operated for the U.S. Department of Energy by Iowa State University under contract no. W-7405-ENG-82.

REFERENCES

1 D. T. Gjerde and J. S. Fritz, *Ion Chromatography*, Hüthig, Heidelberg, 2nd ed., 1987, pp. 139–154.
2 A. Jardy, M. Caude, A. Diop, C. Curvale and R. Rosset, *J. Chromatogr.*, 439 (1988) 137.
3 L. M. Warth, J. S. Fritz and J. O. Naples, *J. Chromatogr.*, 462 (1989) 165.
4 D. T. Gjerde and J. S. Fritz, *Ion Chromatography*, Hüthig, Heidelberg, 2nd ed., 1987, p. 73.

Journal of Chromatography, 482 (1989) 165–173
Elsevier Science Publishers B.V., Amsterdam — Printed in The Netherlands

CHROM. 21 847

HIGH-PERFORMANCE LIQUID CHROMATOGRAPHY FOR OPTICAL RESOLUTION ON A COLUMN OF AN ION-EXCHANGE ADDUCT OF SPHERICALLY SHAPED SYNTHETIC HECTORITE AND OPTICALLY ACTIVE METAL COMPLEXES

YUJI NAKAMURA and AKIHIKO YAMAGISHI*
Department of Chemistry, College of Arts and Sciences, University of Tokyo, Komaba, Meguro-ku, Tokyo 153 (Japan)
and
SATOSHI MATUMOTO, KAZUO TOHKUBO, YUTAKA OHTU and MICHIHIRO YAMAGUCHI
Shiseido Basic Research Laboratories, Nippa-Cho, Kohoku-ku, Yokohama-shi 223 (Japan)
(First received March 16th, 1989; revised manuscript received August 2nd, 1989)

SUMMARY

Optical resolution was accomplished by liquid chromatography on a column packed with an ion-exchange adduct of synthetic hectorite and optically active metal complexes. The metal complexes used were optically active tris(1,10-phenanthroline)-nickel(II) and -ruthenium(II), and were ion exchanged into synthetic hectorite that had been spray-dried to a spherically shaped particle with an average diameter of 5.5 μm. When methanol or ethanol was used as the eluting solvent, the following compounds were resolved completely into enantiomers: 1,1′-binaphthol, 2,2′-diamino-1,1′-binaphthyl, 2,2′-diselecyanato-1,1′-binaphthyl, [5]-helicene, $Co(acac)_3$ (acac = acetylacetonato), $Cr(acac)_3$, $Rh(acac)_3$ and $[Co(acac)_2(en)]^+$ (en = ethylenediamine). The effect of the solvent on selectivity was studied in the resolution of 1,1′-binaphthol with acetonitrile–methanol as the eluent.

INTRODUCTION

In recent years, we have developed a liquid column chromatographic method for resolving organic and inorganic enantiomers on a column of a clay–metal complex adduct[1]. For example, $[\Delta\text{-Ni(phen)}_3]^{2+}$–montmorillonite (phen = 1,10-phenanthroline) was used as a column material for resolving $M(acac)_3$ (M = metal; acac = acetylacetonato)[2]. In comparison with other known chiral adsorbents[3], these materials are characterized by ease of preparation and a high efficiency in resolving wide varieties of compounds with aromatic functional groups.

One difficulty in the present method is the preparation of a clay of uniform particle size. A clay is composed of microcrystalline particles of diameter 0.1–1 μm. These particles are too small to be used as a packing material. In addition, they may collapse to smaller particles under high pressure. In order to overcome this difficulty,

0021-9673/89/$03.50

we have tried to coat a silica gel particle with a film of a clay. Such materials have been found to improve the resolution efficiency greatly[4].

In this study, synthetic hectorite (Laponite XLG, Laporte) was used as the clay material. Tohkubo *et al.*[5] have recently made spherically shaped particles of this material by the spray-dry method. We expected that an adduct of such hectorite particle and an optically active chelate would be ideal as a packing material in high-performance liquid chromatography (HPLC). As a result, high resolutions were attained for a number of inorganic and organic compounds when methanol or ethanol was used as the eluting solvent.

EXPERIMENTAL

$[Ru(phen)_3]Cl_2$ was prepared according to the literature[6]. The complex was resolved by use of potassium antimony *d*-tartrate as a resolving agent. [*Λ*-$Ru(phen)_3$] [antimony *d*-tartrate]$_2$ was converted into the chloride salt by mixing with an anion-exchange resin in the chloride form. [*Δ*-$Ni(phen)_3]Cl_2$ was synthesized as described in the literature[7]. 2,2′-Diamino-1,1′-binaphthyl was also synthesized according to the literature[8]. 2,2′-Diselecyanato-1,1′-binaphthyl was donated by Prof. S. Tomoda (University of Tokyo). $Co(acac)_3$, $Cr(acac)_3$, $Rh(acac)_3$ and $[Co(acac)_2(en)]^+$ (en = ethylenediamine) were synthesized according to the literature[9]. Other compounds were used as purchased.

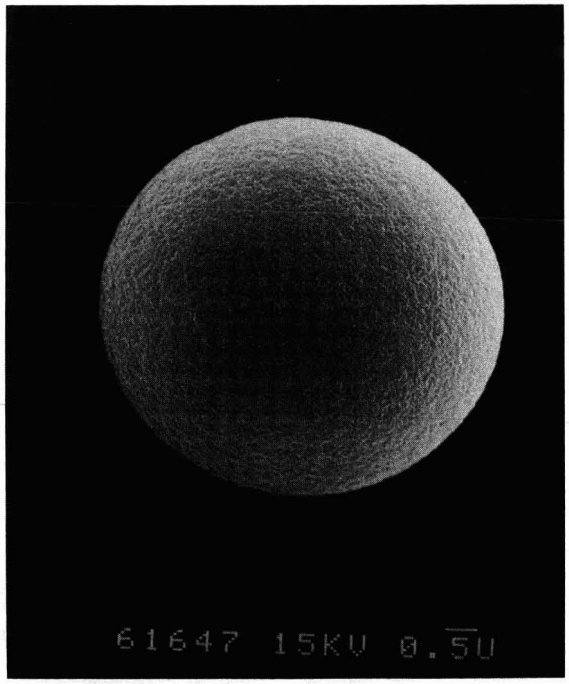

Fig. 1. Electron microphotograph of a particle of spray-dried synthetic hectorite. The diameter of the particle is about 6.5 μm.

The column material was prepared as follows. About 3 g of spray-dried synthetic hectorite (Laponite XLG) (Fig. 1) was dispersed in 100 ml of methanol, to which $1 \cdot 10^{-3}$ mol of optically active $[M(phen)_3]Cl_2$ (M = Ru or Ni) was added as an methanol solution. The mixture was centrifuged and the supernatant solution was separated. Based on a value of the cation-exchange capacity (CEC) of 79 mequiv. per 100 g, about 50% of the CEC was exchanged with the metal complexes. The above material was packed as a slurry in a stainless-steel tube (25 cm × 0.4 cm I.D.). The columns in which larger or smaller amounts of the Ru chelates were exchanged into a clay were prepared in a similar way.

HPLC was performed with a BIP-1 chromatograph (JEOL) equipped with a UVIDEC- 100-VI UV spectrophotometer (JEOL). About 10^{-6} mol of a compound was injected and eluted with methanol or a methanol–organic solvent mixture at a flow-rate of 0.1–1.0 ml/min. The temperature of the column was about 20°C unless indicated otherwise. The UV spectrum of the eluent was measured at 250 nm. The absolute configuration of an enantiomer was determined from the circular dichroism (CD) spectrum. The CD spectra were recorded on a J-20 polarimeter (JEOL).

RESULTS

Fig. 2 shows the chromatogram obtained when 1,1′-binaphthol was eluted with ethanol on a $[\Lambda\text{-Ru(phen)}_3]^{2+}$–hectorite column. Two peaks are observed at elution volumes of 6.8 and 10.6 ml. From the CD spectra, the first and second peaks correspond to the *R* and *S* enantiomers, respectively. The small peak at 3.0 ml is the peak due to chloroform, which was injected to determine the dead volume of the column. The separation factor, α, is defined by

$$\alpha = (t_2 - t_0)/(t_1 - t_0)$$

where t_0, t_1 and t_2 are the elution time for the dead volume, the first peak and the second peak, respectively; α is calculated to be 2.0.

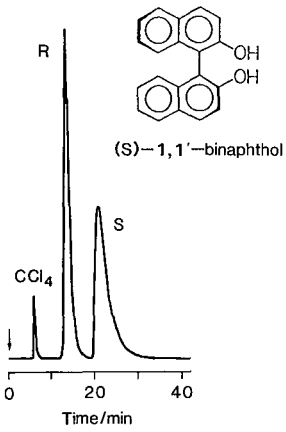

Fig. 2. Chromatogram obtained on elution of 1,1′-binaphthol on a $[\Lambda\text{-Ru(phen)}_3]^{2+}$–hectorite column with ethanol at a flow-rate of 0.2 ml/min.

TABLE I

EFFECT OF FLOW-RATE ON THE ELUTION OF 1,1'-BINAPHTHOL ON A COLUMN OF $[\Delta\text{-Ru(phen)}_3]^{2+}$–HECTORITE WITH ETHANOL AS ELUENT

Flow-rate (ml/min)	*Retention time (min)*[a]	α	R_s
0.2	t_R = 20.58 (622), t_s = 30.18 (500)	2.02	2.21
0.4	t_R = 11.64 (588), t_s = 17.10 (446)	2.00	2.12
1.0	t_R = 5.82 (465), t_s = 8.28 (339)	1.98	1.71

[a] Theoretical plate numbers are shown in parentheses.

Table I shows the effect of the flow-rate on the chromatogram for the resolution of 1,1'-binaphthol. When the flow-rate was varied from 0.3 to 1.0 ml/min, the compound was resolved completely with little change in the separation factor. The resolution factor, R_s, is defined by

$$R_s = 2(t_2 - t_1)/(t_{w1} + t_{w2})$$

where t_{w1} and t_{w2} are the peak widths of the first and second peaks, respectively, R_s was found to decrease with increase in the flow-rate.

The effect of temperature on the separation factor was studied by varying the column temperature from 30 to 50°C. As shown in Fig. 3, the separation factor decreased from 2.9 to 2.5 with this increase in temperature. The peaks of the separated

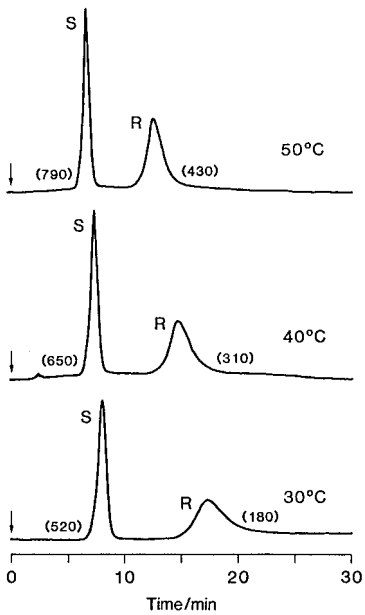

Fig. 3. Effect of the temperature on the elution curve of 1,1'-binaphthol on a column of $[\Delta\text{-Ru(phen)}_3]^{2+}$–hectorite. The figures in parentheses are the theoretical plate numbers of the peaks.

enantiomers were sharper at higher temperature, leading to an increase in the theoretical plate number as indicated in Fig. 3.

The effect of the amount of $[\Delta\text{-Ru(phen)}_3]^{2+}$ adsorbed in a clay was examined when $[Co(acac)_3]$, $[Cr(acac)_3]$ or 1,1′-binaphthol was eluted with ethanol. As shown in Table II, the retention volumes of the $[Cr(acac)_3]$ and 1,1′-binaphthol enantiomers increase with increase in the amount of preadsorbed Ru complex, whereas the retention volumes of the $[Co(acac)_3]$ enantiomers decrease with increase in the amount of preadsorbed Ru complex. The separation factor was lowered with increase in the amount of Ru complex in all the three instances.

Other kinds of binaphthyl derivatives, such as 2,2′-diamino-1,1′-binaphthyl and 2,2′-diselecyanoto-1,1′-binaphthyl, were completely resolved in similar way. 2,2′-Dibromo-1,1′-binaphthyl was partially resolved, since the two peaks overlap with each other. A racemic mixture of [5]-helicene was eluted with ethanol. M-(−)-[5]-helicene was eluted at a retention volume of 19.2 ml as determined from the CD spectrum[10]. The antipode, P-(+)-[5]-helicene, was not eluted with this solvent, but it was recovered from the column when acetonitrile was used as the eluent. P-(+) and M-(−) indicate the right- and left-handed helicites, respectively.

The neutral metal complexes $[Co(acac)_3]$, $[Cr(acac)_3]$ and $[Rh(acac)_3]$ were eluted with ethanol and were completely resolved. A positively charged complex, $[Co(acac)_2(en)]ClO_4$, was eluted with ethanol and completely resolved. The absolute configurations of the eluted enantiomers were determined from their CD spectra[9]. It was found that all these acetylacetonato complexes were eluted in the order Δ- followed by Λ-. Hence the charges of the complexes do not affect the selectivity of resolution on the present column. The results for these complexes are summarized in Table III.

The effect of the addition of acetonitrile to the methanol eluent was studied with the resolution of 1,1′-binaphthol. Table IV gives the chromatographic results when the compound was eluted with acetonitrile–methanol mixtures containing 0, 5, 10, 20 and 100% (v/v) of acetonitrile. The elution curves for the *R* and *S* enantiomers were obtained when each enantiomer was eluted independently with the same solvents.

With increase in the acetonitrile concentration, the separation factor decreased until the column no longer resolved the enantiomers at all at 18% (v/v) of acetonitrile.

TABLE II

EFFECT OF THE AMOUNT OF $[\Delta\text{-Ru(phen)}_3]^{2+}$ EXCHANGED IN THE HECTORITE COLUMN ON THE RETENTION VOLUMES AND ON THE SEPARATION FACTORS (α) OF THE ENANTIOMERS

V_d = Dead volume.

Amount adsorbed (mequiv.)	*Co(acac)₃*			*Cr(acac)₃*			*1,1′-Binaphthol*		
	V(Λ) (ml)	*V(Δ) (ml)*	α	*V(Λ) (ml)*	*V(Δ) (ml)*	α	*V(S) (ml)*	*V(R) (ml)*	α
30	9.3	17.8	2.3	9.6	23.5	3.2	4.6	10.0	4.3
40	7.7	13.8	2.2	10.5	24.3	2.9	8.9	22.1	3.2
50	6.4	10.5	2.1	11.4	24.6	2.6	14.3	37.1	3.0
		V_d = 2.5 ml			V_d = 3.2 ml			V_d = 3.0 ml	

TABLE III

SEPARATION FACTORS FOR THE RESOLUTION OF VARIOUS RACEMIC MIXTURES ON A [*Δ*-Ru(phen)$_3$]$^{2+}$–HECTORITE COLUMN USING ETHANOL AS ELUENT

Compound	*Order of elution*	*Separation factor (α)*
1,1′-Binaphthol	$R \rightarrow S$	2.0
2,2′-Diselecyanato-1,1′-binaphthol	$R \rightarrow S$	1.5
[Co(acac)$_3$]	$\Delta \rightarrow \Lambda$	2.4
[Cr(acac)$_3$]	$\Delta \rightarrow \Lambda$	2.9
[Rh(acac)$_3$]	$\Delta \rightarrow \Lambda$	3.3
[Co(acac)$_2$(en)]$^+$	$\Delta \rightarrow \Lambda$	2.6
[5]-Helicene	M → P	Very large

When the concentration of acetonitrile exceeded 18% (v/v), the order of elution of the enantiomers reversed from *R*–*S* to *S*–*R*. Fig. 4 shows the effect of solvent composition on the separation factor. A similar reversal of the elution order was also confirmed on a column packed with [*Δ*-Ni(phen)$_3$]$^{2+}$–hectorite. On this column, the reversal of selectivity from *S*–*R* to *R*–*S* took place at 14% (v/v) acetonitrile.

Fig. 5 shows the CD spectra of an adduct of [*Λ*-Ru(phen)$_3$]$^{2+}$–hectorite dispersed in either methanol or acetonitrile. The CD spectrum due to adsorbed [*Λ*-Ru(phen)$_3$]$^{2+}$ was displaced downwards when methanol was replaced with acetonitrile. When the amplitude of the negative peak at 425 nm, A_{425}, was plotted against the acetonitrile content, it varied as shown in Fig. 6. A_{425} decreased rapidly until it became constant value at an acetonitrile concentration of 5% (v/v).

Other kinds of nitriles were added to the eluent to study the effect of the structure of the nitrile on the efficiency of resolution of 1,1′-binaphthol. Table V shows the separation factors when the eluent contained 5% (v/v) of nitrile. It is concluded that nitriles of simpler structure such as acetonitrile and propionitrile give the lowest separation factors.

TABLE IV

EFFECT OF MOBILE PHASE COMPOSITION ON THE OPTICAL RESOLUTION OF 1,1′-BINAPHTHOL ON A COLUMN OF [*Δ*-Ru(phen)$_3$]$^{2+}$–HECTORITE

Mobile phase: acetonitrile–methanol.

Acetonitrile concentration (%, v/v)	*Retention time (min)*[a]	α	R_S
0	t_R = 19.12 (1125), t_S = 29.04 (672)	2.09	2.39
5	t_R = 18.40 (1006), t_S = 21.20 (917)	1.35	1.09
10	t_R = 16.28 (1656), t_S = 16.97 (1422)	1.11	0.41
15	t_R = 14.93 (1744), t_S = 15.15 (1509)	1.05	0.15
20	t_S = 13.38 (1525), t_R = 13.48 (1548)	0.97	0.07
50	t_S = 10.00 (1299), t_R = 10.22 (1194)	0.68	0.20
80	t_S = 9.66 (1701), t_R = 9.80 (1789)	0.43	0.15
100	t_S = 9.74 (1848), t_R = 9.91 (1870)	0.32	0.18

[a] Theoretical plate numbers are shown in parentheses.

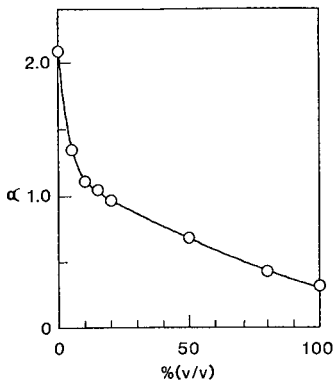

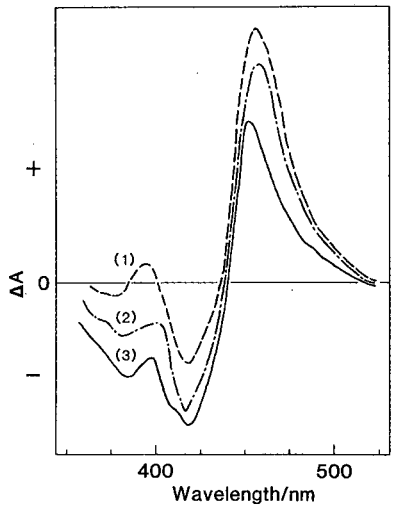

Fig. 4. Plot of the separation factor (α) against the acetonitrile concentration in the eluent. The data were obtained from the results in Table IV.

Fig. 5. Circular dichroism spectra of a free $[\Lambda\text{-Ru(phen)}_3]^{2+}$ ion or $[\Lambda\text{-Ru(phen)}_3]^{2+}$ bound to a colloidally dispersed hectorite. (1) Free $[\Lambda\text{-Ru(phen)}_3]^{2+}$ ion in methanol; (2) colloidally dispersed $[\Lambda\text{-Ru(phen)}_3]^{2+}$–hectorite in methanol; (3) colloidally dispersed $[\Lambda\text{-Ru(phen)}_3]^{2+}$–hectorite in acetonitrile.

DISCUSSION

$[\Lambda\text{-Ru(phen)}_3]^{2+}$– and $[\Delta\text{-Ni(phen)}_3]^{2+}$–hectorite resolve a number of organic and inorganic racemic mixtures when they are eluted with methanol or ethanol. The present results were compared with those observed on a column of silica gel coated with $[\Lambda\text{-Ru(phen)}_3]^{2+}$–montmorillonite[3]. On the latter column, 1,1′-binaphthol was resolved with $\alpha = 2.3$ when the compound was eluted with methanol–water (1:2, v/v) and α decreased with increase in the methanol content in the eluent until no resolution was attained on elution with pure methanol. On the other hand, the present hectorite

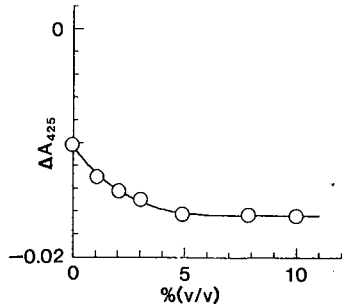

Fig. 6. Plot of the amplitude at 425 nm in the circular dichroism spectra in Fig. 5 against the concentration of acetonitrile in an acetonitrile–methanol mixture.

TABLE V

EFFECT OF NITRILES ON THE EFFICIENCY OF RESOLUTION OF 1,1′-BINAPHTHOL USING NITRILE–ETHANOL (5:95, v/v) MIXTURES AS ELUENT

Nitrile	*Separation factor (α)*
Acetonitrile (CH_3CN)	1.3
Propionitrile (CH_3CH_2CN)	1.3
n-Butyronitrile ($CH_3CH_2CH_2CN$)	1.5
n-Valeronitrile [$CH_3(CH_2)_3CN$]	1.7
Isobutyronitrile [$(CH_3)_2CHCN$]	1.7
Trimethylacetonitrile [$(CH_3)_3CCN$]	1.9

column resolved the same racemic compound completely when pure methanol or ethanol was used as the eluent. Therefore, it is concluded that the present column improves the efficiency of resolution greatly in comparison with the previous column.

There are two possible reasons for the enhancement of resolution efficiency attained with the present column. The first is that the present column contains about 50 times more optically active chelates than the previous column. The number of binding sites may increase by this amount if all of the chelates in a hectorite particle can interact with the analyte molecules. This is confirmed for 1,1′-binaphthol and [$Cr(acac)_3$] from the results in Table II. The retention volumes for these compounds increase with increase in the amount of adsorbed chelates. For [$Co(acac)_3$], however, the retention volume decreases with increase in the amount of adsorbed chelate, and it is not clear why this compound exhibits this reverse tendency. The increased affinity towards an analyte molecule enables one to use organic solvents as eluents. The second reason is that the uniform size distribution and the spherical shape of a particle reduce the disturbances to the flow of the eluent. As a result, the width of a resolved peak is expected to be narrowed. In fact, the widths of the first and second peaks in the chromatogram were about 40 and 100 ml, respectively, when 1,1′-binaphthol was eluted with methanol–water (1:1, v/v) on the previous column of silica gel coated with [*Λ*-$Ru(phen)_3$]$^{2+}$–montmorillonite. In contrast, the corresponding first and second peaks with the present column had widths of only about 2 and 4 ml, respectively. The observed narrow width is partly due to the use of pure methanol instead of methanol–water, as the clay layers swell to a lesser extent in methanol than in water. This leads to less penetration of an analyte molecule into the interlayer space. The non-equilibrium nature of such a penetration process is considered to be one of the main factors in increasing the widths of the separated peaks. The effect of temperature on the chromatogram (Fig. 3) supports this conclusion. The equilibration rate of the penetration increases with increase in temperature, resulting in a narrower peak width at higher temperatures.

The reversal of selectivity with the addition of acetonitrile (Table IV) implies that solvent molecules affect the binding states of the enantiomers in different ways, otherwise a change in solvent composition would never lead to reversal of selectivity. One possibility for the occurrence of this effect is that the enantiomers are adsorbed at different binding sites on the column and that acetonitrile molecules interact specifically with either one of the sites.

The spectral results in Fig. 5 suggest that acetonitrile molecules solvate the Ru chelate more strongly than methanol so that the solvation is complete at an acetonitrile concentration of 5% (v/v). Based on this, the observed effect of acetonitrile in resolving 1,1′-binaphthol might be ascribed to the solvation of $[\Lambda\text{-Ru(phen)}_3]^{2+}$ by acetonitrile molecules, which results in blockage of the binding site for the *S* enantiomer, but has little effect on the binding site for the *R* enantiomer. As a result, the *S* enantiomer is eluted faster than the *R* enantiomer at acetonitrile concentrations higher than 14–18% (v/v). The results in Table V that the smaller nitriles decrease the separation factor more efficiently are consistent with this view, because it is natural to expect that the smaller nitriles will solvate the Ru chelates more strongly.

Several examples have been reported in which a change in solvent composition causes a reversal in chiral selectivity. For example, Lappin *et al.*[11] observed that the electron transfer between $[\text{Co(en)}_3]^{2+}$ and $[\text{Co(edta)}]^{-}$ exhibits different stereoselectivity in water and dimethyl sulphoxide. This result was ascribed to the hydrogen-bonding solvation structures of the reacting complexes in water collapsing in dimethyl sulphoxide. In the present instance also the alcohol molecules are liable to solvate a resolved molecule by hydrogen bonding whereas such bondings collapse in acetonitrile-containing solvents. Therefore, the difference in the abilities of the investigated solvents to form hydrogen bonds is considered to be one of the reasons for the present phenomena.

ACKNOWLEDGEMENT

This work has been supported by a Grant-in-Aid for Scientific Research on the priority area of "Dynamic Interactions and Electronic Processes of Macromolecular Complexes" from the Ministry of Education, Science and Culture of Japan.

REFERENCES

1 A. Yamagishi and M. Soma, *J. Am. Chem. Soc.*, 103 (1981) 4640.
2 A. Yamagishi, *J. Chem. Soc., Chem. Commun.*, (1981) 1168.
3 D. W. Armstrong, *Anal. Chem.*, 59 (1987) 84A.
4 A. Yamagishi, *J. Am. Chem. Soc.*, 107 (1985) 732.
5 K. Tohkubo, S. Matsumoto, M. Yamaguchi, H. Ohtsu and J. Nakamura, *Annual Meeting of the Japan Chemical Socity, Abstracts*, 1988, I-582.
6 C.-T. Lin, W. Bottcher, M. Chou, C. Crenz and N. Sutin, *J. Am. Chem. Soc.*, 98 (1976) 6536.
7 F. P. Dwyer and E. C. Gyarfas, *Proc. R. Soc. N.S.W.*, 83 (1949) 170.
8 K. J. Brown, M. S. Berry and J. R. Murdoch, *J. Org. Chem.*, 50 (1985) 4345.
9 Japan Chemical Society, *New Treatises on Experimental Chemistry*, Vol. VIII, Maruzen, Tokyo, 1975, Ch. V.
10 W. S. Brickell, C. M. Brown and S. F. Mason, *J. Chem. Soc. A*, (1971) 751.
11 A. G. Lappin, R. A. Marusak and P. Osvath, *Inorg. Chem.*, 26 (1987) 4292.

Journal of Chromatography, 482 (1989) 175–187
Elsevier Science Publishers B.V., Amsterdam — Printed in The Netherlands

CHROM. 21 860

HIGH-PERFORMANCE LIQUID CHROMATOGRAPHIC DETERMINATION OF HUMIC ACID IN ENVIRONMENTAL SAMPLES AT THE NANOGRAM LEVEL USING FLUORESCENCE DETECTION[a]

MICHAEL SUSIC* and KEVIN G. BOTO
Australian Institute of Marine Science, P.M.B. No. 3, Townsville M.C., Qld. 4810, Queensland (Australia)
(First received January 27th, 1989; revised manuscript received June 13th, 1989)

SUMMARY

A high-performance liquid chromatographic method for the determination of humic acid in environmental samples is presented. The humic acid is chromatographed as its sodium or calcium complex, eluting as a single, sharp peak. Coral skeletal matter, sea water, river water, soils and plant matter were successfully analysed. The detection limit is 15 ng. The relative standard deviation for a coral skeletal sample is 1.9%. Unusual chromatographic properties such as the occurrence of peak broadening with increased concentration appear to be due to a slow change in the equilibrium composition of humic acid. In solution, fulvic acid showed similar properties to humic acid.

INTRODUCTION

Humic acids are ubiquitous, fluorescent organic compounds that possess acidic properties and readily complex with metal ions and organics. They have been detected in soil[1], sediment[2], lake water[2,3] and sea water[4]. Commercial preparations are commonly obtained from coal beds. Even though the first comprehensive studies of their chemical properties were begun over three decades ago, there is still no agreement on many of their fundamental properties[5,6]. Reports of molecular weight, elemental composition and the nature and levels of moieties vary widely[7–12]. The problem has been contributed to, at least in part, by the poor definition of humic and fulvic acids. Humic acid is regarded as the alkali-soluble extract from soils subjected to varying, but undefined, methods of purification. Fulvic acid is the acid-soluble fraction of these extracts. No definitive measure of purity has been set and "humic acid" extracts no doubt are mixtures of organic compounds derived from plant matter[13].

Humic acid influences many diverse activities and processes[14–17]. The impetus for this study was the discovery that massive corals contain fluorescing bands of fulvic (humic) acid within their skeletal structure[18]. The intensity of these bands is

[a] Contribution No. 484 from the Australian Institute of Marine Science.

0021-9673/89/$03.50

highly correlated with nearby river discharge volumes. This leads to the potential reconstruction of river discharge and rainfall levels[19]. To study and determine the low concentrations of humic acid in coral skeletal matter and to establish its source requires a sensitive and accurate analytical technique. Given the almost routine use of high-performance liquid chromatography (HPLC) for the separation, quantification and purification of a wide variety of organic compounds in recent years, it is surprising that so few HPLC studies of humic acid have been reported. Those that have appeared in the literature are qualitative rather than quantitative[12,20–24].

Our studies show that humic acid can be readily determined on a glass-lined reversed-phase column as the sodium or calcium complex. Although a reversed-phase column was chosen, the retention mechanism is not known. Fluorimetric detection was used, achieving a detection limit at the nanogram level. Humic acid concentrations in coral skeletal matter, sea water, river water, soils and plant matter have been successfully determined.

EXPERIMENTAL

Apparatus

The HPLC system consisted of a Waters Assoc. (Milford, MA, U.S.A.) M6000 pump, U6K injector and 440 UV detector, a Schoeffel Instruments (Westwood, NJ, U.S.A.) FS 970 fluorometer and a Hewlett-Packard (Palo Alto, CA, U.S.A.) 3392A computing integrator. Wherever possible, PTFE capillary tubing obtained from SGE (Ringwood, Victoria, Australia) was used for the chromatographic lines. Access to a Hewlett-Packard 1090M HPLC system with an inbuilt diode-array variable absorbance detector was obtained. A Varian SuperScan 3 absorbance spectrophotometer (Mulgrave, Victoria, Australia) and a Hitachi (Tokyo, Japan) F-4000 fluorescence spectrophotometer were used for samples not requiring fractionation. The Hitachi spectrophotometer was also used to obtain fluorescence spectra of HPLC-purified humic acids by using the flow cell attachment. A Perkin-Elmer 1640 Fourier transform infrared spectrophotometer with disc drive was used to obtain infrared scans.

Columns

Commercial, pre-packed analytical HPLC columns were purchased. All had a particle size of 5 μm except where indicated below. Guard columns contained the same packing as the analytical columns and were used where indicated. An Upchurch Scientific 2-μm in-line precolumn filter (Oak Harbor, WA, U.S.A.) was routinely used to protect the column from sample particulate matter. The following columns were used: SGE ODS, glass-lined (250 × 4 mm I.D.), plus guard column; SGE SAX, glass-lined (250 × 4 mm I.D.); Brownlee (Santa Clara, CA, U.S.A.) RP-18 Spheri-10 (250 × 4.6 mm I.D.), 10-μm particle size (silanized), plus guard column; Brownlee Phenyl Spheri-5 (100 × 4.6 mm I.D.); Brownlee Amino Spheri-5 (100 × 4.6 mm I.D.), plus guard column; Applied Science (State College, PA, U.S.A.) Cyano Spherisorb (250 × 4.6 mm I.D.); Merck (Darmstadt, F.R.G.) 100 Diol LiChrospher (250 × 4.6 mm I.D.), 100 Å pore size, plus guard column; and Merck 100 CH-18/2 LiChrospher (100 × 4.6 mm I.D.), 100 Å pore size.

Chemicals and solvents

Technical-grade humic acid as the sodium salt was purchased from Aldrich (Gillingham, U.K.). Water was purified with a Millipore (Bedford, MA, U.S.A.) purification system. This Super-Q water was further purified by double distillation from potassium permanganate. Analytical-reagent grade sodium chloride from Ajax Chemicals (Auburn, N.S.W., Australia) was heated at 550°C for 16 h to remove humic acid impurities. Concentrated hydrochloric acid and sodium hydroxide were of Aristar grade, purchased from BDH Chemicals (Poole, U.K.). Tetrahydroxy-*p*-benzoquinone, chloranilic acid, arbutin, quercitin, rutin, alizarin, quinalizarin, lawsone, juglone, hydroquinone and *p*-benzoquinone were purchased from Sigma (St. Louis, MO, U.S.A.). All other chemicals were of analytical-reagent grade.

HPLC-grade methanol was obtained from BDH Chemicals and HPLC-grade tetrahydrofuran and acetonitrile from Waters Assoc. These solvents were mixed in varying proportions with Super-Q water. Ammonia from Ajax Chemicals was added to water at a concentration of 0.003% (w/v) (as NH_3) to give the mobile phase that was used in routine analysis. All buffer and salt solutions were prepared by dissolving the appropriate compounds in water.

Humic acid (Aldrich) was purified by mixing it with Super-Q water, adding ammonia solution to adjust the pH to about 8 and carefully decanting the dissolved portion. This solution was precipitated by the addition of concentrated hydrochloric acid, filtered, air-dried at 22°C for 24 h and heat-dried at 80°C for 16 h. The procedure was repeated twice. The low nitrogen content of 0.83% (w/w) indicated that ammonia had not condensed with humic acid.

Sample preparation

The development of the sample preparation procedures for waters and coral skeletal extract are described in the main text. For soils, approximately 50 mg of sample that had been air-dried at ambient temperature for 2 weeks were placed in a 4-ml glass vial and extracted with 2.00 ml of 0.5 *M* sodium chloride–0.3% (w/v) ammonia solution. The sample was manually shaken for 2 min, then sonicated for 1 h. This was left standing at 4°C overnight to allow the particulate matter to settle. The supernatant was withdrawn (20–200 μl) and placed in a 4-ml glass vial. Sodium chloride solution (5 *M*) was added to bring the final sodium chloride concentration to 0.5 *M*. The final volume was brought to 500 μl by the addition of water. Living and senescent leaves of local grasses, trees and shrubs were manually cut into segments of about 1 mm square and freeze-dried for 40 h. Approximately 10 mg were weighed into a 4-ml glass vial. The plant matter was then extracted by the same method that was used for the soil samples, including the dilution step. When local blue-green algal blooms occurred, sea water that contained these organisms was collected. The sample was frozen at −18°C and allowed to thaw at ambient temperature. This ruptured the cells, allowing the organics to leach into the water. An appropriate aliquot was diluted with water and adjusted to a final sodium chloride concentration of 0.5 *M*. All standards were prepared by adding purified humic acid (Aldrich) to a sample matrix. A calibration graph was constructed and used for quantitation. The injection volume was 450 μl for sea water, 100 μl for coral skeletal and river water samples and 50 μl for soil and plant matter extracts.

Dried grasses were extracted with water and the extract was acidified with

concentrated hydrochloric acid to pH <1. The precipitate was filtered, dried and dissolved in dilute sodium hydroxide solution to a final pH of 8. Excess calcium chloride was added and the resulting precipitate was filtered and dried at 80°C. The calcium complex of humic acid was obtained in a similar manner. These samples were used for infrared analysis (potassium bromide disc).

RESULTS AND DISCUSSION

The chromatography of humic acid has been reported using both classical and high-performance techniques. Size-exclusion columns have been most commonly used. When salt solutions were used as the mobile phase, the peak shapes were usually broad and ill-defined. In one study it was shown that the retention time and peak shape of humic acid varied with the ionic strength of the mobile phase[22]. Sharp peaks were obtained when water alone was used as the mobile phase[20–22].

Diol-bonded silica column

We decided to begin our studies with a diol-bonded silica (diol) size-exclusion column. It was expected that our results could then be compared with those of previous studies in which both classical and HPLC size-exclusion columns were used. When phosphate and acetate buffers and sodium chloride solutions were used at concentrations between 0.001 and 2 *M* and the humic acid concentration was between 8 and 50 μg/ml, a non-reproducible broad band eluted. In contrast, when water was used as the mobile phase, a sharp, single peak eluted close to the solvent front. However, with increasing concentrations of humic acid, the peak broadened, although remaining symmetrical. The eluting peak was collected in three equal fractions and re-chromatographed. Each fraction eluted at the average retention time of the original fraction and the peak shape was again symmetrical. The fluorescence (excitation 340 nm; emission >490 nm) to absorbance (340 nm) ratio successively decreased for the three fractions. On the addition of sodium chloride or calcium chloride to each fraction, a single, sharp peak eluted at an increased retention time that was identical for each fraction. Typical chromatograms for a diol column with acetate buffer and water as the mobile phase are shown in Fig. 1.

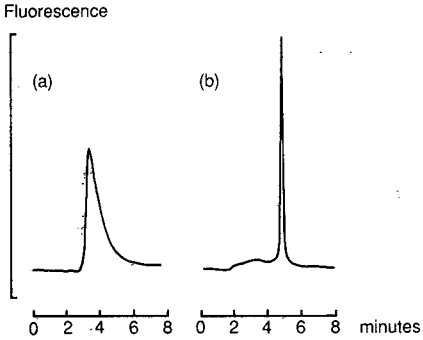

Fig. 1. Peak shape resulting from 1 μg of humic acid injected onto a diol column. Mobile phase: (a) 0.1 *M* sodium acetate solution, pH 6.8; (b) water.

Further unusual properties were observed on investigating the behaviour of humic acid on a Waters Assoc. ODS Sep-Pak cartridge. The retention and elution rate were highly dependent on the humic acid concentration and on the rate and frequency of flushing with water. If the column was allowed to stand for several minutes after a clear eluate was obtained, on renewed flushing a concentrated humic acid solution eluted. This phenomenon could be reproduced by using water, acetonitrile, methanol and tetrahydrofuran in any consecutive elution order.

These characteristics indicated that humic acid in solution was a mixture of components in equilibrium. One component is strongly retained on a reversed-phase column and the other is poorly retained, probably reflecting polarity differences. When disturbed, the equilibrium requires up to several minutes to re-establish, *i.e.*, it is a slow equilibrium. This in turn suggested that the HPLC peak broadening effect was not due exclusively to a size-exclusion mechanism. A slow change in the equilibrium composition of the humic acid could also account for the peak broadening. With water as the mobile phase, the mechanism would almost certainly not be size exclusion. It has been demonstrated previously that size-exclusion columns do not necessarily function in a size-exclusion manner[25].

Other bonded silica columns

When water was used as the mobile phase and < 1 μg of Aldrich humic acid was injected, a single, sharp peak with a low retention time eluted from octyldecylsilyl (ODS), phenyl-bonded silica (phenyl) and cyano-bonded silica (cyano) columns. No peaks eluted from an amino-bonded silica (amino) column or a strong anion-exchange-bonded silica (SAX) column. With phosphate and acetate buffers and sodium chloride solutions in the concentration range 0.001–2 *M*, and with water acidified with perchloric acid to below pH 5, no peaks eluted from an ODS or amino column. The phenyl and cyano columns gave broad, non-reproducible bands with these mobile phases.

Cation complexation

When increasing concentrations of ammonium chloride, sodium chloride, magnesium sulphate and calcium chloride in the range 0.05–1 *M* were added to a standard humic acid (Aldrich) solution (0.02 mg/ml) and chromatographed on an ODS col-

TABLE I

RETENTION TIME AND RELATIVE FLUORESCENCE (EXCITATION 340 nm; EMISSION >418 nm) OF THE FREE AND CATION-COMPLEXED HUMIC ACID ELUTING FROM A GLASS-LINED ODS COLUMN

Solvent flow-rate: 1 ml/min.

Species	*Cation concentration (M)*	*Retention time (min)*	*Relative fluorescence*
Free acid	–	1.36	1.00
Ammonium	0.5	2.10	0.61
Sodium	0.5	2.10	0.91
Magnesium	0.25	2.08	0.63
Calcium	0.2	2.09	0.38

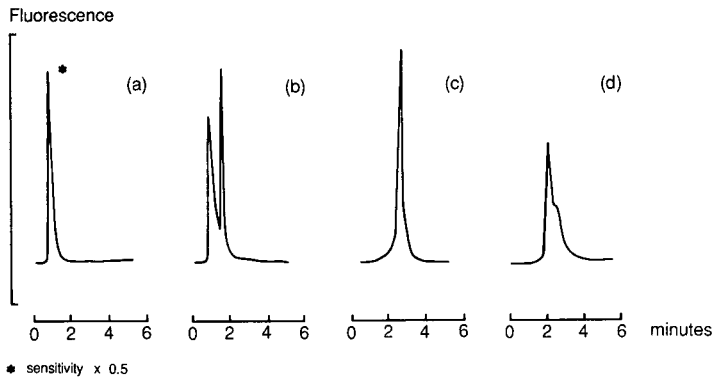

Fig. 2. Succession of peaks obtained when an increasing concentration of sodium chloride is added to 0.02 mg/ml of humic acid and the solution is injected onto an ODS column. Sodium chloride concentration: (a) 0; (b) 0.05; (c) 0.5; (d) 3 *M*.

umn, new peaks and shoulders appeared. The retention times of the existing peaks also increased slightly. The successive chromatograms that were obtained with sodium chloride are shown in Fig. 2. The relative fluorescence of the humic acid peaks resulting from the addition of these salts is given in Table I. Humic acid chromatographed on the diol, cyano and phenyl columns also exhibited similar properties.

In a previous study[2] using paper chromatography, it was recognized that the multiplicity of bands obtained was due to a humic acid–salt interaction. This led to the description of a humic acid–salt interaction hypothesis, but it did not gain general acceptance. When we added calcium chloride to a humic acid solution (2 mg/ml), a precipitate formed immediately and was filtered, washed and dried. It was insoluble in 0.1 *M* sodium hydroxide solution, an excellent solvent for humic acid, but it was soluble in a 0.1 *M* sodium hydroxide–1% (w/v) EDTA solution. This, and the fact that the compound had a 6.3% (w/w) calcium content (by direct current plasma emission analysis), indicated that the humic acid had formed a complex with calcium. When magnesium sulphate was added to the humic acid, a precipitate formed within a few minutes. With sodium chloride and ammonium chloride, a precipitate did not form for several hours. With a more dilute humic acid solution (0.2 mg/ml), no precipitate occurred with any of these salts, but the humic acid complex was strongly retained on an ODS Sep-Pak cartridge. Humic acids are known to complex with metal[26], calcium and hydrogen ions[27]. When sodium chloride and sodium perchlorate were added to the humic acid and subjected to HPLC, a new peak eluted. A new peak did not elute when sodium dodecyl sulphate was added. This indicates that humic acid can complex with sodium ions only in the presence of anions that are poor counter-complexing agents. Our HPLC data indicate that humic acid forms complexes with ammonium and sodium ions. This is in addition to the well known complexes formed with metals such as iron, copper and calcium. As the retention times were increased and the fluorescence was maintained by the addition of salts such as sodium chloride and calcium chloride, all samples and standards were chromatographed as their complexes. Coral skeletal matter was run as the calcium complex and all other samples as their sodium complexes.

Recovery from a reversed-phase column

When samples were injected consecutively (onto any column from which humic acid eluted) within 5 min of each other, a disturbing feature was that the peak size decreased continuously until the peak could not be distinguished from the baseline noise. This generally occurred within about ten injections and was observed for both the free and complexed humic acid. This type of phenomenon had been observed previously with bilins and was overcome in that instance by silylating the ODS column packing material[28]. This approach proved unsuccessful with humic acid, indicating that the problem was not due to irreversible adsorption onto free silanol groups. An increase in the pH of the mobile phase by the addition of ammonia overcame the problem. The elution profile of humic acid against ammonia concentration is shown in Fig. 3. When different columns were used it was found that the humic acid recovery varied considerably. A number of columns were compared using 0.003% (w/v) ammonia solution as the mobile phase. Results are shown in Fig. 4. Two glass-lined ODS columns gave the highest recovery, with similar absolute values. This indicates that humic acid interacts with the stainless-steel surfaces of the columns. Only glass-lined columns are considered suitable for quantitative analysis. To minimize the interaction with other metal components of the HPLC system, capillary PTFE tubing was used where possible. A mobile phase consisting of 0.003% ammonia solution was chosen as a compromise between humic acid recovery and solution pH. This mobile phase, which had a pH of 7.5, was pumped through a single ODS

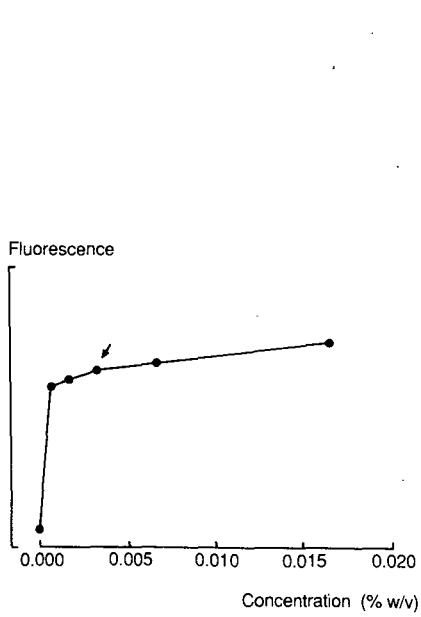

Fig. 3. Recovery of 0.2 μg of humic acid injected onto a glass-lined ODS column as a function of ammonia concentration in the mobile phase. The ammonia concentration used in the analytical procedure is indicated with an arrow.

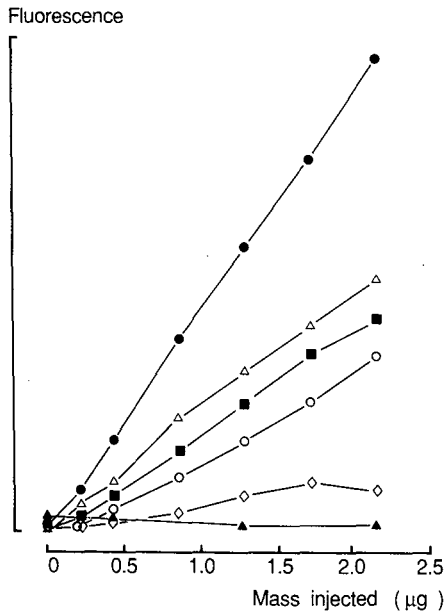

Fig. 4. Relative recoveries for different amounts of humic acid injected onto the following columns: ● = glass-lined ODS; △ = diol; ■ = phenyl; ○ = ODS; ◇ = cyano; ▲ = amino.

glass-lined analytical column protected by a guard column for a period in excess of 500 h. If the guard column was replaced when the peak shape began to deteriorate, there was no discernible change in the chromatographic properties of the system.

The absolute recovery from a glass-lined ODS column was checked by injecting a humic acid standard (Aldrich) with and without the analytical column. With fluorescence detection (excitation 340 nm; emission >418 nm), the recovery was 85.3%. This must be considered as a minimum recovery as it is possible that other components in the standard were not eluted. The method cannot achieve quantitative recovery because of the pH restraint that we imposed to prolong the column life, but the recoveries were found to be consistent. When river and sea water samples were spiked with a standard humic acid solution at a concentration of 0.02 mg/ml, the peak area for these samples (with the blank subtracted) was the same as for a standard humic acid solution in water at this concentration. This indicates that river and sea water do not adversely affect the humic acid recovery. Consecutive injections of humic acid samples dissolved in 0.5 *M* sodium chloride and in 0.25 *M* calcium chloride solutions were made. After the first two injections, no changes in peak area and height could be observed. In the analytical procedure, the column was routinely equilibrated with two 50-μl injections of a 0.2 mg/ml standard humic acid solution.

Fluorescence detection rather than UV absorbance detection was chosen because it showed better sensitivity and selectivity. Absorbance detection was not investigated in any detail, although preliminary studies indicated that absorbance monitoring at 254 nm may give inconsistent results.

The effect of organic modifiers with an ODS column was determined. Methanol, tetrahydrofuran and acetonitrile were mixed with water at concentrations between 5% and 80% (v/v). Little change in retention time was observed, even for high concentrations of the organic solvent. However, with increasing organic solvent concentration, the peak shape deteriorated until the peak could not be distinguished from the baseline noise. The peak shape was also sensitive to the amount of humic acid injected. When 10 μg of humic acid (Aldrich) was injected, a broad band with multiple sub-peaks eluted, similar to the elution profile in a previous study[24]. A comparison of retention mechanisms with that study cannot be made because different mobile phases were used. However, our data indicate that a reversed-phase mechanism is precluded. The equilibrium composition described above may have a significant influence on the mechanism.

Humic acid fluorescence and linearity

The fluorescence excitation spectra of humic acid (Aldrich and environmental samples) solutions changed markedly between concentrations of 0.5 and 140 μg/ml, although the emission spectra remained similar. This phenomenon could be due to a change in the equilibrium composition that we suggested above. Fluorescence at various excitation wavelengths over this concentration range for Aldrich humic acid was measured. Linearity was only obtained at the lower concentrations. The linear range decreased with decreasing excitation wavelength. Because our HPLC detector was fitted with a deuterium lamp, an excitation wavelength of 340 nm was chosen. At this wavelength, a good signal-to-noise ratio could be obtained and initial measurements indicated that linearity could be achieved at normal HPLC concentrations. Emission was measured at >418 nm with the aid of a cut-off filter. With these

wavelength settings, linearity was determined for the HPLC system using coral skeletal, sea water, river water, soil and plant matter samples. Humic acid was added to the sample matrix and the final sodium chloride and calcium chloride concentrations were adjusted to 0.5 and 0.2 *M*, respectively. For a 50-μl injection, linearity was maintained between 0.18 and 2.1 μg of humic acid injected ($r^2 > 0.997$). Coral skeletal, sea water and river water samples did not require dilution owing to their low levels of humic acid. Soil and plant matter extracts required dilution. Above about 3 μg of humic acid injected, peak-broadening effects can begin to occur. Excitation wavelengths below 340 nm can be used for increased sensitivity, but the linear range is diminished. The fluorescence response was also matrix dependent, which necessitated the construction of a calibration graph for each sample matrix.

Spectral properties of the HPLC peaks

The nature of the multiple peaks originating from the successive addition of ammonium, sodium, magnesium and calcium ions was investigated. When the concentrations of ammonium chloride and sodium chloride were about 0.5 *M*, and the concentrations of magnesium sulphate and calcium chloride were about 0.25 *M*, a sharp, single peak eluted from an ODS column with only a minor leading edge but a clearly distinguishable trailing edge at a flow-rate of 0.2 ml/min. The exact concentration that gave a single peak varied from column to column and had to be determined prior to routine analysis. For two glass-lined ODS columns tested, sea water samples could be injected directly without adjustment of the sodium chloride concentration.

Humic acid (Aldrich) was dissolved in 0.5 *M* sodium chloride and injected into an HPLC system fitted with a diode-array detector. Absorbance scans of the eluting peak were taken at millisecond intervals. An HPLC trace and a comparison of the spectra at six points along the peak are shown in Fig. 5. Between 220 and 400 nm the spectral differences were negligible. When the sample was prepared without sodium chloride, the individual spectra were again very similar to each other and also to those obtained with added sodium chloride. These results are similar to those obtained in a previous study[24] and confirm that the humic acid peak does not consist of a mixture of many different components. With an ODS column, two distinct peaks and a shoul-

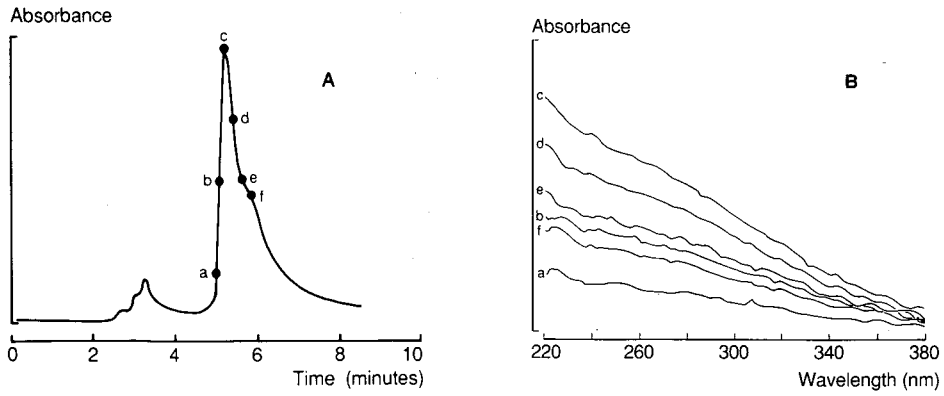

Fig. 5. (A) HPLC 250-nm absorbance trace with (B) spectra from the specified points of an eluting humic acid peak. The absorbance spectra were recorded with a diode-array detector during elution.

der eluted as the sodium chloride or calcium chloride concentration in the sample was increased from 0 to 2 *M*. These peaks are due to the free acid and probably to two cationic complexes. It has been observed previously that humic acid has two binding sites for calcium and hydrogen ions[27]. Sodium ions may complex at the same sites.

Interfering substances

To check for interfering substances, a number of acidic and polar compounds similar to compounds of plant origin were chromatographed, including lawsone, juglone, tetrahydroxy-*p*-benzoquinone, chloranilic acid, hydroquinone, *p*-benzoquinone, quercetin, rutin, arbutin, alizarin and quinalizarin. Chloranilic acid, quercetin and tetrahydroxy-*p*-benzoquinone eluted unresolved from humic acid on a glass-lined ODS column with 254-nm absorbance detection. When dissolved in 0.5 *M* sodium chloride they were also not resolved, coeluting with humic acid. Lawsone coeluted with the sodium complex of humic acid. As only humic acid was fluorescent, however, these compounds did not interfere when fluorescence detection was used.

To guard against possible interfering components in actual samples, the fluorescence ratio for an excitation wavelength of 340 nm relative to 270 nm was routinely monitored. For all humic acid samples tested to date, the ratio rarely varied beyond the limits of 0.25 ± 0.05. This is the ratio that is obtained for a standard Aldrich humic acid, indicating that interfering components are not a problem. The ratio for the peak coeluting with humic acid that was obtained from plant matter was sensitive to the extraction method. A ratio as low as 0.29 was only achieved when 5 ml of extracting solvent were used for about 5 mg of dry plant matter. If the proportion of plant matter was greater than this, the ratio was always higher. When water alone was used to extract the plant matter, many peaks occurred, but they fused into one peak on dilution plus the addition of sodium chloride. On the addition of amino acids and proteins to a standard humic acid solution, new peaks also occurred. The organic compound extracted from plant matter by water was probably complexed with other organic compounds such as amino acids. These organics could simply be replaced by diluting the solution and adding sodium chloride. Direct extraction with a 0.5 *M* sodium chloride–0.3% ammonia solution also overcame the problem.

Application of the method

The supernatant from the acid precipitation of Aldrich humic acid (fulvic acid by definition) was siphoned-off and freeze-dried. The resulting sample was dissolved in water and chromatographed as the free acid and as the sodium complex. The retention times were identical to those obtained for humic acid. The fluorescence ratios for an excitation wavelength of 340 nm relative to 270 nm were 0.25 and 0.26 for the humic and fulvic acids, respectively. In an analogous experiment, the supernatant from a calcium chloride precipitation experiment was chromatographed. The retention time showed that the soluble humic acid fraction was also complexed with calcium. These data indicate that, in solution, humic acid and fulvic acid are very similar.

The HPLC-purified humic acid that remained in the flow cell after diversion of the mobile phase was scanned for fluorescence excitation (240–380 nm; emission 440 nm) and emission (400–600 nm; excitation 340 nm) spectra. The spectra of the Aldrich humic acid were almost identical with those of coral skeletal, sea water, river

water, soil and plant matter samples. At least four different sources of each sample were chromatographed and scanned to confirm this. Because the excitation spectra change with concentration as noted above, samples were prepared to give approximately equal fluorescence responses (excitation 340 nm; emission 440 nm). A surprising result was obtained from plant leaf extracts. Both the retention time of the HPLC peak and its fluorescence excitation and emission spectra were similar to that obtained for humic acid from soils. The calcium complexes of Aldrich humic acid and of a dried grass extract showed almost identical infrared spectra in the region 4000–500 cm^{-1}. These data indicate that plants are a direct source of humic acid, in addition to the generally accepted indirect source. Fulvic acids have been isolated from leaf leachates[29]. For the extract from the algal bloom, there was a small difference in the 280–340-nm region of the fluorescence excitation spectrum compared with the Aldrich humic acid. The emission spectra were similar.

TABLE II

COMPARISON OF HUMIC ACID CONCENTRATIONS OBTAINED BY DIRECT FLUORESCENCE (EXCITATION 340 nm; EMISSION 440 nm) AND HPLC MEASUREMENTS

Sample	*HPLC*	*Direct fluorescence*
Coral skeletal[a] (μg/g)	57.7	116.9
	27.5	71.1
	25.2	51.6
	34.6	78.3
	44.9	85.4
	24.1	77.5
	29.4	62.7
	43.7	84.7
	19.8	38.6
	37.1	78.7
Inshore sea water[b,c] (μg/ml)	0.72	0.71
	0.42	0.47
	0.77	0.90
	0.81	0.81
Offshore sea water[b,d] (μg/ml)	0.11	0.53
	0.09	0.41
	0.08	0.30
	0.11	0.34
River water[b] (μg/ml)	9.10	9.56
	7.94	7.16
	1.79	1.88
	1.41	1.58
Soil[b] (μg/g)	1280	2260
	2060	3920
	711	1470
	5420	8560

[a] Ten samples from a single source.
[b] Four different sources.
[c] Within 500 m of the shore.
[d] 40–90 km offshore.

The chromatographic and fluorescence data indicate that the Aldrich humic acid is similar to humic acids obtained from coral skeletons, sea water, river water, soil and plant leaves, after purification by HPLC. Aldrich humic acid can therefore be used as a standard to determine humic acid in environmental samples. Typical humic acid concentrations in coral skeletons, sea water, river water and soils are given in Table II. The results of the HPLC method are compared with results obtained by measuring the fluorescence levels of the unchromatographed sample. The excitation (240–380 nm; emission 440 nm) and emission (400–600 nm; excitation 340 nm) spectra of unchromatographed coral skeletal, offshore sea water and soil samples were different to those of humic acid, indicating the presence of interfering fluorescent compounds. For these samples, HPLC analysis gave lower humic acid concentrations than direct fluorescence measurements. Direct fluorescence and HPLC measurements gave comparable results for river water and inshore sea water, indicating that humic acid is the major contributor to the fluorescence of these samples. The desirability of determining humic acid by chromatography is indicated by these data.

TABLE III

SUMMARY OF CHARACTERISTICS OF THE HPLC METHOD

Column	Glass-lined ODS (250 × 4.6 mm I.D.)
Mobile phase	0.003% (w/v) ammonia solution
Flow-rate	1 ml/min
Retention time	2.1 min (sodium complex)
Injection volume	50–450 μl
Detection	Fluorescence (excitation 340 nm; emission >418 nm)
Detection limit	15 ng (2 × noise)[a]
Relative standard deviation	(i) 1.9% (n = 8)[b]
	(ii) 0.34% (n = 10)[c]

[a] A detection limit of 1.3 ng was achieved for a sodium complex excited at 255 nm and run on a diol column.

[b] For a coral skeletal sample.

[c] For a river water sample excited at 270 nm.

CONCLUSION

Full details and characteristics of the method are given in Table III. At present the retention mechanism of humic acid on HPLC columns is not known, but the use of an appropriate mobile phase elutes a single, sharp peak from various columns. On an ODS column, humic acid is well resolved from many other polar and acidic compounds, and with fluorescence detection interfering compounds have not been observed. Investigations are in progress to develop a technique that will fractionate the individual components of a purified humic acid. The method described in this paper has been used routinely for the separation and determination of humic acid from many environmental sources. Humic acid environmental levels, their significance and their incorporation into coral skeletal matter will be the subject of a further report.

ACKNOWLEDGEMENTS

We thank Dr. P. Isdale and Mr. E. Daniel for providing the samples of coral skeletal material. We thank Mr. D. Carrick of Australian Analytical Laboratories, Sydney, for enabling us to chromatograph samples with the aid of a diode-array absorbance detector. Mr. F. Tirendi performed the calcium assay on the humic acid complex. Dr. G. Meehan, James Cook University, Townsville, kindly allowed us to use an infrared spectrophotometer.

REFERENCES

1 S. Odén, *Kolloidchem. Beih.*, 11 (1922) 75.
2 J. Shapiro, *Limnol. Oceanogr.*, 11 (1957) 161.
3 O. Aschan, *J. Prakt. Chem., N.F.*, 77 (1908) 172.
4 K. Kalle, *Dtsch. Hydrogr. Ztg.*, 2 (1949) 117.
5 V. C. Farmer and D. L. Pisaniello, *Nature (London)*, 313 (1985) 474.
6 M. Schnitzer, *Nature (London)*, 316 (1985) 658.
7 E. M. Thurman and R. L. Malcolm, in R. F. Christman and E. T. Gjessing (Editors), *Aquatic and Terrestrial Humic Materials*, Ann Arbor Sci. Publ., Ann Arbor, MI, 1983, p. 1.
8 N. Plechanov, B. Joseffsson, D. Dyrssen and K. Lundquist, in R. F. Christman and E. T. Gjessing (Editors), *Aquatic and Terrestrial Humic Materials*, Ann Arbor Sci. Publ., Ann Arbor, MI, 1983, p. 387.
9 C. Steelink, M. A. Mikita and K. A. Thorn, in R. F. Christman and E. T. Gjessing (Editors), *Aquatic and Terrestrial Humic Materials*, Ann Arbor Sci. Publ., Ann Arbor, MI, 1983, p. 83.
10 J. R. Ertel and J. I. Hedges, in R. F. Christman and E. T. Gjessing (Editors), *Aquatic and Terrestrial Humic Materials*, Ann Arbor Sci. Publ., Ann Arbor, MI, 1983, p. 143.
11 M. Lévesque, *Soil Sci.*, 113 (1972) 346.
12 Y. Saito and S. Hayano, *J. Chromatogr.*, 177 (1979) 390.
13 J. P. Martin and K. Haider, in T. K. Kirk, T. Higuchi and H. Chang (Editors), *Lignin Biodegradation: Microbiology, Chemistry and Potential Applications*, Vol. 1, CRC Press, Boca Raton, FL, 1980, p. 89.
14 R. F. C. Mantoura, A. Dickson and J. P. Riley, *Estuar. Coastal Mar. Sci.*, 6 (1978) 387.
15 A. Prakash and D. J. MacGregor, in R. F. Christman and E. T. Gjessing (Editors), *Aquatic and Terrestrial Humic Materials*, Ann Arbor Sci. Publ., Ann Arbor, MI, 1983, p. 481 and references cited therein.
16 A. Prakash, in J. D. Costlow (Editor), *Fertility of the Sea*, Ann Arbor Sci. Publ., Ann Arbor, MI, 1983, p. 351 and references cited therein.
17 S. U. Khan and M. Schnitzer, *Geochim. Cosmochim. Acta*, 36 (1972) 745.
18 K. Boto and P. Isdale, *Nature (London)*, 315 (1985) 396.
19 P. Isdale, *Nature (London)*, 310 (1984) 578.
20 W. S. Gardner and P. F. Landrum, in R. F. Christman and E. T. Gjessing (Editors), *Aquatic and Terrestrial Humic Materials*, Ann Arbor Sci. Publ., Ann Arbor, MI, 1983, p. 203.
21 C. J. Miles and P. L. Brezonik, *J. Chromatogr.*, 259 (1983) 499.
22 G. Becher, G. E. Carlberg, E. T. Gjessing, J. H. Hongslo and S. Monarca, *Environ. Sci. Technol.*, 19 (1985) 422.
23 T. Vartianen, A. Liimatainen and P. Kauranen, *Sci. Total Environ.*, 62 (1987) 75.
24 F. Y. Saleh and D. Y. Chang, *Sci. Total Environ.*, 62 (1987) 67.
25 C. T. Mant, J. M. R. Parker and R. S. Hughes, *J. Chromatogr.*, 397 (1987) 99.
26 J. H. Weber, in R. F. Christman and E. T. Gjessing (Editors), *Aquatic and Terrestrial Humic Materials*, Ann Arbor Sci. Publ., Ann Arbor, MI, 1983, p. 315.
27 B. A. Dempsey and C. R. O'Melia, in R. F. Christman and E. T. Gjessing (Editors), *Aquatic and Terrestrial Humic Materials*, Ann Arbor Sci. Publ., Ann Arbor, MI, 1983, p. 239.
28 S. Schoch, U. Lempert, H. Weischhoff and H. Scheer, *J. Chromatogr.*, 157 (1978) 357.
29 F. H. Frimmel and H. Bauer, *Sci. Total Environ.*, 62 (1987) 139.

Journal of Chromatography, 482 (1989) 189–195
Elsevier Science Publishers B.V., Amsterdam — Printed in The Netherlands

CHROM. 21 825

DIASTEREOMERIC RESOLUTION OF CAROTENOIDS

IV[a]. CAROTENOIDS WITH A 4-HYDROXY-β-END GROUP

TAKASHI MAOKA and TAKAO MATSUNO*
Department of Natural Products Research, Kyoto Pharmaceutical University, Yamashina-ku, Kyoto 607 (Japan)
(Received July 4th, 1989)

SUMMARY

A method is described for the diastereomeric resolution of carotenoids with a 4-hydroxy-β-end group, *viz.*, β-isocryptoxanthin (β,β-caroten-4-ol), isozeaxanthin (β,β-carotene-4,4′-diol) and 4′-hydroxyechinenone (4′-hydroxy-β,β-caroten-4-one). The separation of each carotenoid into individual optical isomers was achieved by high-performance liquid chromatography using a Chiralcel OD [cellulose tris(3,5-dimethylphenylcarbamate) coated on silica gel] chiral resolution column after conversion to the corresponding benzoates.

INTRODUCTION

In the course of our stereochemical studies of naturally occurring carotenoids, we have reported on the diastereomeric resolution of carotenoids with a 3-hydroxy-β-end group (zeaxanthin)[1], 3-hydroxy-4-oxo-β-end group (astaxanthin and phoenicoxanthin)[2,3], a 3-hydroxy-ε-end group (tunaxanthin)[4], 3-oxo-ε-end group (ε,ε-carotene-3,3′-dione)[4], a 2-hydroxy-β-end group (β,β-caroten-2-ol and β,β-carotene-2,2′-diol)[5] and a 2-hydroxy-4-oxo-β-end group (2-hydroxy-echinenone)[5] by high-performance liquid chromatography (HPLC) using a Sumipax-OA 2000 chiral resolution column.

In this paper we report the separation of optical isomers of carotenoids with a 4-hydroxy-β-end group, *viz.*, β-isocryptoxanthin (β,β-caroten-4-ol), isozeaxanthin (β,β-carotene-4,4′-diol) and 4′-hydroxyechinenone (4′-hydroxy-β,β-caroten-4-one).

EXPERIMENTAL

Apparatus

HPLC was carried out on a Waters Model 510 instrument with a Waters Lambda-Max Model 418 LC spectrophotometer set at 450 nm. A 250 × 4.6 mm I.D.

[a] For Part III, see ref. 5.

0021-9673/89/$03.50

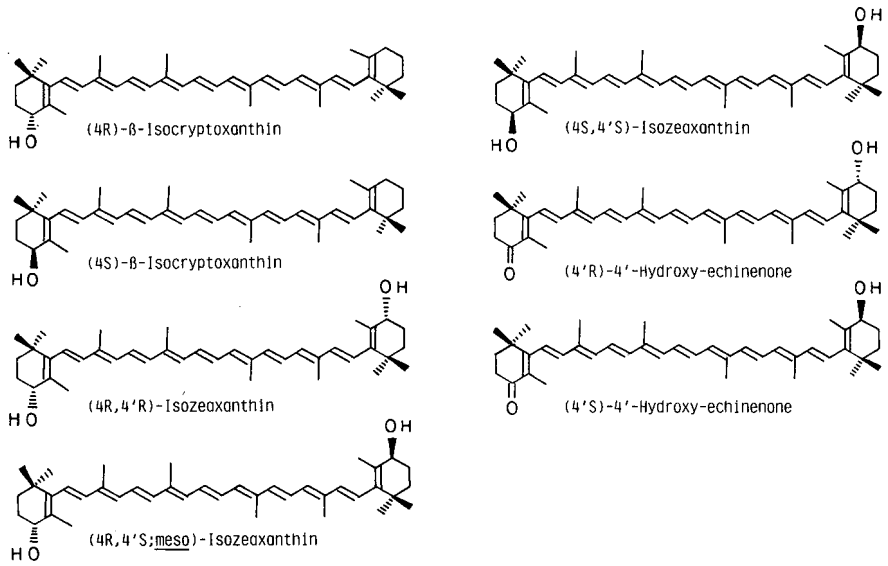

stainless-steel column packed with Chiralcel OD [cellulose tris(3,5-dimethylphenylcarbamate) coated on silica gel; Daicel Chemical Industries, Tokyo, Japan] was used. Visible light absorption spectra (VIS) were recorded in diethyl ether on a Shimadzu UV 240 spectrophotometer. Mass spectra (MS) were recorded with a Hitachi M-80 mass spectrometer using an ionization energy of 25 eV. ^{1}H NMR spectra were recorded on a Varian XL-300 spectrometer at 300 MHz in $CDCl_3$ solution. Circular dichroism (CD) spectra were obtained with a Jasco J-500 C spectropolarimeter in diethyl ether–isopentane–ethanol (5:5:2) (EPA) solution at 20°C.

Preparation of racemic β-isocryptoxanthin from echinenone

Reduction of echinenone (β,β-caroten-4-one) (0.5 mg) isolated from sea urchins purchased at a local fish market with sodium borohydride (10 mg) in methanol (20 ml) for 30 min at 20°C provided racemic β-isocryptoxanthin (0.4 mg). The reduction product was purified by preparative thin-layer chromatography (TLC) on silica gel G with acetone–*n*-hexane (3:7).

Preparation of racemic 4'-hydroxy-echinenone and isozeaxanthin from canthaxanthin

Reduction of canthaxanthin (β,β-carotene-4,4'-dione) (1 mg) (Hoffmann-La Roche) with sodium borohydride (10 mg) in methanol (20 ml) for 15 min at 20°C provided racemic 4'-hydroxyechinenone (0.1 mg) and racemic isozeaxanthin (0.6 mg). These two reduction products were separated by preparative TLC on silica gel G with acetone-*n*-hexane (3:7).

Preparation of benzoates of β-isocryptoxanthin, isozeaxanthin and 4'-hydroxy-echinenone.

Preparation of benzoates of these carotenoids was carried out by the method described previously[1,4].

Saponification of benzoates of β-isocryptoxanthin, isozeaxanthin and 4'-hydroxy-echinenone

Saponification of these benzoates was carried out by routine procedure[6].

RESULTS AND DISCUSSION

Separation of racemic β-isocryptoxanthin into (4R)- and (4S)-β-isocryptoxanthin

The separation of the two stereoisomers of β-isocryptoxanthin from a racemic mixture was achieved by HPLC on a Chiralcel OD column after conversion to the corresponding monobenzoate as shown in Fig. 1. *Cis* isomers in the polyene chain were also separated from the corresponding all-*trans* isomers. The *cis* isomers were not identified. Saponification of each separated monobenzoate gave optically pure (4*R*)- and (4*S*)-β-isocryptoxanthin. The identification of each stereoisomer was based on CD spectral data as shown in Fig. 2. Peaks 1 and 2 represent (4*R*)- and (4*S*)-β-isocryptoxanthin, respectively.

(4*R*)-β-Isocryptoxanthin (0.1 mg available) showed VIS, λ_{max} 425 (shoulder), 449 and 476 nm and no *cis* peak; MS, *m/z* 552 [M^+, compatible with $C_{40}H_{56}O$], 534 [$M-18]^+$, 460 [$M-92]^+$ and 446 [$M-106]^+$; ^{1}H NMR, δ 1.02 s (3H, CH_3-16), 1.03 s (6H, CH_3-16',17'), 1.05 s (3H, CH_3-17), 1.72 s (3H, CH_3-18'), 1.84 s (3H, CH_3-18), 1.97 s (12H, CH_3-19,20,19',20'), 2.02 m (2H, H-4'), 4.01 t (1H, H-4), 6.1–6.8 m (14H, olefinic H); and CD ($\Delta\varepsilon$), 242 (+4.0), 262 (0), 282 (−2.6), 312 (0) and 345 nm (+0.7). These data were completely identical with those of (4*R*)-β-isocryptoxanthin synthesized by Haag and Eugster[7].

(4*S*)-β-Isocryptoxanthin (0.1 mg available) showed the same VIS, MS and ^{1}H NMR spectral data as those of (4*R*)-β-isocryptoxanthin and showed CD ($\Delta\varepsilon$), 242 (−4.0), 262 (0), 282 (+2.6), 312 (0) and 345 nm (−0.7).

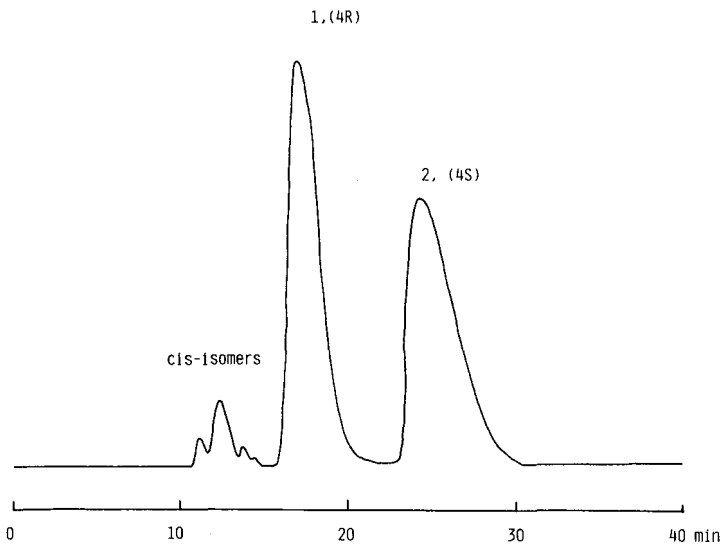

Fig. 1. Separation of (4*R*)- and (4*S*)-β-isocryptoxanthin monobenzoates (20 μg available in one separation). Column, Chiralcel OD (250 × 4.6 mm I.D.); mobile phase, *n*-hexane–ethanol–N,N-diisopropylethylamine (100:0.2:0.05); flow-rate, 0.5 ml/min; detection, 450 nm.

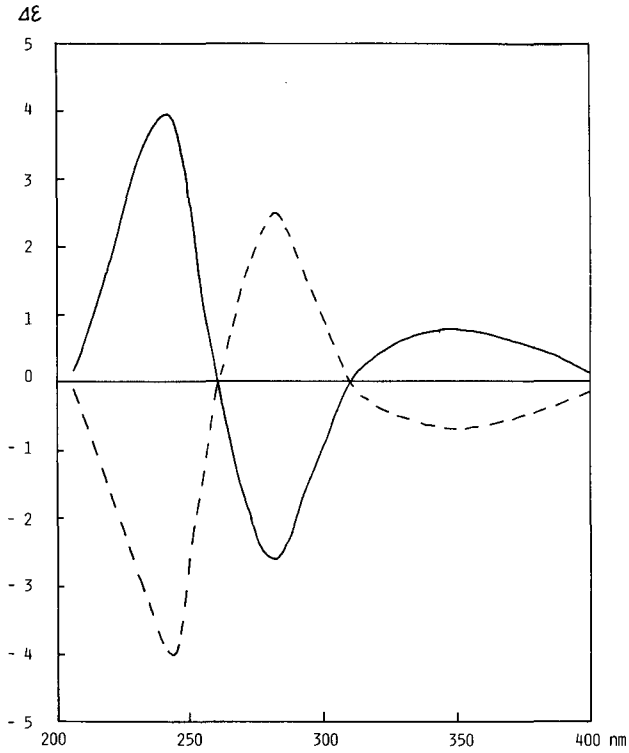

Fig. 2. CD spectra of (4*R*)-β-isocryptoxanthin (——) and (4*S*)-β-isocryptoxanthin (– – – –) in EPA at 20°C.

Separation of racemic isozeaxanthin into (4R,4′R)-, (4R,4′S;meso)- and (4S,4′S)-isozeaxanthin

The separation of the three stereoisomers of isozeaxanthin from a racemic mixture was achieved by HPLC on a Chiralcel OD column after conversion to the corresponding dibenzoate as shown in Fig. 3. *Cis* isomers were also separated from the corresponding all-*trans* isomers. The *cis* isomers were not identified. Saponification of each separated dibenzoate gave optically pure (4*R*,4′*R*)-, (4*R*,4′*S*;*meso*)- and (4*S*,4′*S*)-isozeaxanthin. The identification of each stereoisomer was based on CD spectral data as shown in Fig. 4. Peaks 1, 2 and 3 represent (4*R*,4′*R*)-, (4*R*,4′*S*;*meso*)- and (4*S*,4′*S*)-isozeaxanthin, respectively.

(4*R*,4′*R*)-Isozeaxanthin (0.1 mg available) showed VIS, λ_{max} 425 (shoulder), 449 and 476 nm and no *cis* peak; MS, *m/z* 568 [M^+, compatible with $C_{40}H_{56}O_2$], 550 [$M-18]^+$, 532 [$M-36]^+$, 476 [$M-92]^+$ and 462 [$M-106]^+$; ^{1}H NMR, δ 1.02 s (6H, CH_3-16,16′), 1.05 s (6H, CH_3-17,17′), 1.84 s (6H, CH_3-18,18′), 1.97 s (12H, CH_3-19,20,19′,20′), 4.01 t (2H, H-4,4′) and 6.1–6.8 m (14H, olefinic H); and CD ($\Delta\varepsilon$), 243 (+5.0), 262 (0), 282 (−5.9), 312 (0) and 346 nm (+1.0). These data were completely identical with those of (4*R*,4′*R*)-isozeaxanthin synthesized by Haag and Eugster[8].

(4*R*,4′*S*;*meso*)-Isozeaxanthin (0.2 mg available) showed the same VIS, MS and ^{1}H NMR data as those of (4*R*,4′*R*)-isozeaxanthin and showed no optical activity in CD.

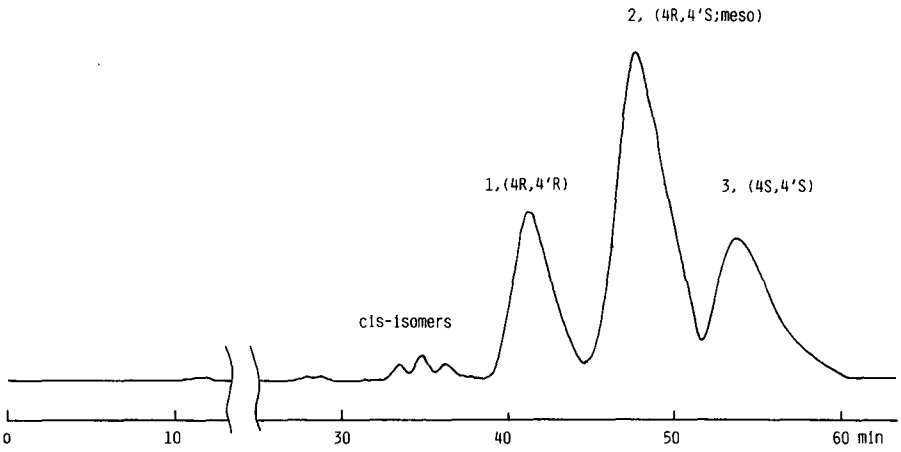

Fig. 3. Separation of (4*R*,4′*R*)-, (4*R*,4′*S*;*meso*)- and (4*S*,4′*S*)-isozeaxanthin dibenzoates (10 μg available in one operation). Column, Chiralcel OD (250 × 4.6 mm I.D.); mobile phase, *n*-hexane–ethanol–N,N-diisopropylethylamine (100:0.5:0.05); flow-rate, 0.5 ml/min; detection, 450 nm.

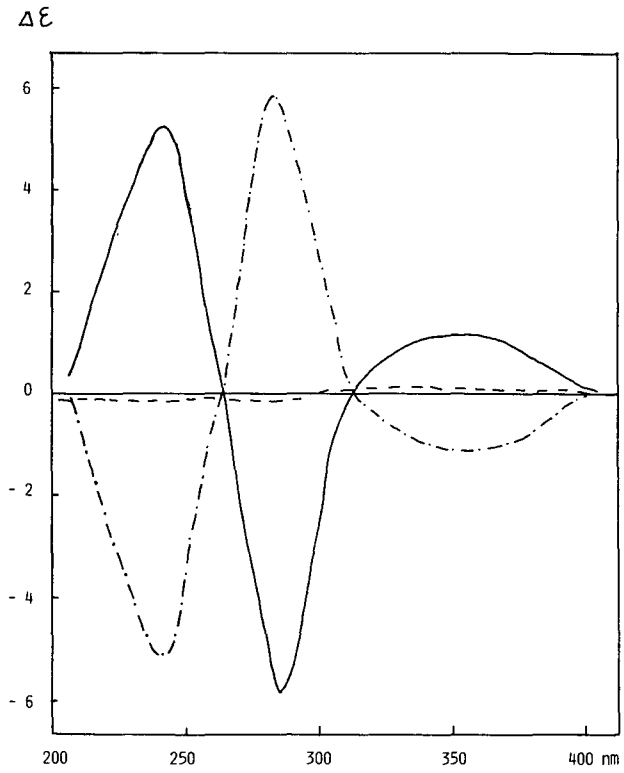

Fig. 4. CD spectra of (4*R*,4′*R*)-isozeaxanthin (——) (4*R*,4′*S*;*meso*)-isozeaxanthin (– – – –) and (4*S*,4′*S*)-isozeaxanthin (– · – · –) in EPA at 20°C.

(4*S*,4′*S*)-Isozeaxanthin (0.1 mg available) showed the same VIS, MS and ^{1}H NMR data as those of (4*R*,4′*R*)-isozeaxanthin and showed CD ($\Delta\varepsilon$), 243 (−5.0), 262 (0), 282 (+5.9), 312 (0) and 346 nm (−1.0).

Separation of racemic 4′-hydroxyechinenone into (4′R)- and (4′S)-4′-hydroxyechinenone

The separation of the two stereoisomers of 4′-hydroxyechinenone from a racemic mixture was ahieved by HPLC on a Chiralcel OD column after conversion to the corresponding monobenzoate as shown in Fig. 5. *Cis* isomers were also separated from the corresponding all-*trans* isomers. The *cis* isomers were not identified. Saponification of each separated monobenzoate gave optically pure (4′*R*)- and (4′*S*)-4′-hydroxyechinenone. The identification of each stereoisomer was based on CD spectral data as shown in Fig. 6. Peaks 1 and 2 represent (4′*R*)- and (4′*S*)-4′-hydroxyechinenone, respectively.

(4′*R*)-4′-Hydroxyechinenone (0.05 mg available) showed VIS, λ_{max} 455–460 nm and no *cis* peak; MS, *m/z* 566 [M$^+$, compatible with $C_{40}H_{54}O_2$], 548 [M − 18]$^+$, 474 [M − 92]$^+$ and 460 [M − 106]$^+$; ^{1}H NMR, δ 1.02 s (3H, CH_3-16′), 1.05 s (3H, CH_3-17′), 1.20 s (6H, CH_3-16,17), 1.84 s (3H, CH_3-18′), 1.88 s (3H, CH_3-18), 1.98 s (9H, CH_3-20,19′,20′), 2.00 s (3H, CH_3-19), 2.51 t (2H, H-3) 4.01 t (1H, H-4′) and 6.1–6.8 m (14H, olefinic H); and CD ($\Delta\varepsilon$), 240 (0), 252 (+1.1), 270 (0), 298 (−1.8), 330 (0) and 350 nm (+0.5). These data were completely identical with those of (4′*R*)-4′-hydroxyechinenone synthesized by Haag and Eugster[7].

(4′*S*)-4′-Hydroxyechinenone (0.05 mg available) showed the same VIS, MS and ^{1}H NMR data as those of (4′*R*)-4′-hydroxyechinenone and showed CD ($\Delta\varepsilon$), 240 (0), 252 (−1.1), 270 (0), 298 (+1.8), 330 (0) and 350 nm (−0.5).

Concerning the stereoisomers of carotenoids with a 4-hydroxy-β-end group, only (4*R*)-stereoisomers, *i.e.* (4*R*)-β-isocryptoxanthin, (4*R*,6′*R*)-α-isocryptoxanthin, (4′*R*)-4′-hydroxyechinone, (4*R*)-isorubixanthin and (4*R*,4′*R*)-isozeaxanthin, have so far been synthesized by Haag and Eugster[7,8]; (4*S*)-stereoisomers have not yet been reported.

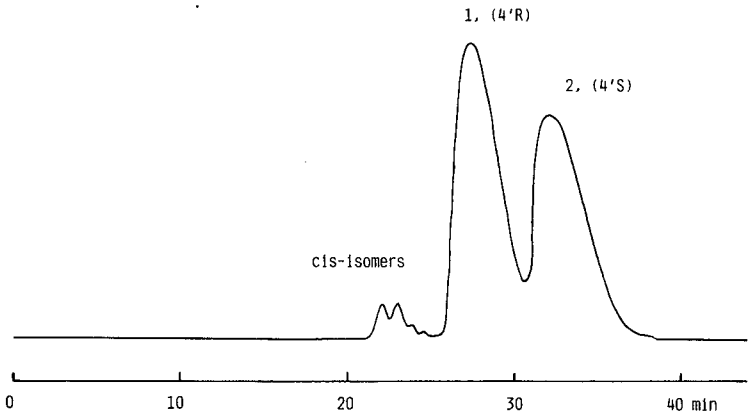

Fig. 5. Separation of (4′*R*)- and (4*S*′)-4′-hydroxyechinenone monobenzoates (10 μg available in one separation). Column, Chiralcel OD (240 × 4.6 mm I.D.); mobile phase, *n*-hexane–ethanol–N,N-diisopropylethylamine (100:0.2:0.05); flow-rate, 0.5 ml/min; detection at 450 nm.

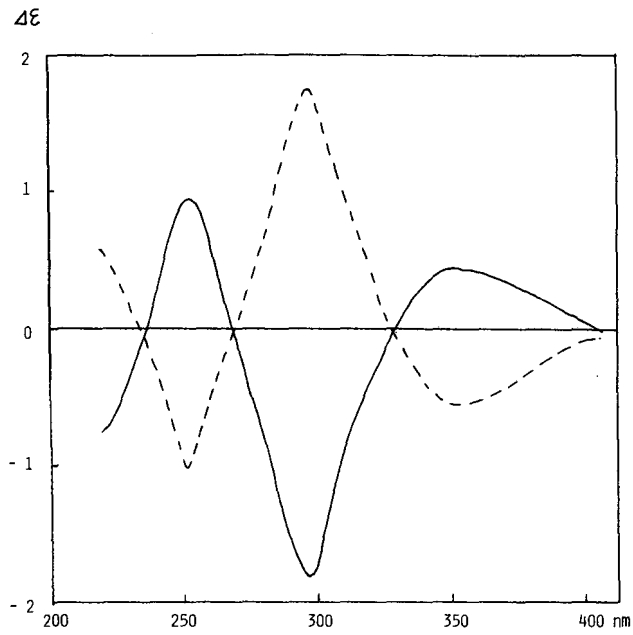

Fig. 6. CD spectra of (4′*R*)-4′-hydroxyechinenone (——) and (4′*S*)-4′-hydroxyechinenone (– – –) in EPA at 20°C.

REFERENCES

1 T. Maoka, A. Arai, M. Shimizu and T. Matsuno, *Comp. Biochem. Physiol. B*, 83 (1986) 121.
2 T. Matsuno, T. Maoka, M. Katsuyama, M. Ookubo, K. Katagiri and H. Jimura, *Nippon Suisan Gakkaishi*, 50 (1984) 1598.
3 T. Maoka, K. Komori and T. Matsuno, *J. Chromatogr.*, 318 (1985) 122.
4 Y. Ikuno, T. Maoka, M. Shimizu, T. Komori and T. Matsuno, *J. Chromatogr.*, 328 (1985) 387.
5 T. Maoka and T. Matsuno, *J. Chromatogr.*, 478 (1989) 379.
6 T. Matsuno, T. Akita and M. Hara, *Nippon Suisan Gakaishi*, 39 (1973) 51.
7 A. Haag and C. H. Eugster, *Helv. Chim. Acta*, 68 (1985) 1897.
8 A. Haag and C. H. Eugster, *Helv. Chim. Acta*, 65 (1982) 1795.

Journal of Chromatography, 482 (1989) 197–205
Elsevier Science Publishers B.V., Amsterdam — Printed in The Netherlands

CHROM. 21 852

FOAM COUNTER-CURRENT CHROMATOGRAPHY OF BACITRACIN

I. BATCH SEPARATION WITH NITROGEN AND WATER FREE OF ADDITIVES

HISAO OKA[a]
Laboratory of Technical Development, National Heart, Lung, and Blood Institute, National Institutes of Health, Bethesda, MD 20892 (U.S.A.)
KEN-ICHI HARADA and MAKOTO SUZUKI
Faculty of Pharmacy, Meijo University, Tempaku, Nagoya 468 (Japan)
HIROYUKI NAKAZAWA
Institute of Public Health, Tokyo 108 (Japan)
and
YOICHIRO ITO*
Laboratory of Technical Development, National Heart, Lung, and Blood Institute, National Institutes of Health, Bethesda, MD 20892 (U.S.A.)
(First received May 18th, 1989; revised manuscript received August 2nd, 1989)

SUMMARY

A foam counter-current chromatographic method utilizing a true counter-current movement between nitrogen and distilled water through a long narrow coiled tube is described. Samples introduced into the coil are separated according to their foaming capability: foam-active materials generate foam and quickly move with nitrogen toward one end of the coil while the remainder are carried with the liquid stream in the opposite direction and eluted through the other end of the coil. The utility of the method was demonstrated in the fractionation of commercial bacitracin (BC). Hydrophobic components including BC-A, BC-F and several minor components were enriched with foam and collected in decreasing order of hydrophobicity, whereas hydrophilic components were eluted with the liquid in decreasing order of polarity. The results indicate that foam-active components can be effectively separated by foam counter-current chromatography using nitrogen and distilled water without a surfactant or other additives.

INTRODUCTION

Recently, a great improvement in foam separation technology has been achieved by the development of foam counter-current chromatography (CCC)[1],

[a] Visiting Scientist from the Aichi Prefectural Institute of Public Health, Nagoya 462, Japan.

0021-9673/89/$03.50

which uses a long coiled column in a centrifugal force field. Introduction of a sample mixture into the coiled column, either batchwise or continuously, results in the separation of the sample components: molecules with a foam-producing capacity or foam affinity quickly move with the foaming stream and are collected through the foam outlet, whereas the remainder of the molecules are carried with the liquid stream in the opposite direction and eluted through the liquid outlet. This method has been successfully applied to various test samples: ionic compounds were collected with suitable surfactants, and surface-active proteins were separated in phosphate buffer solution to prevent denaturation of the molecules[1–3]. However, this original foam CCC method requires the removal of surfactants or other additives after fractionation.

As many natural products exhibit foaming capacity in an aqueous solution, foam CCC may be possible without surfactants or other additives for the isolation and enrichment of these natural products. In a previous paper[4], we briefly introduced a foam CCC method for bacitracin (BC) components using nitrogen gas and distilled water entirely free from surfactants and other additives. This paper describes in detail the successful application of foam CCC to the separation of BC components without any surfactants and other additives.

EXPERIMENTAL

Apparatus for foam CCC

Fig. 1 shows a cross-sectional view of the foam counter-current chromatograph. The apparatus holds a pair of holders symmetrically 20 cm from the central axis. The gear-driven holder (upper) is equipped with a coiled column, and the pulley-driven holder (lower) is used for mounting a counterweight for balancing the centrifuge system. The desired planetary motion of the gear-driven holder is produced by the use of a countershaft equipped with a gear and a toothed pulley. The stationary gear mounted on the central pipe of the centrifuge is coupled to the identical planetary gear affixed on the countershaft to rotate the countershaft on the rotary frame. This motion is further conveyed to the column holder by coupling the toothed pulley on the countershaft to an identical pulley on the coil holder shaft with a toothed belt. Consequently, as the rotary frame is driven by the motor, the coil holder undergoes a synchronous planetary motion in such a way that it revolves around the central axis of the centrifuge and simultaneously rotates about its own axis at the same angular velocity in the same direction. As described elsewhere[1], this planetary motion permits the bundle of flow tubes to rotate with the rotary frame without twisting, thus allowing both gas and liquid to flow in and out through the rotating coil without the use of a conventional rotary seal device, which would become a potential source of leakage and cross-contamination. The revolutional speed of the apparatus can be regulated up to 1000 rpm with a speed control unit (Bodine Electric, Chicago, IL, U.S.A.).

The column design is illustrated schematically in Fig. 2. The coil, consisting of a 10 m × 2.6 mm I.D. PTFE tube with a capacity of 50 ml, is equipped with five flow channels: liquid feed line and foam collection line at the tail and gas feed line and liquid collection line at the head, while the sample feed line opens at the middle portion of the coil. In the actual column design, the gas and liquid feed lines each enter into the coil through a Kel-F three-way adaptor at the respective terminus

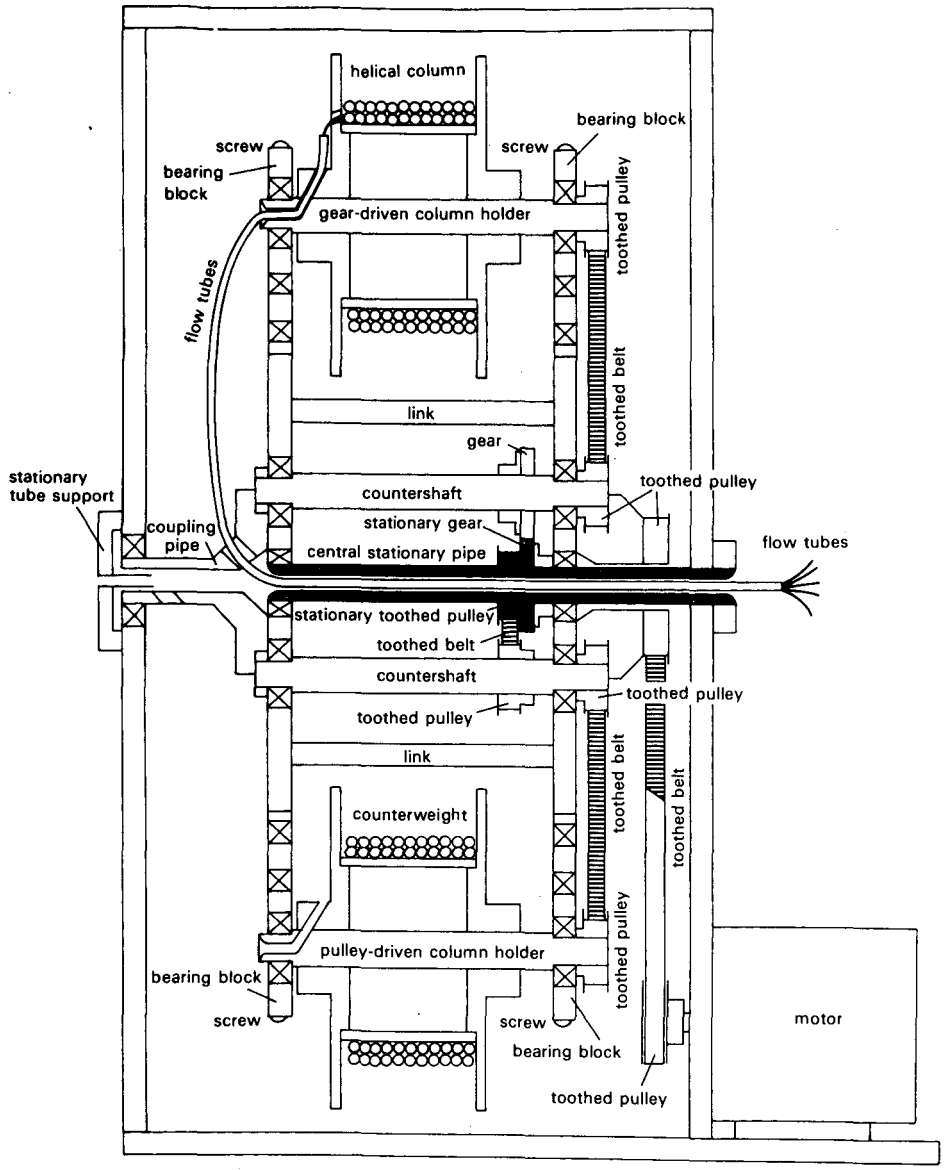

Fig. 1. Illustration of foam counter-current chromatograph.

where the tubing extends into the coil for about one turn (50 cm) to prevent the fed fluid from flowing back through the nearby outlet at the same terminus. The liquid is pumped with a Milton-Roy Minipump through the tail and collected from the head while nitrogen is introduced through the head directly from a gas cylinder at 80 p.s.i., and the generated foam is collected from the tail as indicated in Fig. 2 (the head–tail relationship of the rotating coil is conventionally defined by an Archimedean screw

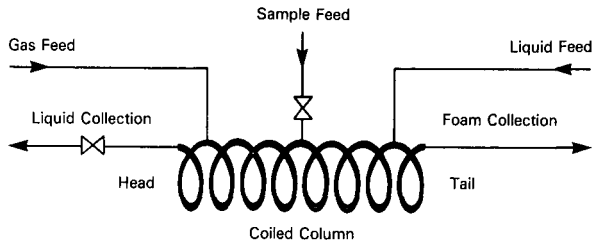

Fig. 2. Column design for foam CCC.

force where all objects of different densities are driven toward the head of the coil). The liquid flow through the liquid collection line is regulated with a needle valve (Washington Valve, Rockville, MD, U.S.A.) while the foam collection line is left open to the air.

Procedure for foam CCC

Separation was initiated by the simultaneous introduction of distilled water at the desired flow-rate from the tail and nitrogen at 80 p.s.i. from the head into the rotating coil at 500 rpm while the needle valve on the liquid collection line was fully open (13.5 turns). After a steady-state hydrodynamic equilibrium had been reached, the pump was stopped and 0.5 ml of a sample solution containing bacitracin (Sigma, St. Louis, MO, U.S.A.) at 1% (w/v) in distilled water was injected through the sample port. After the desired standing time, opening of the needle valve was adjusted to the desired level and the pumping resumed. Effluents through the foam and liquid outlets were each manually fractionated at 15-s intervals. Elution curves of BC from the foam and liquid outlets were obtained by spectrophotometric analysis of each fraction at a measurement wavelength of 234 nm, and an aliquot of each fraction was also analysed by reversed-phase high-performance liquid chromatography (HPLC).

HPLC conditions

A chromatograph equipped with a constant-flow pump (LC-6A; Shimadzu, Kyoto, Japan) was used with a variable-wavelength UV detector (SPD-6A; Shimadzu) operated at 234 nm. The separations were performed on Capcell Pak C_{18} (150 mm × 4.6 mm I.D.) (Shiseido, Tokyo, Japan) with methanol–0.04 *M* disodium hydrogenphosphate solution (62:38) as the mobile phase at a flow-rate of 1.0 ml/min.

RESULTS AND DISCUSSION

Bacitracin (BC) is a basic cyclic peptide antibiotic commonly used as a feed additive for livestock. It consists of more than 20 components, but the chemical structures of these components are still unknown except the major active component BC-A and its oxidation product BC-F. Under the present HPLC conditions, BC was separated into more than 15 components, as shown in Fig. 3. Generally, hydrophilic compounds show shorter retention times than hydrophobic compounds under reversed-phase HPLC conditions. We consider that BC-A is more hydrophilic than BC-F, which elutes earlier in HPLC. In this study, we used this definition to establish

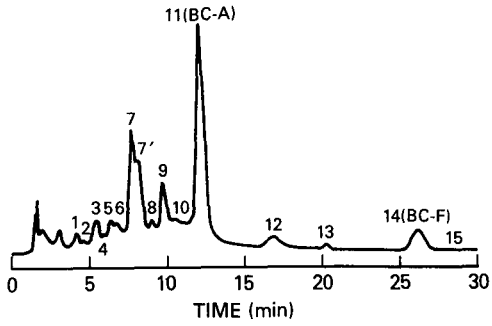

Fig. 3. High-performance liquid chromatogram of the original bacitracin. For HPLC conditions, see Experimental.

the polarity of BC components; special attention was also paid to peaks 3, 7, 11 and 14 to evaluate the separation of bacitracin components by foam CCC.

Optimization of foam CCC conditions

Using a set of fixed conditions for nitrogen flow-rate, sample size, fractionation rate and the column rotation speed, as described under Experimental, we investigated the effects of the liquid flow-rate, opening of the needle valve at the liquid outlet and standing time after sample injection on the separation efficiency. The results are summarized in Table I. Liquid flow-rates lower than 3.2 ml/min failed to elute foam, whereas flow-rates higher than 3.2 ml/min gave a less efficient separation between peaks 11 and 14. Consequently, 3.2 ml/min was selected as the liquid flow-rate. The degree of opening of the needle valve at the liquid outlet was found to be an important parameter. When the valve was opened less than 0.5 turn (fully open: 13.5 turns), all peaks showed less efficient separation. On opening the valve between 0.5 and 0.8 turn, peak 7 eluted from the foam outlet, whereas the same peak eluted from the liquid outlet with the valve opening between 0.8 and 1.2 turn. Valve opening more than 1.2 turn gave no foam fraction. Accordingly, we adjusted the needle valve opening to 0.8 turn in the subsequent work. The length of the standing time after sample injection also affects the foam separation. Standing times less than 5 min gave an inefficient separation between peaks 11 and 14, and no foam eluted at standing times over 5 min. Therefore, 5 min was selected as the optimum standing time. The standing time permits the injected sample components to distribute along the length of the coil according to their foam-producing capacity.

Separation of bacitracin components

The separation of BC components was carried out using the optimum foam CCC conditions determined above. Elution curves for BC from the foam and liquid outlets were obtained manually by spectrophotometric analysis of each fraction, which were also analysed by reversed-phase HPLC.

Foam fraction. The elution curve for BC from the foam outlet shows three major peaks, as indicated by arrows in Fig. 4. The fractions corresponding to these three peaks were subjected to HPLC analysis. As shown in Fig. 5A, the most hydrophobic compounds with the longest retention time in HPLC analysis corresponding

TABLE I

OPTIMIZATION OF OPERATING CONDITIONS FOR FOAM COUNTER-CURRENT CHROMATOGRAPHY OF BACITRACIN

Sample size, 5 mg in 0.5 ml of distilled water; nitrogen gas pressure, 80 p.s.i.; revolution speed, 500 rpm; fractionation rate, 15 s per tube.

Parameter	*Conditions*	*Results*
Liquid flow-rate	<3.2 ml/min	Failure to elute foam
	>3.2 ml/min	Lower efficiency of separation (peaks 11 and 14)
Needle valve at liquid outlet	<0.5 turn open	Lower efficiency of separation (all peaks)
	0.5–0.8 turn open	Peak 7 elutes from foam outlet
	0.8–1.2 turn open	Peak 7 elutes from liquid outlet
	>1.2 turn open	No foam
Standing time after sample injection	<5 min	Lower efficiency of separation (peaks 11 and 14)
	>5 min	Intermittent foam elution

to peaks 14 and 15 were eluted in the first fraction with a small amount of less hydrophobic components corresponding to peaks 11 and 13. Each component showed substantial enrichment relative to that in the original sample solution. Peaks 14 and 15 were enriched 2.8 and 2.2 times, respectively. Peak 15 is hardly visible in the HPLC trace of the original sample owing to the low concentration, but the same peak

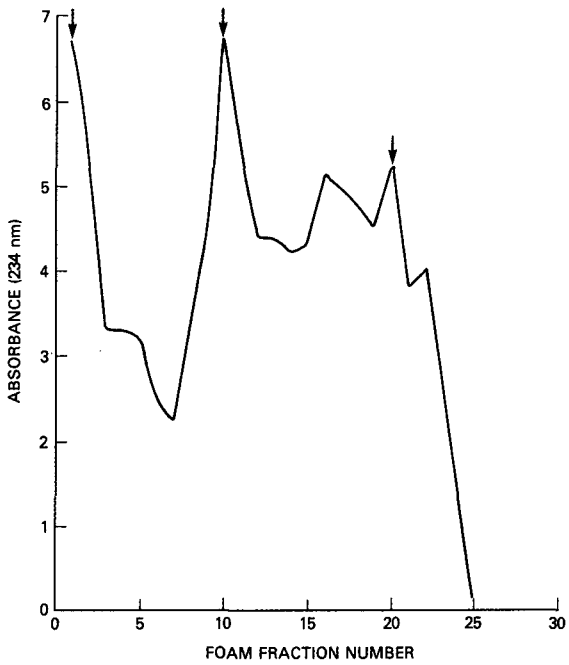

Fig. 4. Elution curve of bacitracin from foam outlet. Foam CCC conditions: liquid flow-rate, 3.2 ml/min; needle valve at liquid outlet, 0.8 turn open; standing time after sample injection, 5 min; nitrogen pressure, 80 p.s.i.; revolution speed, 500 rpm; sample size, 5 mg in 0.5 ml of distilled water; fractionation rate, 15 s per tube.

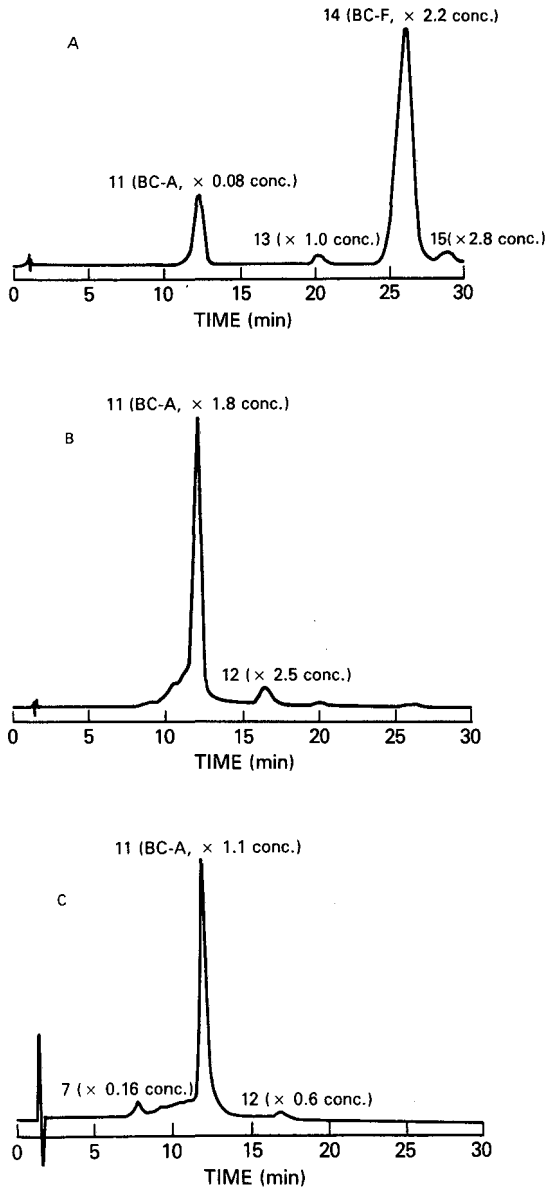

Fig. 5. High-performance liquid chromatograms of bacitracin in foam fractions. For HPLC conditions see Experimental. (A) First foam fraction; (B) tenth foam fractions; (C) twentieth foam fraction.

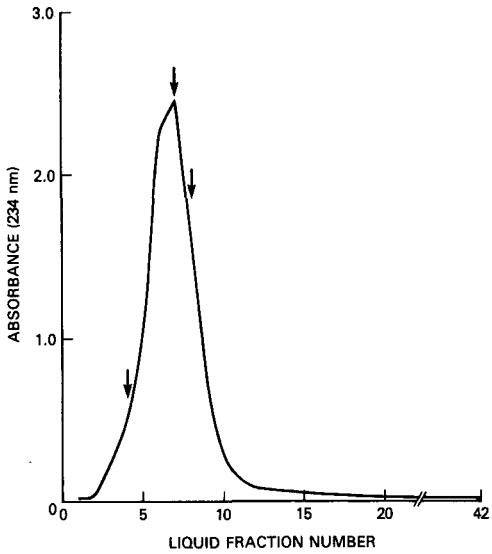

Fig. 6. Elution curve of bacitracin from liquid outlet. Foam CCC conditions are described in Fig. 4.

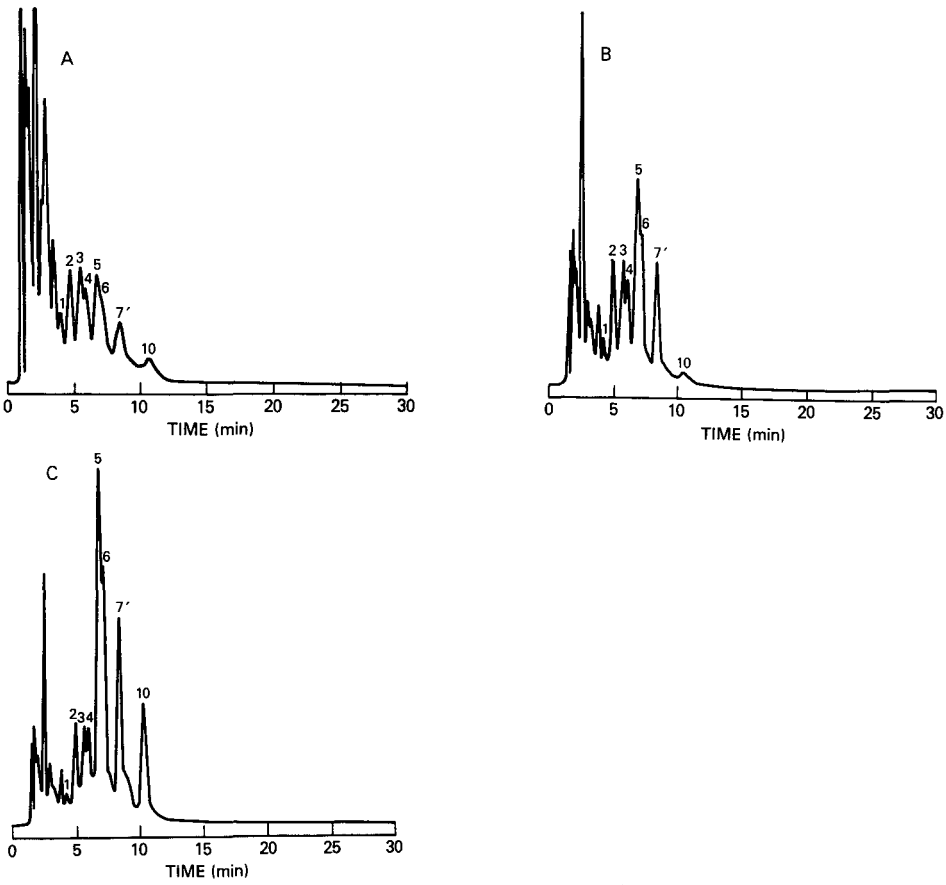

Fig. 7. High-performance liquid chromatograms of bacitracin in liquid fractions. For HPLC conditions, see Experimental. (A) Fourth liquid fraction; (B) sixth liquid fraction; (C) ninth liquid fraction.

is clearly observed in this chromatogram. In the tenth fraction (Fig. 5B), BC-A (peak 11) was almost isolated from other components while enriched 1.8 times. In the twentieth fraction (Fig. 5C), peak 7 appeared on the chromatogram while peak 11 still remained as the major peak. Components with higher polarity, including peaks 1–6, were undetected in the foam fraction. These results clearly indicate that the BC components are separated in the order of hydrophobicity of the molecules and enriched in the foam fractions.

Liquid fraction. As shown in Fig. 6, the elution curve from the liquid fractions is different from that obtained from the foam fractions. Although only a single peak is observed, HPLC analysis of fractions 4, 6 and 9, as indicated by arrows, yielded interesting results.

The HPLC trace of the fourth liquid fraction shows, in addition to peaks 1–10, a group of more hydrophilic components which are hardly visible in the chromatogram of the original sample owing to the low concentration (Fig. 7A). In the sixth fraction, these hydrophilic compounds tend to disappear and peaks 2–10 dominate (Fig. 7B). In the ninth fraction, peaks 5 and 7′ still remain as the main peaks whereas the intensity of peak 10 is considerably enhanced compared with that in the sixth fraction (Fig. 7C). Later fractions showed no additional peaks. These results clearly indicate that BC components elute in decreasing order of their polarity in the liquid fractions. As described above, the liquid fractions obtained from our prototype apparatus gave inefficient fractionation of hydrophilic components. Nevertheless, these results clearly demonstrate the potential capability of the present foam CCC method.

CONCLUSION

Using foam CCC, we were able to separate the components of BC in the order of their hydrophobicity without any surfactants or other additives. The method provides a number of advantages over other chromatographic methods: (1) enrichment and concentration of foam-active components; (2) minimum decomposition or deactivation of biological samples; (3) no adsorptive sample loss into the solid support matrix; (4) no risk of contamination; (5) easy recovery of the sample after fractionation; and (6) low cost in operation. Therefore, we believe that the method has great potential in the isolation and enrichment of various natural and synthetic products in research laboratories and industrial plants. The method also permits continuous operation by continuous sample feeding. These results will be reported elsewhere in the near future.

REFERENCES

1 Y. Ito, *J. Liq. Chromatogr.*, 8 (1985) 2131.
2 M. Bhatnagar and Y. Ito, *J. Liq. Chromatogr.*, 11 (1988) 21.
3 Y. Ito, *J. Chromatogr.*, 403 (1987) 77.
4 H. Oka, K. Harada, M. Suzuki, H. Nakazawa and Y. Ito, *Anal. Chem.*, 61 (1989) 1998.

Journal of Chromatography, 482 (1989) 207–214
Elsevier Science Publishers B.V., Amsterdam — Printed in The Netherlands

CHROM. 21 826

DETERMINATION OF THE ABSOLUTE NUMBER OF MOLES OF AN ANALYTE IN A FLOW-THROUGH SYSTEM FROM PEAK-AREA MEASUREMENTS

G. TORSI*, G. CHIAVARI, C. LAGHI and A. M. ASMUNDSDOTTIR[a]
Dipartimento di Chimica G. Ciamician, Università di Bologna, Via Selmi 2, 40126 Bologna (Italy)
and
F. FAGIOLI and R. VECCHIETTI
Dipartimento di Chimica, Università di Ferrara, Via Borsari 46, 44100 Ferrara (Italy)
(First received November 22nd, 1988; revised manuscript received July 26th, 1989)

SUMMARY

A simple model is proposed for the determination of the absolute amount of an analyte when non-destructive detection systems are used in high-performance liquid chromatography and flow-injection analysis. The method requires only a knowledge of the cell thickness, molar absorptivity of the analyte and flow-rate if absorption is measured. The data obtained with a commercial apparatus are consistent with the model both for a compound with well known spectroscopic characteristics (K_2CrO_4) and for common organic substances such as toluene and *p*-nitroaniline. A systematic error of *ca.* 18% is present with the detector used for all analytes. The possible origin of this error is discussed.

INTRODUCTION

Quantitative results in high-performance liquid chromatography (HPLC) and flow-injection analysis (FIA) are generally based on peak-height or peak-area measurements using calibration graphs or other calibration methods. However, no information about the absolute amount of the analyte present in the sample is obtained, as both the analyte and the standard undergo the same physical and chemical processes with possible losses through various mechanisms. In this paper, we present a method for determining the absolute number of moles of an analyte from peak-area measurements in flow-through systems such as HPLC and FIA when the analytical signal is obtained through a detector which measures a physical property of intensive nature such as light absorption, fluorescence, electrical conductivity, electrode potential or refractive index. An amperometric sensor can be included if the current passing through the elctrodes is so low that mass-transfer phenomena can

[a] On leave from the University of Iceland.

0021-9673/89/$03.50

practically be ignored. These detectors can be classified as non-destructive[1] and related equations for chromatographic analysis can be found in a recent publication[2].

In this paper, the theoretical treatment will be restricted to light absorption detectors because the derivation is similar to that given for atomic absorption spectrometry with electrothermal atomization[3,4,7–9] and because the experimental verification of the model is very easy. The extension of the equations derived here to other types of detectors is generally trivial.

In order to determine the absolute number of moles in a flow-through absorption system, one has to measure the flow-rate of the mobile phase, the cell thickness and the molar absorptivity of the analyte at the selected wavelength. The cell thickness is obtained from the manufacturer of the detector, the molar absorptivity from the litterature or by measuring it in the normal way and the flow-rate from the selected value in the HPLC system.

As in the final equation new parameters are introduced (ε, b and F), the accuracy and precision of the analysis will be lower. However, the often tedious and sometimes expensive calibration procedures are eliminated. In addition, data obtained under widely different experimental conditions can be compared. Of course, it is always possible to follow the usual calibration methods. In this instance, if one is sure that no analyte has been lost, the product εb can be obtained, from which either one can be calculated if the other is known.

The final equation derived and tested in this paper has already been obtained for chromatographic measurements[2,5]. However, it has always been associated with peaks of gaussian shape and has never been used for measuring the absolute amount of an analyte as proposed here. As we are interested in the analytical aspects of the problem, the form of the peak is immaterial because in the theoretical treatment no assumptions are made about the form of the peak. We are concerned only with peak overlapping because, in such an event, the measurement of the area is less precise.

The same considerations can be made about the influence of cell design on the form of the peak[6]. For this reason, the large body of literature dealing with chromatographic peak generation and cell design is not considered.

In fact, peak-area data have always been used in everyday measurements because it is considered to be the most dependable parameter in calibration procedures, independent of the peak shape. In this paper we show that, at least with the detector used, it is possible to make absolute measurements. The model was verified by using an RP C_{18} column with an ion of well known spectroscopic characteristics (CrO_4^{2-}) which shows no interaction with the stationary phase. For this reason, the peaks are skewed gaussian, similar to those obtained in FIA measurements. Two other substances were analysed to test the model, more like those encountered in normal HPLC measurements, *viz.*, toluene and *p*-nitroaniline (PNA), chosen for their availability in sufficiently pure form and, with PNA, for the presence in its spectrum of peaks at different wavelengths.

THEORETICAL

The starting equation for absorption measurements is the Lambert–Beer law:

$$A = \varepsilon bc = 10^3 \varepsilon N \tag{1}$$

where A is the absorbance, c (mol/l) the concentration, b (cm) the cell thickness, N the number of moles/cm^2 in the light path and ε the molar absorptivity. A and ε are referred to a fixed wavelength. The multiplying factor 10^3 is used to maintain the numerical value of ε. The assumptions made in deriving the Lambert–Beer law are also valid for eqn. 1. However, it is not an essential requirement that the analyte molecules are uniformly distributed along the cell light path; it is sufficient that they are uniformly distributed in planes perpendicular to the optical beam[3]. In this event, only the final part of eqn. 1 is meaningful.

As in a flow-through system N, and therefore A, are time dependent, eqn. 1 is rewritten as

$$A(t) = 10^3 \varepsilon N(t) \tag{2}$$

The function $N(t)$, as already mentioned, has been extensively studied for HPLC and FIA systems. It can be defined by a convolution integral[3,4] of the type

$$N(t) = 1/S_c \int_0^{t'} S(t')R(t - t')\, dt' \tag{3}$$

where S_c (cm^2) is the cross-section (assumed constant) of the cell, t is a dummy variable and $S(t)$ and $R(t)$ are the number of moles of analyte entering and leaving the cell per unit time, respectively. If we take the integral of both sides between the limits 0 and ∞, we obtain

$$\int_0^{\infty} N(t)\, dt = 1/S_c \int_0^{\infty} S(t)\, dt \int_0^{\infty} R(t)\, dt \tag{4}$$

or

$$\int_0^{} N(t)\, dt = N(0)\tau(r)/S_c \tag{4a}$$

where $N(0)$ and $\tau(r)$ are the total number of moles passed through the cell and the equivalent time constant of the removal function, more directly perceivable as the average time spent by a mole of the analyte in the cell, respectively. If we now return to eqn. 2 and take the integral, we obtain

$$\int_0^{\infty} N(t)\, dt = \frac{1}{10^3 \varepsilon} \int_0^{\infty} A(t)\, dt = \frac{1}{10^3 \varepsilon} A(i) \tag{5}$$

where $A(i)$ (min) is the area of the peak of the analyte under study. Then, by combining eqns. 4a and 5, we obtain

$$A(i) = 10^3 \varepsilon N(0) \tau(r) / S_c \tag{6}$$

In this equation, all quantities, except $\tau(r)$ can easily be measured. In HPLC and FIA, $\tau(r)$ can be expressed as the ratio of the cell colume, V (cm^3), to the flow-rate, F (cm^3/min), which is assumed to be constant. Then we have

$$A(i) = 10^3 \varepsilon N(0) V / F S_c \tag{7}$$

By expressing V as the product of b and S_c, we arrive at the final equation:

$$A(i)\ F = 10^3 \varepsilon b N(0) \tag{8}$$

The experimental validation of eqn. 8 is very easy as all the terms can be obtained by direct measurements. Its limits lie in the non-linearity of the absorption measurements and in the deviation of the experimental conditions from those assumed in the model. The most important deviations are that the light beam is not composed of rays parallel to each other and homogeneously distributed in the planes perpendicular to the beam, that the analyte is not homogeneously distributed in planes perpendicular to the beam and that the flow-rate is not constant. The limits of the Lambert–Beer law are well known. As the bandwidth of the instrument used is large (see below), care must be taken to use concentrations low enough to obtain a linear response.

With the present trend toward miniaturization, the physical limitations on the beam and the parallelism of its rays inside the cell are certainly difficult to implement. The second deviation is equivalent to invoking a plug-flow regime. As the flow is assumed to be laminar under the experimental conditions in this work, distorsions due to different velocities in the planes perpendicular to the flow and the beam are unavoidable. No problems should be encountered in controlling the flow-rate with modern pumping systems.

The time constant of the detector electronics has not been considered in deriving eqn. 8, because peak-area measurements are independent of the detector response rate.

EXPERIMENTAL

All experiments were carried out with the same Varian 2510 liquid chromatograph, equipped with a Varian 2550 spectrophotometric detector, the monochromator of which has a bandwidth of 8 nm, a Rheodyne 7125 injector with 10-, 20- and 50-μl loops and a Perkin-Elmer LC-100 integrator. An Erbasil C_{18} (10 μm) analytical column (250 × 4.6 mm I.D.) was used. Absorption measurements were carried out with a Perkin-Elmer Model 551 instrument with a 2-nm bandwidth. K_2CrO_4 was dissolved in the aqueous mobile phase containing 0.05 M Na_2HPO_4. Toluene and PNA were also dissolved in the mobile phase, which was water–methanol (25:75, v/v).

The chemicals, purchased from Carlo Erba, were of analytical-reagent grade and were recrystallized from deionized or distilled water before use. Methanol (HPLC grade) was used as received. Doubly distilled water was used throughout. All measurements were carried out at room temperature (20–25°C).

Calibration of the system

Before starting the designed measurements, a series of calibrations were made in order to reduce the systematic errors as much as possible. Such calibrations are essential for absolute measurements. In our case, a cautiosus approach was necessary because the chromatographic instruments are not designed for such calibrations.

The calibration of the Perkin-Elmer spectrometer was performed by measuring the molar absorptivity of K_2CrO_4, which is well known[10,11]. Calibration graphs for all the analytes were obtained in the usual way. The spectrometric system of the chromatograph was checked by circulating the analyte solutions for a sufficiently long time until no change in absorbance was detected. As absorbance is not dependent on flow-rate, and as the cell thickness was the same (1.0 cm), no difference should have been observed between the two sets of measurements. However, it was found that the slopes of the calibration graphs obtained with the chromatographic detector were low up to 3%. As the standard deviation of the slopes of the calibration graphs was *ca.* 0.5%, it was concluded that the difference was significant. The observed systematic error presumably arises from different bandwidths of the instruments and/or from the cell thickness being different from the given value. As we measure the product εb, the two effects can be separated by measuring the actual value of b. This measurement is not necessary, however, because by using the experimental value of εb the relevant systematic error is corrected. The flow-rate was obtained by measuring the time needed to deliver a known volume of eluent at the exit of the cell.

The output of the detector and its linearity were controlled with a high-impedence voltmeter by checking the correspondence between the digital output used in the calibration graphs and the output voltage. The integrator was controlled by feeding a known voltage for a known time.

The injection loops of 10, 20 and 50 μl were calibrated as follows: about 100-fold concentrated solutions of the analyte used for normal chromatographic separation were injected using different loops. A 10-ml volume of mobile phase was then collected to ensure that all the sample was eluted. The concentrations were measured on the Perkin-Elmer instrument by making use of the calibration graphs obtained previously. The actual volumes found were 12, 22 and 51 μl, respectively. The systematic errors found are probably due to an imperfect fit of the loops in the injector.

RESULTS AND DISCUSSION

Figs. 1 and 2 show the influence of injection volume and flow-rate obtained with K_2CrO_4 solutions. The analyte concentration, flow-rate and volume injected varied between $0.8 \cdot 10^{-4}$ and $4 \cdot 10^{-4}$ M, 0.5 and 5 cm^3/min and 10 and 50 μl, respectively.

Only part of the data are shown here because they are all clustered together. One can see that the ratio $A(i)F/10^3\varepsilon bN(0)$ is higher than the theoretically expected value. It is not significantly influenced by the injection volume and increases slightly with increasing flow-rate. The dependence of peak area on the number of moles of K_2CrO_4 at constant flow-rate is shown in Fig. 3. Similar data obtained at constant flow-rate and with a 10-μl loop for toluene and PNA are shown in Fig. 4.

In Figs. 3 and 4, the experimental data lie on a straight line as expected, as the peak area changes linearly with the amount of analyte. Table I shows the numerical values of the slope and intercept of these lines. They are fairly good except for toluene.

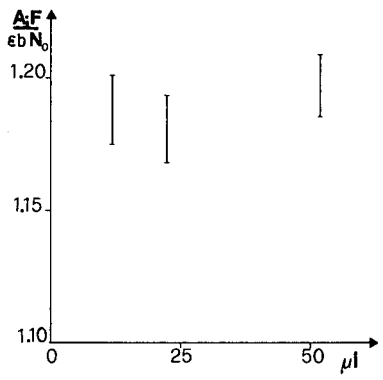

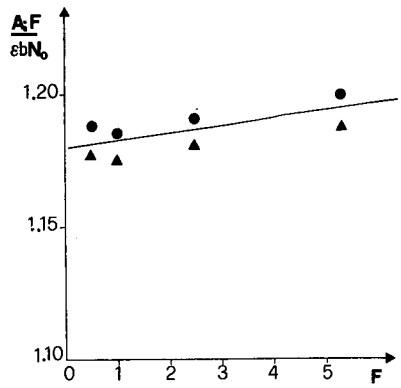

Fig. 1. Influence of volume injected at constant flow-rate. Analyte, K_2CrO_4; flow-rate, 1.01 cm^3/min; concentration $2 \cdot 10^{-4}$ *M*. The bars represent 95% confidence intervals.

Fig. 2. Influence of flow-rate. Analyte, K_2CrO_4; nominal volume of loop, (●) 10 and (▲) 50; concentration, $2 \cdot 10^{-4}$ *M*. The straight line is the regression line of the experimental points.

The reason for the latter discrepancy is the low energy available at such low wavelengths and the sharpness of the peak with associated problems with peak-area measurements due to baseline instability and wavelength irreproducibility.

As already seen, the slope shows a systematic error of about 18% independent of analyte and wavelength. The origin of this error is unknown and the answer must wait

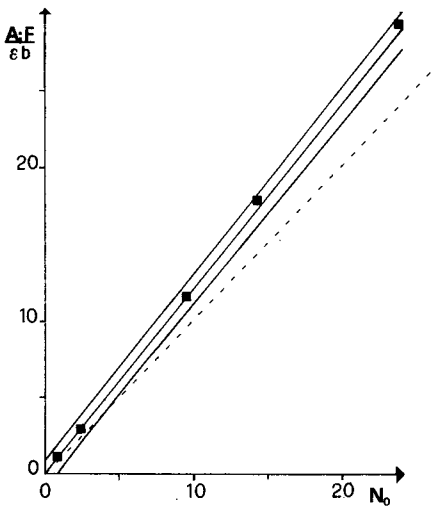

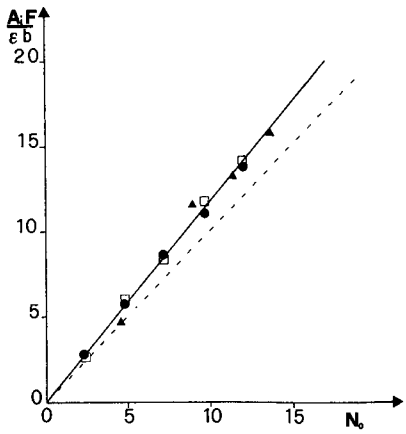

Fig. 3. Calibration graph at constant flow-rate (1.01 cm^3/min) for K_2CrO_4 for different loops and concentrations. λ_{max} = 373 nm. The dashed line is the ideal line. The outer lines represent the 95% confidence limits.

Fig. 4. Calibration graph for toluene [(▲) λ_{max} = 206 nm] and PNA [λ_{max} = (●) 376 and (□) 228 nm]. Flow-rate, 1.01 cm^3/min; volume of loop, 12 μl.

TABLE I

PARAMETERS OF THE STRAIGHT LINES SHOWN IN FIGS. 3 AND 4

Substance	λ_{max} *(nm)*	*r*	*Slope*	*Intercept*
PNA	376	0.9999	1.16 ± 0.02	$+0.06 \pm 0.19$
PNA	228	0.9983	1.20 ± 0.04	-0.10 ± 0.32
Toluene	206	0.9874	1.19 ± 0.13	$+0.04 \pm 1.27$
K_2CrO_4	373	0.9992	1.19 ± 0.10	$+0.10 \pm 0.23$

further investigation. The presence of the same error for different analytes and different wavelengths indicates a physical effect. The first part of the chromatographic system that must be checked is the microcell. In a microcell, as already noted, the beam rays are not parallel, as required by the model. We have seen, however, that when the cell is filled with a homogeneous solution the error, if present, is very small. Therefore, the systematic error found here should be linked to the passage of analyze through the cell at variable concentration. Our suggestion is a combined effect of non-parallelism of the beam and non-homogeneity of the analyte in the planes perpendicular to the beam, which we know is present as a consequence of the laminar flow. This hypothesis was confirmed by direct measurements of deviations of light beams in chromatographic cells when concentration gradients are present[12]. A model that takes into account such deviations is, of course, much more complex and outside the scope of this paper.

CONCLUSION

The data presented, seem to follow the model proposed fairly closely. The systematic error of 18% presumably originates from instrumental deviations between the requirements of the model and actual experimental conditions. In spite of this high systematic error, which is independent of wavelength and analyte, the utility of the method from an analytical point of view is good. We are now extending the work to other systems to investigate the origin of the above error. Experiments will also be carried out on real mixtures to establish the advantages of absolute calibrations.

ACKNOWLEDGEMENTS

Financial support from CNR (Contributo 8800088.03 and 0905/6-861725) is gratefully acknowledged. One of us, A.M.A., expresses her thanks to the Ministero degli Esteri, for a scholarship in Italy. We also thank Dr. Mustafa Ozcimder (University of Samsun, Turkey) for useful discussions.

REFERENCES

1 S. Dal Nogare and R. S. Juvet, *Gas–Liquid Chromatography*, Wiley-Interscience, New York, 1962, p. 188.
2 J. P. Novak, *Quantitative Analysis by Gas Chromatography*, Marcel Dekker, New York, 2nd ed., 1988, Ch. 3.
3 S. L. Paveri-Fontana, G. Tessari and G. Torsi, *Anal. Chem.*, 46 (1974) 1032.
4 M. G. T. van der Broek and L. de Galan, *Anal. Chem.*, 49 (1977) 2176.

5 L. M. MacDowell, W. E. Barber and P. W. Carr, *Anal. Chem.*, 53 (1981) 1373.
6 D. C. Stone and J. F. Tyson, *Anal. Chim. Acta*, 179 (1986) 427.
7 B. V. L'vov, *Spectrochim. Acta*, Part B, 33 (1978) 153.
8 D. C. Baxter and W. Frech, *Spectrochim. Acta*, Part B, 42 (1978) 1005.
9 R. Vecchietti, F. Fagioli, C. Locatelli and G. Torsi, *Talanta*, 36 (1989) 743.
10 R. W. Burke, E. R. Deardogg and O. Menis, *J. Res. Natl. Bur. Stand.*, (1972) 76A469.
11 E. A. Johnson, *Photoelectron Spectrosc. Group Bull.*, 17 (1967) 505.
12 K. Peck and M. D. Morris, *J. Chromatogr.*, 448 (1988) 193.

Journal of Chromatography, 482 (1989) 215–226
Elsevier Science Publishers B.V., Amsterdam — Printed in The Netherlands

CHROM. 21 873

SOME NEW OBSERVATIONS ON THE EQUIVALENT CARBON NUMBERS OF TRIGLYCERIDES AND RELATIONSHIP BETWEEN CHANGES IN EQUIVALENT CARBON NUMBER AND MOLECULAR STRUCTURE

OLDRICH PODLAHA* and BENGT TÖREGÅRD
Karlshamns AB, S-374 82 Karlshamn (Sweden)
(First received January 31st, 1989; revised manuscript received August 8th, 1989)

SUMMARY

A further development, giving more reproducible results, of the procedure for calculating equivalent carbon numbers (ECNs) is presented. The reproducibility is listed. ECNs define the order of elution of triglycerides and give information as to where the peak of a defined triglyceride will appear in the chromatogram. The ECN values of triglycerides are, to a reasonable degree, equal to the sum of their partial ECN values (fatty acid ECN values). They thus reflect the contribution of each fatty acid to the chromatographic properties of the total triglyceride molecule. A list of basic data is presented and the changes in ECN values are described, together with the corresponding changes in the triglyceride molecule.

INTRODUCTION

As early as 1950 Martin[1] reported the relationship between the free energy of the separation process in chromatography and the structure of the chromatographed molecule. The relationship is frequently discussed in later papers[2–5].

In 1954 Ray[6] described the linear relationship between the logarithms of retention times (t_R) and carbon numbers (CN) of the members of a homologous series. This relationship can be used to identify the components/peaks in a chromatogram; however, it is necessary to compensate for the day-to-day variations in the chromatographic process and to achieve this normally two methods are used.

According to the first method, the retention times are expressed as relative retention times (RRT), with reference to one of the peaks in the chromatogram (in lipid analysis usually the peak of triolein). All the peaks are thus characterized in relation to one defined point of the chromatogram.

Goiffon *et al.*[7,8] presented a system based on RRTs, used in high-performance liquid chromatography (HPLC). The system shows close correlation between the molecular structures of defined triglycerides and their retention times.

Perrin and Naudet[2] presented a table of RRTs for a series of triglycerides, and Stolyhwo *et al.*[9] discussed the features of the system. Sempore and Bezard[3] found the parallelism between of RRTs and ECNs, and presented a linear regression plot of RRTs *versus* ECNs.

0021-9673/89/$03.50

In the second method two standards (in lipid analysis saturated triglycerides are preferred) are added to the sample. The peaks in the chromatogram are then related to the line, represented by the two points. The system of Kovats indexes, developed for the gas chromatography (GC) of structurally similar substances such as pharmaceutical products, uses the two-point principle[4,10].

In the area of lipid analysis the same principle has been used for identification of fatty acids in GC. In this way it is possible to characterize all the peaks in the chromatogram at once, using only two standard substances. As standard substances saturated fatty acids were used, and the values obtained were called "equivalent chain lengths" (ECL)[11,12].

It was shown that the same principal relationships were valid even in reversed-phase (RP) HPLC. However, only a few papers dealing with retention indices in RP-HPLC have been published[5,13–17].

In this laboratory, we have developed a system similar to ECLs for the identification of triglyceride components/peaks in RP-HPLC of glyceride oils and fats[18–21]. In order to emphasize the similarity the units were called "equivalent carbon numbers" (ECNs), and the base in this case was the homologous series of saturated triglycerides.

This paper develops further the ECN system, based on three standard points, to obtain a more exact position of the reference line. This is a continuation of earlier work, in which mainly graphical results were presented[19]. The aim is to present a list of ECN values of some triglyceride model substances, and show some of the relationships between the variations in the ECN values and the structural changes in triglyceride molecules by the use of figures and tables.

The term equivalent carbon number (ECN) in this and in all previous publications from this laboratory is definitely not identical with the term "partition number" (PN), though it is used in that way by many workers. This is evident because the ECN values are not integers, contrary to PNs, just as ECNs are relative (equivalent) numbers[22].

The notion of PNs, sometimes also called ECNs, was useful in the early days of the technique, when resolving power was relatively limited[3,22–24].

EXPERIMENTAL

Apparatus

An Optilab 593l liquid chromatograph, Tecator, a refractive index detector equipped with a 10-mm measuring cell and a Rheodyne injection block with a 10-μl loop were used. Two 25 cm Hibar RP-18 columns (Merck, ser.nos. 410 728 and 204 551, 5 μm particle diameter, 4 mm I.D.) were coupled in series and thermostated to 30°C. An HP reporting integrator 3390A was also used.

Materials

Model triglycerides, purity 99%, were purchased from Larodan (Malmö, Sweden).

Propionitrile for synthesis (Merck) was distilled before use and before each reuse from Siccapent (Merck). Toluene p.a. (Merck) was used without further purification).

Fatty acid symbols

La = Lauric acid (C12:0); M = myristic acid (C14:0); P = palmitic acid (C16:0); Po = palmitoleic acid (C16:1,9c); Pe = petroselinic acid (C16:1,6c); St = stearic acid (C18:0); O = oleic acid (C18:1,9c); El = elaidic acid (C18:1,9t); L = linoleic acid (C18:2,9c,12c); Ln = linolenic acid (C18:3,9c,12c,15c); Ad = arachidic acid (C20:0); Ao = *cis*-11-eicosenoic acid (C20:1,11c); Be = behenic acid (C22:0); E = erucic acid (C22:1,13c).

Procedure

Volumes of 10 μl of working solution (*ca.* 0.6% in propionitrile–toluene, 3:2, v/v) were injected into the column. The mobile phase was propionitrile at a flow-rate of *ca.* 0.5 ml/min.

Calculation of ECN values

An AB800 microcomputer (Luxor, Sweden) was used, with our own BASIC program, which can be obtained on request.

RESULTS AND DISCUSSION

Definitions and calculations of ECNs

According to the principal definition of ECNs[19], the retention times of the triglycerides studied are related to the retention times of saturated triglycerides. This gives a basis for the uniform consideration of the data.

The basic relation between the logarithms of the corrected retention times and the ECNs of the saturated triglycerides (by definition equal to the carbon number) is linear, as shown in Fig. 1. Theoretically, for construction of the line only two points

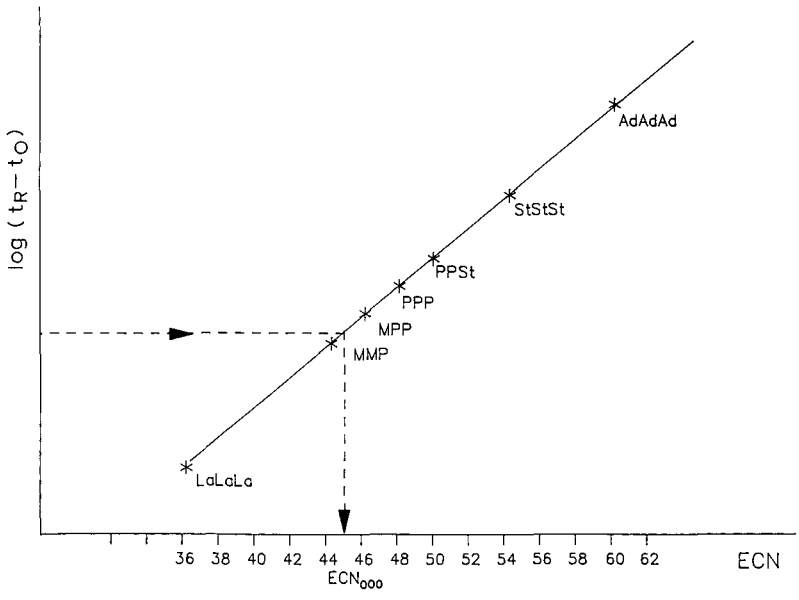

Fig. 1. Plot of log $(t_R - t_0)$ *versus* the carbon number of saturated triglycerides and the interpretation of ECN_{OOO}.

are necessary, but it is not possible to determine exactly the value of t_0 from the chromatogram and therefore a third point is needed before the exact position of the line can be determined. The procedure using three standards gives very reproducible ECN values and can be used for the determination of the void volume of the column system, t_0.

In this laboratory a spiking solution is used, containing trilaurin and tristearin as outer points for the definition of the standard line and trimyristin as the third point defining t_0 and thus the position of the line.

In principle, the above-mentioned considerations can be expressed by three equations:

$$\log(t_{R,LaLaLa} - t_0) = k \cdot CN + b$$

$$\log(t_{R,MMM} - t_0) = k \cdot CN + b$$

$$\log(t_{R,StStSt} - t_0) = k \cdot CN + b$$

where t_0 (dead time), k and b are the three unknowns. The computer program calculates t_0 and ECN values.

A similar standard solution containing a further component, triolein (OOO), is used to test colums and to characterize their polarity, which is expressed as ECN of triolein. Only pairs of column giving in combination $ECN_{OOO} = 45.16 \pm 0.02$ are used in this work. Table I lists polarity values for eighteen tested Merck Hibar RP-18 columns.

Relation of ECN values to structural changes in the triglyceride molecule

ECN values of some triglycerides, their reproducibilities and other molecular characteristics are presented in Table II. The values were determined experimentally by spiking the standard or sample solutions with LaLaLa, MMM and StStSt.

The ECN values of triglycerides can be considered as sums of "partial" fatty acid ECN values and can thus be calculated by addition with reasonable accuracy[19]. The partial ECN values for fatty acids are presented in Table III. These can also be used as preliminary information concerning unknown peaks.

TABLE I

POLARITIES OF SOME HIBAR RP-18 COLUMNS EXPRESSED AS ECN_{OOO}

Serial No.	*ECN_{OOO}*	*Serial No.*	*ECN_{OOO}*
110 445	45.15	410 728	45.13
204 551	45.16	410 800	45.10
208 749	45.05	415 207	44.82
303 452	45.11	415 208	45.32
308 514	45.12	415 212	45.32
308 532	45.09	415 242	45.21
308 572	45.12	415 277	45.21
314 884	45.19	420 509	45.24
314 894	45.11	423 251	45.26

TABLE II

ECN VALUES OF DIFFERENT TRIGLYCERIDES AND THEIR REPRODUCIBILITY

Triglyceride type	*ECN*			*CN*	*Double bonds*	
	Value	*S.D.*	*Number of determinations*		*Number*	*Composed of*
LaLaLa[a]	36.00			36	0	
MMP[a]	44.00			44	0	
MPP[a]	46.00			46	0	
PPP[a]	48.00			48	0	
PPSt[a]	50.00			50	0	
PStSt[a]	52.00			52	0	
StStSt[a]	54.00			54	0	
AdAdAd[a]	60.00			60	0	
MPO[b]	45.17	0.015	10	48	1	0 + 0 + 1c
PPO[a]	46.97	0.044	10	50	1	0 + 0 + 1c
PPEl[a]	47.42	0.003	9	50	1	0 + 0 + 1t
PStO[a]	48.99	0.008	7	52	1	0 + 0 + 1c
StStO[a]	50.97	0.006	6	54	1	0 + 0 + 1c
StStEl[a]	51.36	0.003	9	54	1	0 + 0 + 1t
StOAd[a]	52.80	0.009	11	56	1	0 + 0 + 1c
StOBe[a]	54.72	0.006	9	58	1	0 + 0 + 1c
OAdAd[b]	54.68		1	58	1	0 + 0 + 1c
MPL[b]	42.79	0.017	7	48	2	0 + 0 + 2c
MOO[a]	44.10	0.005	9	50	2	0 + 1c+ 1c
PPL[b]	44.54	0.054	10	50	2	0 + 0 + 2c
POO[a]	46.05	0.008	7	52	2	0 + 1c+ 1c
PStL[b]	46.46	0.039	6	52	2	0 + 0 + 2c
StOO[a]	47.99	0.005	6	54	2	0 + 1c+ 1c
StOEl[a]	48.37	0.005	9	54	2	0 + 1c+ 1t
StStL[a]	48.45	0.013	7	54	2	0 + 0 + 2c
StElEl[a]	48.78	0.004	9	54	2	0 + 1t+ 1t
OOAd[a]	49.92	0.007	16	56	2	0 + 1c+ 1c
OOBe[a]	51.79	0.018	11	58	2	0 + 1c+ 1c
MMLn[a]	38.56	0.003	9	46	3	0 + 0 + 3c
PoPoPo[a]	39.50	0.006	9	48	3	1c+ 1c+ 1c
POL[b]	43.65	0.021	8	52	3	0 + 1c+ 2c
OOO[a]	45.17	0.032	7	54	3	1c+ 1c+ 1c
StOL[b]	45.57	0.063	8	54	3	0 + 1c+ 2c
PePePe[a]	46.33	0.004	9	54	3	1c+ 1c+ 1c
ElElEl[a]	46.27	0.007	11	54	3	1t+ 1t+ 1t
StStLn[a]	46.42	0.000	9	54	3	0 + 0 + 3c
OLAd[a]	47.49	0.008	11	56	3	0 + 1c+ 2c
AoAoAo[a]	50.51	0.010	9	60	3	1c+ 1c+ 1c
EEE[a]	55.93	0.013	7	66	3	1c+ 1c+ 1c
PLL[b]	41.09	0.022	7	52	4	0 + 2c+ 2c
OOL[b]	42.79	0.017	7	54	4	1c+ 1c+ 2c
LLL[a]	38.18	0.005	7	54	6	2c+ 2c+ 2c
LnLnLn[a]	32.34	0.044	23	54	9	3c+ 3c+ 3c

[a] ECN values using synthetic model triglycerides.
[b] ECN values by analysis of fractions.

TABLE III

PARTIAL ECN VALUES OF FATTY ACIDS

Partial ECN values of saturated fatty acids are equal their carbon numbers.

Fatty acid	*Partial ECN value*
Po	13.12
O	15.05
El	15.43
L	12.73
Ln	10.81
Ao	16.83
E	18.64

ECNs and CNs of the triglycerides, when plotted, give the diagram presented in Fig. 2. The family of almost parallel lines indicates that each change in the triglyceride molecule causes a particular change in ECN, as it will be shown in the following text. The diagram can thus give the first indication about the possible composition of an unknown fraction/peak, displaying the tentative carbon numbers and numbers of double bonds (NDB) and their composition.

The lines on this diagram can also be expressed as regression lines. The calculated regression parameters are listed in Table IV. The lines in the table are specified by the degree of unsaturation and the combination of double bonds in the molecule. The

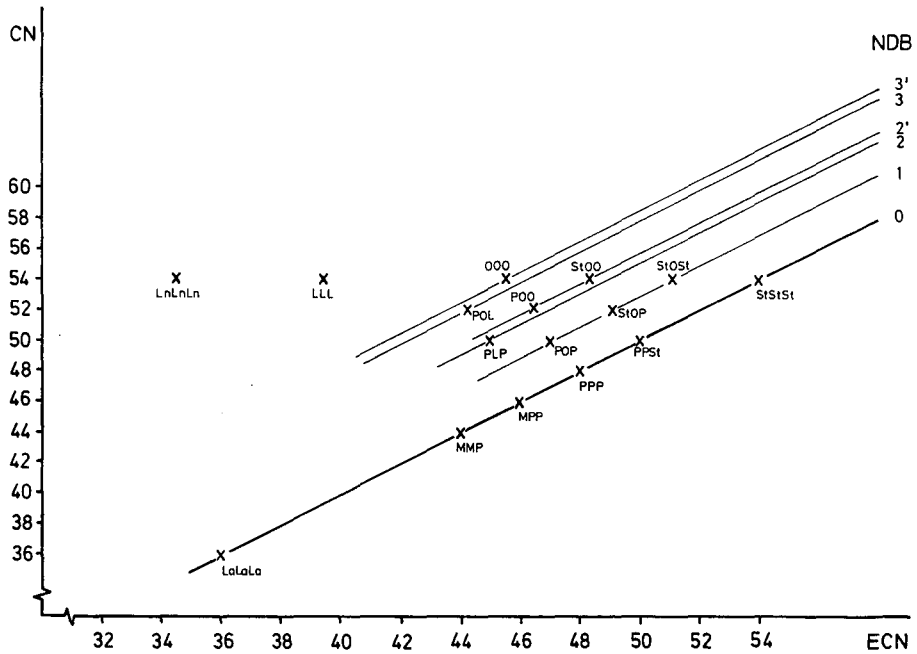

Fig. 2. Graphical representation of the relationship of ECN values to carbon numbers (CN). Curve: 0 = saturated triglycerides; 1 = one monounsaturated fatty acid; 2 = two unsaturated fatty acids; 2′ = one diunsaturated fatty acid; 3 = three monounsaturated fatty acids; 3′ = one monounsaturated and one diunsaturated fatty acid. Two 25 cm Hibar RP-18 columns, 4 mm I.D.; mobile phase: acetone–acetonitrile (64:36, v/v).

TABLE IV

REGRESSION PARAMETERS FOR THE LINES IN FIG. 2

Line combination of double bonds	*Slope*	*Intercept*	*n*	*Correlation*
0 + 0 + 0	1.00000	0.00000	7	1.00000
0 + 0 + 1	1.03539	1.30878	7	0.99984
0 + 1 + 1	1.03890	4.16420	5	0.99997
0 + 0 + 2	1.02822	4.21171	3	0.99997
1 + 1 + 1	1.03093	7.43300	2	–
0 + 1 + 2	1.04167	6.53125	3	1.00000
0 + 0 + 3	1.01911	6.70318	2	–

parameters are calculated using only triglycerides containing saturated and unsaturated fatty acids with methylene-interrupted double bonds in the *cis*-configuration starting from the 9-position and upwards, *i.e.* the natural vegetable oil fatty acids. It can be seen that the slope parameters of the lines are virtually equal and the lines are thus parallel, with the slight exception of the line for saturated triglycerides. The other parameter, the intercept, increases as expected with the number of double bonds. In addition, significant differences in this parameter are observed even for triglycerides with different double-bond combinations in the molecule.

According to the definition, the ECN values of saturated triglycerides are equal to their carbon numbers. Their ECN values thus increase by two units with a change of two in carbon number. The differences in ECNs with a change of two carbon atoms in unsaturated triglycerides are somewhat lower than two, and statistically significant. From Table V it can be seen that the mean difference is -1.94 and that the mean value has a total S.D. of 0.04. In this table the differences are presented in groups according to the degree and combination of unsaturation, and show no deviation between the groups.

These results confirm the observation, based on the regression line analysis, that the lines for the unsaturated triglycerides are reasonable parallel to each other, but not to that for the saturated triglycerides, which has a slightly lower slope parameter than the unsaturated ones.

The changes in ECN through the incorporation of one or more double bonds in a saturated triglyceride molecule are presented in Table VI. When the first double bond is introduced into the saturated triglycerides the differences between the ECN values rise with increasing carbon number. This is explained by the lower slope of the saturated triglyceride line in comparison with the line for unsaturated triglycerides (Table VI, column 2). Those figures are therefore not used in any calculation.

The real lowering of ECN by introduction of one double bond can be estimated from the introduction of a second and further double bonds in an already unsaturated triglyceride, and this value is *ca.* -2.89 ECN, with an S.D. of 0.08 ECN (Table VI).

The examples in the Table VII, however, show that the increment of one double bond, through an exchange of one monounsaturated fatty acid for a diunsaturated one, produces an ECN change that is lower than that in the case discussed above, *i.e.* -2.47 ECN, with an S.D. of 0.07 ECN. Only one measurement can be presented for

TABLE V

DIFFERENCE IN ECN AFTER CN CHANGE OF 2

Triglycerides	*Change in ECN*	*Triglycerides*	*Change in ECN*		*Triglycerides*	*Change in ECN*		
			0+1+1	*0+0+2*		*1+1+1*	*0+1+2*	*0+0+3*
MPO to PPO	−1.96	MOO to POO	−2.00		(PoPoPo to OOO)/3	−1.94		
PPO to PStO	−1.97	POO to StOO	−1.94		POL to StOL		−1.92	
PStO to StStO	−1.94	StOO to OOAd	−1.93		StOL to OLAd		−1.97	
StStO to StOAd	−1.94	MPL to PPL		−1.95	(MMLn to StStLn)/4			−1.96
StOAd to StOBe	−1.86	PPL to PStL		−1.92				
StOAd to StOBe	−1.86	PStL to StStL		−1.97				
Mean (total)	−1.935							
S.D. (total)	0.037							

TABLE VI

DIFFERENCE IN ECN WITH INCREMENT OF ONE DOUBLE BOND BY ONE MONOUNSATURATED FATTY ACID (CN CONSTANT)

Triglycerides	*Change in ECN*	*Triglycerides*	*Change in ECN*	*Triglycerides*	*Change in ECN*	*Triglycerides*	*Change in ECN*
MPO to MPSt	−2.99	POO to PStO	−2.94	OOO to StOO	−2.82	POL to PStL	−2.81
PPO to PPSt	−3.03	StOO to StStO	−2.98			StOL to StStL	−2.88
PStO to PStSt	−3.01	OOAd to StOAd	−2.88			OOL to StOL	−2.78
StStO to StStSt	−3.03	StOEl to StStEl	−2.99				
StOAd to StStAd	−3.20						
StOB to StStBe	−3.28						
OAdAd to StStBe	−3.32						
Mean total ($n=8$)		2.89					
S.D.		0.079					

TABLE VII

DIFFERENCES IN ECN WITH CHANGES BY ONE DOUBLE BOND THROUGH THE CHANGE FROM LOWER TO HIGHER UNSATURATED FATTY ACID (CN CONSTANT)

Triglycerides	*Change in ECN*	*Triglycerides*	*Change in ECN*
MPL to MPO	−2.42	StStLn to StStL	−2.02
PPL to PPO	−2.43		
PStL to PStO	−2.53		
StStL to StStO	−2.52		
PLL to POL	−2.56		
OOL to OOO	−2.38		
OLAd to OOAd	−2.43		
Mean	−2.47		−2.02
S.D.	0.068		

the exchange of one diunsaturated fatty acid for a triunsaturated one, which gave a still lower difference, −2.02 ECN. These observations can be related to the effect of the positioning of the double bond in the fatty acid chain, shown in the Table VIII.

When the double bond moves along the fatty acid chain in a triglyceride, the ECN value changes. This is shown in Table VIII by three examples, which explain why tripetroselinin (3 × C18:1,6c), triundecanoin (3 × C20:1,11c) and trierucin (3 × C22:1,13c) do not fit the line for triunsaturated triglycerides containing three isolated double bonds (1 + 1 + 1), as defined by tripalmitolein (3 × C16:1,9c) and triolein (3 × C18:1,9c). PoPoPo and OOO, like most naturally occurring fatty acids, have their first double bond just in the 9 position.

It was not possible to find fatty acids C20:1,9c and C22:1,9c, or triglycerides based on them, to measure the ECN values experimentally. Instead the values were calculated from the regression line. The values are therefore, to some degree, uncertain. Tripetroselinin was measured experimentally as standard. Nevertheless, the results show that the displacement of one double bond in the vicinity of C-9 of a fatty acid chain in a triglyceride to a vicinal carbon atom produces a change in ECN of between 0.07 and 0.13 units.

No attempt was made to explain this effect, because of the lack of basic experimental data. However, the values presented can partially explain the observed low

TABLE VIII

DIFFERENCES IN ECN WITH CHANGES IN THE POSITION OF THE DOUBLE BOND ALONG THE FATTY ACID (FA) CHAIN

Triglycerides	*Difference*	*Difference per FA*	*Difference per FA and per carbon atom*
(PePePe to OOO)/3	+1.16	+0.39	+0.13
(AoAoAo to 3 × C20:1,Δ9)/3	−0.47	−0.16	−0.08
(EEE to 3 × C22:1,Δ9)/3	−0.88	−0.29	−0.07

TABLE IX

DIFFERENCES IN ECN AFTER ADDITION OF BROMINE TO THE OLEIC ACID DOUBLE BOND IN MONOUNSATURATED TRIGLYCERIDES

Triglyceride	*ECN*		
	Not treated (both isomers)	*Bromine added*	
		Symmetrical	*Unsymmetrical*
PPO	46.97	44.70	44.91
PStO	48.99	46.71	46.93
StStO	50.97	48.65	48.88
StOO	47.99	44.02	44.10

differences in ECN when a monounsaturated fatty acid is exchanged for a diunsaturated, or a diunsaturated for a triunsaturated one.

Each new double bond in C_{18} fatty acids, for example, is created in a position three carbon atoms further away from the carboxyl group, which represents an ECN difference of 0.21–0.33 units. This does not explain the whole difference of 0.42 (2.89 minus 2.47), but possibly the greater part of it.

It was shown[21] with four isomeric pairs (rac-PPO and rac-POP, rac-PStO and rac-POSt, rac-StStO and rac-StOSt, and rac-StOO and rac-OStO) that the position of the unsaturated fatty acid in the triglyceride has no measurable influence on the ECN value.

A special case, however, is the change in ECN with addition of bromine to the oleic acid double bond in monounsaturated triglycerides. Bromine addition was performed directly in pentane solution[21,25]. Table IX shows the results obtained with four isomer pairs. The addition of bromine enhances the polarity of the triglyceride, shortens the retention time and reduces the ECN value. The two possible positions where the unsaturated fatty acid can be placed are thus not equivalent. The difference of more than 0.20 between the ECN of the two isomers is sufficient to allow the peaks of the isomer pairs to be half separated at *ca.* 40 000 and nearly completely separated at 80 000 theoretical plates.

The transition from a *cis* to a *trans* double bond (Table X) enhances the retention time and thus the ECN value by 0.40 units per double bond. Trielaidin thus has a lower polarity than triolein.

TABLE X

DIFFERENCE IN ECN WITH CHANGE FROM A *cis* TO A *trans* DOUBLE BOND

Triglycerides	*Change in ECN*	*Triglycerides*	*Change in ECN*	*Triglycerides*	*Change in ECN*
PPO to PPEl	−0.45	StOO to StOEl	−0.39	(OOO to ElElEl)/3	−0.37
StStO to StStEl	−0.39	(StOO to StElEl)/2	−0.40		
Mean total ($n=5$)			−0.40		
S.D.			0.03		

TABLE XI

VARIATION IN ECN VALUE AS MOLECULAR STRUCTURE CHANGES

Change in molecular structure	*Difference in ECN*	*S.D.*
Increase of carbon number by 2 in sat. triglycerides (defin.)	2.00	–
Increase of carbon number by 2 in unsat. triglycerides	1.94	0.04
Increment of one double bond from sat. to monounsat. fatty acid	2.89	0.08
Increment of one double bond from monounsat. to diunsat. fatty acid	2.47	0.07
Increment of one double bond from diunsat. to triunsat. fatty acid	2.02	–
Addition of bromine to the double bond in monounsat. triglyceride	2.29 (sym.) 2.07 (unsym.)	– –
Moving of one double bond from carbon atom in the vicinity of Δ^9	0.07–0.13	–
Change of one *cis*-double bond to one *trans*-double bond	0.40	0.03

CONCLUSIONS

Equivalent carbon numbers are based on the same log t_R *versus* carbon number relation as ECL values and Kovats indices. In our laboratory ECN values are used in the HPLC of lipids, but they can be used with other homologous series of organic compounds. The calculation, using only three standard points, gives the ECN values for all peaks in a chromatogram.

ECN values define the order of elution of triglycerides from a modern RP-HPLC column. The ECNs denote the hypothetical carbon numbers of hypothetical saturated triglycerides and thus give a direct indication of the position of a peak in the chromatogram. For example, the peak of triolein, OOO (ECN = 45.17) will appear between the peaks of trimyristin, MMM (ECN = 42.00) and tripalmitin, PPP (ECN = 48.00); or, more exactly, between the peaks of MMP (ECN = 44.00) and MPP (ECN = 46.00).

It was demonstrated that ECN values are very stable and can be used directly as characterizing parameters for the components in a given HPLC triglyceride peak. Arranged in a diagram as in Fig. 2, the ECN values can give the first tentative information about an unknown peak (carbon number, and the number and positions of double bonds).

The ECN value of a triglyceride is the sum of the partial fatty acid ECN values. These can then give further initial information about the qualitative content of a peak.

The measured changes in ECN values in relation to the changes in the molecule under the reported experimental conditions are as listed in Table XI.

REFERENCES

1 A. J. P. Martin, *Biochem. Soc. Symp.*, 3 (1950) 4.
2 J. L Perrin and M. Naudet, *Rev. Fr. Corps Gras*, 30 (1983) 279.
3 G. Sempore and J. Bezard, *J. Chromatogr.*, 366 (1986) 261.
4 E. Kovats, *Helv. Chim. Acta*, 41 (1958) 1915.
5 J. K. Baker and Ch.-Y. Ma, *J. Chromatogr.*, 169 (1979) 107.
6 N. H. Ray, *J. Appl. Chem.*, 4 (1954) 25.
7 J. P. Goiffon, C. Reminiac and M. Olle, *Rev. Fr. Corps Gras*, 28 (1981) 167.
8 J. P. Goiffon, C. Reminiac and D. Furon, *Rev. Fr. Corps Gras*, 28 (1981) 199.
9 A. Stolywho, H. Colin and G. Guiochon, *Anal. Chem.*, 57 (1985) 1342.
10 A. Wehrli and E. Kovats, *Helv. Chim. Acta*, 42 (1959) 2709.
11 T. K. Miwa, K. L. Mikolajczak, F. R. Earle and I. A. Wolff, *Anal. Chem.*, 32 (1960) 1739.
12 T. K. Miwa, *J. Am. Oil Chem. Soc.*, 35 (1963) 1739.
13 F. D. Gunstone, *Topics in Lipid Chemistry*, Logos, London, 1970, pp. 108–109.
14 J. K. Baker, R. E. Skelton, T. N. Riley and J. R. Bagley, *J. Chromatogr. Sci.*, 18 (1980) 153.
15 R. M. Smith, *J. Chromatogr. Sci.*, 236 (1982) 313.
16 A. Shalby, Zs. Budvari-Brany and G. Szasz, *J. Liq. Chromatogr.*, 7 (1984) 1133.
17 R. M. Smith, *Trends Anal. Chem.*, 3 (1984) 186.
18 B. Herslöf, O. Podlaha and B. Töregård, *J. Am. Oil Chem. Soc.*, 56 (1979) 864.
19 O. Podlaha and B. Töregård, *J. High Resolut. Chromatogr. Chromatogr. Comm.*, 5 (1982) 553.
20 B. Töregård, O. Podlaha and B. Püschl, *Lebensm. Wiss. u. Technol.*, 17 (1984) 77.
21 O. Podlaha and B. Töregård, *Fette, Seifen, Anstrichm.*, 86 (1984) 243.
22 O. Podlaha, *J. Chromatogr.*, 410 (1987) 509.
23 C. Litchfield, *Analysis of Triglycerides*, Academic Press, New York, London, 1972, p. 86.
24 W. W. Christie, *HPLC and Lipids*, Pergamon Press, Oxford, 1987.
25 E. Geeraert and D. De Scheppper, *J. High Resolut Chromatogr. Chromatogr. Comm.*, 6 (1983) 123.

Journal of Chromatography, 482 (1989) 227–233
Elsevier Science Publishers B.V., Amsterdam — Printed in The Netherlands

CHROM. 21 934

Note

Gas chromatography-based method for assigning the configurations of allylic and benzylic alcohols and for determining their optical purities

YULIN HU[a] and HERMAN ZIFFER*
Laboratory of Chemical Physics, National Institute of Diabetes and Digestive and Kidney Diseases, Bethesda, MD 20892 (U.S.A.)
(First received April 20th, 1989; revised manuscript received August 30th, 1989)

We recently demonstrated that it is possible, with rare exceptions, to account for the optical purities[1], as well as the configurations, of alcohols prepared by enantioselective hydrolysis of the corresponding racemic acetates using the mold *Rhizopus nigricans*[1–4]. Estimates of enantiomeric excesses of alcohols formed in these kinetic resolutions were based on electrical, steric and polarizability parameters obtained from the literature and on quantitative hydrolysis data. The experimental values for enantiomeric excess were obtained from rotation measurements; consequently, the data employed in formulating the correlations would be subject to large errors. The desire for a more precise analytical technique prompted a search for a better method. That search was also influenced by a recent observation[4] that the configuration of one allylic alcohol formed in these hydrolyses was not the expected one based on the rule given in ref. 1. Thus, an independent method of assigning the configurations of allylic alcohols was also sought. A recently developed reaction by Sharpless *et al.*[5] is now widely used by organic chemists for the preparation of chiral allylic and epoxy alcohols of a predictable configuration. While we are unaware of any discrepancies between predicted and observed configurations of alcohols prepared using this reaction, a simple method of verifying a configurational assignment of an allylic alcohol, obtained using the Sharpless procedure, should prove useful. We describe here a method of assigning the configurations of allylic and benzylic alcohols that employs the relative retention times of the diastereomeric esters formed with (−)-camphanic acid, from an Ultra 1 (Hewlett-Packard) capillary gas chromatography (GC) column. In addition, the GC separation provides analytical data on the optical purity of the alcohol.

Many of our preparations of chiral alcohols employ microbial transformations; thus it is frequently necessary to analyze small quantities of impure alcohols. To avoid the extensive purification necessary for optical and NMR methods, a chromatographic procedure to separate and characterize diastereomers appeared ideal. Although milligram quantities were employed to prepare the camphanate esters, reaction conditions can be modified to use much less material.

[a] On leave from Shanghai Institute of Materia Medica, Chinese Academy of Science, 319 Yue-Yang Road, Shanghai 200031, China.

0021-9673/89/$03.50

While separations of diastereomeric esters have been used to determine optical purity, many of the derivatives were developed for the analysis of saturated alcohols[6–8] and for correlating the elution order of diastereomers with their configuration[9–11]. The procedure developed by Doolittle and Heath[7] employes (*S*)-tetrahydro-5-oxo-5-furancarboxylic acid while Brooks and Gilbert[10] utilizes α-phenylbutyric acid in a modification on a microscale of Horeau and Kagan's procedure[11]. Analogous studies using elution order from high-performance liquid chromatography (HPLC) columns have been described[12–16]. Thus, there is ample precedent for employing chromatographic procedures for determining enantiomeric excess and for making configurational assignments based on elution order. Camphanate esters of allylic alcohols have been employed by several investigators to resolve allylic alcohols[17,18] and by others to assign a molecules configuration[19]. Deger *et al.*[16] employed HPLC and GC for the separation of camphanate esters of allylic alcohols. Deger *et al.*[16] and Bergot *et al.*[20] have cautioned against overestimating the reliability of configurational assignments based on elution order. Despite these cautionary comments a series of thirteen racemic cyclic allylic alcohols were esterified with (−)-camphanyl chloride. We found that all of the diastereomeric esters could be separated on a 25 m × 0.2 mm I.D. Ultra capillary GC column. The configuration of the more rapidly eluted diastereomer was assigned using samples of known configuration. The resulting data were examined to determine if the elution order of a diastereomer could be correlated with the configuration of the alcohol.

EXPERIMENTAL

General procedure for the preparation of camphanate esters

A solution of 0.002–0.010 g of the alcohol in methylene chloride (1–2 ml) was reacted overnight at room temperature with 1.2 equiv. of camphanyl chloride in the presence of 1 equiv. of 4-dimethylaminopyridine. The reaction mixture was treated with water (1 ml), the methylene chloride layer was separated, washed, dried and concentrated. The crude ester was then purified by flash chromatography on silica gel.

Analysis

The analyses were done using a Hewlett Packard 5890A gas chromatograph equipped with a 25 m × 0.2 mm I.D. Ultra 1 capillary column and an HP 3392A integrator. The alcohols employed for this study were all prepared by literature methods and their spectroscopic properties were in agreement with those expected for their structures. The peaks in the chromatogram were identified using camphanates of alcohols enriched in one enantiomer, the absolute stereochemistry of which had previously been established. Data on the specific rotations and the configurations of the alcohols used to identify the diastereomeric camphanate ester more rapidly eluted from the column is given in Table I.

RESULTS AND DISCUSSION

The data obtained for the chromatographic behavior of camphanate esters of a series of (*E*)- and (*Z*)-cycloalk-2-en-1-ols (compounds **1–13**) on a 25 m × 0.2 mm I.D. Ultra 1 cross-linked capillary column is summarized in Table II. Success in

TABLE I

DATA ON THE SPECIFIC ROTATIONS AND ABSOLUTE STEREOCHEMISTRIES OF THE ALCOHOLS EMPLOYED IN ASSIGNING THE ABSOLUTE STEREOCHEMISTRY OF THE DIASTEREOMERIC CAMPHANATES

Compound	*Specific rotation in chloroform (enantiomeric excess)*	*Absolute stereochemistry of enantiomer in excess*	*Compound*	*Specific rotation in chloroform (enantiomeric excess)*	*Absolute stereochemistry of enantiomer in excess*
1	+5.7 (14)	*R*	**13**	−4.6 (49)	*R*
2	+18 (15)	*R*	**14**	+23 (91)	*S*
3	−17 (22)	*S*	**15**	+27 (81)	*S*
4	−28 (79)	*R*	**16**	+30 (91)	*R*
5	−7.5 (35)	*S*	**17**	−89 (>95)	*S*
6	+55 (97)	*R*	**18**	−71 (99)	*S*
7	−24 (52)	*R*	**19**	+45 (91)	*R*
8	−38 (78)	*R*	**20**	−1.5 (91)	*R*
9	−85	*R*	**21**	+37 (61)	*R*
10	−118 (46)	1*R*, 2*R*	**22**	+26 (53)	*R*
11	−49 (85)	*R*	**23**	+26 (77)	*S*
12	−2.0	*R*	**24**	−17 (98)	*R*

separating diastereomeric camphanates of cyclic allylic alcohols prompted us to extend this study to include benzylic alcohols. Camphanate esters of several benzylic alcohols were prepared (compounds **14**–**19**) and their chromatographic properties examined. The esters were readily separated; data are included in Table II. Although no systematic effort was made to explore the scope and limitations of the GC-based method, the chromatographic behavior of several other camphanates were examined. The esters of saturated acyclic alcohol **25** and of the cyclohexanol derivative **26** were *not* separated on the Ultra 1 capillary column. However, esters of the homobenzylic alcohol **21** were readily separated.

Since the method proved valuable in determining enantiomeric excesses of benzylic and allylic alcohols, an effort was made to learn whether the elution order of a diastereomer correlated with the configuration of the alcohol. As mentioned briefly in the introduction, chiral allylic alcohols are important synthetic intermediates and their configurations are frequently assigned from the method of preparation. It is therefore important to identify compounds where the configuration might have been incorrectly assigned. Information on the configuration of the ester preferentially eluted (first peak) is given in Table II; it shows that the alcohol has the configuration shown in Fig. 1. The presence of substituents on C-2 or C-3 of a cycloalk-2-en-ol does *not* alter this correlation between elution order and configuration of the ester. Furthermore, the correlation between the configuration of the alcohol and the elution order of the ester is also independent of the *cis* or *trans* nature of the double bond.

The configuration of a benzylic alcohol preferentially eluted from the column is also accounted for by the structure in Fig. 1, if the double bond is incorporated into an aromatic ring. For phenylalkyl carbinols, replacing an ethyl group by a trifluoromethyl group (compounds **22** and **23**) does not affect the relation between elution order and configuration. Since critical factors which affect the differential binding of diastereomeric esters to the column are unknown, *assignments based on this correla-*

TABLE II

SEPARATION BY GC OF DIASTEREOMERIC CAMPHANATES OF ALLYLIC, BENZYLIC AND MISCELLANEOUS ALCOHOLS ON A 25-m ULTRA 1 COLUMN

Compound	*Oven temp. (°C)*	*First peak*		*Second peak*		*Alpha value*	*Ref.*
		Retention time (min)	*Absolute stereochemistry*	*Retention time (min)*	*Absolute stereochemistry*		
1	140[a]	10.13		10.23		1.02	4
2	160[a]	7.52	*R*	7.71	*S*	1.03	4
3	200	11.79	*R*	12.23	*S*	1.04	4
4	175[a]	10.55	*R*	11.26	*S*	1.07	4
5	170	7.78	*R*	7.92	*S*	1.02	4
6	200	5.43	*R*	5.76	*S*	1.06	4
7	170	11.85	*R*	12.05	*S*	1.02	18
8	190[a]	8.97	*R*	9.13	*S*	1.02	13
9	200[a]	12.81	*R*	13.09	*S*	1.02	13
10	180–220[b]	32.33	*R*	32.77	*S*	1.01	21, 22
11	210–240[b]	19.06	*R*	19.16	*S*	1.01	21, 22
12	250–270[b]	12.41	*R*	12.53	*S*	1.01	21, 22
13	250–270[b]	14.76	*R*	14.97	*S*	1.01	26
14	190	7.46	*R*	7.88	*S*	1.06	3
15	190	10.50	*R*	11.26	*S*	1.07	3
16	210	5.89	*R*	6.34	*S*	1.08	3
17	210	7.65	*R*	7.92	*S*	1.04	24
18	250–270[b]	15.55	*R*	15.88	*S*	1.02	13
19	230[a]	7.06	*R*	7.35	*S*	1.04	13
20	230	7.03	*R*	7.35	*S*	1.04	25
21	240	15.46	*R*	15.87	*S*	1.03	27
22	220	12.15	*R*	12.71	*S*	1.05	2
23	150	9.64	*S*	9.79	*R*	1.02	2
24	240	13.56	*S*	15.19	*R*	1.12	2
25	160	9.07		9.07		1.00	–
26	200	11.01		11.01		1.00	–

[a] Temperature programmed to rise 1°C/min.

[b] The column used for these measurements was physically different one from that used for the other measurements, although it was purchased from the same source with the same specifications.

tion must be treated as tentative. There are several reports in which the elution order of one member of a homologous series unexpectedly differs from that of the others in the series[16,20]. Configurational assignments based on elution order data therefore should be verified using an independent method, *i.e.*, chiroptical measurements or the use of enzymic or microbially mediated reactions. If independent assignments differ, the configuration must be rigorously determined by a direct method, *i.e.*, chemical conversion into a compound of established configuration or by an X-ray crystallographic determination.

One factor that has been found to alter the relationship between the relative

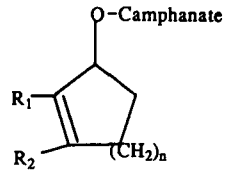

1 n = 1, $R_1 = R_2 = H$
2 n = 2, $R_1 = R_2 = H$
3 n = 2, R_1 = Ph, R_2 = H
4 n = 2, R_1 = H, R_2 = Br
5 n = 3, $R_1 = R_2 = H$
6 n = 3, R_1 = Br, R_2 = H
7 n = 4, $R_1 = R_2 = H$
8 n = 5, $R_1 = R_2 = H$
9 n = 6, $R_1 = R_2 = H$

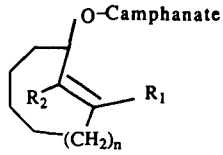

10 n = 1, $R_1 = R_2 = H$
11 n = 2, $R_1 = R_2 = H$
12 n = 4, $R_1 = R_2 = H$
13 n = 5, $R_1 = R_2 = H$

retention time of diastereomeric benzylic camphanates is the presence of substituents on the methylene group adjacent to the carbinol carbon, *e.g.*, 4,4-dimethyl-1,2-benzocyclohexen-3-ol (**24**). The configuration of the enantiomer more rapidly eluted from the column *differed* from that predicted using the relationship proposed in ref. 4. Since we have no data on the elution order of other 4-substituted 1,2-benzocycloalken-3-yl camphanates, this observation should alert other investigators to be extremely careful in assigning the configurations of 4-substituted cyclic benzylic camphanates from their elution order. Surprisingly, a similar change in the relationship between elution order and configuration of 4-substituted 1,2-benzocycloalken-3-ols and the unsubstituted parent compounds was noted for the elution of enantiomers of these alcohols from type 1A chiral Pirkle HPLC column[2].

The ability to separate diastereomeric camphanates has been helpful in solving several problems. In the course of resolving 1-acenaphthenol, a metabolite of acenaphthene[21], this separations technique was used to monitor the resolution and make a tentative configurational assignment of the (−)-enantiomer. The ester of (−)-1-acenaphthenol was the more rapidly eluted diastereomer, suggesting that it was the (*R*)-alcohol. This deduction was confirmed by an X-ray structure analysis[22]. This procedure was also used to establish enantiomeric excesses of substituted and unsubstituted 1,2-benzocycloalken-3-ols (**13** and **16**). The alcohols were not resolved on a type 1A Pirkle HPLC column[1–4,23,24]. Finally, the analytical method was used to assign the configuration of (−)-(*E*)-cyclooct-2-en-1-ol[25]. Treatment of the (*E*)-isomer with silver ion to convert it into the (*Z*)-isomer yielded a mixture of isomers

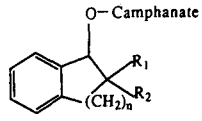

14 n = 1, $R_1 = R_2 = H$ **17** n = 4, $R_1 = R_2 = H$

15 n = 2, $R_1 = R_2 = H$ **18** n = 5, $R_1 = R_2 = H$

16 n = 3, $R_1 = R_2 = H$ **19** n = 6, $R_1 = R_2 = H$

24 n = 2, $R_1 = R_2 = CH_3$

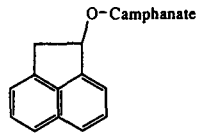

20

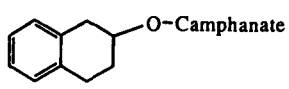

21

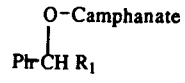

22 $R_1 = C_2H_5$

23 $R_1 = CF_3$

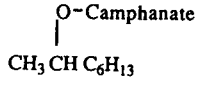

25

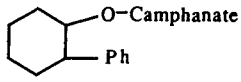

26

whose separation was very difficult. When the camphanate esters of this mixture were prepared it was possible to separate all of the diastereomeric esters by GC. The chromatogram was also used to assign the configuration of the predominant diastereomer of (*Z*)-cyclooct-2-en-1-ol. The use of these GC-based separations with sensitive detection systems, *e.g.*, mass spectrometers would result in far greater sensitivity than is possible with NMR-based methods.

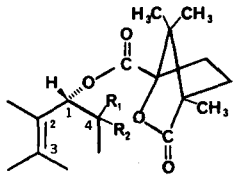

Fig. 1. Configuration at the carbinol carbon of the ester formed with (−)-camphanic that is more rapidly eluted from an Ultra 1 capillary column.

CONCLUSION

It is possible to identify the predominate enantiomer and to analyze the enantiomeric excesses of a large number of allylic and benzylic alcohols by esterifying them with (−)-camphanic acid and separating the resulting diastereomers on a capillary GC column. Data on the relative retention times of a diastereomer have been correlated with the configurations about the carbinol carbon.

ACKNOWLEDGEMENT

We wish to record our appreciation to the late Dr. Ulrich Weiss for stimulating and valuable discussions.

REFERENCES

1 M. Charton and H. Ziffer, *J. Org. Chem.*, 52 (1987) 2400.
2 H. Ziffer, K. Kawai, M. Imuta and C. Froussios, *J. Org. Chem.*, 48 (1983) 3017.
3 M. Kasai, K. Kawai, M. Imuta and H. Ziffer, *J. Org. Chem.*, 49 (1984) 675.
4 S. Ito, M. Kasai, H. Ziffer and J. V. Silverton, *Can. J. Chem.*, 65 (1987) 574.
5 K. B. Sharpless, C. H. Behrens, T. Katsuki, A. W. M. Lee, V. S. Martin, M. Taketani, S. M. Viti, F. J. Walker and S. S. Woodward, *Pure Appl. Chem.*, 55 (1983) 589.
6 R. W. Souter, *Chromatographic Separations of Stereoisomers*, CRC Press, Boca Raton, FL, 2nd ed., 1986, pp. 11–47.
7 R. E. Doolittle and R. R. Heath, *J. Org. Chem.*, 49 (1984) 5041.
8 P. E. Sonnet and R. R. Heath, *J. Chromatogr.*, 238 (1982) 41.
9 W. Pereira, V. A. Bacon, W. Patton and B. Halpern, *Anal. Lett.*, 3 (1970) 23.
10 C. J. W. Brooks and J. D. Gilbert, *Chem. Commun.*, (1973) 194.
11 A. Horeau and H. B. Kagan, *Tetrahedron*, 20 (1964) 2431.
12 M. Kasai, C. Froussios and H. Ziffer, *J. Org. Chem.*, 48 (1983) 459.
13 R. E. Doolittle and R. R. Heath, *J. Org. Chem.*, 49 (1984) 5041.
14 W. H. Pirkle, J. M. Finn, J. L. Schreiner and B. C. Hamper, *J. Am. Chem. Soc.*, 103 (1981) 3964.
15 W. H. Pirkle and J. L. Schreiner, *J. Org. Chem.*, 46 (1981) 4988.
16 W. Deger, M. Gessner, G. Heusinger, G. Singer and A. Mosandl, *J. Chromatogr.*, 366 (1986) 385.
17 L. Luche, J. C. Damiano and P. Crabbé, *J. Chem. Res. Synop.*, (1977) 32.
18 L. Luche, J. C. Damiano and P. Crabbé, *J. Chem. Res. Miniprint*, (1977) 443.
19 A. Mosandl, G. Heusinger and M. Gessner, *J. Agric. Food Chem.*, 34 (1986) 119.
20 B. J. Bergot, F. C. Baker, E. Lee and D. A. Schooley, *J. Am. Chem. Soc.*, 101 (1979) 7432.
21 M. J. Schocken and D. T. Gibson, *Appl. Environ. Microbiol.*, 48 (1984) 10.
22 Y. Hu, H. Ziffer and J. V. Silverton, *Can. J. Chem.*, 67 (1989) 60.
23 Y. Hu and H. Ziffer, *J. Chromatogr.*, submitted for publication.
24 M. Kasai and H. Ziffer, *J. Org. Chem.*, 48 (1983) 712.
25 A. Balan and H. Ziffer, in preparation.
26 S. Ito, H. Ziffer and J. V. Silverton, *Acta Crystallogr.*, C45 (1989) 515.
27 H. Arawa, N. Torimoto and Y. Musui, *Tetrahedron Lett.*, (1968) 4115.

Journal of Chromatography, 482 (1989) 234–239
Elsevier Science Publishers B.V., Amsterdam — Printed in The Netherlands

CHROM. 21 882

Note

Modifications to a high-speed counter-current chromatograph for improved separation capability

I. SLACANIN, A. MARSTON and K. HOSTETTMANN*
Institut de Pharmacognosie et Phytochimie, Ecole de Pharmacie de l'Université de Lausanne, Rue Vuillermet 2, CH-1005 Lausanne (Switzerland)
(Received June 7th, 1989)

Counter-current chromatography (CCC) is a liquid–liquid partition method without solid supports that permits the separation of very diverse samples[1]. The development of high-speed CCC (HSCCC) has led to a dramatic decrease in separation times by using a multilayer coil coaxially mounted on a holder rotating at high revolutional speeds[2]. HSCCC with the Ito multi-layer coil separator–extractor has found numerous applications in, for example, the fields of antibiotics[3], flavonoids[4] and alkaloids[5].

As part of our investigation into the use of centrifugal counter-current chromatography (or centrifugal partition chromatography) for the separation of natural products[6], we have introduced certain modifications to the Ito instrument in order to allow the following manipulations: (a) injection of sample without stopping the solvent flow, (b) variation of the relative proportions of the two phases in the coil and (c) reversal of phase flow.

EXPERIMENTAL

Separations were carried out at *ca.* 20°C with an Ito multi-layer coil separator–extractor (P.C., Potomac, MD, U.S.A.), equipped with a 2.6 mm I.D. coil (volume 360 ml). Ancillaries included a sample loop (with six-way valve) and a second valve to permit rapid switching of the solvent to the "head" or "tail" ends of the coil. The chromatograph was connected to two Waters Assoc. 6000A high-performance liquid chromatographic (HPLC) pumps (see Fig. 1), pump A for delivery of the upper phase and pump B for delivery of the lower phase of any biphasic solvent system.

For normal operation, the immobile coil was first filled with stationary phase. After commencing rotation, mobile phase was then introduced. When the mobile phase was the lower phase, solvent was pumped into the "head" end of the coil and when the mobile phase was the upper phase, it was pumped into the "tail" end of the coil. At the point where stationary phase no longer eluted from the coil and stable conditions were obtained, the sample was introduced via the sample loop.

By varying the speeds of the pumps, both the flow-rate of the eluate and the composition of the stationary phase in the coil could be regulated. In order to introduce a certain volume of upper (or lower) phase, the two phases were pumped

0021-9673/89/$03.50

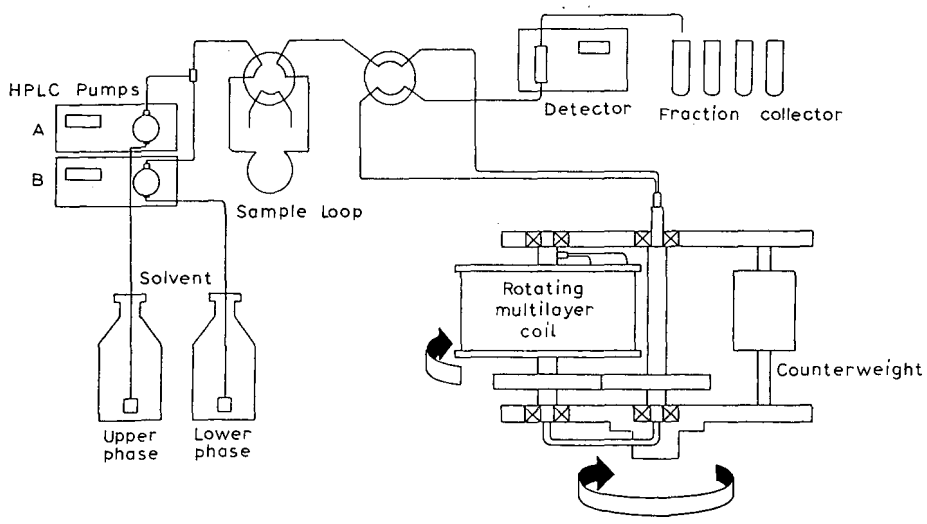

Fig. 1. Ito multi-layer coil separator–extractor and solvent pumping system.

simultaneously into the immobile coil at the required flow-rates before commencing rotation. For example, if 80% lower phase was desired in the coil, lower phase was pumped into the non-rotating coil at 8 ml/min with pump B and upper phase at 2 ml/min with pump A. When the coil had been filled, pumping was stopped and rotation was started. After allowing a few minutes for stabilization, the necessary mobile phase (upper or lower phase of the solvent system) was passed into the instrument and the sample was loaded. Solvent introduction via the "head" or "tail" ends of the coil was selected as above. At the end of a separation run, the proportions of the two phases in the coil could be checked by blowing out the solvent with nitrogen.

The instrument was connected to a Uvicord 2238 SII detector (254 nm) (LKB, Bromma, Sweden), a Model 600 chart recorder (W + W Scientific, Basle, Switzerland) and an LKB Ultrorac II fraction collector. Samples were dissolved in equal amounts of the two solvent phases before injection.

RESULTS AND DISCUSSION

Variation of phase ratios

By altering the proportion of stationary phase in the coil (by changing the relative flow-rates of the two HPLC pumps; see Experimental), the retention times of peaks in the chromatogram could be changed at will. This phenomenon is illustrated by a separation of anthranoid pigments from a root bark light petroleum (b.p. 60–80°C) extract of *Psorospermum febrifugum* (Guttiferae)[6] (Fig. 2). With the upper phase of the non-aqueous solvent system hexane–acetonitrile-methanol (40:25:10) as the mobile phase, the elution order was as shown on the left-hand side of Fig. 2. Use of the lower phase as the mobile phase gave the reverse elution profile. In Fig. 2a–c, increasing amounts of lower phase in the coil increased retention times, whereas in

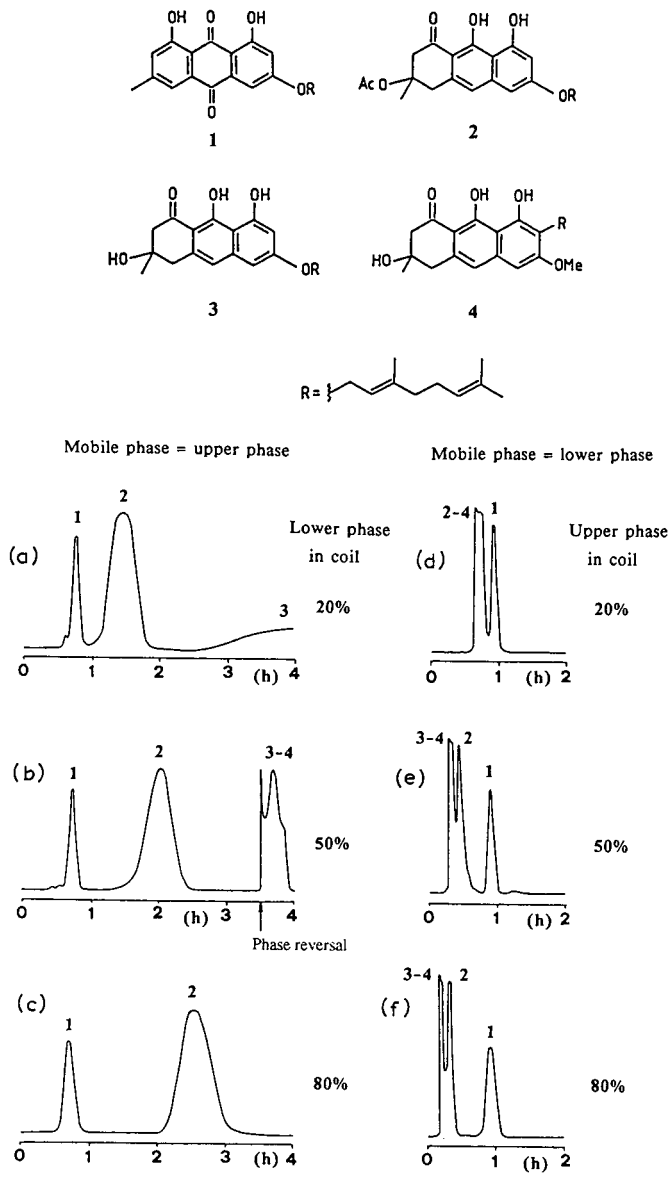

Fig. 2. Separation of *P. febrifugum* root bark pigments on an Ito CCC instrument with different compositions of the stationary phase. Solvent system, hexane–acetonitrile–methanol (40:25:10); sample 100 mg of light petroleum extract; flow-rate, 4 ml/min; rotational speed, 700 rpm; detection, 254 nm. Ac = Acetyl; Me = methyl.

Fig. 2d–f, increasing amounts of upper phase in the coil decreased retention times. Interestingly, the elution time of **1** was hardly affected by changing the stationary phase composition in either of the two modes.

Phase reversal

Fig. 3a shows the separation of the flavonoids hesperetin (**5**), kaempferol (**6**) and quercetin (**7**) with the lower phase of the solvent system chloroform–methanol–water (33:40:27) as the mobile phase. By using the upper phase as the mobile phase (Fig. 3b), a considerably longer separation time resulted.

Starting the separation of flavonoids **5**–**7** with the upper phase as mobile phase and then changing to the lower phase after elution of quercetin (**7**) gave a dramatic increase in separation speed (Fig. 3c). This phase reversal during the separation (or "reversed-phase" operation) was achieved by activating a four-way valve between the solvent delivery system and the coil (Fig. 1), without stopping the instrument. The only difference between Fig. 3b and c (apart from the separation time) is the change in order of elution of **5** and **6**. In this example, the coil was filled at the beginning of the run with 50% of each component of the two-phase solvent system by pumping upper phase with pump A (5 ml/min) and lower phase with pump B (5 ml/min) simultaneously, before sample injection. Other initial phase ratios for "reversed-phase" operation were feasible and could be achieved by adjusting the relative flow-rates of pumps A and B.

"Gradient" elution

By pumping simultaneously the lower phase with one HPLC pump and the upper phase of a two-phase system with the other HPLC pump, it was possible to change the proportions of phases in the coil during a separation run. In the example shown (Fig. 4), the coil of the chromatograph was first filled with equivalent amounts

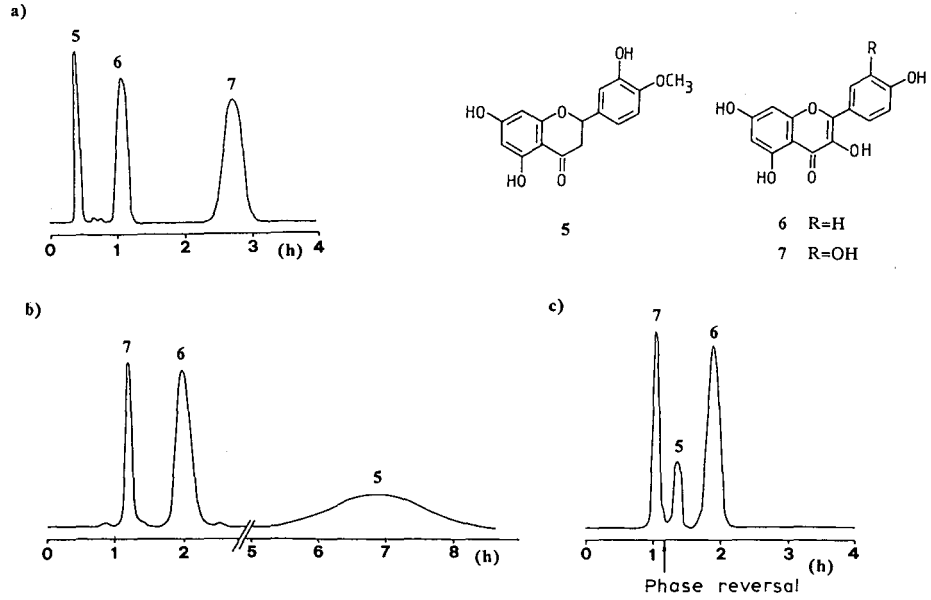

Fig. 3. CCC separation of hesperetin (**5**), kaempferol (**6**) and quercetin (**7**) with the Ito instrument. Solvent system, chloroform–methanol–water (33:40:27); detection, 254 nm; rotational speed, 700 rpm; flow-rate, 3 ml/min; sample, 15 mg. (a) Mobile phase, lower phase; (b) mobile phase, upper phase; (c) mobile phase, upper phase to 70 min, then lower phase.

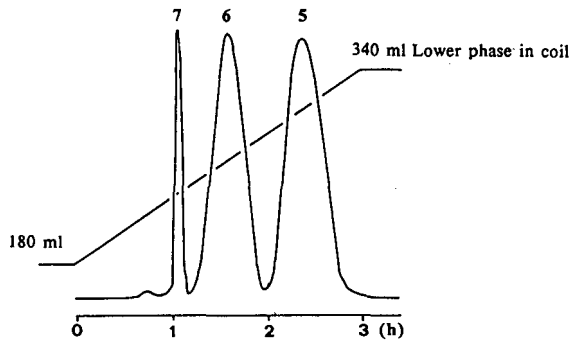

Fig. 4. CCC separation of flavonoids **5–7** with the Ito instrument using "gradient" elution. Mobile phase: upper phase (4 ml/min) and lower phase (1 ml/min). Conditions as in Fig. 3.

of upper and lower phases of the solvent system chloroform–methanol–water (33:40:27) (see Experimental). A mixture of flavonoids **5–7** was then injected. By pumping upper phase through the apparatus at 4 ml/min and lower phase at 1 ml/min, the content of lower phase in the coil increased from 180 to 340 ml over 3 h. The separation of the three flavonoids was thus achieved in a time 5 h shorter than that shown in Fig. 3b.

CONCLUSION

The above examples show some of the separation possibilities available to the multi-layer coil separator-extractor with separate pumping of the upper and lower phases of a biphasic solvent system. Choice of solvents can be guided by silica gel thin-layer chromatography (with the water-saturated non-aqueous phase as solvent)[6] and, when the biphasic system has been decided upon, the rates of elution of injected compounds can be varied by changing the ratio of stationary to mobile phase. Once the sample has been injected, the required mobile phase can be pumped through the machine with no subsequent loss of stationary phase from the coil. Accurate control of the flow-rate and of the composition of stationary phase in the separation coil is permitted, allowing "gradient" elution and phase reversal. In addition, phase reversal, previously described for analytical HSCCC[7,8], has now been applied to the preparative Ito instrument. With the aid of these developments, it is possible to expand the area of operation of the Ito multi-layer coil separator–extractor and introduce a greater degree of flexibility when establishing experimental parameters.

ACKNOWLEDGEMENT

Financial support from the Swiss National Science Foundation is gratefully acknowledged.

REFERENCES

1 K. Hostettmann, M. Hostettmann and A. Marston, *Preparative Chromatography Techniques—Applications in Natural Product Isolation*, Springer, Berlin, 1986.
2 Y. Ito, *CRC Crit. Rev. Anal. Chem.*, 17 (1986) 65.
3 R. R. Rasmussen and M. H. Scherr, *J. Chromatogr.*, 386 (1987) 325.
4 T.-Y. Zhang, D.-G. Cai and Y. Ito, *J. Chromatogr.*, 435 (1988) 159.
5 J. Quetin-Leclercq and L. Angenot, *Phytochemistry*, 27 (1988) 1923.
6 A. Marston, C. Borel and K. Hostettmann, *J. Chromatogr.*, 450 (1988) 91.
7 T.-Y. Zhang, L. K. Pannell, Q.-L. Pu, D.-G. Cai and Y. Ito, *J. Chromatogr.*, 442 (1988) 455.
8 T.-Y. Zhang, L. K. Pannell, D.-G. Cai and Y. Ito, *J. Liq. Chromatogr.*, 11 (1988) 1661.

Journal of Chromatography, 482 (1989) 240–245
Elsevier Science Publishers B.V., Amsterdam — Printed in The Netherlands

CHROM. 21 898

Note

Determination of sunscreen agents in cosmetic products by reversed-phase high-performance liquid chromatography

KAZUO IKEDA*, SUKEJI SUZUKI and YOHYA WATANABE

Tokyo Metropolitan Research Laboratory of Public Health, 24-1, Hyakunicho 3 chome, Shinjuku-ku, Tokyo 169 (Japan)

(First received June 9th, 1989; revised manuscript received August 10th, 1989)

Cosmetic products containing sunscreen agents are widely available. Sunscreen agents are used to protect the skin against sunburn and to prevent the degradation of cosmetic products by sunlight. However, the regular application of these products may cause irritation and allergic or photoallergic contact dermatitis[1,2]. In order to ascertain which sunscreen agents are present in commercial cosmetic products and to prevent undesirable side-effects, simple and reliable methods for the simultaneous determination of sunscreen agents are required.

A few methods have been proposed for the identification and determination of sunscreen agents in cosmetic products, based on gas–liquid chromatography[3] and high-performance liquid chromatography (HPLC)[4–9]. Cumpelik[3] determined 2-ethoxyethyl 3-(4-methoxyphenyl)-2-propenoate (Cinoxate), 2-ethylhexyl 4-(dimethylamino)benzoate (Escalol 507) and 2-ethylhexyl 3-(4-methoxyphenyl)-2-propenoate (Parsol MCX) by temperature-programmed gas chromatography after silanization. Gagliardi *et al.*[7] assayed (2-hydroxy-4-methoxyphenyl)phenylmethanone (Oxybenzone), Escalol 507, 1-[4-(1,1-dimethylethyl)phenyl]-3-(4-methoxyphenyl)-1,3-propanedione(Parsol 1789) and Parsol MCX by HPLC. These procedures are relatively time consuming and laborious because of the complex sample pretreatment and extraction steps required, and therefore are not suitable for the routine analysis of cosmetic products.

In this paper we describe a reversed-phase HPLC method for the rapid and simultaneous determination of six sunscreen agents {Cinoxate, Oxybenzone, 1-[4-(1-methylethyl)phenyl]-3-phenyl-1,3-propanedione (Eusolex 8020), Escalol 507, Parsol 1789 and Parsol MCX} in cosmetic products involving a simple extraction for sample preparation.

EXPERIMENTAL

Reagents and materials

The following materials and reagents were used: Cinoxate (Givaudan, courtesy of Kokuritu Eisei Shikenjo, Tokyo, Japan), Oxybenzone (Tokyo Kasei Kogyo, Tokyo, Japan), Eusolex 8020 (Merck, courtesy of Kanto Chemical, Tokyo, Japan), Escalol 507 (Van Dyk, courtesy of Ina Trading, Tokyo, Japan), Parsol 1789 and

0021-9673/89/$03.50

Parsol MCX (Givaudan, Tokyo, Japan). All other chemicals were of HPLC grade. Water was deionized and distilled from glass apparatus. All solvents and solutions for HPLC analysis were filtered through an FR-40 Fuji Film Micro Filter (pore size 0.4 μm) and vacuum degassed by sonication before use.

Standard solutions

Stock solutions of standards were prepared by dissolving the appropriate amount of sunscreen agent in tetrahydrofuran (THF). A set of standard solutions were produced by diluting aliquots of the stock solutions with THF to 50 ml in volumetric flasks. The concentrations of each compound for the calibration graphs ranged from 1 to 10 μg/ml and from 10 to 100 μg/ml.

Sample solutions

Taking into account the content of sunscreen agents in the cosmetic products, about 0.05–5.0 g of the latter were weighed accurately in a 50-ml beaker, diluted to about 20-ml with THF, dissolved by sonication and transferred into a 50-ml volumetric flask. The beaker was rinsed twice with 5-ml portions of THF and the rinsings were combined in the volumetric flask. The solution was diluted to volume with THF. An aliquot of the solution was filtered through a 0.4 μm membrane filter prior to HPLC analysis.

High-performance liquid chromatography

The HPLC system consisted of a Model 665A-12 pump (Hitachi, Tokyo, Japan), a Model 7125 injector equipped with a 20 μl sample loop (Rheodyne, Cotati, CA, U.S.A.) and a Model 665A-21 variable-wavelength UV detector (Hitachi). Chromatograms and peak areas were obtained with a Model 883A reporting integrator (Hitachi). A TSKgel ODS-80T_M (particle size 5 μm, 15 cm × 4.6 mm I.D.; TOSOH, Tokyo, Japan) analytical column was used at 40°C. The mobile phase was methanol–THF–water (4:6:6) at a flow-rate of 1.0 ml/min. The UV detector was operated at 325 nm with a sensitivity of 0.04 a.u.f.s.

By means of the injection valve, 5 μl of the prepared sample solution and standard solution were chromatographed under the operating conditions described above. Quantitation was based on the peak area of the sample.

RESULTS AND DISCUSSION

Fig. 1 shows the UV spectrum of the sunscreen agents in ethanol. The absorbance maxima for Cinoxate, Oxybenzone, Escalol 507, Eusolex 8020, Parsol 1789 and Parsol MCX are 302, 286 (second maxima at 325 nm), 309, 345, 358 and 308 nm, respectively. However, UV monitoring with the absorbance maxima could not be used because it was required to determine these compounds simultaneously. As the absorbances of the individual sunscreen agents were similar from 320 to 330 nm, as shown in Fig. 1, the UV monitoring wavelength was selected as 325 nm.

Fig. 2 shows the chromatogram of a standard mixture of sunscreen agents. Six sunscreen agents were eluted as fairly symmetrical peaks, well resolved from each other. Gagliardi *et al.*[7] reported that Escalol 507, Parsol 1789 and Parsol MCX were eluted almost at the same time on a reversed-phase ODS column using a mobile phase

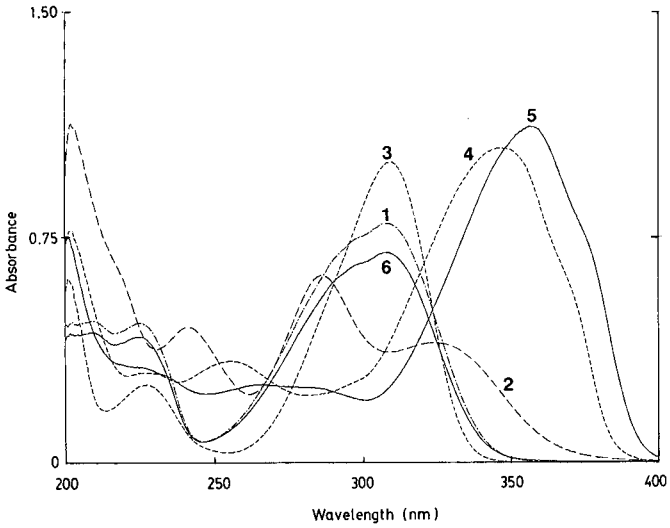

Fig. 1. Absorption spectrum of sunscreen agents. Conditions: cell length, 1 cm; concentration, 10 mg/l. 1 = Cinoxate; 2 = Oxybenzone; 3 = Escalol 507; 4 = Eusolex 8020; 5 = Parsol 1789; 6 = Parsol MCX.

system with an ion-pair partition process. Under our chromatographic conditions, good separation among Escalol 507, Parsol 1789 and Parsol MCX was achieved using methanol–THF–water (4:6:6) as the mobile phase.

Calibration graphs were constructed by plotting the peak area *vs.* the concentration of standard injected. Good linearity over the ranges 1–10 μg/ml and 10–100 μ/ml for each sunscreen agent was obtained; the plots passed through the origin.

Recovery tests were carried out on cosmetic products for the evaluation of the reproducibility and accuracy of the proposed method. Six cosmetic products were

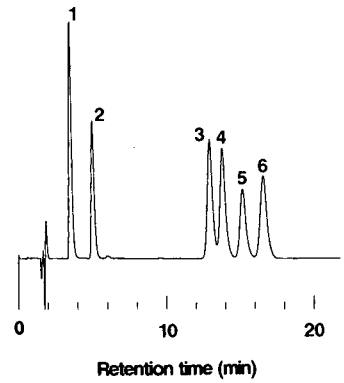

Fig. 2. Liquid chromatogram of sunscreen agents. Conditions: column, TSKgel ODS-80T$_M$ (150 mm × 4.6 mm I.D.); eluent, methanol–THF–water (4:6:6); flow-rate, 1.0 ml/min; column temperature, 40°C; injection volume, 5 μl. Peaks: 1 = Cinoxate; 2 = Oxybenzone; 3 = Escalol 507; 4 = Eusolex 8020; 5 = Parsol 1789; 6 = Parsol MCX.

TABLE I

RECOVERIES OF SUNSCREEN AGENTS FROM COSMETICS

The amounts of standard samples added were as follows: suntan, 1–2% (w/w); foundation, 1% (w/w); lipstick, 1% (w/w); hair rinse, 0.2% (w/w); milk lotion, 0.1% (w/w); lotion, 0.1% (w/w). C.V. = coefficient of variation (n = 3).

Cosmetic	*Cinoxate*		*Oxybenzone*		*Escalol 507*	
	Recovery (%)	*C.V. (%)*	*Recovery (%)*	*C.V. (%)*	*Recovery*	*C.V. (%)*
Suntan	98.3	1.3	100.2	2.8	99.5	3.7
Foundation	101.2	1.7	99.1	1.5	96.7	0.7
Lipstick	104.4	3.4	100.9	3.2	100.4	1.4
Hair rinse	98.3	1.3	98.1	0.8	97.0	2.5
Milk lotion	97.1	2.4	98.1	2.2	98.7	1.3
Lotion	97.2	1.6	99.6	2.7	100.9	2.3
	Eusolex 8020		*Parsol 1789*		*Parsol MCX*	
	Recovery (%)	*C.V. (%)*	*Recovery (%)*	*C.V. (%)*	*Recovery (%)*	*C.V. (%)*
Suntan	99.0	2.0	97.3	0.9	99.9	0.7
Foundation	92.4	0.5	93.6	0.9	99.9	1.2
Lipstick	100.2	1.6	99.5	2.0	102.3	1.3
Hair rinse	97.4	2.2	97.3	0.4	99.8	0.4
Milk lotion	100.0	1.0	99.0	1.0	97.5	0.2
Lotion	98.3	2.2	98.7	1.5	98.6	0.9

spiked with the amounts of the agents reported in Table I and subjected to the whole procedure. As shown in Table I, excellent recoveries and precision were observed.

The proposed method was applied to the determination of sunscreen agents in 33 samples of commercial cosmetic products. The results obtained are shown in Table II. None of the cosmetic products contained Eusolex 8020. Foundations, lipsticks, hair tonics and shampoos contained one of the sunscreen agents investigated; suntans and milk lotions contained a combination of two or three of Oxybenzone, Escalol 507

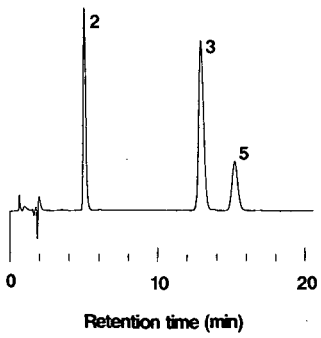

Fig. 3. Liquid chromatogram of sunscreen agents in a commercial milk lotion. Peaks: 2 = Oxybenzone; 3 = Escalol 507; 5 = Parsol 1789.

and Parsol 1789. Several cosmetic products contained less than 0.1% of the sunscreen agents. In such instances, it is concluded that the sunscreen agents are used to prevent the degradation of the cosmetic products. Fig. 3 shows a typical chromatogram for a milk lotion. The peaks of the sunscreen agents did not suffer interference from other cosmetic ingredient in any of the samples examined.

In conclusion, the proposed method is useful for the simultaneous determination of six sunscreen agents in cosmetics products. This method is very simple, precise and accurate, and is suitable for the routine analysis of cosmetics.

TABLE II

CONTENTS OF SUNSCREEN AGENTS IN COSMETICS

Sample	*No.*	*Concentration (%, w/w)*				
		Cinoxate	*Oxybenzone*	*Escalol 507*	*Parsol 1789*	*Parsol MCX*
Suntan	1		2.6	6.7		2.4
	2		4.3	8.8		
	3		3.0	3.4		
	4		0.7	3.8		
	5		0.39	3.6		
Foundation	1			2.9		
	2				0.0091[a]	
	3			0.45		
	4			0.68	0.49	
	5				0.0031[a]	
	6	0.20				
	7			4.2		
	8			0.10		
	9					2.2
	10					1.5
	11					3.0
Lipstick	1					1.1
	2		2.9			
	3					2.2
Milk lotion	1		0.10	0.10	0.033	
	2		0.10	0.10	0.053	
	3		0.051			
Lotion and hair tonic	1	0.10				
	2					0.023
	3		0.0093[a]			
	4		0.020			
	5		0.099			
	6		0.048			
Hair rinse and shampoo	1			0.17		
	2			0.0081[a]		
	3		0.10			
	4		0.010[a]			
	5		0.10			

[a] The range of the calibration graph used was 1–10 μg/ml.

ACKNOWLEDGEMENTS

The author thanks Kokuritu Eisei Shikenjo, Kanto Chemical, Ina Trading and Givaudan for supplying Cinoxate, Eusolex 8020, Escalol 507, Parsol 1789 and Parsol MCX, respectively.

REFERENCES

1 S. Schauder and H. Ippen, *Photodermatology*, 3 (1986) 140.
2 J. S. C. English, I. R. White and E. Cronin, *Contact Derm.*, 17 (1987) 159.
3 B. M. Cumpelik, *Cosmet. Toilet.*, 97 (1982) 67.
4 H. Koenig and R. Ryschka, *Fresenius Z. Anal. Chem.*, 315 (1983) 434.
5 H. Koenig, *Fette Seifen Anstrichm.*, 86 (1984) 37.
6 H. S. I. Tan, R. Sih, S. E. Moseley and J. L. Lichtin, *J. Chromatogr.*, 291 (1984) 275.
7 L. Gagliardi, A. Amato, A. Basili, G. Cavazzutti and D. Tonelli, *J. Chromatogr.*, 408 (1987) 409.
8 T. Ohshima and E. Saito, *Gekkan Yakuji*, 29 (1987) 2477.
9 L. Gagliardi, G. Cavazzutti, L. Montanarella and D. Tonelli, *J. Chromatogr.*, 464 (1989) 428.

Journal of Chromatography, 482 (1989) 246–251
Elsevier Science Publishers B.V., Amsterdam — Printed in The Netherlands

CHROM. 21 884

Note

Selected-ion monitoring of 4-vinyl-1-cyclohexene in acrylonitrile–butadiene–styrene polymer products and food simulants

SHIGERU TAN*, TAKASHI TATSUNO and TARO OKADA

Institute of Food Hygiene, Japan Food Hygiene Association, 6-1, Jingu-mae 2-chome, Shibuya-ku, Tokyo 150 (Japan)

(First received April 20th, 1989; revised manuscript received August 11th, 1989)

In recent years, there has been increasing concern with the migration of substances from packaging materials into foods, particularly that of monomers from plastics. Because the extent of monomer migration is related to its concentration in a polymer, it is important to determine residual levels. As evidence has been presented linking the inhalation of vinyl chloride with the occurrence of angiosarcoma[1,2] of the liver, attention has been directed to the possible presence of other monomer residues in food packaging materials. Residual data have been published for styrene[3,4], vinylidene chloride[5–8], acrylonitrile[9,10] and butadiene [11,12].

1,3-Butadiene (BD) is widely used industrially, especially as a polymer component in the manufacture of synthetic rubber and copolymers such as acrylonitrile–butadiene–styrene (ABS) resins, which are resularly used for packaging foodstuffs.

BD is a vinyl-substituted ethylene and, like vinyl chloride, it is believed to be metabolized in humans via an epoxide intermediate[13]. BD monoxide has been found to have mutagenic activity in bacteria[13]. Moreover, in an inhalation test[14] with BD and 4-vinyl-1-cyclohexene (VCh), a BD dimer, the ciliated epithelium of rat trachea was considerably stripped and the cilia themselves were greatly stunted.

Although the determination of BD in plastics by gas chromatography with flame ionization detection (GC–FID) has been described previously[11,12], there are no reports of the chromatographic determination of VCh in plastics. When we previously analysed BD-based polymers for VCh[15], none could be detected in polybutadiene household wrapping films, but ABS products were found to contain VCh. Retail ABS polymer products can be analysed for VCh by selected-ion monitoring (SIM), and this technique is now routinely used in many laboratories as a highly specific chromatographic detector for quantitative measurements in the selected-ion mode. It offers the additional advantage of much greater sensitivity than FID.

Because of its possible toxicity, we were interested in measuring residual VCh in ABS polymer products and establishing its potnetial for migration into foods using two lots of food-grade ABS sheets. In testing extractables from food packaging materials, it is customary to use food-simulating solvents rather than foods themselves. This practice was followed in the procedures described here, using water, 4% acetic acid, 20% ethanol and *n*-heptane as food simulants.

0021-9673/89/$03.50

EXPERIMENTAL

Materials

Retail ABS products were purchased from supermarkets and food-grade ABS sheets were prepared and their surface areas were simply measured for migration experiments; the sheet thickness was 1.05 mm.

4-Vinyl-1-cyclohexene was obtained from Tokyo Chemical Industries (Tokyo, Japan), UV-grade N,N-dimethylformamide (DMF) from Wako (Osaka, Japan) and organic solvents were of analytical-reagent grade.

Determination of VCh in ABS products

Sample preparation. ABS products were cut into narrow strips (*ca.* 1 cm × 0.2 cm). Samples of about 1.0 g were weighed accurately into volumetric flasks and the volume was adjusted to 20 ml with DMF. The volumetric flasks were then capped and left overnight to dissolve the plastic.

Selected-ion monitoring. A Shimadzu GC-9A gas chromatograph was coupled through an all-glass jet separator to a Shimadzu QP-1000 quadrapole mass spectrometer. Chromatography was carried out on a 0.5 m × 3 mm I.D. glass column packed with 15% DC-550 silicone on 60–80-mesh Gasport A (Gasukuro Kogyo, Tokyo, Japan) held at 60°C for 3.5 min and then programmed to 120°C at 20°C/min to remove DMF, using helium as the carrier gas at a flow-rate of 40 ml/min. The injection temperature was 200°C, the analysis time 7.5 min and the stabilization time about 10 min.

The mass spectrometer was operated in the electron-impact mode (electron energy 70 eV, trap current 60 μA) and maintained at 250°C. Multiple ion monitoring of the ions at *m/z* 54 (base peak of VCh) and 79 was done under computer control.

ABS products analysis. Volumes of 5 μl of polymer solutions in DMF were injected into the gas chromatograph–mass spectrometer under the conditions described above. Determination of VCh in the ABS products was based on peak-area measurement and from a calibration graph for a VCh in DMF standard analysed immediately prior to the sample.

Determination of VCh in food simulants

Sample preparation. An extractability test was adapted from the food sanitation law of Japan[16] for use in this study. The four food simulants used were as follows: water to simulate non-acid aqueous food products, 4% acetic acid as the solvent for acidic food products, 20% ethanol to simulate alcoholic food products and *n*-heptane to simulate foods containing free oil or fat.

ABS sheets of area 100 cm^2 were placed with 200 ml of food simulants (a rate of 2 ml per cm^2) in a closed container. When water, 4% acetic acid and 20% ethanol were used, each container was maintained for 30 min in a water-bath at 60°C, and when *n*-heptane was used, for 1 h in a forced-air oven at 25°C. After being in contact with each other, the ABS sheets in the container were removed and each eluate was allowed to cool to room temperature, and then treated as follows.

Water and 4% acetic acid. A 50-ml aliquot of the eluate was extracted with 20 ml of *n*-hexane for 10 min in a separating funnel, the aqueous layer was shaken with 20 ml of *n*-hexane and the combined organic layers were dried over 2 g of anhydrous

sodium sulphate. The organic layer was transferred into volumetric flasks and the volume was adjusted to 50 ml with *n*-hexane.

20% Ethanol. To avoid emulsion formation, 2.5 g of sodium chloride were added to 50 ml of eluate and the procedure as described above was followed for the water and 4% acetic acid sample preparation.

n-Heptane. The eluates were used directly as sample solutions.

Selected-ion monitoring. Identical apparatus and conditions to those already described were used.

Food simulant analysis. Volumes of 10 μl of *n*-hexane extract solutions in volumetric flasks and *n*-heptane eluates were injected into the gas chromatograph–mass spectrometer system under the conditions described above. Determination of VCh in the food simulants that had migrated from ABS sheets was based on peak-area measurement and from the calibration graph for the VCh in *n*-hexane or *n*-heptane standard analysed immediately prior to the sample.

RESULTS AND DISCUSSION

VCh (b.p. 126–127°C) is well suited for liquid sampling. As a liquid at ambient temperature, it is readily handled with volumetric glassware. It is readily soluble in all the organic solvents used in this study. VCh elutes well ahead of DMF on a DC-550 silicone GC column and is well separated from any interferents present.

Gaschromatographic–mass spectrometric confirmation of VCh requires a high level of specificity at low sample concentrations to be maintained. The full mass scan of VCh revealed that the two ions at *m/z* 54 and 79 constituted the base peak and *ca.* 60% of the relative intensity. Multiple ion monitoring, *i.e.*, monitoring of peaks from a limited number of ions, of these two ions was carried out to enhance the sensitivity beyond that obtainable by full mass scans. The specificity for VCh was maintained in the multiple ion monitoring mode by careful attention to the relative areas of the monitored ions.

Determination of VCh levels in polymers

VCh levels in ABS products purchased from retail outlets were determined by injecting solutions of the polymer. The retention time for VCh was 2.9 min. The VCh levels found in ABS products in this study varied with each sample (Table I), ranging from 29 to about 200 mg/kg. VCh in ABS sheet was confirmed by correspondence of

TABLE I

OBSERVED LEVELS OF 4-VINYL-1-CYCLOHEXENE IN RETAIL ABS PRODUCTS

Product		*4-Vinyl-1-cyclohexene (mg/kg)*
Food-grade sheet:	1	104
	2	205
Ladle		132
Grater		88
Lunch tray:	1	110
	2	29

TABLE II

MIGRATION OF 4-VINYL-1-CYCLOHEXENE (VCh) FROM TWO LOTS OF FOOD-GRADE ABS SHEETS TO *n*-HEPTANE FROM 1 TO 10 DAYS AT 25°C

Lot No.	*Surface area (cm^2)*	*Weight (g)*	*Volume of n-heptane (ml)*	*Level of VCh (mg/kg)*	*Total VCh found (mg/kg)*	*Day*	*Concentration of VCh found in solvent (mg/kg)*	*Calculated total VCh extracted (μg)*	*Total VCh extracted (%)*
1	100	5.7	200	104	593	1	0.30	60	10
						5	0.62	124	21
						8	0.69	138	23
						10	0.72	144	24
2	100	5.7	200	205	1169	1	0.46	92	8
						5	0.88	176	15
						8	0.96	192	16
						10	1.02	204	17

the retention times, ion profiles and relative areas of the monitored ions with those of VCh standards.

A 5% solution of polymer in DMF was used because higher concentrations became cloudy when cooled to room temperature. The limit of quantification on direct injection of about 5 μl of these 5% solutions was about 0.5 mg/kg for VCh, equivalent to about 10 mg/kg of VCh in the polymer. The recovery of VCh added to 5% ABS polymer solution was 89–103% in the range of 40–80 μg per sample and the coefficient of variation was 5.4%.

Determination of VCh in food simulants

This SIM procedure is very useful in migration studies with food simulants where the concentrations of VCh may be extremely low. Such studies often require higher analytical sensitivity and much lower noise than can be achieved by GC–FID. Food simulants spiked with VCh at concentrations of 2.5 and 5.0 μg were prepared. The recoveries of VCh were found to be 98–100, 102–97 and 94–91% from water, 4% acetic acid and 20% ethanol, respectively. Blank food simulants should be tested to ensure the absence of extraneous chromatographable compounds eluting at the retention time of VCh.

Migration experiments

To illustrate the applicability of the method, experiments were performed to determine the extent of migration of VCh into water, 4% acetic acid, 20% ethanol and *n*-heptane and the approximate rates. VCh levels were determined in two lots of food-grade ABS sheets. ABS lots 1 and 2 contained 104 and 205 mg/kg of residual VCh, respectively. Duplicate sheets of each lot, measuring approximately 100 cm^2, weighing 5.7 g and 1.05 mm in thickness, were then immersed in water, 4% acetic acid or 20% ethanol for 30 min at 60°C and in *n*-heptane from 2 h up to 10 days at 25°C.

No migration of VCh from the two lots of food-grade ABS sheets into the four food simulants was found, with a detection limit of 0.05 mg/kg, under the effluent conditions of the sanitation law of Japan for total migration from various polymers. Migration levels into *n*-heptane were monitored periodically for up to 10 days because VCh itself shows some tendency to migrate into oily foodstuffs. These analyses, given in Table II, gave concentrations of 0.72 and 1.02 mg/kg of VCh in *n*-heptane for lots 1 and 2, respectively. These concentrations represent total migrations of approximately 24 and 17%, respectively, of the residual VCh from ABS sheets into *n*-heptane.

REFERENCES

1 P. L. Viola, A. Bigotti and A. Caputo, *Cancer Res.*, 31 (1971) 516.
2 C. Maltoni, *Ambio*, 4 (1975) 18.
3 S. Tan and T. Okada, *J. Food Hyg. Soc. Jpn.*, 19 (1978) 172.
4 J. Gilbert and J. R. Startin, *J. Chromatogr.*, 205 (1981) 434.
5 T. J. Birkel, J. A. G. Roach and J. A. Sphon, *J. Assoc. Off. Anal. Chem.*, 60 (1977) 1210.
6 H. C. Hollifield and T. McNeal, *J. Assoc. Off. Anal. Chem.*, 61 (1978) 537.
7 S. Tan and T. Okada, *J. Food Hyg. Soc. Jpn.*, 20 (1979) 223.
8 J. Gilbert, M. J. Shepherd, J. R. Startin and D. J. McWeeny, *J. Chromatogr.*, 197 (1980) 71.
9 R. J. Steichen, *Anal. Chem.*, 48 (1976) 1398.
10 S. Tan and T. Okada, *J. Food Hyg. Soc. Jpn.*, 20 (1979) 228.

11 S. Tan and T. Okada, *J. Food Hyg. Soc. Jpn.*, 22 (1981) 150.
12 J. R. Startin and J. Gilbert, *J. Chromatogr.*, 294 (1984) 427.
13 C. de Meester, F. Poncelet, M. Roberfroid and M. Mercier, *Biochem. Biophys. Res. Commun.*, 80 (1978) 298.
14 A. K. Armitage and D. H. Pullinger, presented at the *18th Annual Meeting of the International Institute of Synthetic Rubber Producers, Inc., May 2–7, 1977, Monte Carlo*, p. 53.
15 S. Tan and T. Okada, *J. Food Hyg. Soc. Jpn.*, 22 (1981) 155.
16 *Notification No. 20*, Ministery of Health and Welfare, February 16, 1982.

Journal of Chromatography, 482 (1989) 252–257
Elsevier Science Publishers B V., Amsterdam — Printed in The Netherlands

CHROM. 21 915

Note

Purification of argininosuccinase by high-pressure immunoaffinity chromatography on monoclonal anti-argininosuccinase–silica

LARRY R. MASSOM and HARRY W. JARRETT*,[a]

Department of Biology, Indiana University–Purdue University at Indianapolis, Indianapolis, IN 46223 (U.S.A.)

(First received May 24th, 1989; revised manuscript received August 23rd, 1989)

Purification of enzymes is typically a long and tedious process. However, once a specific antibody directed against an enzyme is obtained, enzyme purification can be shortened by the use of immunological techniques. These techniques include the immobilization of antibodies against the desired enzyme on such supports as Sepharose and agarose for use in low-pressure affinity chromatography (LPAC). This method can greatly simplify enzyme purification and reduce the time required. However, LPAC may still require days of laboratory work before a pure enzyme is obtained. The time required for column work can be shortened considerably by using high-pressure affinity chromatography (HPAC) instead of LPAC. The use of HPAC requires that the antibody be immobilized on supports such as silica which can withstand the high pressures associated with HPAC. Josic *et al.*[1] immobilized an antibody against glycoprotein GP 105 (a membrane bound protein) on silica and demonstrated its effectiveness in purifying GP 105. Ohlson *et al.*[2] have immobilized polyclonal antibodies against transferrin and have shown quantitative recovery of pure transferrin. However, the elution conditions used by Josic *et al.*[1] included a detergent and pH 2.4 and those used by Ohlson *et al.*[2] included pH 1.3. These conditions are likely to denature many proteins. The purification of an active enzyme by this method has yet to be demonstrated. We describe here the synthesis of an antibody–silica HPAC column and its use to purify active argininosuccinase from a crude homogenate using conditions less harsh (pH 3, no detergent) than those previously employed[1,2].

MATERIALS AND METHODS

Chromatography

All high-pressure chromatography was at room temperature (20°C) using a Varian 5000 (ternary gradient) chromatograph outfitted with a Jasco UV–VIS detector, a Gilson 321/401 autosampler, and an Apple II Plus computer to serve as an integrator using the Chromatochart software (Interactive Microware, State College, PA, U.S.A.).

---

[a] Present address: Department of Biochemistry, University of Tennessee, 800 Madison Avenue, Memphis, TN 38163, U.S.A.

0021-9673/89/$03.50

Preparation of anti-argininosuccinase

Anti-(beef)argininosuccinase (subclass IgG_1) was obtained from hybridoma culture media (Dulbecco's Modified Eagle Medium, IgG_1 concentration approximately 10 μg/ml) provided by Dr. Merrill Benson and William Kuster, DRTC Hybridoma Core, Indiana University Medical Center, Indianapolis, IN, U.S.A. A volume of 20 ml of the above medium was mixed with 20 ml of a saturated solution of ammonium sulfate in 10 m*M* sodium phosphate, pH 7.0. The mixture was held at 5°C for 30 min and centrifuged (10 000 *g*, 10 min, Sovall RC-5 centrifuge). The precipitant was resuspended in 3 ml of 10 m*M* sodium phosphate, 1 *M* sodium sulfate, pH 7.0 (buffer A).

Further purification of the anti-argininosuccinase was accomplished by HPAC using a protein A–silica column[3]. 1.5 ml of the ammonium sulfate fractionated anti-argininosuccinase was applied to the column which was equilibrated in buffer A. During sample loading, the flow-rate was 0.1 ml/min. The column was washed for 5 min with buffer A at 1 ml/min, and then eluted with 10 m*M* sodium phosphate, 1 *M* sodium sulfate, pH 3.0 (buffer B) also at 1 ml/min. The effluent was monitored at 280 nm. Fractions of 1 ml were collected in tubes containing 0.1 ml of 0.5 *M* sodium phosphate, pH 12 which, after mixing, gave a final pH for each fraction of about 7.5. The final combined volume from processing two 1.5-ml portions of the ammonium sulfate fractionated antibody was 3.2 ml of 18 μg/ml antibody (assuming $E^{1\%}_{280\,nm}$ = 14.0) at pH 7.52.

Synthesis of anti-argininosuccinase–silica

All reactions were conducted at room temperature (20°C) unless otherwise stated. An amount of 1.0 g of 3-glycidyloxypropyl silica (7 μm bead, 500 Å pore) was incubated with 3.2 ml of the above solution containing the purified anti-argininosuccinase while shaking for 36 h. The support was washed with buffer A, and excess coupling sites on the silica were quenched by incubating the support for 24 h with 3.0 ml of buffer A containing 0.5 *M* 2-aminoethanol. The support was then washed with buffer A and *ca.* 0.3 g was packed into a 30 × 4.6 mm I.D. stainless-steel column (Alltech, Deerfield, IL, U.S.A.).

Purification of argininosuccinase

The source of argininosuccinase was a 5% crude beef liver extract (approximately 30.9 μg of argininosuccinase per ml) provided by Dr. Philip Snodgrass, Veterans Administration Medical Center, Indianapolis, IN, U.S.A.).

The anti-argininosuccinase column was equilibrated with 10 m*M* sodium phosphate, 100 m*M* sodium sulfate, pH 7.0 (buffer C) at a flow-rate of 1 ml/min. Injected were 200 μl of a 1/10 dilution of the beef liver extract (buffer C was the diluent) on the column which was then washed for 5 min with buffer C. The column was eluted using 10 m*M* sodium phosphate, 100 m*M* sodium sulfate, pH 3.0 buffer (buffer D). The effluent was monitored at 280 nm and 1-ml fractions were collected in test tubes containing 0.1 ml of 0.5 *M* sodium phosphate, pH 12 to rapidly adjust the effluent to pH 7.5 as previously described.

Purity of fractions were determined by sodium dodecylsulfate polyacrylamide gel electrophoresis (SDS-PAGE, 5% acrylamide and 0.25% bis-acrylamide) using the method of Laemmi[4]. Argininosuccinase activity was measured using the method described by Havir *et al.*[5]

Storage

When not in use, the antibody–silica column was stored in buffer C at 4°C. No other special precautions or washed were taken.

Capacity of the anti-argininosuccinase column

One unit of argininosuccinase is defined as that which will form 1.0 μmole of L-arginine from L-argininosuccinate per minute at pH 7.5 and 37°C as determined by the formation of urea. A volume of 500 μl of buffer C containing 2 units of pure argininosuccinase (Sigma, St. Louis, MO, U.S.A.) was loaded onto the column under the same conditions used for the beef liver extract. The effluent was collected and assayed for argininosuccinase activity. A volume of 1000 μl containing 4 units of the pure argininosuccinase solution was also tested and gave similar results.

RESULTS AND DISCUSSION

Anti-argininosuccinase was purified on the Protein A–Silica column (data not shown); based on previous experience, the eluted fractions were considered to be pure anti-argininosuccinase[3]. This purified monoclonal antibody was then coupled to glycidyloxypropyl–silica, presumably by the scheme depicted in Fig. 1.

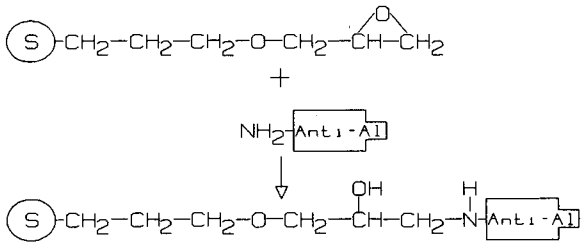

Fig. 1. Coupling of anti-argininosuccinase to silica. An amount of 1 g of 3-glycidyloxypropyl–silica reacted with 3.2 ml of a solution containing purified anti-argininosuccinase (Anti-Al) in 10 m*M* sodium phosphate, 1 *M* sodium sulfate, pH 7.5. Amino groups on the anti-argininosuccinase (*e.g.*, ε-amino groups on lysyl side chains) are thought to have reacted with the epoxide group on the silica ("S") to form a covalent bond and providing a seven atom spacer between the silica and the antibody.

The anti-argininosuccinase–silica column was next used to purify argininosuccinase from a crude liver extract containing 0.021 units of activity, as shown in Fig. 2. SDS-PAGE of the eluted fractions showed a single band (Fig. 3) with a relative mobility identical to that observed for pure argininosuccinase in other experiments (data not shown). In the eluted fractions 0.013 units of argininosuccinase activity were present.

When either 2 or 4 units of pure argininosuccinase was loaded on the column, most of the activity was recovered in the unretained fractions indicating that the column was saturated in both instances and elution in either case gave 0.12 units. Thus, the capacity of the column (containing 0.3 g of the support) corresponds to 0.4 units of argininosuccinase per gram silica.

After approximately a dozen runs over a period of 3 months (longest time tested), there was no evidence of deterioration in the antibody column's performance

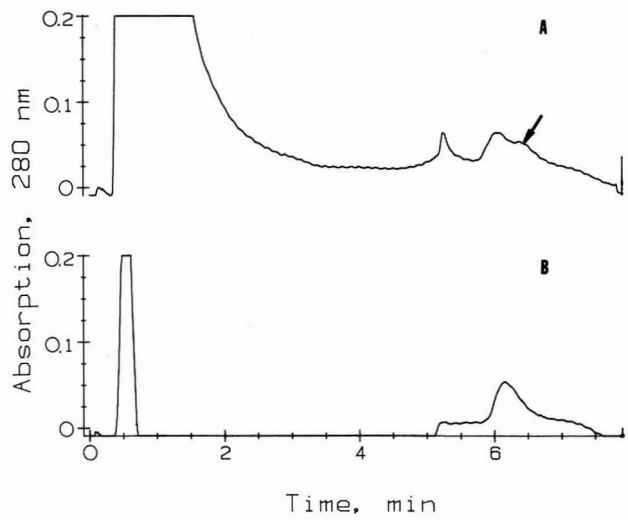

Fig. 2. Purification of argininosuccinase on anti-argininosuccinase–silica. (A) Purification of argininosuccinase on the anti-argininosuccinase–silica column. A volume of 200 μl of 1/10 diluted beef liver extract containing 0.021 units of argininosuccinase was loaded onto the column equilibrated in buffer C. Approximately 5 min later the column was eluted with buffer D. The amount of argininosuccinase retained by and eluted from the column was small (0.013 units) and the arrow indicates the largest change in the chromatogram as compared to the baseline illustrated in (B). Activity measurements confirm the elution of argininosuccinase at the position indicated; the remaining argininosuccinase activity was found in unretained fractions eluting before 3 min. The baseline (B) consisted of the same protocol used for (A) except the load consisted only of buffer C with no sample included.

using the elution regimen described. A Protein A column has been used with a similar protocol[3] in our lab for more than $1\frac{1}{2}$ years without a noticeable decline in activity. Josic *et al.*[1], using somewhat harsher elution conditions has noted such deterioration. Ohlson *et al.*[2] used pH 1.3 for elution but unfortunately did not discuss the durability of their columns. Since pH 3 is adequate to ensure elution and columns remain stable over long periods using these conditions,the milder elution regimen described here is preferable.

The coupling of antibodies directly to high-performance liquid chromatographic supports for immunoaffinity purification of antigens appears to be promising. Here, using a column based upon a monoclonal antibody, argininosuccinase was purified from a crude liver extract to apparent homogeneity in a single purification step requiring less than 10 min. Argininosuccinase retains its biological activity under the conditions used; the monoclonal antibody on the column also appears stable even after repeated uses over several months. Some enzymes can be purified in an active state; argininosuccinase is such an enzyme. However, it should not be expected that all enzymes would remain active under the conditions used; for example, previously we found that arginase is inactivated by the pH 3 used for elution[3]. For such pH sensitive enzymes, it may be possible to develop an additional elution protocol tailored to the sensitivities of individual enzymes. High concentrations of some salts (*e.g.* potassium thiocyanate) have been effective in LPAC and may be applicable to HPAC.

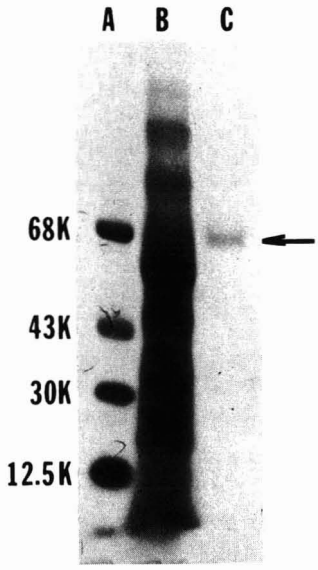

Fig. 3. SDS-PAGE of purified argininosuccinase from liver extract. Unretained and eluted fractions from a separation of crude beef liver extract under the conditions described for Fig. 2 were examined by SDS-PAGE including 2-mercaptoethanol in the sample buffer (reducing conditions). The gel was 5% acrylamide and 0.25% bis-acrylamide. In order from left to right, the lanes contained: (A) molecular weight standards (in descending order bovine serum albumin, ovalbumin, carbonic anhydrase, and cytochrome *c*); (B) the unretained fractions; and (C) material eluted at pH 3. Lane C shows a single band with a molecular weight slightly less than the bovine serum albumin standard (*i.e.*, 68 K). This is very near the reported molecular weight of argininosuccinase subunit reported by Schulze *et al.*[6] and the relative mobility (R_F) is the same as that observed for authenic argininosuccinase in other experiments. K = kilodaltons.

Direct coupling of antibodies to HPAC supports will probably be of most value in situations where repeated purification of a particular antigen is needed or for quantitative assays as suggested by Ohlson *et al.*[2]. Immunoaffinity purification of antigen–antibody complexes using protein A–silica[1,3] does not require the synthesis of new supports for each antibody–antigen pair and may be more practical in some cases.

ACKNOWLEDGEMENTS

We would like to thank Mr. William Foster (Alltech, Deerfield, IL, U.S.A.) and Robert L. Sheppard (Krannett Institute of Cardiology, Indianapolis, IN, US.A.) for excellent technical assistance, Drs. Philip Snodgrass and Corrine Ulbright (Veterans Administration Medical Center, Indianapolis, IN, U.S.A.) for the enzymes, and Dr. Merrill Benson and William Kuster (DRTC Hybridoma Core, Indiana University Medical Center, Indianapolis, IN, U.S.A.) for the monoclonal antibody. This work was supported in part by NSF (DMB8707013) and NIH (GM43609).

REFERENCES

1 D. Josic, W. Hofmann, R. Habermann, J. D. Schulzke and W. Reuter, *J. Clin. Chem. Clin. Biochem.*, 26 (1988) 559.
2 S. Ohlson, B. M. Gudmundssom, P. Wilkstrom and P. O. Larsson, *Clin. Chem.*, 34 (1988) 2039–2043.
3 L. R. Massom, C. Ulbright, P. Snodgrass and H. W. Jarrett, *BioChromatogr.*, 4 (1989) 144–148.
4 U. K. Laemmli, *Nature (London)*, 227 (1970) 680.
5 E. A. Havir, H. Tamir, S. Ratner and R. C. Warner, *J. Biol. Chem.*, 240 (1965) 3079.
6 I. T. Schulze, C. J. Lusty and S. Ratner, *J. Biol. Chem.*, 245 (1970) 4534.

Journal of Chromatography, 482 (1989) 258–261
Elsevier Science Publishers B.V., Amsterdam — Printed in The Netherlands

CHROM. 21 927

Note

Separation of the enantiomers of a triester of 2,2-difluorocitrate

P. CAMILLERI*, R. E. DOLLE, R. NOVELLI and C. J. SALTER
Smith Kline & French Research Limited, The Frythe, Welwyn, Herts. AL6 9AR (U.K.)
(Received July 17th, 1989)

Racemic fluorocitrates have been used extensively in studies[1–4] related to the blocking of the citric acid cycle. They inhibit a number of enzymes such as aconitase[1] and succinic hydrogenase[2]. In the case of monofluorocitrate, only the (−)-enantiomer is biologically active, displaying sever CNS toxicity. Because of the lack of toxicity associated with the corresponding (+)-enantiomer of monofluorocitrate, it has been used as an NMR probe for the quantitative estimation of magnesium ions in a biological environment[6]. Although the fluorine atoms in 2,2-difluorocitric acid are not magnetically equivalent, and lead to two distinguishable signals in the fluorine NMR spectrum, difluoro citrate has not yet been used as an NMR probe. Separation of the enantiomers of the citric acid analogue **1** is not only of interest to afford knowledge on the biochemistry of these substances, but may also provide a useful precursor for a versatile NMR probe.

The enantiomers of 2,2-difluorocitrate have not been separated either by chemical or chromatographic methods. In this article, we describe the successful chromatographic separation of the antipodes of **1** and their characterisation by polarimetry and circular dichroism.

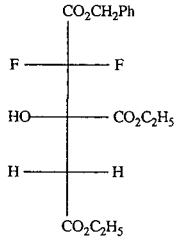

1

EXPERIMENTAL

Chemicals

n-Hexane (Rathburn) and propan-2-ol (BDH) were filtered through a Millipore Durapor 0.45-μm membrane filter and degassed with helium before use. Racemic **1** was prepared from the known diethyl difluorocitrate[7] and treatment with phenyldiazomethane.

0021-9673/89/$03.50

High-performance liquid chromatography (HPLC)

The HPLC system used to carry out the chromatographic separation of the enantiomers of **1** consisted of a Perkin-Elmer Series 4 liquid chromatograph, a Perkin-Elmer ISS-100 autoinjector and a Kratos Spectroflow 783 variable-wavelength absorbance detector operated at 210 nm. For the analytical separations the chiral column (250 × 4.9 mm I.D.) was of the Pirkle type (supplied by Hichrom) and was packed with (L)-N-(3,5-dinitrobenzoyl)leucine covalently bound to 3-aminopropyl silica (particle size 5 μm). The column was operated at 0°C. The best separation of the enantiomers was achieved using *n*-hexane–propan-2-ol as the mobile phase (97:3) at a flow-rate of 1 ml min^{-1}.

The preparation of about 40 mg of each of the two enantiomers was carried out using the same type of column packing as above. However, in this case the dimensions of the semi-preparative column were 250 × 8.0 mm I.D. Again, the same solvent ratio was used and the flow-rate was set at 2 ml min^{-1}.

Polarimetry and circular dichroism

In order to determine the enantiomeric composition of the separated enantiomers of **1**, their specific rotation $[\alpha]_D^T$ was measured using a Perkin-Elmer 241 polarimeter set at a wavelength of 589 nm (sodium D-line). Optical rotation was determined in a cell of 100 mm pathlength. Each of the enantiomers was dissolved in acetonitrile and equilibrated at 25°C before the specific rotation was measured. The concentrations of the (+)- and (−)-enantiomers were 9.6 and 9.2 mg ml^{-1}, respectively.

The circular dichroism (CD) spectra of the enantiomers were recorded from 350 to 225 nm on a Jasco J-600 spectropolarimeter, using a 10-mm pathlength cell thermostatted at 25°C. The (+)- and (−)-enantiomers were dissolved in acetonitrile, at concentrations of 0.96 and 0.92 mg ml^{-1}, respectively.

RESULTS AND DISCUSSION

The analytical separation of the enantiomers of **1** is shown in Fig. 1. The (−)-enantiomer elutes faster than the (+)-form. The retention times are 21.2 and 22.6

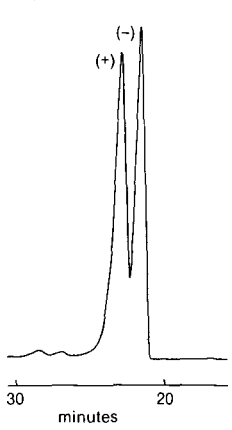

Fig. 1. HPLC separation of the enantiomers of **1**. For conditions, see Experimental.

min, respectively, and the corresponding separation factor, α, is 1.08.

To obtain about 40 mg of each of the two enantiomers a semi-preparative column was used. This enabled the injection of about 2-mg quantities of **1**. Fig. 2a shows a typical chromatogram obtained on this column. The rather peculiar shape of the peaks is due to overloading. Three fractions were collected. The first and third fractions gave the (−)- and (+)-enantiomer in 97 and 90% purity as determined by rechromatography on the analytical column using hexane–propan-2-ol (99:1) and a flow-rate of 1 ml min^{-1} (Fig. 2b and c). This purity was adequate for partial characterisation and for our research purposes.

The specific rotations $[\alpha]_D^{25}$ for fractions 1 and 3 were measured as −7.6 and +6.6. Taking into account the level of impurities of the (+)- and (−)-forms in either of the two fractions, the specific rotation of the pure enantiomers was calculated at about 8.1 with the appropriate sign.

The CD curves obtained from fractions 1 and 3 are shown in Fig. 3. As expected from the purity of the (−)- and (+)-enantiomers in the two fractions, one of these spectra is weaker than the other. The CD curves obtained in the wavelength range of 270–235 nm are due to the phenyl chromophore in **1**, which also gives rise to near-UV absorption maxima at 261, 257 and 252 nm with extinction coefficients of about 400 1 mol^{-1} cm^{-1}. The CD band with a peak at 243 nm, which does not coincide with any

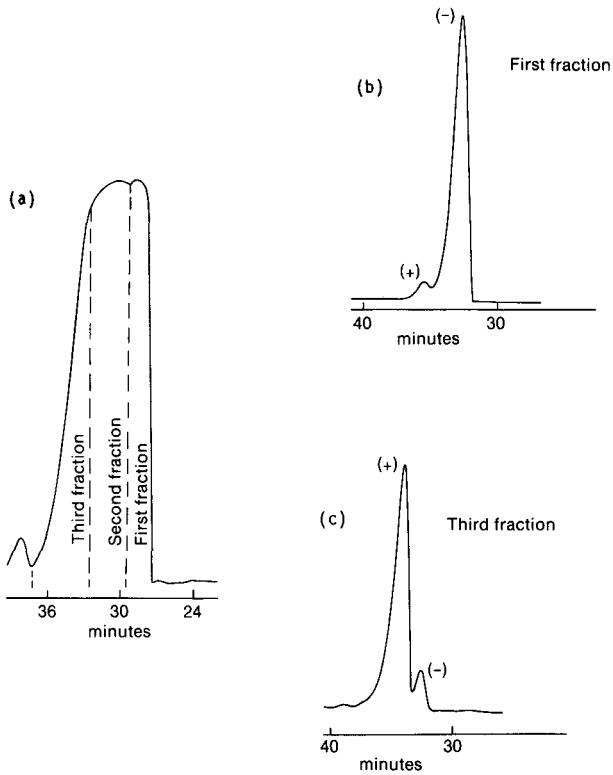

Fig. 2. Preparative HPLC of **1**. (a) Racemic mixture chromatographed on a semi-preparative column; (b) first fraction and (c) third fraction from (a) rechromatographed on an analytical column.

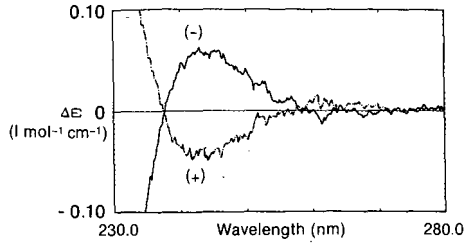

Fig. 3. CD spectra of the first and third fractions (see Fig. 2) denoted by (−) and (+), respectively. $[\alpha]_D^{25}$ = −7.6 and +6.6.

of the UV absorption maxima, is probably due to the summation of two or more underlying positive and negative bands arising from the phenyl chromophore coupling with the two carbonyl chromophores of the ethyl ester groups in **1**.

In conclusion, the simple preparation procedure described in this note allows the preparation of milligram quantities of the (−)- and (+)-enantiomers of an ester of 2,2-difluorocitric acid in purity >90%. Larger quantities can be prepared using a larger preparative column and higher purity material can easily be obtained by rechromatography.

REFERENCES

1 F. L. M. Pattison and R. A. Peters, in F. A. Smith (Editor), *Handbook of Experimental Pharmacology*, Vol. XX, Part 1, Springer, New York, 1966, p. 387.
2 D. W. Fanshier, L. W. Gottwald and E. Kan, *J. Biol. Chem.*, 239 (1964) 425.
3 R. V. Brunt, R. Eisenthal and S. A. Symons, *FEBS Lett.*, 13 (1971) 89.
4 S. Herford and P. D. J. Weitzman, *FEBS Lett.*, 114 (1980) 339.
5 R. J. Dummel and E. Kun, *J. Biol. Chem.*, 244 (1969) 2966.
6 H. L. Kirschenlohr, J. C. Metcalfe, P. G. Morris, G. C. Rodrigo and G. A. Smith, *Proc. Natl. Acad. Sci. U.S.A.*, 85 (1988) 9017.
7 M. S. Raasch, *U.S. Pat.*, 2 824 888 (1958); *C.A.*, 52 (1958) 12901h.

PUBLICATION SCHEDULE FOR 1989

Journal of Chromatography and Journal of Chromatography, Biomedical Applications

MONTH	J	F	M	A	M	J	J	A	S	O	N	D
Journal of Chromatography	461 462 463/1	463/2 464/1	464/2 465/1 465/2	466 467/1 467/2	468 469 470/1 470/2	471 472/1 472/2 473/1	473/2 474/1 474/2 475	476 477/1 477/2	478/1 478/2 479/1	479/2 480	481 482/1	482/2 483 484 485
Bibliography Section		486/1		486/2		486/3		486/4		486/5		486/6
Biomedical Applications	487/1	487/2	488/1 488/2	489/1 489/2	490/1 490/2	491/1	491/2	492 493/1	493/2 494	495	496/1 496/2	497

INFORMATION FOR AUTHORS

(Detailed *Instructions to Authors* were published in Vol. 478, pp. 453–456. A free reprint can be obtained by application to the publisher, Elsevier Science Publishers B.V., P.O. Box 330, 1000 AH Amsterdam, The Netherlands.)

Types of Contributions. The following types of papers are published in the *Journal of Chromatography* and the section on *Biomedical Applications:* Regular research papers (Full-length papers), Notes, Review articles and Letters to the Editor. Notes are usually descriptions of short investigations and reflect the same quality of research as Full-length papers, but should preferably not exceed six printed pages. Letters to the Editor can comment on (parts of) previously published articles, or they can report minor technical improvements of previously published procedures; they should preferably not exceed two printed pages. For review articles, see inside front cover under Submission of Papers.

Submission. Every paper must be accompanied by a letter from the senior author, stating that he is submitting the paper for publication in the *Journal of Chromatography*. Please do not send a letter signed by the director of the institute or the professor unless he is one of the authors.

Manuscripts. Manuscripts should be typed in double spacing on consecutively numbered pages of uniform size. The manuscript should be preceded by a sheet of manuscript paper carrying the title of the paper and the name and full postal address of the person to whom the proofs are to be sent. Authors of papers in French or German are requested to supply an English translation of the title of the paper. As a rule, papers should be divided into sections, headed by a caption (*e.g.*, Summary, Introduction, Experimental, Results, Discussion, etc.). All illustrations, photographs, tables, etc., should be on separate sheets.

Introduction. Every paper must have a concise introduction mentioning what has been done before on the topic described, and stating clearly what is new in the paper now submitted.

Summary. Full-length papers and Review articles should have a summary of 50–100 words which clearly and briefly indicates what is new, different and significant. In the case of French or German articles an additional summary in English, headed by an English translation of the title, should also be provided. (Notes and Letters to the Editor are published without a summary.)

Illustrations. The figures should be submitted in a form suitable for reproduction, drawn in Indian ink on drawing or tracing paper. Each illustration should have a legend, all the *legends* being typed (with double spacing) together on a *separate sheet.* If structures are given in the text, the original drawings should be supplied. Coloured illustrations are reproduced at the author's expense, the cost being determined by the number of pages and by the number of colours needed. The written permission of the author and publisher must be obtained for the use of any figure already published. Its source must be indicated in the legend.

References. References should be numbered in the order in which they are cited in the text, and listed in numerical sequence on a separate sheet at the end of the article. Please check a recent issue for the layout of the reference list. Abbreviations for the titles of journals should follow the system used by *Chemical Abstracts.* Articles not yet published should be given as "in press" (journal should be specified), "submitted for publication" (journal should be specified), "in preparation" or "personal communication".

Dispatch. Before sending the manuscript to the Editor please check that the envelope contains three copies of the paper complete with references, legends and figures. One of the sets of figures must be the originals suitable for direct reproduction. Please also ensure that permission to publish has been obtained from your institute.

Proofs. One set of proofs will be sent to the author to be carefully checked for printer's errors. Corrections must be restricted to instances in which the proof is at variance with the manuscript. "Extra corrections" will be inserted at the author's expense.

Reprints. Fifty reprints of Full-length papers, Notes and Letters to the Editor will be supplied free of charge. Additional reprints can be ordered by the authors. An order form containing price quotations will be sent to the authors together with the proofs of their article.

Advertisements. Advertisement rates are available from the publisher on request. The Editors of the journal accept no responsibility for the contents of the advertisements.

Industry Research Studies and Technical-Market Analyses of Membrane & Separations and Biotechnology

JBC-080 CHROMATOGRAPHY

As large scale purification processes become increasingly important, so will the role of chromatography in their development. This BCC report is a technical-market guide for chromatography manufacturers, suppliers, investors, planners and users. It examines the chromatography market in terms of existing and new separation techniques, chromatographs and materials. GC, LC, HPLC, TLC, IonLC and GPC are covered in an in-depth look at the technologies, materials, markets, manufacturers and competition - both domestic and foreign. The study also looks into the newly emerging affinity chromatography techniques, evaluates and forecasts their applications potential, future availability and market impact.
Published November 1988 *150 pages* *Price: $1950.00*

JBC-046R MEMBRANE MICROFILTRATION

Improved filter technology, legislation requiring waste clean-up, and the possibility of economic advantages in reclaiming certain by-products or starting materials have worked in favor of developing high-tech filtration markets. BCC report analyzes the markets, technology and companies involved in high-tech filtration. Stand-alone applications and materials examined include those used for the biotechnology/biomedical industry, the ethical drug market, the semiconductor/electronic applications market, chemicals and other fluid processing, processed foods & beverages market, and environmental and waste clean-up. An industry sector that uses or needs pure and/or particulate-free liquids, discharges waste materials or is involved in biotechnology is a potential high-tech filtration market.
Published July 1988 *160 pages* *Price: $1950.00*

JBGB-112 INORGANIC MEMBRANES

This exciting, new, improved group of materials is being investigated by major materials companies worldwide. BCC report analyzes the new developments and technologies that make it all possible. It estimates markets and reviews fabrication techniques for materials such as inorganic dynamic membranes; ceramic, glass, and ceramic-like membranes; alumina; and surface modifications for microfiltration and ultrafiltration. The companies involved, the important research, current and new applications and the advantages and disadvantages of these new materials are discussed in detail.
Published April 1989 *131 pages* *Price: $2450.00*

JBC-107 ADVANCED NOVEL SEPARATIONS

Novel separations are on the cutting edge of separations technology. Although many have yet to be commercialized, they offer new and innovative approaches that will improve separation efficiencies and reduce costs. BCC report examines technologies such as exsorption, supercritical and solvents, and capillary zone electrophoresis; analyzes their applications and markets; assesses the opportunities they offer; and investigates the activities of the manufacturers currently involved.
Published July 1989 *76 pages* *Price: $1750.00*

JBC-060 THE DIAGNOSTIC REAGENTS INDUSTRY

BCC report on diagnostic reagents industry tells what the new and better diagnostic products are, who makes them, and the markets they impact on, together with forecasts and sales by category of reagents and by application. Report discusses strategic options within the diagnostic reagents industry, as well as choices available if acquiring diagnostics from outside the industry.
Published March 1987 *162 pages* *Price: $1950.00*

JBC-088 THE DYNAMIC MONOCLONAL AND POLYCLONAL ANTIBODY BUSINESS

BCC report identifies and describes MAb and PAb products, discusses their advantages and limitations, looks into the emerging defined antibody blends as well as FAbs, SAbs, CAbs and HAbs. The report also reviews the current status of MAb and PAb manufacturing processes including support products. Also covered is the emerging field of organic chemicals applications and other new applications. This BCC report lists the extensive number of products and suppliers; describes applications; analyzes markets by customer, origin, and Ig class; and estimates current and projected sales with explanations.
Published May 1989 *Price: $2650.00*

JBC-084 MICROORGANISM TESTING MARKETS

BCC report examines recent technological advances in microorganism testing, as well as conventional technologies used. It assesses the present and likely future markets for products in human clinical, veterinary, agricultural, environmental and sterility testing applications. The study describes the new DNA gene probes and monoclonal antibodies, and evaluates their potential vis-a-vis chemical dyes and stains, nutrient growth media, microscopy and automated equipment. Market size, product sales, suppliers and impact of regulations are discussed.
Published February 1988 *184 pages* *Price: $1950.00*

JBC-073 SEPARATIONS SYSTEMS FOR COMMERCIAL BIOTECHNOLOGY

A variety of different high technologies are applied for biotechnology separations. These include membrane-based separations as well as ion, gel, and affinity chromatography. BCC explores commercial operations that handle product volumes ranging from 50 gm to pounds and evaluates the separations techniques such as ultra-centrifuge and slow cytometer used to achieve optimum reactions. The value of the separation technology is explored by type with trends and forecasts for the next five to ten years.
Published July 1988 *179 pages* *Price: $2250.00*

JBC-056 AMINO ACID PRODUCTS & TECHNOLOGY

BCC report details developments in biotechnology and protein synthesis which are opening markets for amino acid products, or modify established processes pointing to the effects of these advances, where opportunities exist and where market potential is declining. Report reviews products in each of five groups - research and analytical, animal feed supplements, food grade amino acids for human food and nutrition, medical/pharmaceutical, and chemical intermediates. Each group is examined for how amino acids are made, which are used, current and projected values for products and services, patterns of supply and demand, production capacity, firms making and using amino acids, and strategic positions for market participants.
Published April 1987 *145 pages* *Price: $1750.00*

JBC-103 EXPANDING HORIZONS FOR GENE PROBES

This BCC report discusses the technology for making gene probes and identifies niche opportunities for suppliers of biochemicals, fluorescent and other types of probe tags, other kinds of chemicals and DNA synthesizers. As the Human Genome Project gathers momentum, opportunities for new gene probes will expand geometrically. This report provides quantified data on market sizes and sales potentials for the growing list of gene probe applications.
Published March 1989 *98 pages* *Price: $1950.00*

Plus: Custom Studies, Conferences, Newsletters, Focus Groups

CALL, WRITE OR FAX

Business Communications Company, Inc. • 25 Van Zant Street, Norwalk, CT 06855 U.S.A.
Phone: (203) 853-4266 • FAX: (203) 853-0348 • TELEX: 6502934929 (via WUI)